Creep Characteristics and Shear Strength of Recycled Asphalt Blends

by

Jeffery M. Schaper

A Thesis Presented in Partial Fulfillment
of the Requirements for the Degree
Master of Science

Approved April 2011 by the
Graduate Supervisory Committee:

Edward Kavazanjian, Chair
Claudia Zapata
Sandra Houston

ARIZONA STATE UNIVERSITY

May 2011

ABSTRACT

The trend towards using recycled materials on new construction projects is growing as the cost for construction materials are ever increasing and the awareness of the responsibility we have to be good stewards of our environment is heightened. While recycled asphalt is sometimes used in pavements, its use as structural fill has been hindered by concern that it is susceptible to large long-term deformations (creep), preventing its use for a great many geotechnical applications. While asphalt/soil blends are often proposed as an alternative to 100% recycled asphalt fill, little data is available characterizing the geotechnical properties of recycled asphalt soil blends. In this dissertation, the geotechnical properties for five different recycled asphalt soil blends are characterized. Data includes the particle size distribution, plasticity index, creep, and shear strength for each blend. Blends with 0%, 25%, 50%, 75% and 100% recycled asphalt were tested. As the recycled asphalt material used for testing had particles sizes up to 1.5 inches, a large 18 inch diameter direct shear apparatus was used to determine the shear strength and creep characteristics of the material. The results of the testing program confirm that the creep potential of recycled asphalt is a geotechnical concern

when the material is subjected to loads greater than 1500 pounds per square foot (psf). In addition, the test results demonstrate that the amount of soil blended with the recycled asphalt can greatly influence the creep and shear strength behavior of the composite material. Furthermore, there appears to be an optimal blend ratio where the composite material had better properties than either the recycled asphalt or virgin soil alone with respect to shear strength.

To my wife and children, whom without their love, patience and understanding this would have not been possible.

To my Grandmother, whom without her inspiration, I would have never gone beyond my years at Mizzou.

To Doug Lattin, whom for the past ten years has given me the confidence and support to finish this work.

To John Patterson, whom without his mentoring I would have quit just short of the finish line.

ACKNOWLEDGMENTS

I would like to thank Dr. Edward Kavazanjian for his instruction, guidance and assistance throughout my graduate school studies at Arizona State University. He has been an important part of my growth both academically and professionally. His mentoring was invaluable in completing this research.

I would also like to acknowledge and thank the other members of my committee, Dr. Claudia Zapata and Dr. Sandra Houston. I have enjoyed being in their classes and have learned much from both of them, and in particular from Dr. Zapata.

Peter Goguen was instrumental in keeping the testing equipment running. I am especially grateful for his tireless patience through all of the problems encountered.

Lastly, I would like to acknowledge those who helped me with my research in one fashion or another; Bongseong Seo who taught me how to use the equipment and was very helpful working through early problems; Eric Iglesias and Pengbo Yuan for their manual labor in helping prepare specimens.

TABLE OF CONTENTS

CHAPTER Page

CHAPTER Page

LIST OF TABLES

LIST OF FIGURES

Figure Page

CHAPTER 1

INTRODUCTION

1.1 Overview

Recycled asphalt product (RAP), the recycled material that is the resultant product of the removal of asphaltic concrete pavements that have reached the end of their service life, is fast finding its way onto many construction projects. RAP is a natural choice for use as a recycled material because its main constituent is well controlled, processed and durable mineral aggregate. RAP is readily available on any roadway construction project which includes the removal and replacement of the existing asphalt. RAP material is already commonly being used for base and subbase materials. RAP material is also being incorporated on a limited basis into new asphaltic concrete mixtures, typically at a rate of 10 to 20 percent by weight.

As good of a product RAP material may be, much research still remains to adequately characterize the material to the satisfaction of many engineers. Currently many transportation agencies are still hesitant to use RAP because of the lack of information about its properties. The Arizona Department of Transportation, for example, stockpiles thousands of cubic yards of RAP material every year. One of the main concerns about the

behavior of RAP as an engineered material is that it also contains asphalt cement, usually on the order of 3 to 10 percent by weight. The affects of the asphalt cement on the behavior of the RAP material is not fully understood. The potential for increased compressibility under constant stress, or creep, because of the asphalt cement content of RAP is one negative affect that has been documented. This alone limits the use of RAP in a great many applications, particularly with regard to its use as structural fill.

1.2 Research Goals

Some research is available that addresses RAP material and its potential for use in construction applications. For example, Rathje et al. (2006) at the University of Texas has investigated the use of RAP material for use as backfill for mechanically stabilized earth wall systems. Consentino et al. (2003) at the Florida Institute of Technology has investigated the use of RAP material, as well as RAP soil blends as a base or subbase material. The previous research on shear strength and creep potential were performed using triaxial tests.

The objectives for this research is to further characterize the material properties, shear strength and compressibility of RAP and RAP-soil blends. In harmony with maximizing the use of

RAP material, my research is focused on evaluating the behavior of RAP and RAP-soil blends as well as evaluating the potential use of RAP material as general structural fill material.

1.3 Potential Contributions

It is estimated that over 100 million tons of asphaltic concrete is removed from U.S. roads on an annual basis as a result of ongoing resurfacing and widening construction projects (Kuennen, 2007). The importance of reclaiming and reusing this material has grown over the past several decades as the asphalt construction industry gravitates towards becoming more sustainable and environmentally responsible. The use of recycled asphaltic concrete (RAP) is becoming even more important as the cost of oil is skyrocketing and the availability of suitable materials for roadway construction is declining (Eighmy, & Magee, 2001). For these reasons it is important to be able to maximize the applicable uses for recycled RAP material.

The potential for creep is of real concern for RAP material and consequently has limited the practical use of RAP material in construction. RAP-soil blends have been proposed as a means of decreasing the potential for creep. Furthermore, blending soil with RAP, may improve the shear strength and compaction characteristics of the blended material over straight 100 percent

RAP material. The test data and conclusions of this thesis will help to better understand the behavior of RAP and RAP-soil blends.

CHAPTER 2

BACKGROUND

2.1 Literature

Limited research has previously been done investigating the properties of RAP and evaluating its use in certain construction applications. In preparation for my own research and in interpreting the results of my findings, I conducted several literature searches and read numerous articles pertaining to the engineering applications of RAP material.

A search of the ASU library electronic catalog for the phrase "recycled asphalt product" resulted in 2,874 references pertaining to the general subject. By including the terms "RAP" and "Properties" in the search, the number was reduced to only 52 publications. Of these references, 25 were journal articles, 11 were dissertations, 9 were articles in popular trade publications, and 7 were newspaper articles. The majority of these references only refer to RAP in a limited passing context and do not address directly the compressive or shear strength properties of RAP. In all, 4 references were found that were most applicable to my research in that they addressed the engineering properties of RAP.

In addition to searching for background references addressing RAP material, my research also addressed the subjects of bound in matrix material and on the effects of the coefficient of uniformity on the soil skeleton. These references were specifically targeted to help evaluate the results of my research on the behavior of asphalt/soil blends. A brief summary for each of the relevant references follows.

2.1.1 University of Texas studies. The University of Texas began characterizing RAP, as well as crushed concrete, and investigating its applicability for backfill of mechanically stabilized earth (MSE) wall systems in 2001 (Rathje et al., 2001). This research was sponsored by the Texas Department of Transportation. Their first report was a state-of-the-art review of the design of MSE walls and the engineering issues related to the backfill material. This report outlined some basic characteristics for RAP material, including grain size distribution, specific gravity and compaction characteristics.

In 2002, a second report was completed by the University of Texas presenting the results of initial durability and geotechnical tests for RAP and crushed concrete (Rathje et al., 2002). This report expanded the basic characterization of the RAP material to include consolidated-drained shear strength and

hydraulic conductivity from triaxial testing, in addition to some short term and long term corrosion studies. The triaxial testing was performed with 4 inch diameter and 8 inch tall specimens, with particles larger than 0.67 inches removed. Triaxial tests were performed with confining pressures ranging from 5 psi to 50 psi. The results from this triaxial testing found the effective stress friction angle for RAP to be 39° and the effective cohesion of 8 psi.

In 2006, the University of Texas released a third report evaluating RAP and crushed concrete as backfill for MSE walls (Rathje et al., 2006). This report summarized the work that they had been performing for the past several years and put it into context with regards to the current specifications for MSE wall backfill. This report also introduced some further test data for RAP and crushed concrete, including pullout resistance and creep potential. Testing for consolidated-drained shear strength was performed using a large direct shear machine, having a 20 inch square shear box, however the results from this testing for the RAP were discarded due to problems with creep during the tests.

2.1.2 Florida Institute of Technology (FIT) study. FIT also performed some research with RAP to develop a specification for the Florida Department of Transportation for the

use of RAP as a base, subbase or general fill material (Consentino et al., 2003). Their report includes a wide range of test results performed on RAP, including laboratory and in-situ stiffness testing, dry unit weight, compaction characteristics, permeability, consolidated-drained triaxial shear testing and some preliminary measurements of creep. Triaxial tests were performed at confining pressure of 5 psi and 15 psi. The results of the friction angle for 100 percent RAP was found to be 44° and the cohesion was found to be 4.9 psi.

This report also addresses RAP-soil blends. Compaction, shear strength and creep tests were performed with a blend of fine sand material at blend percentages of 80 percent RAP and 60 percent RAP, by weight. The USCS classification of the fine sand used in this study is poorly graded sand to clayey sand, SP-SC. The fine sand material was 99.9 percent passing the #40 sieve and 10.4 percent passing the #200 sieve. The fines had a liquid limit of 39 and a plasticity index of 15. FIT concluded that the friction angle decreases and cohesion increases as the RAP content decreases. In addition, the 80 percent and 60 percent blends yielded denser materials than either the RAP material or the fine sand alone.

2.1.3 Other pertinent studies. To investigate the observed behavior of RAP and RAP-soil blends based on the test results from my research, in which the compaction and shear strength properties were observed to improve when a small amount of soil was blended with the RAP, I researched a conference paper presented by J.P. Giroud regarding geotextile and granular filter criteria (Giroud, 2010). In this work, Giroud discuses the effects of the coefficient of uniformity, Cu, on the soil skeleton. Giroud documents that when Cu for a soil is less than 3, the coarsest particles in the soil remain in continuous contact, forming a skeleton in which the smaller particles are trapped. For soils with a Cu greater than 3, the coarsest soil particles are not in contact with one another, and instead are floating within the matrix of the smaller particles.

Eric Stuart Lindquist wrote a dissertation on the strength and deformation properties of mélange (Lindquist, 1994), a material composed of strong, stiff blocks inside a matrix that is weaker and softer. From his research he concluded that the internal friction angle of the mélange increased as the block proportion of the specimen tested increased. While Lindquist's research was not directly applicable to this thesis, as with the case of Giroud, the background discussion about the effects of

the overall material matrix was valuable for the evaluation of the findings of my research.

2.2 Findings

The University of Texas and the Florida Institute of Technology have actively been researching the properties of RAP in an attempt to characterize RAP and evaluate its applicability as backfill material. The shear strength tests conducted so far have been consolidated-drained triaxial tests on RAP that has been scalped of the larger particles. The University of Texas made some attempts to test to test the shear strength of RAP with a large direct shear machine, however was unsuccessful and chose not to publish those results (Rathje et al., 2006). Preliminary creep testing that has been performed has concluded that RAP is susceptible to creep.

CHAPTER 3

TESTING PROGRAM AND METHODOLOGY

3.1 Sources of Material

Two different materials were used in the testing program; recycled asphalt pavement (RAP) and a native soil material representative of the type of soil that is typically found in the Phoenix valley.

The RAP material was obtained from a large stockpile located at the Arizona Department of Transportation (ADOT) Salt River office. This stockpile of RAP material consists of milled asphalt pavement that has been removed from various ADOT projects over the past several years. The total volume of RAP in this stockpile is approximately 20,000 cubic yards. For the purposes of this testing program, all of the RAP material used was sampled from one face of the stockpile.

RAP material was sampled on two separate occasions; July 30, 2008 and February 11, 2009. On each occasion the RAP material was sampled from the same face of the stockpile and placed into ten five-gallon buckets. The maximum particle size of the sampled RAP material was approximately 3 inches, however, to facilitate testing and comply with the ASTM D3080 and ASTM D2435 requirements concerning the maximum particle size

relative to equipment dimensions, the sampled RAP was screened to remove particles greater than 1.5 inches in dimension. The samples were then blended to provide a uniform RAP material.

The blending soil used in the testing program was obtained from a stockpile of export material on the ADOT Loop 202 (Red Mountain Freeway) Power Road to University Road project in Mesa, Arizona. The stockpile was located between McKellips Road and Brown Road, just east of the Red Mountain Freeway. This material was stockpiled over a period from early 2008 until mid-July 2008 by Pulice Construction, Inc. The approximate volume of material in this stockpile was about 200,000 cubic yards and consisted of predominantly clayey sand material taken from the upper 2 feet of the subsurface profile in this same area.

Material was sampled from this stockpile also on two separate occasions; September 18, 2008 and February 13, 2009. Material was sampled from random locations throughout the stockpile on each occasion and blended together to provide a uniform material for testing.

Six different blends of the RAP and blending soil materials were investigated in the testing program. The blends consisted of 100 percent 1.5 inch minus RAP material, 100% RAP material

scalped on the ¾ inch sieve, 75% 1.5 inch minus RAP and 25% soil, 50% 1.5 inch minus RAP and 50% soil, 25% 1.5 inch minus RAP and 75% soil and 100 percent soil alone.

3.2 Testing Equipment

The maximum particle size of the blended RAP material made it difficult to evaluate its potential for creep using traditional laboratory equipment. Typical oedometers having a diameter of 3 inches were not practical for testing the RAP with a maximum aggregate size of 1.5 inches. Because the larger particle sizes were mostly milled pieces of asphaltic concrete, it was not desirous to screen the RAP material over a sieve size that would have allowed for the use of traditional oedometers, as it is believed that the behavior of RAP is influenced by the asphalt on the larger particles. Instead, it was decided that the RAP would be tested using the 18-inch diameter direct shear apparatus in the Arizona State University Enamel Hogue Geotechnical Laboratory. This equipment is capable of handling the larger particle sizes and allows for the shear strength of the material to be evaluated in addition to its creep potential.

Evaluations of shear strength by Rathje et al. (2002) and Consentino et al. (2003) were performed using triaxial specimens. It should be noted that there are differences between

the direct shear and triaxial tests. In general it is widely believed that the triaxial method for evaluating shear strength is more accurate (Bardet, 1997). This is because the direct shear test places non-uniform strains on the specimen and forces the failure on a horizontal plane. It is well documented that the peak friction angle obtained from direct shear tests is generally about 2° higher than that obtained using triaxial testing (Bardet, 1997). The advantage for using direct shear testing in this case, however, is the ability to test aggregate particle sizes up to 1.5 inches. Additionally, the direct shear apparatus will allow for compression testing of the RAP and RAP-soil blends in the unsaturated drained condition.

3.2.1 Large scale direct shear apparatus. The large scale direct shear apparatus consists of an 18-inch diameter steel shear box within a steel loading frame. An attached high pressure pump supplied lateral loading and a smaller pump was attached to provide a normal load through hydraulic actuators. A photo of the large scale direct shear frame is included as Figure 3.1.

The shear box is 18-inches in height and is divided into bottom and top portions along a horizontal plane, with the bottom portion of the box measuring six-inches in height and the

top portion of the box measuring 12-inches in height. The top and bottom of the shear box can be fitted together (aligned) during sample preparation with four ½-inch diameter bolts. The bottom plate of the shear box is grooved to facilitate drainage of the specimen.

Figure 3.1. Large scale direct shear apparatus

The bottom 2 inches of the shear box were filled with an incompressible gravel material and then capped with a steel plate. This was done in order to accommodate the desired specimen height of 8 inches. By eliminating the bottom 2 inches of the shear box, the shear plane would be closer to the middle of the 8 inch tall compacted specimen.

3.3 Data Acquisition

Four variables were measured and recorded during testing; the normal load, the axial displacement, the lateral load, and the lateral displacement. The axial and lateral displacements were measured using two separate low-voltage digital linear variable displacement transducers (LVDT), each mounted to the loading frame. Lateral and normal loads were measured using pressure transducers that were mounted in line with the hydraulic system. All of the transducers were connected to a digital signal conditioning and control unit which was controlled by computer, as displayed in Figure 3.2. Data readings were taken at 80 second intervals during the compression phases of testing and at 0.1 second intervals during the shear phase.

3.4 Specimen Fabrication

The procedure used to fabricate specimens for large scale creep and direct shear tests are presented in this section. While it would have been desirable to use an American Society for Testing and Materials (ASTM) test method for the direct shear and compression tests, no ASTM test method is available for the large scale direct shear tests. For this reason, the following procedure was developed to fabricate specimens that were relatively consistent between tests. The general intent of this

procedure was to follow the appropriate ASTM standard as closely as possible, deviating only as necessary to accommodate the equipment being used.

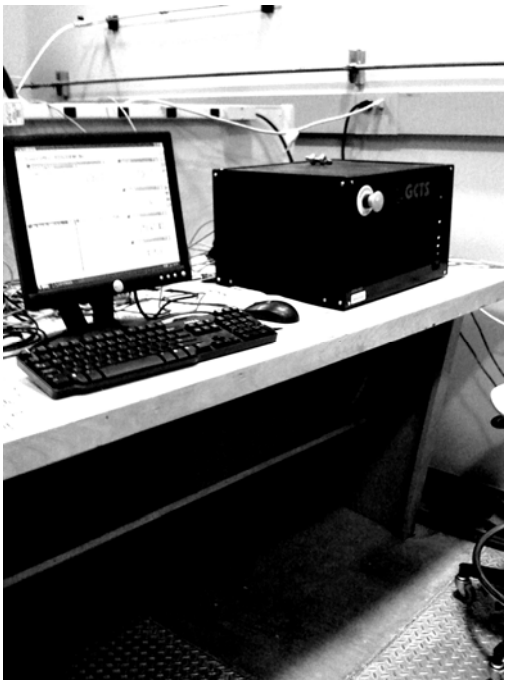

Figure 3.2. Computer and digital signal conditioning and control device used during testing.

3.4.1 Large scale specimens. The target dimension of the specimens used in the 18 inch diameter direct shear apparatus was 8 inches in height, having a total volume of 1.18 cubic feet. Each specimen was compacted to a density of approximately 91 percent of the maximum dry density as determined using ASTM D698 Method C. The material used for the ASTM D698 Method C test method is screened over a ¾ inch

sieve, therefore to correct the maximum density and optimum moisture for the oversize particles, ASTM D4718 was used. The target moisture content for each specimen was 2 percent below optimum moisture. The density and moisture conditions were chosen to simulate field conditions. The specimens were fabricated directly in the large shear box, using the following process.

3.4.1.1 Preparing the blended material. A specific blend of RAP material and soil was targeted for each specimen. Material for all specimens was proportioned by weight. The blend percentages for each specimen are outlined in the fabrication schedule presented in Table 3.1.

Using the appropriate compaction characteristics for the desired blend (as determined per ASTM D698), the required weight of the specimen was calculated. Appropriate weights of dry RAP and dry soil were blended together to achieve the correct blend percentage. This material was then thoroughly mixed to produce a uniform matrix of RAP and soil. Water was added to the mixture to bring it to the desired moisture content. The mixture was then again thoroughly mixed to provide a consistent material.

3.4.1.2 Loading and compacting the specimen. Prior to loading the specimen into the direct shear device, the top section of the shear box was carefully lowered onto and aligned with the bottom section to create a smooth-wall cylinder within which to compact the specimen. The two shear box sections were bolted together at each corner to prevent the box from moving during compaction. The RAP-soil blend was introduced into the shear box in three approximately equal lifts. Three lifts was chosen to avoid having a lift boundary at the same location as the horizontal shear plane and thus potentially introduce an artificial weak shear plane at the shear plane location. The target compacted lift thickness was 2.67 inches; however, the compaction process was difficult and often resulted in lifts that were thicker than the target value after compaction.

Each lift was compacted using the 30-pound slide hammer as depicted in Figure 3.3. However, a slide rod was not used during compaction; instead a rope handle was fastened to the hammer to facilitate lifting and dropping the hammer onto the sample. The hammer was dropped approximately 20 to 30 times of times on each lift as necessary to achieve a final compacted lift thickness as close to 2.67 inches as possible

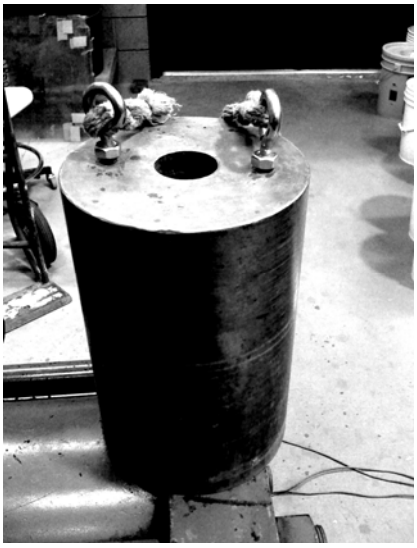

Figure 3.3. 30-pound hammer used for compaction

Each lift was compacted using the 30-pound slide hammer as depicted in Figure 3.3. However, a slide rod was not used during compaction; instead a rope handle was fastened to the hammer to facilitate lifting and dropping the hammer onto the sample. The hammer was dropped approximately 20 to 30 times of times on each lift as necessary to achieve a final compacted lift thickness as close to 2.67 inches as possible.

The final height of the first compacted specimen measured 7.65 inches below the top of the shear box, indicating a specimen height of 8.35 inches. The percent compaction of the specimen based on this final achieved height is 91% of the maximum dry density per ASTM D698. Although slightly lower than the target density desired (95 percent) for testing, it

proved more difficult than beneficial to further compact the specimen and it was determined that 91% relative compaction would be sufficient for this testing program. The inside of the shear box was marked at the top of the specimen and all further specimens were compacted to achieve this same height. This process provided a level of uniformity between test specimens, as they all were thereby compacted to the same density.

3.4.1.3 Placement of top caps. After compaction of the final lift, a steel plate and a hand level were used to assist in leveling the top of the specimen as much as possible. The top surface was checked at 6 points to insure a level surface for axial loading. Following leveling, two top caps were placed on top of the specimen. Each top cap measured 5 inches in height and weighed approximately 230 pounds. The two caps were necessary to raise the loading surface 2 inches above the top of the shear box. Additionally, a 2 inch thick steel spacer plate was placed onto the top cap to further raise the loading surface and to provide a surface suitable for seating of the compression pistons used to apply the normal load.

The combined weight of the two top caps and the steel spacer plate was approximately 573 pounds, providing an initial overburden pressure of 325 pounds per square foot (psf) to the

specimen. This initial overburden pressure was considered as the seating pressure for the specimen, and was thereafter factored into the total normal pressure placed onto the specimen.

3.4.2 Traditional specimens. In addition to the large scale specimens, two specimens were also prepared for compressibility testing using a traditional dead-weight consolidation frame. The first specimen consisted entirely of soil and the second specimen entirely of RAP material; no blends were tested with the traditional dead-weight consolidation frame. The procedure for preparing these specimens was in strict accordance with ASTM D2435, the standard test method for one-dimensional consolidation properties of soils. The only deviation from this test method was with respect to the maximum particle size. In these tests, material passing a 3/8 inch sieve was remolded into a 2.41 inch inside diameter ring. A picture of the traditional dead-weight consolidation frame used for testing is presented in Figure 3.4.

3.5 Fabrication and Testing Schedule

Each large diameter specimen took approximately 4 to 6 hours to prepare prior to the start of the compression testing. It was common to fabricate the specimens early in the morning so that the first load increment was applied by 8:00 am, and

subsequent load increments were applied after 24 hours. There were two shear boxes available, however, because of the difficulty in preparing a specimen outside of the direct shear frame and then having to move the box into the frame, only one specimen was prepared at a time. The schedule for the large diameter compression and shear testing is presented in Table 3.1.

Figure 3.4. Traditional dead-load consolidation frame

Table 3.1

Schedule of Specimen Fabrication

Test No.	Specimen Description	σ_n at Shear	Fabrication Date	Shear Date
1	100% RAP	1000 psf	08/14/08	08/15/08
2	100% RAP	2000 psf	08/26/08	08/28/08
3	100% RAP	4000 psf	08/29/08	09/01/08
4	100% RAP	4000 psf	09/02/08	09/05/08
5	100% RAP (Scalped)	2000 psf	09/05/08	09/09/08
6	100% RAP	2000 psf	09/12/08	09/16/08
7	75% RAP Blend	2000 psf	09/26/08	09/29/08
8	50% RAP Blend	2000 psf	10/02/08	10/03/08
9	25% RAP Blend	2000 psf	10/09/08	10/10/08
10	100% Soil	2000 psf	10/10/08	10/13/08
11	75% RAP Blend	2000 psf	02/16/09	02/18/09
12	75% RAP Blend	2000 psf	02/20/09	02/22/09
13	50% RAP Blend	2000 psf	02/23/09	02/25/09
14	100% Soil (Traditional Scale)	N/A	03/01/11	N/A
15	100% RAP (Traditional Scale)	N/A	03/05/11	N/A

CHAPTER 4

MATERIAL PROPERTIES

4.1 Recycled Asphalt Product

Although RAP itself is not a processed material, its primary constituent component, asphaltic concrete, is a heavily controlled processed material. As a result, it is expected that the material properties of RAP, with the exception of particle size, will generally be consistent regardless of the source of the asphaltic concrete. The particle size of the RAP, largely a function of the milling operation, can however vary widely from a very coarse granular material to a relatively fine granular material.

The RAP material used for this research was obtained from a large stockpile. The stockpile itself varied greatly from location to location. Samples were taken from a cut face on one side of the stockpile and then combined and split to provide some uniformity with the RAP material used in each specimen. The grain size curve for the homogenized RAP material, presented in Figure 4.1, indicates that the RAP material is fairly well graded (Cu=20, Cc=0.9). However the actual USCS classification of the RAP material as determined by ASTM D2485 is GP, poorly graded gravel with sand, due to the low value for the coefficient

of curvature, Cc. There are very few fines in the material and RAP exhibits no plasticity.

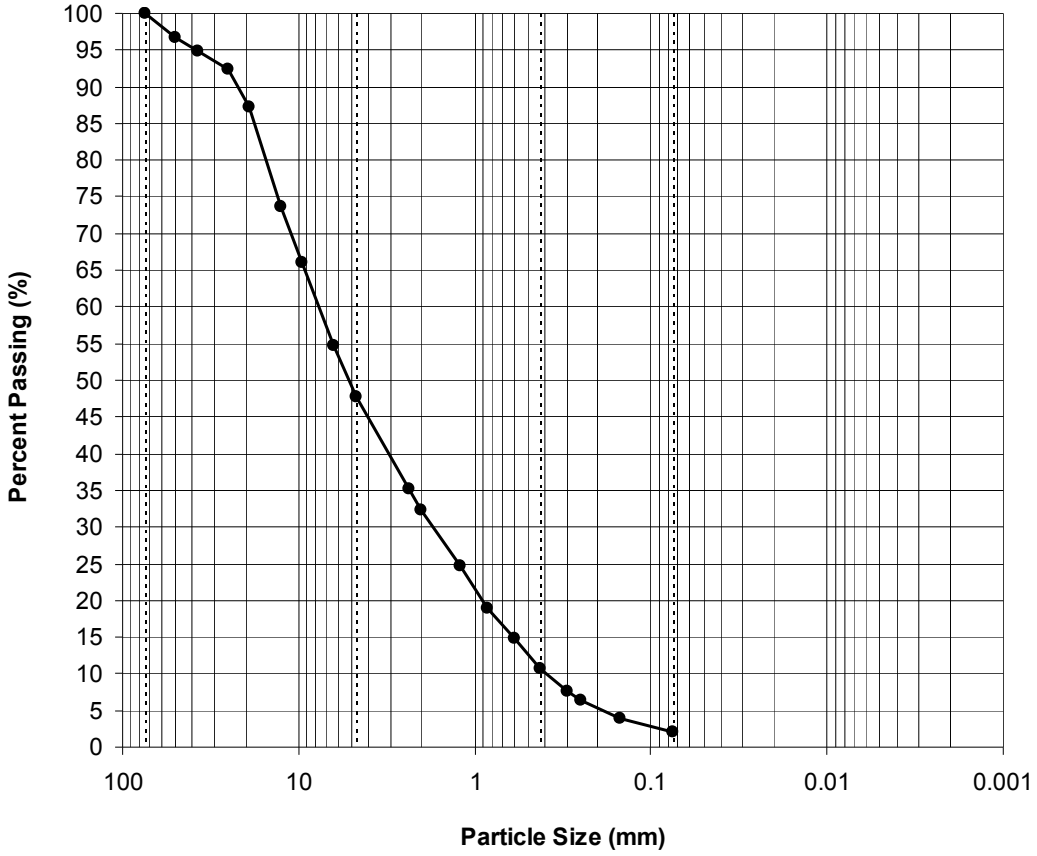

Figure 4.1. Grain size distribution of RAP material

The compaction characteristics of the 100 percent RAP material was determined using standard proctor compactive effort, in accordance with ASTM D-698 Method C. The maximum density, as shown in Figure 4.2, was determined to be 121.2 pounds per cubic feet and the corresponding optimum moisture was 7.8 percent. These values are typical for granular materials in the Phoenix area, and suggest that the 100 percent RAP

material has a specific gravity of approximately 2.40 based upon the location of the "wet" side of the compaction curve compared to the zero air voids curve for Gs = 2.40. This is consistent with the specific gravity typically obtained for asphaltic concrete materials.

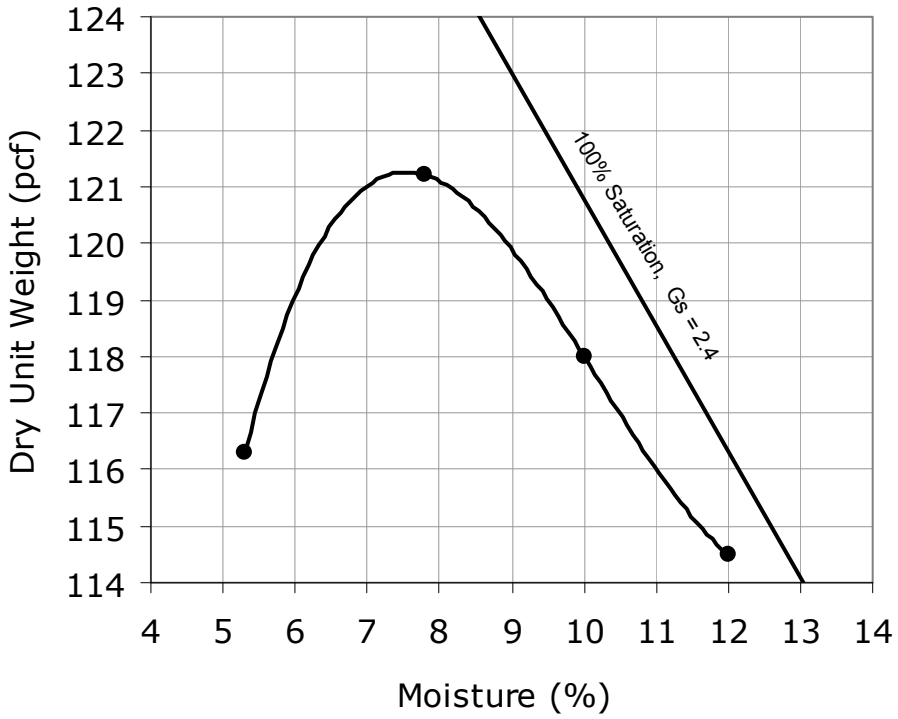

Figure 4.2. Compaction characteristics of the RAP material

4.2 Blend Soil

It is anticipated that blend soil used with RAP material in practice would be highly variable and dependent on site conditions for a particular construction project. The blend soil used for this testing program was chosen to represent fill

material that is typically encountered on construction projects in Maricopa County, Arizona. The grain size distribution of the blend soil, presented in Figure 4.3, again indicates that the material is fairly well graded (Cu=184, Cc=1.64), however the USCS classification is SM to SC, silty to clayey sand. The blend soil exhibited moderate plasticity, with a liquid limit of 24 and a plasticity index of 7, resulting in a classification of ML-CL fror the fines.

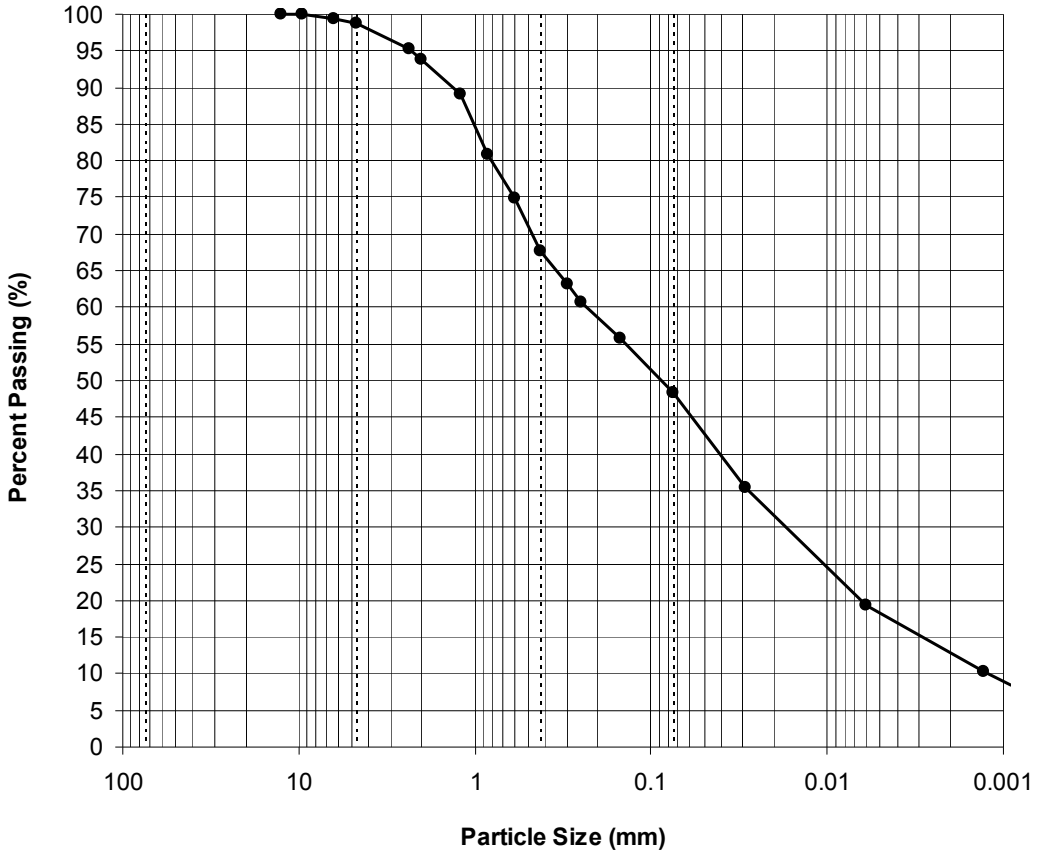

Figure 4.3. Grain size curve of the blending soil used during the testing program

The compaction characteristics of the blend soil, as determined using ASTM D-698, Method A, are presented in Figure 4.4. The zero air voids curve presented in Figure 4.4 suggests a specific gravity of around 2.55 to 2.60. A specific gravity test was not performed.

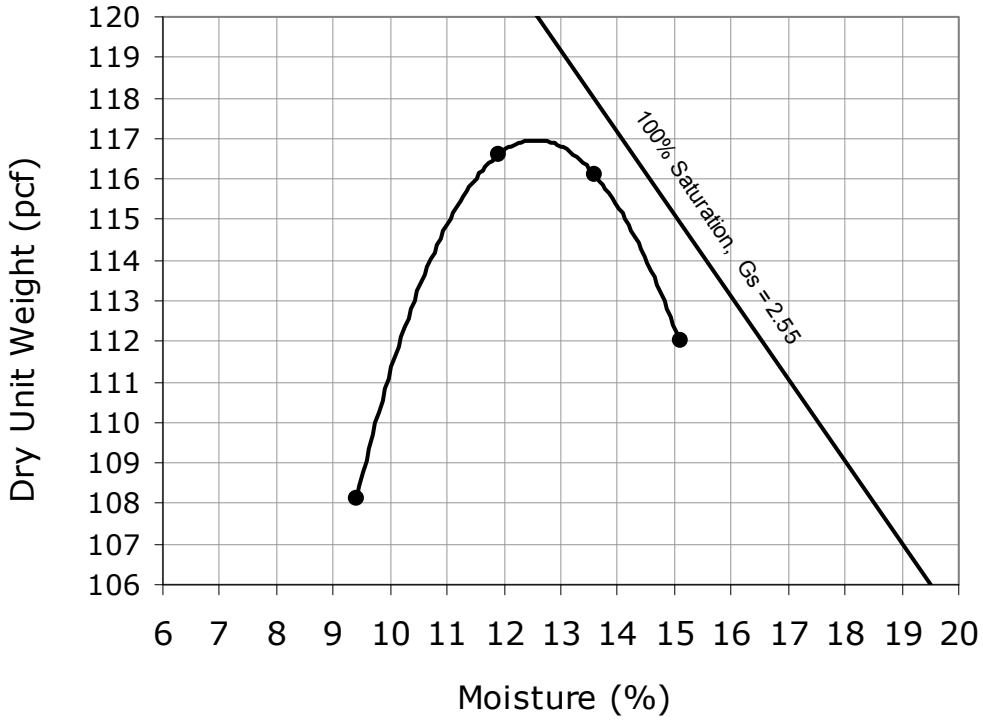

Figure 4.4. Compaction curve for the blend soil used

4.3 RAP Blends

Three different mixtures of RAP and soil were blended in the laboratory for testing purposes. RAP and soil were blended to create materials with RAP contents of 75, 50 and 25 percent by weight. Grain size analyses for each blend were not performed;

however the calculated composite gradations for each blend, as well as the RAP material and blend soil, are presented in Table 4.1. The Atterberg limits for each blend were determined. The blend with only 25 percent RAP material still maintained some plasticity, but the blends with higher RAP percentages were all found to be non-plastic.

Table 4.1

Material Properties of RAP and RAP Blends

	RAP Content				
Particle Size	100%	75%	50%	25%	0%
1 1/2" (37.5mm)	95	96	97	99	
1" (25mm)	92	94	96	98	
3/4" (19mm)	87	90	94	97	
1/2" (12.5mm)	74	80	87	93	
3/8" (9.5mm)	66	74	83	91	100
#4 (4.75mm)	48	61	73	86	99
#8 (2.36mm)	35	50	65	80	95
#10 (1.9mm)	32	48	63	79	94
#16 (1.2mm)	25	41	57	73	89
#30 (0.6mm)	15	30	45	60	75
#40 (0.425mm)	11	25	39	53	68
#50 (0.3mm)	8	21	35	49	63
#100 (0.15mm)	4	17	30	43	56
#200 (0.075mm)	2	14	25	37	48
D_{60}	7.76	4.63	1.55	0.60	0.224
D_{30}	1.68	0.60	0.15	0.05	0.021
D_{10}	0.39	0.04	0.011	0.004	0.001
Cu	20	106	142	140	184
Cc	0.93	1.81	1.38	0.98	1.64
Liquid Limit				15	24
Plasticity Index	NP	NP	NP	3	7
Maximum Density (pcf)	121.3	128.8	123.7	117.8	117.0

The compaction characteristics for each blend were determined in the same manner as the RAP and soil materials individually, using ASTM D698, Method C. The compaction curves for the RAP-soil blends are presented in Figures 4.5, 4.6 and 4.7. It is interesting to note that the maximum density of the 75 percent RAP blend, approximately 128.7 pcf, is considerably higher than either the RAP material (approximately 121.2 pcf) or the blend soil material (approximately 117.0 pcf) alone.

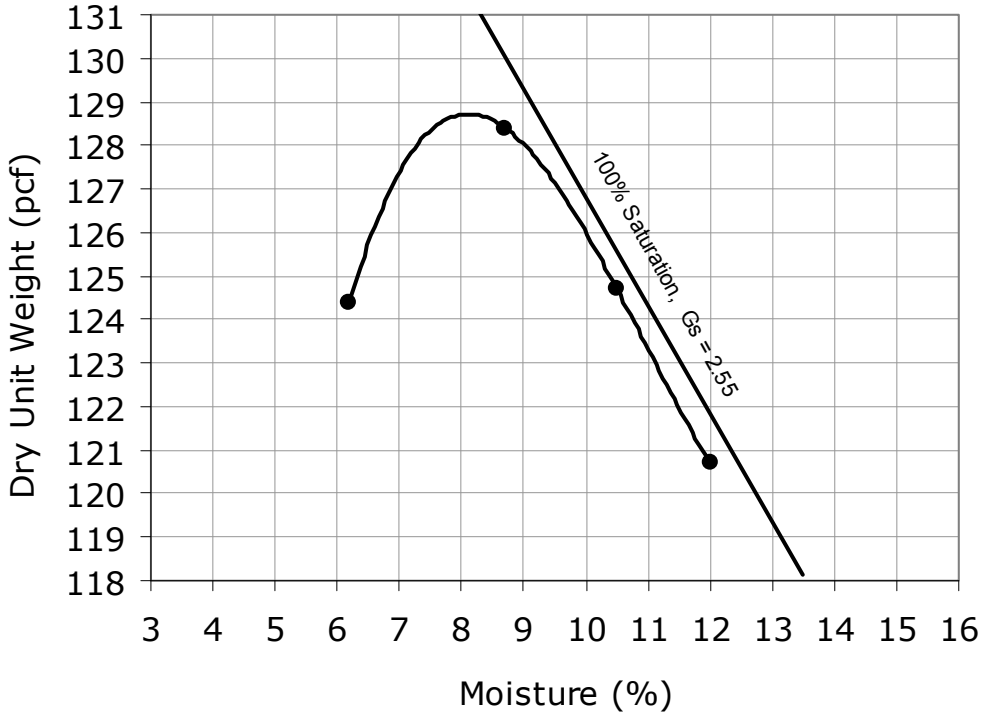

Figure 4.5. Compaction curve for the 75% RAP blend

The unit weight of the 50 percent RAP blend is also somewhat higher than either constituent component. It is my opinion that a

small amount of blend soil provides finer materials that fill the void spaces between the larger RAP particles and results in a more dense overall soil fabric. As the amount of blend soil increases, this effect is diminished, until the blend soil fabric overcomes the RAP material at percentages greater than around 50 percent.

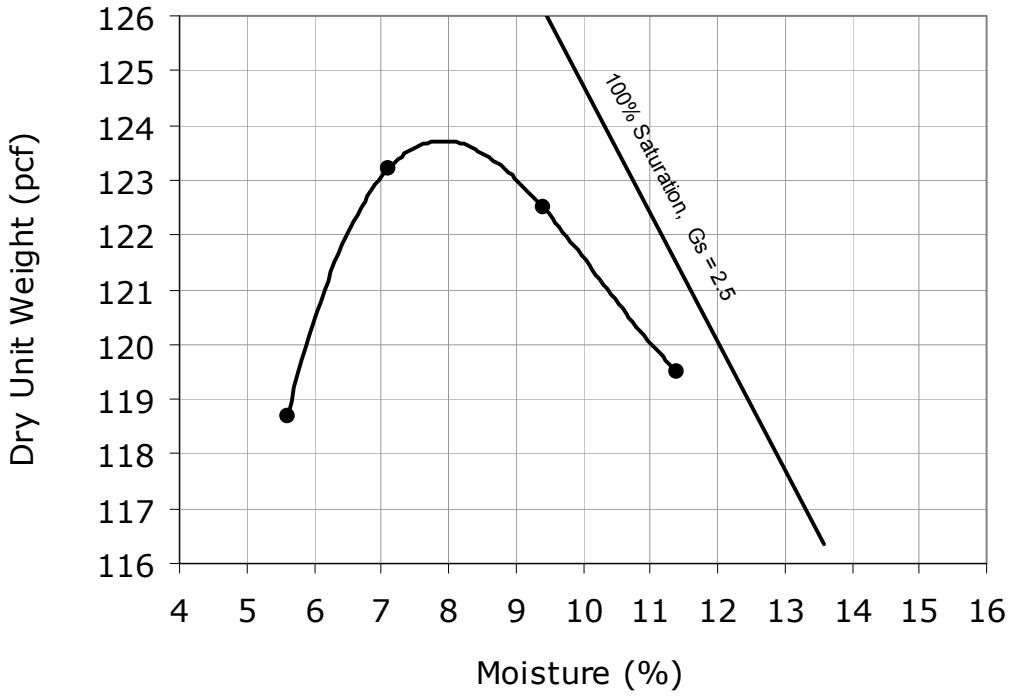

Figure 4.6. Compaction curve for the 50% RAP blend

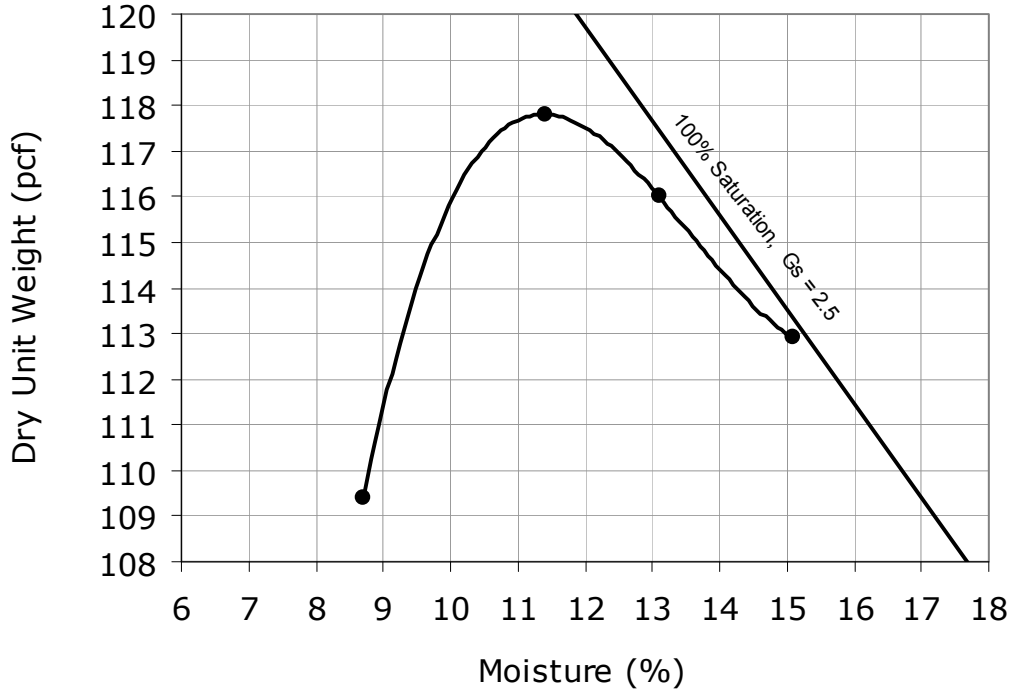

Figure 4.7. Compaction curve for the 25% RAP blend

CHAPTER 5

COMPRESSIBILITY OF RAP AND RAP SOIL BLENDS

The compressibility of the RAP material, the soil material, and each blend was tested using the large scale direct shear apparatus. All specimens were tested in the unsaturated drained condition. Load increments of normal pressure for each specimen were chosen in conjunction with the schedule for shear testing. The summary of these results are presented in Table 5.1. Test data sheets for all specimens can be found in Appendix B.

5.1 Determining Primary and Secondary Compressibility

Due to the tendency of RAP to creep, a consistent method had to be developed to determine the end of primary compression and the initiation of secondary compression for each load increment. Fur consistency, the point of 100 percent primary consolidation for each load increment was estimated using the time-deformation curve from square root of time method. This method was chosen because the square root of time method provided a more noticeable straight line trend over the initial readings than the log of time method. As illustrated in Figure 5.1, the deformation of the specimen was plotted on the abscissa against the square root of time plotted on the ordinate.

Table 5.1

$C_{c\varepsilon}$ and $C_{\alpha\varepsilon}$ for RAP and RAP blends

Specimen No.	% RAP	σ_n (psf)	$C_{\alpha\varepsilon}$	$C_{c\varepsilon}$	$C_{\alpha\varepsilon}/C_{c\varepsilon}$
1	100%	1000	0.004	-	-
2	100%	1500	0.001	0.062	0.012
		3250	0.002	0.062	0.036
3	100%	1180	0.037	0.432	0.087
		2000	0.028	0.432	0.064
		4000	0.038	0.432	0.087
4	100%	1000	0.025	0.320	0.079
		2000	0.022	0.320	0.070
		4000	0.030	0.320	0.094
5 (scalped)	100%	1000	0.021	0.251	0.085
		2000	0.021	0.251	0.084
6	100%	1000	0.020	0.299	0.067
		2000	0.024	0.299	0.081
7	75%	1000	0.021	0.233	0.089
		2000	0.017	0.233	0.074
8	50%	2000	0.009	-	-
9	25%	2000	0.023	-	-
10	0%	2000	0.008	-	-

A line was drawn through the initial readings exhibiting a straight line trend and the slope of that line was determined. A second line was then drawn extending from the point where the straight line portion of the plot crossed the vertical axis (i.e., time equal to zero) and at a slope equal to 1.15 times the slope of the initial

straight line. The intersection of this second line with the compression curve represents the point of 90 percent primary compression. The deformation at this point, designated as d_{90}, represents 90 percent of the primary compression. An additional 10 percent was added to d_{90} to determine the amount of deformation at 100 percent primary compression, d_{100}. The time required to reach d_{100}, designated as t_{100} was then determined from the plot. The secondary compressibility index, $C_{\alpha\varepsilon}$, was then obtained from the time-deformation curve from log of time method. The slope of a straight line between the deformation at t_{100} and the final deformation measurement was considered to represent $C_{\alpha\varepsilon}$.

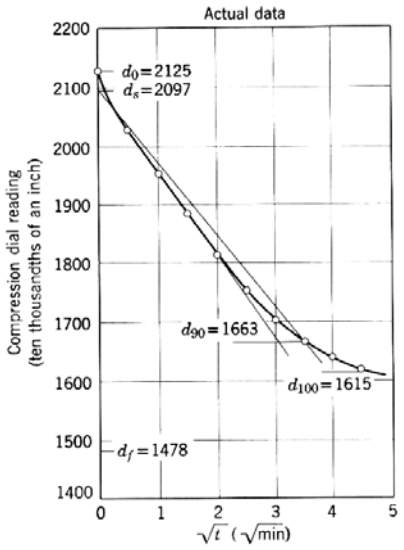

Figure 5.1. Determination of d_{100} using the square root of time method (Lambe and Whitman, 1967).

The primary compressibility index, $C_{c\varepsilon}$, was obtained from the primary compression values for the specimens tested at multiple normal pressures. From a chart of the percent of strain plotted along the abscissa versus the normal pressure plotted on a log scale along the ordinate, $C_{c\varepsilon}$ was calculated as the slope of the line formed by the points. In all cases, the points obtained between 1,000 psf and 4,000 psf of overburden pressure formed a relatively straight line. Since it is highly unlikely that the RAP material has ever experienced 4,000 psf of overburden pressure, it is reasonable to assume that this line represents the virgin compression line.

5.2 Compressibility of RAP

Specimen 1, composed of 100 percent RAP only was tested at a single normal pressure of 1,000 psf. This first specimen experienced several problems during the compression phase. These issues were related to maintaining the pump pressure during the test. It was learned during this early test that the pump has a difficult time maintaining pressures for an extended period of time, particularly at low pressures. This problem was not until late into the test and likely resulted in a lower than expected secondary compressibility index, $C_{\alpha\varepsilon}$, due to the pump fluctuations.

Specimen 2 was the first specimen tested at more than one overburden pressure. As with specimen number 1, problems with the pump resulted in difficulty achieving the desired normal pressures of 1000 psf and 2000 psf. As a result, the normal pressures ended up being 1500 psf and 3250 psf. Furthermore, the pump pressure was not constant throughout the test and likely resulted in lower than expected primary and secondary compressibility.

Following the first two trial specimens, the operation of the pump was significantly improved and proved to be much more reliable for the remainder of the specimens tested. Specimens 3 and 4 were both tested at normal pressures of 1,000 psf, 2,000 psf and 4,000 psf. Specimen 6 was tested at normal pressures of 1,000 psf and 2,000 psf. Reasonably consistent primary and secondary compressibility results were obtained from these three specimens. Specimen 5 was also tested at overburden pressures of 1,000 psf and 2,000 psf, but the specimen was prepared using RAP material that was scalped on the ¾-in. (19.0 mm) sieve, so the results are not directly comparable to the results for the other tests.

Based on the results of specimens 3, 4 and 6, the primary compressibility index for the 1.5 inch minus RAP material is

between 0.30 and 0.43, as presented in Figure 5.2. The secondary compressibility index was observed to be in the range of 0.02 to 0.038. The ratio of $C_{\alpha\varepsilon}/C_{c\varepsilon}$ is commonly reported as a material property that remains reasonably constant over the range of normal stresses encountered in practice (Holtz and Kovacs, 1981). For RAP material, my research demonstrates that $C_{\alpha\varepsilon}/C_{c\varepsilon}$ is approximately 0.08, which indicates that RAP material does indeed have high secondary compressibility, as this value is within the range reported for organic soils and peats (Mesri and Godlewski, 1977).

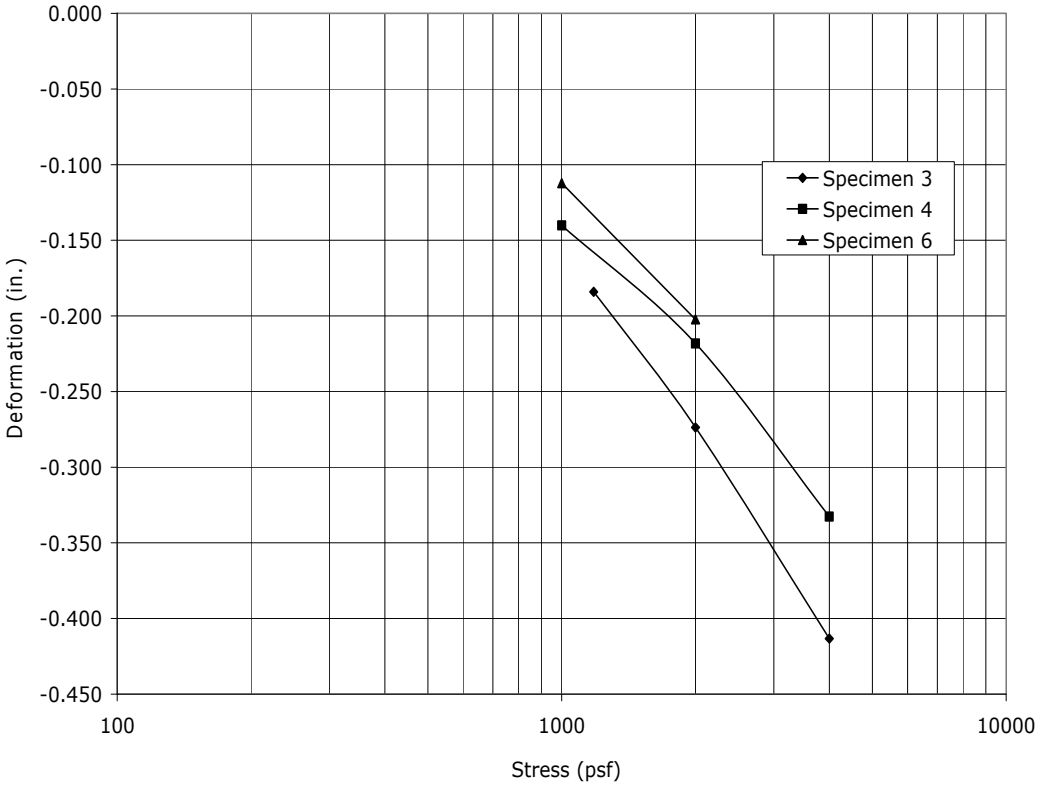

Figure 5.2. Primary compression curves for 1.5 inch minus RAP

In addition to the large scale compression testing, a single test was performed on scalped RAP material using a traditional oedometer. The specimen was fabricated in a 2.41-inch inside diameter ring and at a unit weight and moisture content similar to that of the corresponding large scale specimens. The RAP material used for this test was screened over a 3/8 inch sieve prior to testing to accommodate the smaller ring. The results of the traditional compression test are presented in Table 5.2. $C_{c\varepsilon}$ was found to be 0.011. $C_{\alpha\varepsilon}$ was found to be 0.006 at a normal stress of 1,000 psf and 0.001 for normal stresses of 2,000 and 4,000 psf. The ratio of $C_{\alpha\varepsilon}/C_{c\varepsilon}$ was calculated as 0.054 at a normal stress of 1,000 psf and 0.091 at normal stresses of 2,000 and 4,000 psf.

Table 5.2

$C_{c\varepsilon}$ and $C_{\alpha\varepsilon}$ for RAP tested in a 2.41 inch diameter oedometer

Specimen No.	% RAP	σ_n (psf)	$C_{\alpha\varepsilon}$	C_c	$C_{\alpha\varepsilon}/C_c$
14	100%	1000	0.0006	0.011	0.054
		2000	0.0010	0.011	0.091
		4000	0.0010	0.011	0.091

5.3 Secondary Compressibility Index of RAP Blends

Beginning with specimen 7, the RAP material was blended with a various percentages of soil and then tested for

compressibility. Specimen 7 consisted of 75 percent 1.5 inch minus RAP and 25 percent soil. Specimen 8 consisted of equal amounts of 1.5 inch minus RAP material and soil. Specimen 9 contained 25 percent 1.5 inch minus RAP and 75 percent soil.

Beginning with specimen 8, problems with maintaining a constant pump pressure at low pressures during testing prevented obtaining compression data at the 1,000 psf overburden pressure. Specimens 8 and 9 were only tested at 2,000 psf and therefore $C_{c\varepsilon}$ data for these two blends is unavailable.

The 75 percent RAP blend still exhibited considerable secondary compression, but for the 50 percent RAP blend, the secondary compressibility dropped off significantly. This was not the case, however, for specimen 9 (25 percent RAP), which exhibited an unusually high amount of primary compression. It is believed that the large primary compression resulted in t_{100} occurring earlier than it should have and ultimately resulted in larger than normal secondary compression.

5.4 Compressibility of the Blend Soil

For reference, the compressibility of the blend soil alone was also tested. The blend soil was tested both using the large scale apparatus as well as using a traditional oedometer. The

large scale test of the blend soil was performed only at 2,000 psf and, as a result, $C_{c\varepsilon}$ data is not available. Using the traditional oedometer, $C_{\alpha\varepsilon}$ and $C_{c\varepsilon}$ were both obtained. The results of the large scale test can be found in Table 5.1, while the traditional test results are presented in Table 5.3.

Table 5.3

$C_{c\varepsilon}$ and $C_{\alpha\varepsilon}$ for the blend soil tested in a 2.41 inch diameter oedometer

Specimen No.	% RAP	σ_n (psf)	$C_{\alpha\varepsilon}$	C_c	$C_{\alpha\varepsilon}/C_c$
15	0%	1000	0.0006	0.011	0.057
		2000	0.0006	0.011	0.057
		4000	0.0002	0.011	0.018

The large scale test indicates that the secondary compressibility index of the blending soil is about 3 to 4 times lower than that of the RAP material. This result further supports the observation that RAP material exhibits high secondary compressibility.

5.5 Discussion

The ratio of $C_{\alpha\varepsilon}/C_{c\varepsilon}$ for the 100 percent RAP indicates that RAP does exhibit high secondary compression. While the research of others such as Rathje et al. (2006) and Consentino et al. (2003) did not use the ratio of $C_{\alpha\varepsilon}/C_{c\varepsilon}$ to evaluate

secondary compressibility, we all agree that the potential for creep with RAP is high. Incorporating blending soil with the RAP material had a significant impact on the secondary compressibility at a blend of 50 percent RAP with 50 percent soil. The test data shows that the secondary compressibility of the RAP-soil blend at the 50 percent blend is approximately the same as the soil alone. Consentino et al. (2003) had similar findings with a 20 percent blend of RAP and soil. While there is disagreement between my test results and the results of Consentino as to the blend percentage where the creep associated with the RAP material is mitigated, we both agree that blending soil with RAP material has the potential to significantly reduce the large deformations associated with secondary compressibility.

The values for both the primary and secondary compressibility indexes obtained with the traditional oedometer for 100 percent RAP are considerably lower than those obtained using the large scale test. While the wide discrepancy between the large scale tests and the traditional scale test raises questions as to the validity of the large scale testing, it seems more likely that it indicates the inadequacy of using scalped material to test RAP compressibility. Even though the absolute

values of $C_{\alpha\varepsilon}$, and $C_{c\varepsilon}$ were different, the ratios of $C_{\alpha\varepsilon}/C_{c\varepsilon}$ are relatively similar and still suggest that the RAP material has high secondary compressibility.

The ratio of $C_{\alpha\varepsilon}/C_{c\varepsilon}$ using the traditional oedometer is within the range for inorganic soils, 0.025 to 0.060, as suggested by Mesri and Godlewski (1977). Since $C_{c\varepsilon}$ was not obtained for the blending soil using the large direct shear apparatus, there is no correlation with the traditional oedometer for $C_{c\varepsilon}$ or the ratio of $C_{\alpha\varepsilon}/C_{c\varepsilon}$. For the value of $C_{\alpha\varepsilon}$, as with the RAP material, there is not a good correlation between the large scale test and the traditional scale test for the blending soil alone. Again, this may suggest a problem with the large scale equipment.

CHAPTER 6

SHEAR STRENGTH OF RAP AND RAP SOIL BLENDS

The shear strength for thirteen large scale test specimens was evaluated using the direct shear method under consolidated-drained condition. The direct shear test method is an appropriate method for determining the shear strength of the granular RAP material and blended soils, as these materials will likely be free draining and should completely consolidate under relatively rapidly under applied normal stresses.

At the conclusion of secondary compression and at the desired normal stress for each specimen, the upper portion of the shear box was lifted approximately ½ inch to facilitate shearing the specimen without excessive frictional resistance between the top and bottom of the shear box. The normal load and the height of the specimen were closely monitored and maintained as much as possible while lifting the top portion of the shear box. For specimens 1 and 2, the top portion of the shear box was only lifted approximately ¼ inch. However in both cases the gap between the top portion and the bottom portion closed during shearing. For this reason it was chosen to go with a ½ inch gap for all subsequent tests.

All specimens were sheared at a constant rate of lateral displacement of 0.2 inches per minute; approximately 1.1 percent of the 18 inch diameter specimens per minute. Measurements were taken until lateral displacements reached 20 percent of the specimen diameter, or 3.6 inches. The shear strength data for the 100 percent RAP material, RAP-soil blends and the soil alone are summarized in Table 6.1.

Table 6.1

Shear Strength of RAP and RAP Blends.

% RAP	Specimen #	σ_n (psf)	Φ_{sec}
100%	3	4000	61.5
	4	4000	60.0
	6	2000	61.2
100% (Scalped)	5	2000	62.2
75%	7	2000	71.4
	11	2000	74.1
	12	2000	73.0
50%	8	2000	65.7
	13	2000	63.9
25%	9	2000	64.9
0%	10	2000	52.3

6.1 Shear Strength of RAP

The first four specimens consisted entirely of 1-1/2 inch minus RAP material and were sheared at 1,000 psf, 3,250 psf, and 4,000 psf normal stresses. Duplicate tests were conducted at the 4,000 psf normal stress. Specimen 6 also consisted entirely of 1-1/2 inch minus RAP material and was sheared under a normal stress of 2,000 psf. Together the direct shear results for the five 100 percent RAP specimens are plotted on the Mohr-Coulomb diagram in Figure 6.1. Based upon the data shown in Figure 6.1, the shear strength envelope for the 100 percent RAP compacted to 91 percent relative compaction per ASTM D698 Method C was determined, as represented by a friction angle, Φ, of 42.4° and a cohesion, c, of 3500 psf.

The results of these five direct shear tests contain some inconsistencies that should be noted. The cohesion of 3,500 psf appears to be significantly higher than normally expected for a granular material. While it is anticipated that the asphalt cement contained in the material will provide some level of true cohesion, it is unlikely that the true cohesion is as high as these results indicate.

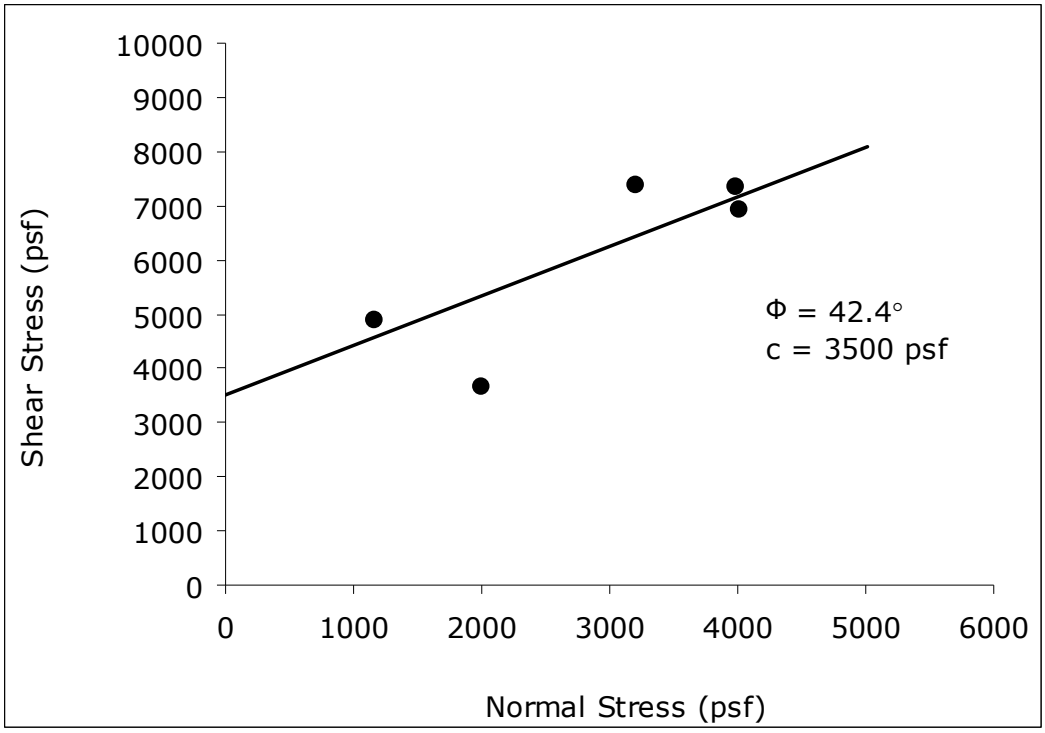

Figure 6.1. Φ and c for RAP material

In addition to the questionably high cohesion, the shear strength of the first two specimens, tested at 1,000 psf and 3,250 psf normal stresses respectively, seem to have resulted in shear strengths that are significantly higher than expected when presented with the rest of the data. This is likely the result of the top section of the shear box coming into contact with the bottom section during the shearing operation, which would undoubtedly result in higher shear strengths. This problem was corrected with subsequent specimens by increasing the gap between the top and bottom sections to ½-inch.

Figure 6.2 presents two alternative shear strength envelopes for the 100 percent RAP material after removing the problematic data for the first two tests. For the first interpretation, the secant friction angle, Φ_{sec}, was used. The secant friction angle assumes that the material is cohesionless. While this may not be strictly correct, the secant friction angle provides a good basis for comparison of the shear strength between specimens tested at a similar normal stress using different percentages of RAP. Using this method, Φ_{sec} for the RAP material is 60.8°. A second shear strength envelope was developed after discarding the problematic data by assuming cohesion equal to 1,150 psf, the value found by Rathje et al (2006). This second method of interpretation yielded a friction angle of 55.7° to go with the cohesion of 1,150 psf.

To evaluate the sensitivity of the tests results to particle size, it was decided to also evaluate the shear strength of 100 percent RAP material that was scalped over a ¾ inch sieve. The shear strength of the RAP material scalped over a ¾" sieve was tested under a single normal stress of 2,000 psf with Specimen 5. The resulting secant friction angle, as presented in Figure 6.3, is 62.2°. The secant friction angle for the scalped material is

slightly higher than but consistent with the shear strength of the 1.5 inch minus RAP specimens.

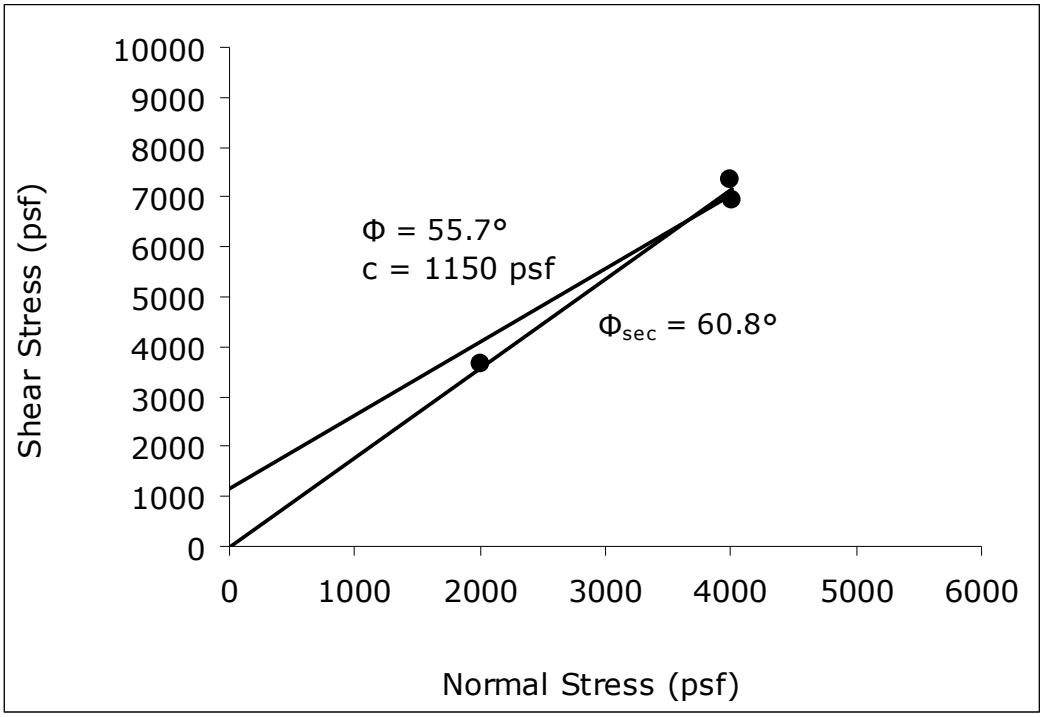

Figure 6.2. Φ_{sec} for RAP material

6.2 Shear Strength of RAP Blends

Six specimens, representing the three separate RAP blends, were tested for shear strength. Each of the RAP blend specimens were tested at a normal stress of 2,000 psf. Three tests were conducted on specimens with 75 percent RAP, two tests were conducted on the 50 percent RAP-soil blend, and one test was conducted at the 25% RAP-soil blend. The shear strength envelopes for the 75, 50 and 25 percent blends are presented in Figures 6.4, 6.5 and 6.6 respectively.

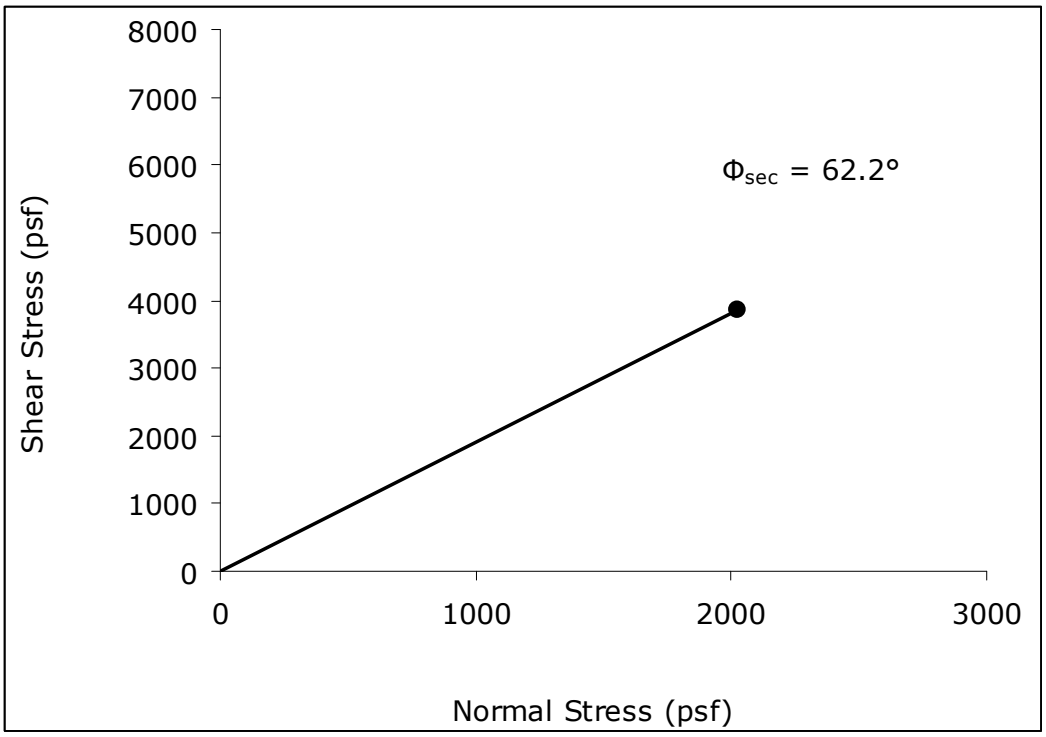

Figure 6.3. Φ_{sec} for RAP material scalped over a ¾-inch sieve

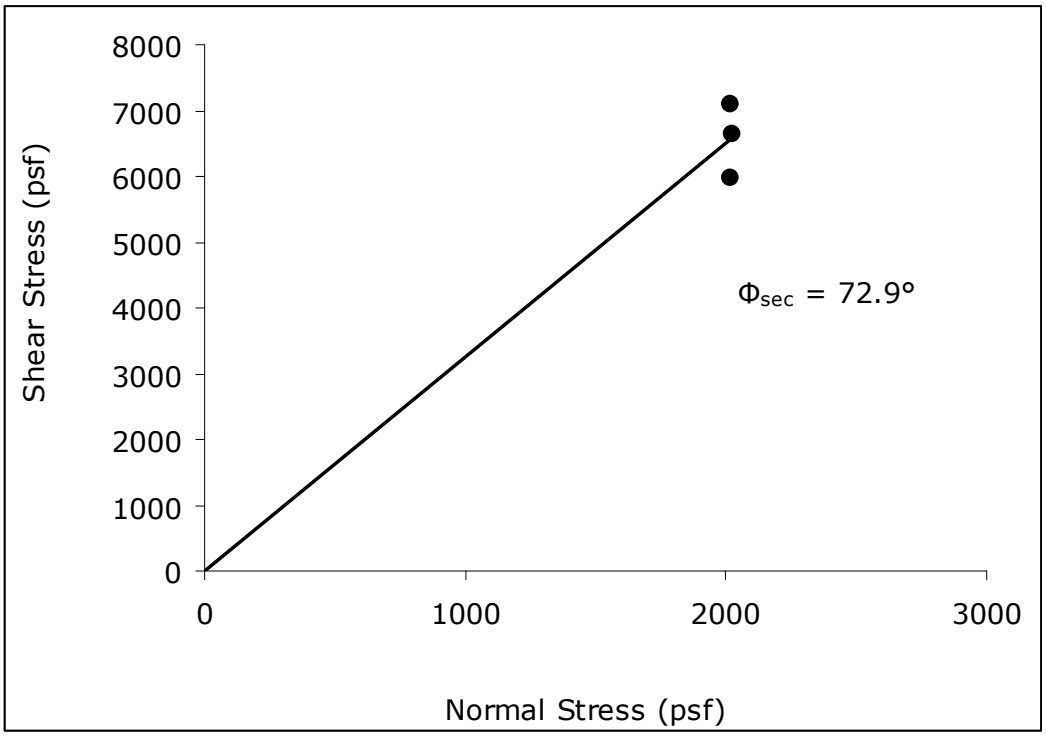

Figure 6.4. Φ_{sec} for the 75% RAP blend material

The secant friction angle of the 75 percent RAP blend material was 72.9°. This secant friction angle is significantly higher than that obtained from the RAP material alone. It is believed that this is the due to the blend material filling in the voids of the RAP soil, resulting in an overall stronger soil matrix. A similar effect was observed with the compaction characteristics for the 75 percent blend, as discussed in Chapter 4. Evaluating the extent of this benefit is beyond the scope of my research; however it does suggest that a small amount of fine material can significantly improve the strength of RAP-soil blends.

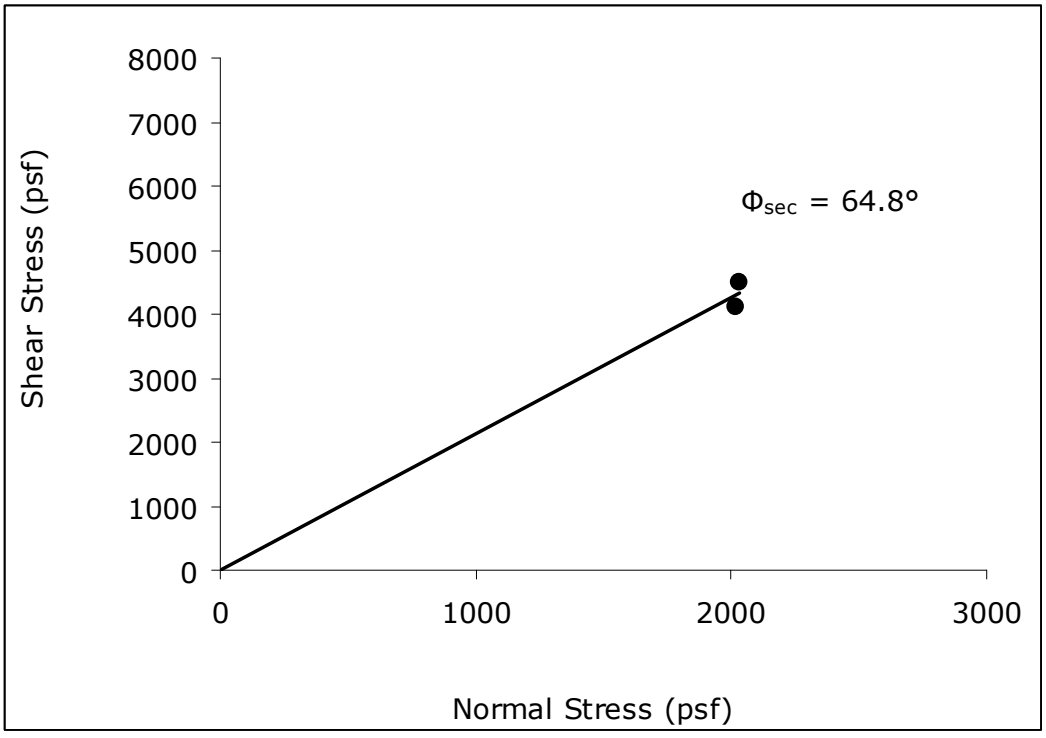

Figure 6.5. Φ_{sec} for the 50% RAP blend material

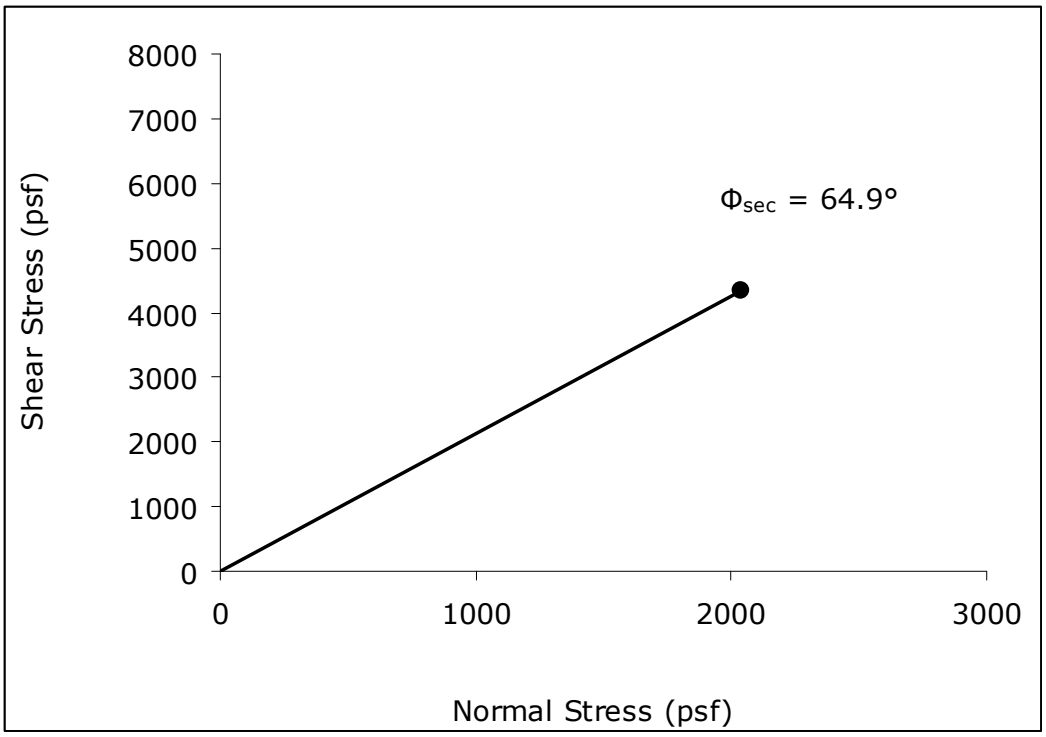

Figure 6.6. Φ_{sec} for the 25% RAP blend material

The 50 percent and 25 percent RAP blends both have similar secant friction angles, 64.8° and 64.9°, respectively. As in the case of the scalped RAP material, these secant friction angles are slightly higher than but consistent with the secant friction angle for the RAP material alone.

6.3 Shear Strength of the Blending Soil

Specimen 10, consisting of only blending soil material was also tested in direct shear under a normal stress of 2,000 psf and at a relative compaction of 90 percent per ASTM D698 Method A. This test was performed to provide a point of reference as to the shear strength of the blend soil alone when

tested in the same large direct shear apparatus. The result of this test, presented in Figure 6.7, yielded a secant friction angle of 52.3°. This shear strength would seem to be somewhat high for a well graded silty sand. However, as noted earlier, the secant friction angle does not necessarily provide a measurement of the actual shear strength parameters as it ignores the cohesion component. The intent of using the secant friction angle is to provide a basis for comparison between the specimens. With that in mind, it can be seen that the blend soil is substantially weaker than the RAP material or any of the RAP-soil blends.

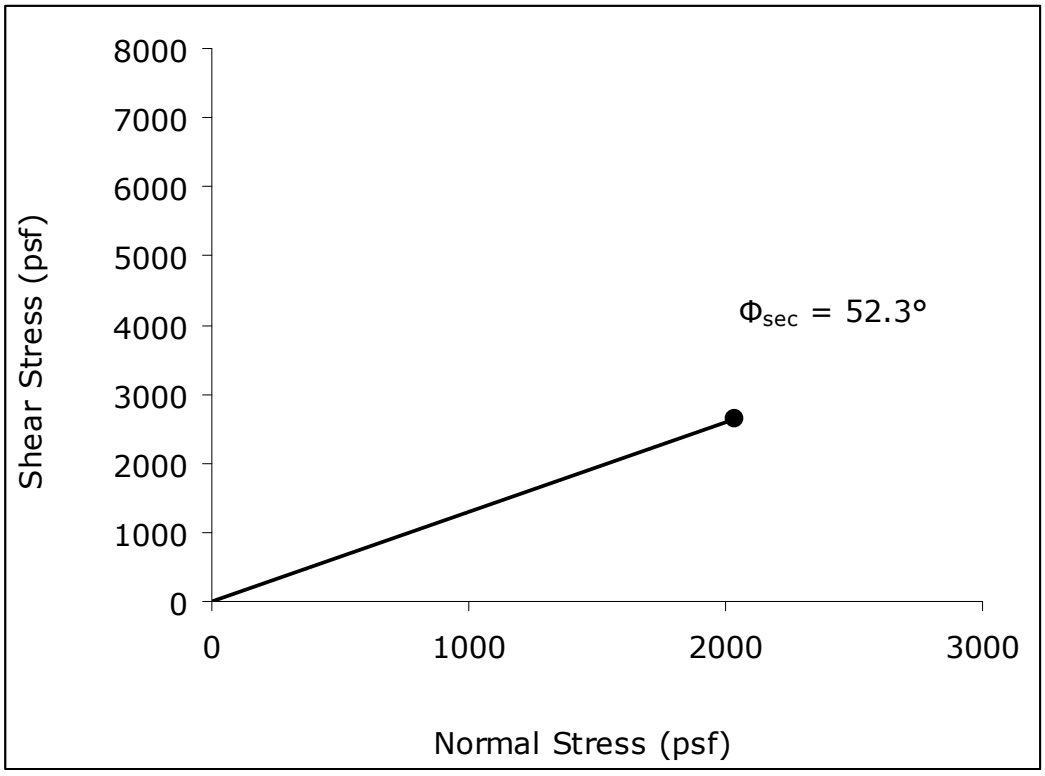

Figure 6.7. Φ_{sec} for the blending soil used

6.4 Discussion

The shear strength of the RAP material, as determined using the large direct shear apparatus, appears to be somewhat higher than other research performed using triaxial specimens. The secant friction angle for the 1.5 inch minus RAP alone was found to be 60.8°. Research performed at the University of Texas by Rathje et al. (2006) using consolidated-drained triaxial specimens found the effective friction angle of RAP to be 37° and the cohesion of RAP to be around of 1,150 psf. The Florida Institute of Technology found the friction angle of RAP to be 44° and the cohesion to be around 700 psf. As shown in Figure 6.2, when using the same cohesion for RAP as determined by the University of Texas, the friction angle was found to be 55.7°. This result is still significantly higher than that obtained by either Rathje et al. (2006) or Consentino et al. (2003).

The friction angles presented in Table 6.1 are all secant friction angles and are therefore not direct comparisons with the results obtained by past research. The cohesion term of the shear strength is assumed to be zero when evaluated using a secant friction angle. Neglecting the cohesion term of the shear strength of RAP and RAP blends is not entirely appropriate. It has been documented that RAP does have real cohesion; a result

of the asphalt binder fusing the particles together (Rathje et al., 2006). Table 6.2 presents friction angles for the various RAP blends for three different assumed cohesions; 0 psf, 1,150 psf as documented by Rathje et al. (2006), and 3,500 psf as presented in Figure 6.1. The results for the friction angles presented in Table 6.2 indicate that the friction angle of RAP is relatively high, even with a cohesion term included.

Table 6.2

Φ for Varying Amounts of Cohesion

	Percent RAP (by weight)			
c, psf	100%	75%	50%	25%
0	60.8	72.9	64.8	64.9
1150	55.7	69.6	57.3	57.5
3500	39.3	56.7	21.7	22.6

It would appear from the results of the direct shear tests performed on the RAP blends that a significant improvement to the shear strength occurs when RAP is blended with soil. This finding is contrary to what was observed by Consentino et al. (2003), in which the friction angle of a 20 percent RAP-soil blend decreased from 44° to 41°. Consentino et al. (2003) also observed, however, that the cohesion of the RAP-soil blend

increased from 605 psf to 1,325 psf with the 20 percent RAP-soil blend. Due to the increase in cohesion, Consentino et al. (2003) concludes that the shear strength of the 20 percent RAP blend was comparable with that of 100 percent RAP that they tested.

It is important to note that the consolidated-drained direct shear tests performed on the RAP and RAP-soil blends for this thesis have not been scalped of the larger particles (except for specimen 5 which was scalped on the ¾ inch sieve). The inclusion of these larger particles may have a significant impact on the shear strength of the RAP and RAP-soil blends. All of the comparative shear strength data has been scalped to accommodate testing in 4 inch diameter triaxial cells. For this reason, additional testing with the large scale direct shear apparatus should be performed to verify the impact that the larger particles may have on the shear strength properties of RAP and RAP-soil blends.

CHAPTER 7

CONCLUSIONS AND RECOMMENDATIONS

7.1 Summary

Based on the findings of my research, several general conclusions can be drawn about RAP and RAP blends. The findings presented herein represent only a very limited testing program, and further testing should be performed to further confirm these conclusions. That being said, I believe the following conclusions can help to further the understanding of material properties and strength characteristics of RAP material and RAP-soil blends.

7.1.1 Compaction characteristics of RAP and RAP blends. The density of the RAP-soil blends was significantly higher than that of either the RAP material or the blending soil alone. This is likely due to the resultant grading of the RAP-soil blends being more well-graded than the RAP material alone. With the 75 percent and 50 percent RAP blends, the finer material of the blending soil is able to fill in the voids of the RAP material. With the 25 percent blend, it would appear that the RAP particles are floating in the matrix of the blending soil, and the resultant density is very similar to the blending soil alone. The results of my research are confirmed by the findings of

Consentino et al. (2003), which also found increased densities for the 80 percent and 60 percent RAP blends. This suggests that blending RAP into soil, at blend percentages of 50 percent or more RAP by weight, could significantly increase the density of the soil and could be used as a means of improving the shear strength of general fill materials where perhaps creep potential is not of great concern.

7.1.2 Compressibility of RAP and RAP blends. RAP material by itself is fairly well documented as exhibiting high secondary compressibility, or creep, potential and this fact has further been substantiated by my research. The parameter used to quantify the level of secondary compressibility was the ratio of $C_{\alpha\varepsilon}/C_{c\varepsilon}$. Mesri and Godlewski (as cited in Holtz, & Kovacs, 1981) summarized data on the ratio of $C_{\alpha\varepsilon}/C_{c\varepsilon}$ and determined that the range for inorganic soils is about 0.025 to 0.06. The results of the RAP material tested in this research yield higher values than that, values around 0.08. Comparison with typical values from Mesri and Godlewski cited in Holtz and Kovaks (1981) suggests that RAP exhibits secondary compressibility of around the same magnitude as organic soils.

Due to experimental difficulties, the only blend specimens that I was able to obtain a ratio of $C_{\alpha\varepsilon}/C_{c\varepsilon}$ for were the 75

percent RAP blends. At this blend ratio the material still had a $C_{\alpha\varepsilon}/C_{c\varepsilon}$ ratio representative of organic soil, measuring around 0.08 as well. Unfortunately, equipment problems prevented me from being able to determine $C_{c\varepsilon}$ for the 50 percent and 25 percent blends. In looking at only the secondary compressibility index, $C_{\alpha\varepsilon}$, for the 50 percent blend, there does seem to be an indication that $C_{\alpha\varepsilon}$ is approaching that of the blend soil. It seems logical that as the soil becomes dominant in the RAP-soil blend, $C_{\alpha\varepsilon}$ should approach that of the soil. It may be that a 50 percent blend of RAP and soil mitigates the negative potential for excessive creep that RAP material alone exhibits.

7.1.3 Shear Strength of RAP and RAP blends. It would appear as though the shear strength of RAP material is high, on the same order of magnitude or greater than other granular materials. It may also be concluded that RAP material can significantly improve the shear strength properties of soils when blended together. This is best exemplified with the 75 percent RAP-soil blend, in which the friction angle was found to be substantially higher than either of the constituent components. Even at low RAP contents, however, the shear strength of the resultant blend was found to be at least as high as RAP alone and higher than the soil. Because of this, RAP may be considered

as a viable material for improving the shear strength of low strength soils used in general fills.

Due to the large size of the RAP particles it is absolutely important to use a large scale direct shear machine to determine the shear strength of RAP. The correlation that I performed between a large scale test and a traditional sized test was not very good. However, refinement of the procedures used and additional testing may help to improve the correlation.

7.1.4 Evaluation of RAP as Structure Backfill. One of the original objectives for this testing program was to evaluate the potential for using RAP as backfill material for structures. Past research by Rathje et al. (2006) has evaluated the use of RAP as an MSE backfill material. However, these investigators did not address the use of RAP blends as MSE wall backfill or the use of RAP or RAP Blends as a general structure backfill material. Rathje et al. (2006) rejects RAP material for use as MSE backfill for permanent structures due to the creep potential of the material, but, as shown in this research, blending RAP with soil may mitigate creep effects.

The data from this research agrees with the conclusion that RAP exhibits considerable potential for creep. However, for the backfill of structures where some long-term settlement can

be tolerated, RAP is likely a suitable material. RAP can be milled and crushed to meet virtually any material gradation requirements, and is a dense material that compacts easily. With the addition of a small amount of soil, as with the 75% RAP blend, the density and compaction of the resultant blend was even better. RAP and RAP blends exhibit relatively high shear strength, which is typically desirous for backfill material behind structures. Furthermore, even though RAP is a cohesive material, RAP is very different from clay. RAP material is a free draining material and does not require drainage considerations behind structures as typical cohesive materials do. Hydraulic conductivity tests were not performed as part of this research. However, Rathje et al. (2006) report that the RAP tested at the University of Texas had a hydraulic conductivity equal to 5.5 $x10^{-4}$ cm/s at a confining pressure of 50 psi.

7.2 Recommendations

I have several recommendations with regards to further research efforts at Arizona State University on the general topic of the characteristics of RAP and RAP blends. These recommendations have been developed based on a working knowledge of the current equipment available for use during the

testing and on several ideas that may be worth exploring in a broader research program.

7.2.1 Limitations of the test equipment. During the testing for this research a couple of issues were experienced with the equipment that should be addressed before further research is conducted. The first issue involves the preparation of the specimens inside the shear box for the large direct shear apparatus. The size and weight of the shear box and top caps made them prohibitively difficult to move around. A hydraulic hand lift was available to assist in moving these components. However, the combined weight of the mold, sample and top caps really pushed the limits of the lift. The first sample was prepared and compacted on the ground, outside of the direct shear frame. For safety reasons, it was decided that subsequent specimens would be prepared with the mold already in the direct shear frame. This made it difficult to compact the specimens as there was limited room above the shear box to raise and drop the compaction hammer. I would recommend that a fork lift be used in the future to accommodate the preparation of the specimens outside of the frame. Due to limited space in the geotechnical lab, this may also involve moving the large scale direct shear apparatus to another location.

Due to the surface area of the specimen, fairly large pump pressures were required to produce the desired axial and lateral stresses on the specimens. This required the use of the large pump in the basement for the lateral loads and a smaller pump for the axial loads. During my testing, I experienced numerous problems with the smaller pump and its associated equipment. The ability to hold a constant pressure for 24 hours or more was the biggest problem. This problem seemed to be exaggerated at lower pressures. The only way to maintain constant pressure with the pump was to keep constant watch on the pump pressure and make adjustments as needed. For testing that spans several days, this was just not practical. I would strongly recommend that these issues be resolved before any further testing is performed.

Because of the problems with the pump, it would have been ideal to perform long term compression testing on the ground using dead loads. This was not performed for my research because of a couple of issues. First and foremost was the safety factor of trying to move a loaded shear box into the direct shear frame for shear testing following the compression testing. Secondly, a large amount of weight is necessary to produce the desired pressures due to the size of the specimen.

For example, in order to produce 2,000 psf of pressure on the surface area of an 18 inch diameter circle (1.76 square feet), 3,520 pounds of dead load is necessary. This is the equivalent of placing a small car on top of the specimen. Again this is not practical and would not be necessary if the smaller pump was in good working order.

7.2.2 Recommendations for further research. The limited testing performed during the research for this thesis really just scratches the surface of the testing that is required to truly characterize RAP blends. At a minimum, I would recommend additional compression and shear strength tests at the same blend ratios as performed for this research to further confirm the validity of the results. I would also recommend, if possible, that tests for compressibility span several days up to a week. This would help to better evaluate the secondary compressibility of the blends. Additionally, compression testing performed over a wider range of overburden pressures would help to better evaluate $C_{c\varepsilon}$. Direct shear testing should also be performed over a wider range of overburden pressures to develop a more accurate shear strength envelope.

Since the end goal for researching RAP blends is to hopefully identify an easy solution for mitigating the potential for

creep, I recommend that further methods for potentially mitigating the creep potential of RAP also be evaluated. Future research should include varying the moisture content during compaction to evaluate the effect this might have on creep, varying the type of blend soil added to the RAP as well as investigating the effects of applying heat during compaction, which could perhaps have the effect of fusing the material together.

7.3 Conclusions

RAP is an abundant material that is finding its way onto construction projects all over the country. While this may be due in part to the diligent promotion of incorporating recyclable materials into construction, the real driving factor behind this is its availability as a cheap construction material. Research such as this will help us to understand how RAP material will function in a variety of construction applications. Hopefully the end result will be the successful use of RAP material in the future for applications that are presently not being considered because of a lack of understanding about RAP behavior.

REFERENCES

ASTM International (2008). Standard test method for particle-size analysis of soils (ASTM D422). *Annual Book of ASTM Standards*. West Conshohocken, PA: American Society for Testing and Materials.

ASTM International (2008). Standard test method for laboratory compaction characteristics using standard effort (ASTM D698). *Annual Book of ASTM Standards*. West Conshohocken, PA: American Society for Testing and Materials.

ASTM International (2008). Standard test method for one-dimensional consolidation properties of soils (ASTM D2435). *Annual Book of ASTM Standards*. West Conshohocken, PA: American Society for Testing and Materials.

ASTM International (2008). Standard practice for classification of soils for engineering purposes (ASTM D2487). *Annual Book of ASTM Standards*. West Conshohocken, PA: American Society for Testing and Materials.

ASTM International (2008). Standard test method for direct shear test of soils under consolidated drained conditions (ASTM D3080). *Annual Book of ASTM Standards*. West Conshohocken, PA: American Society for Testing and Materials.

ASTM International (2008). Standard test method for liquid limit, plastic limit, and plasticity index of soils (ASTM D4318). *Annual Book of ASTM Standards*. West Conshohocken, PA: American Society for Testing and Materials.

ASTM International (2008). Standard practice for correction of unit weight and water content for soils containing oversize particles (ASTM D4718). *Annual Book of ASTM Standards*. West Conshohocken, PA: American Society for Testing and Materials.

Bardet, J.P. (1997). Experimental soil mechanics. Upper Sadle River, NJ: Prentice-Hall, Inc.

Cosentino, P.J., Kalaajin, E.H., Shieh, C.S., Mathurin, W.K.J., Gomez, F.A., Cleary, E.D., and Treeratrakoon, A. (2003). Developing specifications for using recycled asphalt pavement as base, subbase or general fill materials, phase II (FL/DOT/RMC/06650-7754). Melbourne, FL: Florida Institute of Technology.

Eighmy, T.T., and Magee, B.J. (2001). The road to reuse. *Civil Engineering*, *71*(9), 66-71

Giroud, J.P. (2010). Development of criteria for geotextile and granular filters: 9th International Conference on Geosynthetics (pp. 45-64). Guaruja, Brazil.

Holtz, R.D, and Kovacs, W.D. (1981). An introduction to geotechnical engineering. Upper Saddle River, NJ: Prentice-Hall, Inc.

Kuennen, T. (2007, October 1). The economics of recycling. *Rock Products*, Retrieved from http://rockproducts.com/index.php/features/59-features/6691.html.

Lambe, T.W., and Whitman, R.V. (1967). Soil mechanics. John Wiley and Sons: New York, NY.

Lindquist, E.S. (1994). The strength and deformation properties of melange. Ph.D. Dissertation. Department of Civil Engineering: University of California at Berkeley.

Mesri, G., and Godlewski, P.M. (1977). Time- and stress-compressility interrelationship. *Journal of the Geotechnical Division, ASCE, 103(GT5)*, 417-430.

Rathje, E.M., Rauch, A.F., Folliard, K.J., Trejo, D., Little, D., Viyanant, Ogall, M., and Esfellar, M., (2001). Recycled asphalt pavement and crushed concrete backfill: state-of-the-art review and material characterization. (FHWA/TX-0/4177-6). Austin, TX: Center for Transportation Research.

Rathje, E.M., Rauch, A.F., Folliard, K.J., Trejo, D., Little, D., Viyanant, Ogall, M., and Esfellar, M., (2002). Recycled asphalt pavement and crushed concrete backfill: results from initial durability and geotechnical tests. (FHWA/TX-02/4177-2). Austin, TX: Center for Transportation Research.

Rathje, E.M., Rauch, A.F., Trejo, D., Folliard, K.J., Viyanant, C., Esfellar, M., Jain, A., and Ogall, M. (2006). Evaluation of crushed concrete and recycled asphalt pavement as backfill for mechanically stabilized earth walls (FHWA/TX-06/0-4177-3). Austin, TX: Center for Transportation Research.

APPENDIX A

MATERIAL PROPERTIES DATA SHEETS

PARTICLE SIZE ANALYSIS OF SOILS
ASTM D422
RAP MATERIAL

CONSTANTS		
L_2	140	(Hydrometer bulb length, mm)
V_B	67000	(Hydrometer bulb volume, mm^3)
A	2780	(Cross-sectional area of sedimentation cylinder, mm^2)
°C	21.3	(Temp of suspending medium, °C)
n	9.70E-04	$n = 0.00249 - 0.000497 Ln(°C)$
G	2.65	(Specific gravity of soil particles)
a	1.00	$a = \frac{G}{G-1} \times 0.623$
W_H	552.70	(Hydrometer analysis sample weight)
W	1	(mass of air-dried soil for hygroscopic moisture, g)
W_1	1	(mass of oven-dried soil for hygroscopic moisture, g)
HM	1.000	(Hygroscopic moisture correction factor, HM = W_1 / W)
w	552.70	W_H x HM

Hydrometer Calibration

Calibration Intercept	32.507
Calibation Slope	-2.0872
2nd Order Term	0.0363

SIEVE ANALYIS		
Size	Weight Ret	%Pass
in. (mm)	g	%
3" (75)	0.0	100.0
2" (50)	255.5	96.7
1" (25)	330.9	92.4
3/8" (9.5)	2040.5	66.0
1/4" (6.25)	867.5	54.8
#4 (4.75)	543.0	47.8
Pan	3696.1	
Total	7733.5	
#8 (2.36)	145.7	35.2
#10 (2.00)	31.8	32.4
#16 (1.20)	89.9	24.7
#30 (0.60)	112.8	14.9
#40 (0.425)	47.7	10.8
#50 (0.300)	37.0	7.6
#100 (0.150)	41.4	4.0
#200 (0.075)	21.8	2.1
Pan	0.0	
Elut	202.1	
Total	552.7	

PERCENTAGE OF SOIL IN SUSPENSION **Hydrometer Start Time: 8:15 AM**

T	R_H	Temp	Corrected R_H	R_a $R_H * a$	P $\frac{R_a}{w} * 100$	%Pass $\frac{P * \%P_{200}}{100}$	L_1 $105 - (1.64 * R_a)$	L $L_1 + 58$	d $\sqrt{\frac{30 * \eta * L}{980(G-1)T}}$
2									
5									
15									
30									
60									
250									
1440									
2880									

HYDROMETER ANALYSIS	
Smaller Than:	Percent
.02 mm	
.002 mm	
.001 mm	

MAXIMUM DRY DENSITY & OPTIMUM MOISTURE OF SOILS
ASTM D698

RAP MATERIAL

WEIGHT OF MOLD 6415.0 g SPECIFIC GRAVITY 2.40

VOLUME OF MOLD 0.0751 ft^3 % OVERSIZE 13.0

% WATER ADDED	WT. OF SAMPLE AND MOLD	WET WT OF SAMPLE	WET DENSITY	MOISTURE SAMPLE		% MOISTURE	DRY DENSITY
				WET WT.	DRY WT.		
(%)	(g)	(g)	(lb/ft3)	(g)	(g)	(%)	(lb/ft3)
2	10586.8	4171.8	122.5	475.8	451.9	5.3%	116.3
4	10865.8	4450.8	130.7	434.8	403.3	7.8%	121.2
6	10836.7	4421.7	129.8	519.4	472.2	10.0%	118.0
8	10783.5	4368.5	128.2	354.5	316.5	12.0%	114.5

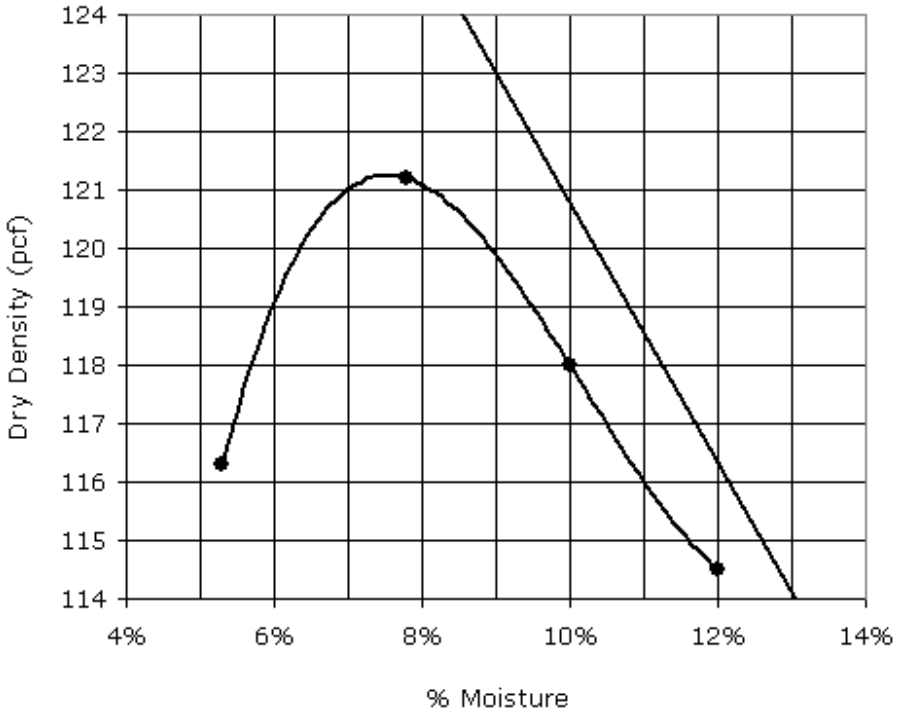

		ADJUSTED FOR OVERSIZE
MAXIMUM DENSITY	121.2	123.0
OPTIMUM MOISTURE	7.8	6.9

PARTICLE SIZE ANALYSIS OF SOILS
ASTM D422
BLEND SOIL

CONSTANTS		
L_2	140	(Hydrometer bulb length, mm)
V_B	67000	(Hydrometer bulb volume, mm^3)
A	2780	(Cross-sectional area of sedimentation cylinder, mm^2)
°C	21.3	(Temp of suspending medium, °C)
n	9.70E-04	$n = 0.00249 - 0.000497 Ln(°C)$
G	2.65	(Specific gravity of soil particles)
a	1.00	$a = \frac{G}{G-1} \times 0.623$
W_H	100.60	(Hydrometer analysis sample weight)
W	14.94	(mass of air-dried soil for hygroscopic moisture, g)
W_1	14.73	(mass of oven-dried soil for hygroscopic moisture, g)
HM	0.986	(Hygroscopic moisture correction factor, HM = W_1 / W)
w	99.19	W_H x HM

Hydrometer Calibration

Calibration Intercept	32.507
Calibation Slope	-2.0872
2nd Order Term	0.0363

SIEVE ANALYIS		
Size	Weight Ret	%Pass
in. (mm)	g	%
3" (75)	0.0	100.0
2" (50)	0.0	100.0
1" (25)	0.0	100.0
3/8" (9.5)	1.8	99.9
1/4" (6.25)	6.3	99.4
#4 (4.75)	8.6	98.7
#8 (2.36)	44.5	95.3
#10 (2.00)	17.9	93.9
Pan	1216.0	
Total	1295.1	
#16 (1.20)	5.0	89.2
#30 (0.60)	11.0	78.8
#40 (0.425)	6.0	73.1
#50 (0.300)	8.0	65.5
#100 (0.150)	12.0	54.1
#200 (0.075)	9.0	45.6
Pan	1.5	
Elut	46.7	
Total	99.2	

PERCENTAGE OF SOIL IN SUSPENSION **Hydrometer Start Time: 8:15 AM**

T	R_H	Temp	Corrected R_H	R_a $R_H * a$	P $\frac{R_a}{w} * 100$	%Pass $\frac{P * \%P_{200}}{100}$	L_1 $105 - (1.64 * R_a)$	L $L_1 + 58$	d $\sqrt{\frac{30 * n * L}{980(G-1)T}}$
2	42	21.2	37	37.0	37	35.0	44.32	102.32	0.03034
5	35	21.2	30	30.0	30	28.4	55.8	113.8	0.02024
15	30	21.3	25	25.0	25	23.7	64	122	0.01210
30	27	21.3	22	22.0	22	20.8	68.92	126.92	0.00872
60	25	21.5	21	21.0	21	19.9	70.56	128.56	0.00621
250	21	21.5	17	17.0	17	16.1	77.12	135.12	0.00312
1440	16	21.2	11	11.0	11	10.4	86.96	144.96	0.00135
2880	12	21.2	7	7.0	7	6.6	93.52	151.52	0.00097

HYDROMETER ANALYSIS	
Smaller Than:	Percent
.02 mm	28
.002 mm	13
.001 mm	8

MAXIMUM DRY DENSITY & OPTIMUM MOISTURE OF SOILS
ASTM D698

BLEND SOIL

WEIGHT OF MOLD 4204.0 g SPECIFIC GRAVITY 2.55

VOLUME OF MOLD 0.0333 ft^3 % OVERSIZE 0.0

% WATER ADDED	WT. OF SAMPLE AND MOLD	WET WT OF SAMPLE	WET DENSITY	MOISTURE SAMPLE		% MOISTURE	DRY DENSITY
				WET WT.	DRY WT.		
(%)	(g)	(g)	(lb/ft3)	(g)	(g)	(%)	(lb/ft3)
2	5990.3	1786.3	118.3	397.4	363.3	9.4%	108.1
4	6174.8	1970.8	130.5	545.1	487.1	11.9%	116.6
6	6196.2	1992.2	131.9	445.8	392.4	13.6%	116.1
8	6151.2	1947.2	128.9	455.7	395.9	15.1%	112.0

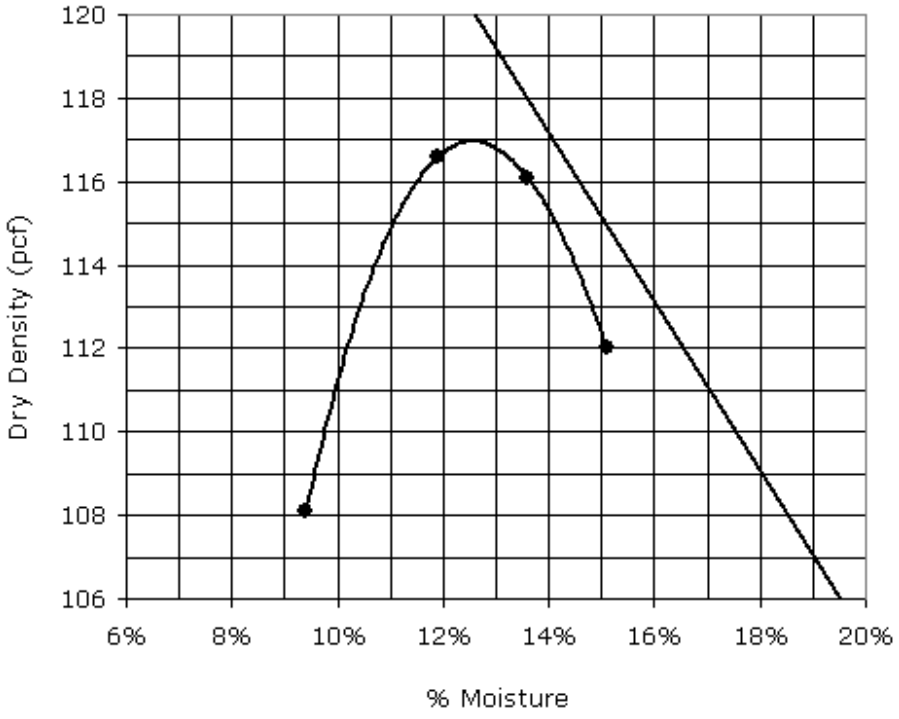

		ADJUSTED FOR OVERSIZE
MAXIMUM DENSITY	117.0	117.0
OPTIMUM MOISTURE	12.5	12.5

MAXIMUM DRY DENSITY & OPTIMUM MOISTURE OF SOILS
ASTM D698

75% RAP BLEND

WEIGHT OF MOLD 6415.0 g SPECIFIC GRAVITY 2.55

VOLUME OF MOLD 0.0751 ft^3 % OVERSIZE 10.0

% WATER ADDED	WT. OF SAMPLE AND MOLD	WET WT OF SAMPLE	WET DENSITY	MOISTURE SAMPLE		% MOISTURE	DRY DENSITY
				WET WT.	DRY WT.		
(%)	(g)	(g)	(lb/ft3)	(g)	(g)	(%)	(lb/ft3)
2	10915.5	4500.5	132.1	405.7	382.0	6.2%	124.4
4	11169.5	4754.5	139.6	387.7	356.7	8.7%	128.4
6	11109.0	4694.0	137.8	530.9	480.5	10.5%	124.7
8	11020.1	4605.1	135.2	545.8	487.3	12.0%	120.7

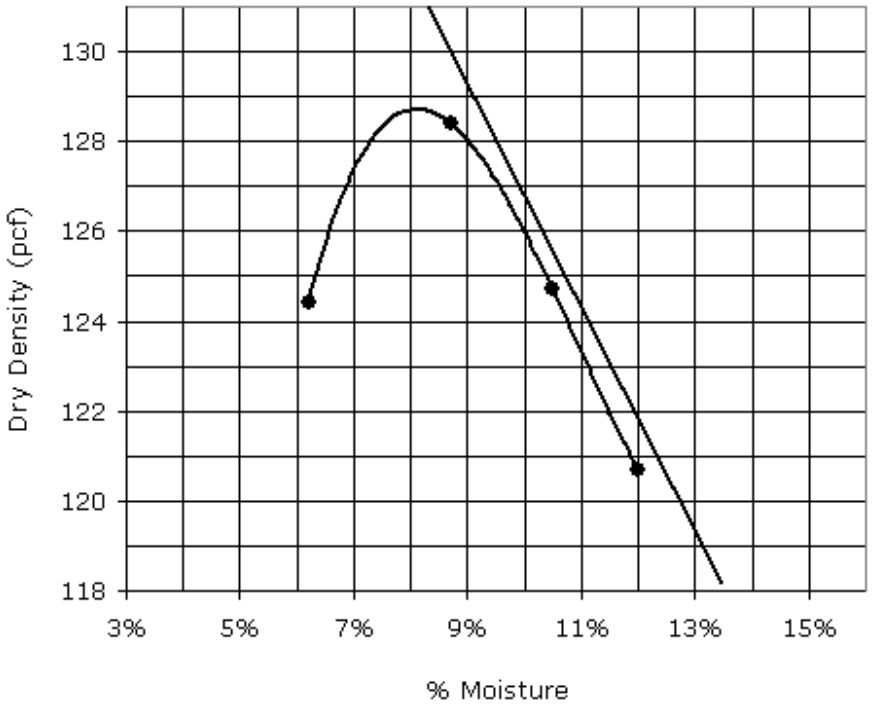

		ADJUSTED FOR OVERSIZE
MAXIMUM DENSITY	128.8	130.3
OPTIMUM MOISTURE	8.2	7.5

MAXIMUM DRY DENSITY & OPTIMUM MOISTURE OF SOILS
ASTM D698

50% RAP BLEND

WEIGHT OF MOLD 6415.0 g SPECIFIC GRAVITY 2.50

VOLUME OF MOLD 0.0751 ft^3 % OVERSIZE 6.0

% WATER ADDED	WT. OF SAMPLE AND MOLD	WET WT OF SAMPLE	WET DENSITY	MOISTURE SAMPLE		% MOISTURE	DRY DENSITY
				WET WT.	DRY WT.		
(%)	(g)	(g)	(lb/ft3)	(g)	(g)	(%)	(lb/ft3)
2	10685.0	4270.0	125.3	510.0	483.0	5.6%	118.7
4	10909.8	4494.8	131.9	481.6	449.7	7.1%	123.2
6	10980.3	4565.3	134.0	461.6	421.9	9.4%	122.5
8	10949.9	4534.9	133.1	433.4	389.0	11.4%	119.5

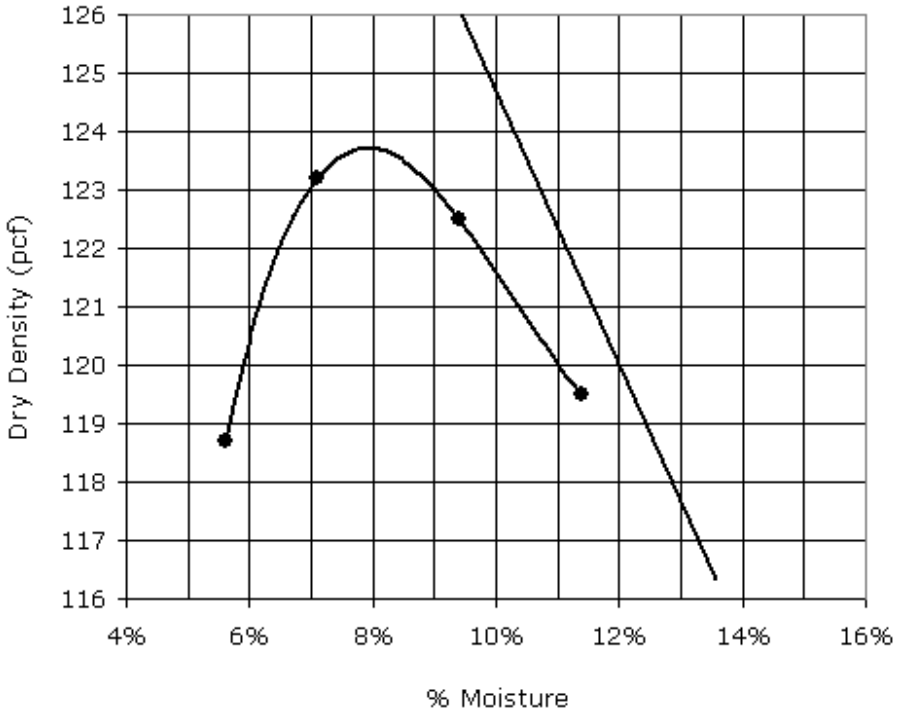

		ADJUSTED FOR OVERSIZE
MAXIMUM DENSITY	123.7	124.7
OPTIMUM MOISTURE	7.8	7.4

MAXIMUM DRY DENSITY & OPTIMUM MOISTURE OF SOILS
ASTM D698

25% RAP BLEND

WEIGHT OF MOLD 6415.0 g SPECIFIC GRAVITY 2.50

VOLUME OF MOLD 0.0751 ft^3 % OVERSIZE 3.0

% WATER ADDED	WT. OF SAMPLE AND MOLD	WET WT OF SAMPLE	WET DENSITY	MOISTURE SAMPLE		% MOISTURE	DRY DENSITY
				WET WT.	DRY WT.		
(%)	(g)	(g)	(lb/ft3)	(g)	(g)	(%)	(lb/ft3)
2	10466.0	4051.0	118.9	419.4	385.8	8.7%	109.4
4	10885.4	4470.4	131.2	453.7	407.3	11.4%	117.8
6	10884.2	4469.2	131.2	419.7	371.1	13.1%	116.0
8	10841.7	4426.7	129.9	401.0	348.4	15.1%	112.9

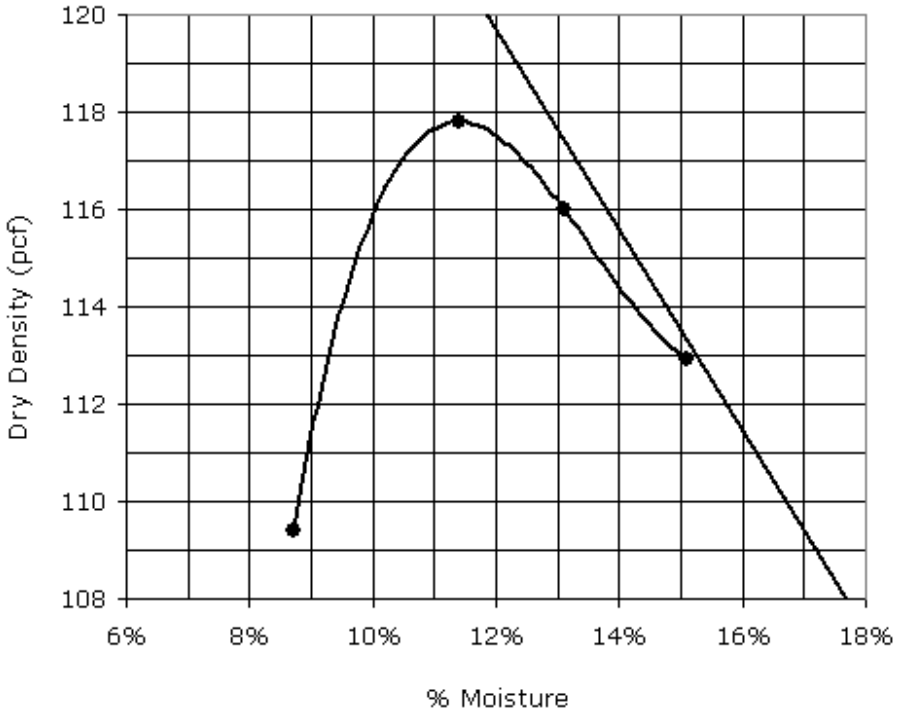

		ADJUSTED FOR OVERSIZE
MAXIMUM DENSITY	117.8	118.5
OPTIMUM MOISTURE	11.4	11.1

APPENDIX B

COMPRESSIBILITY TEST DATA

Time-Deformation Curve

Specimen #1
-1 1/2" RAP
σ_n = 1000 psf

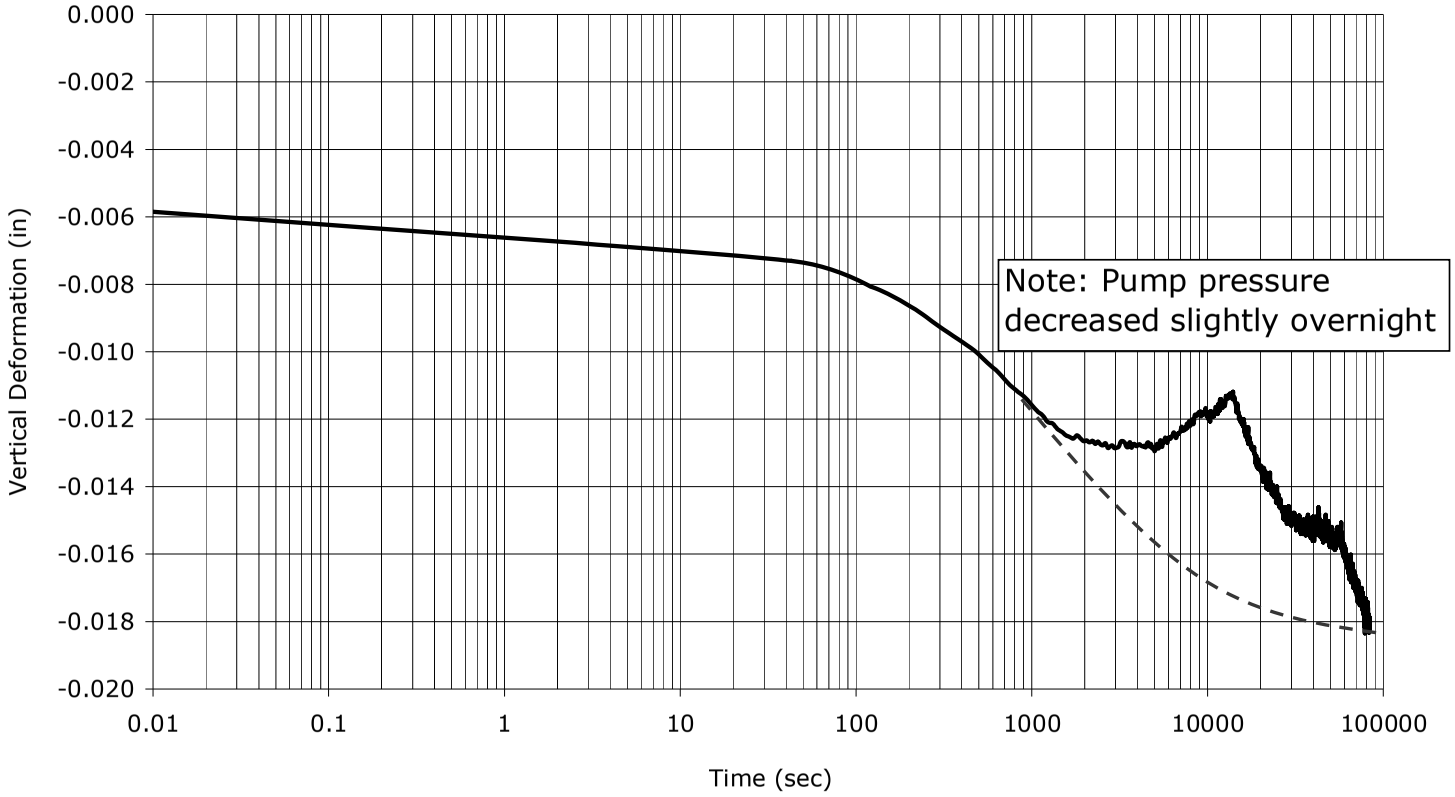

Time-Deformation Curve

Specimen #1
-1 1/2" RAP
σ_n = 1000 psf

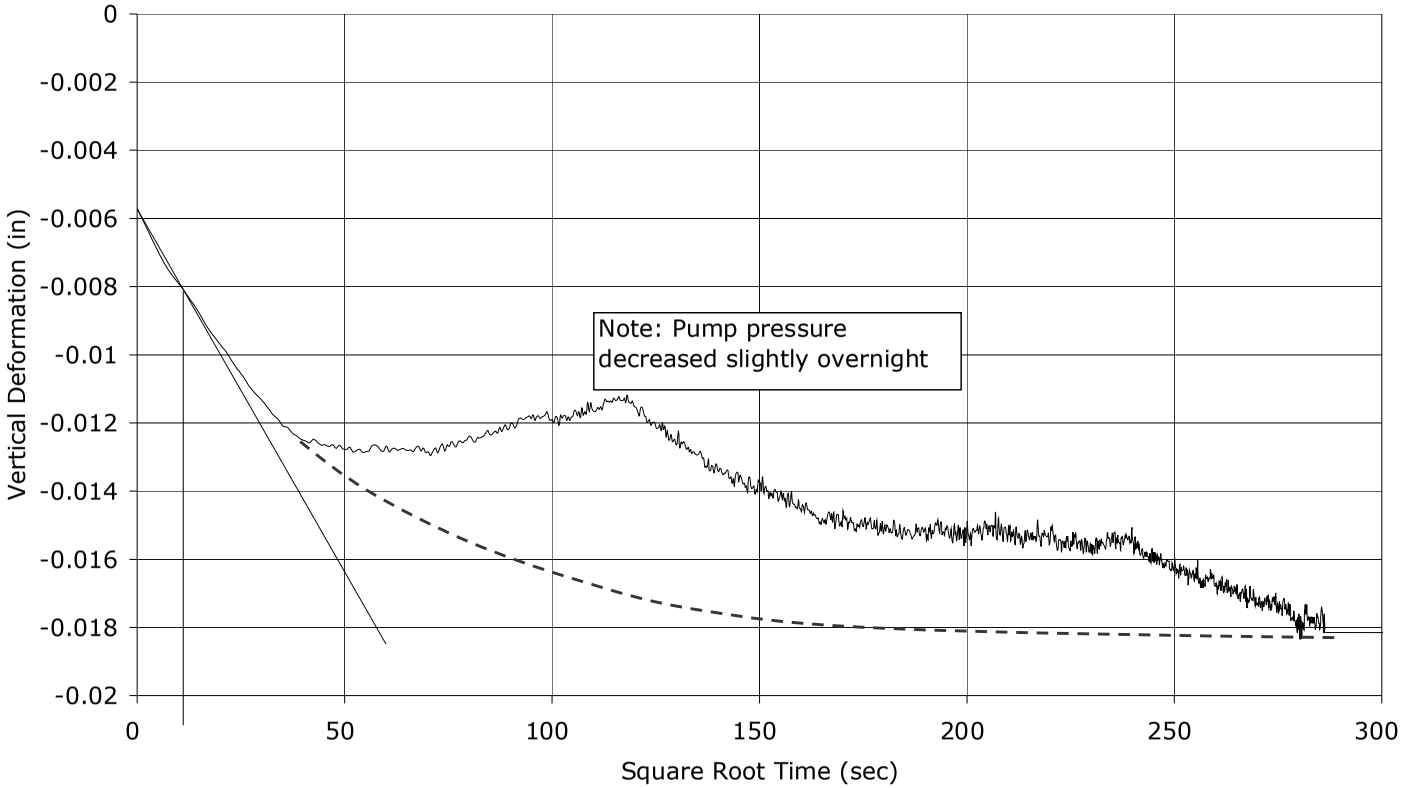

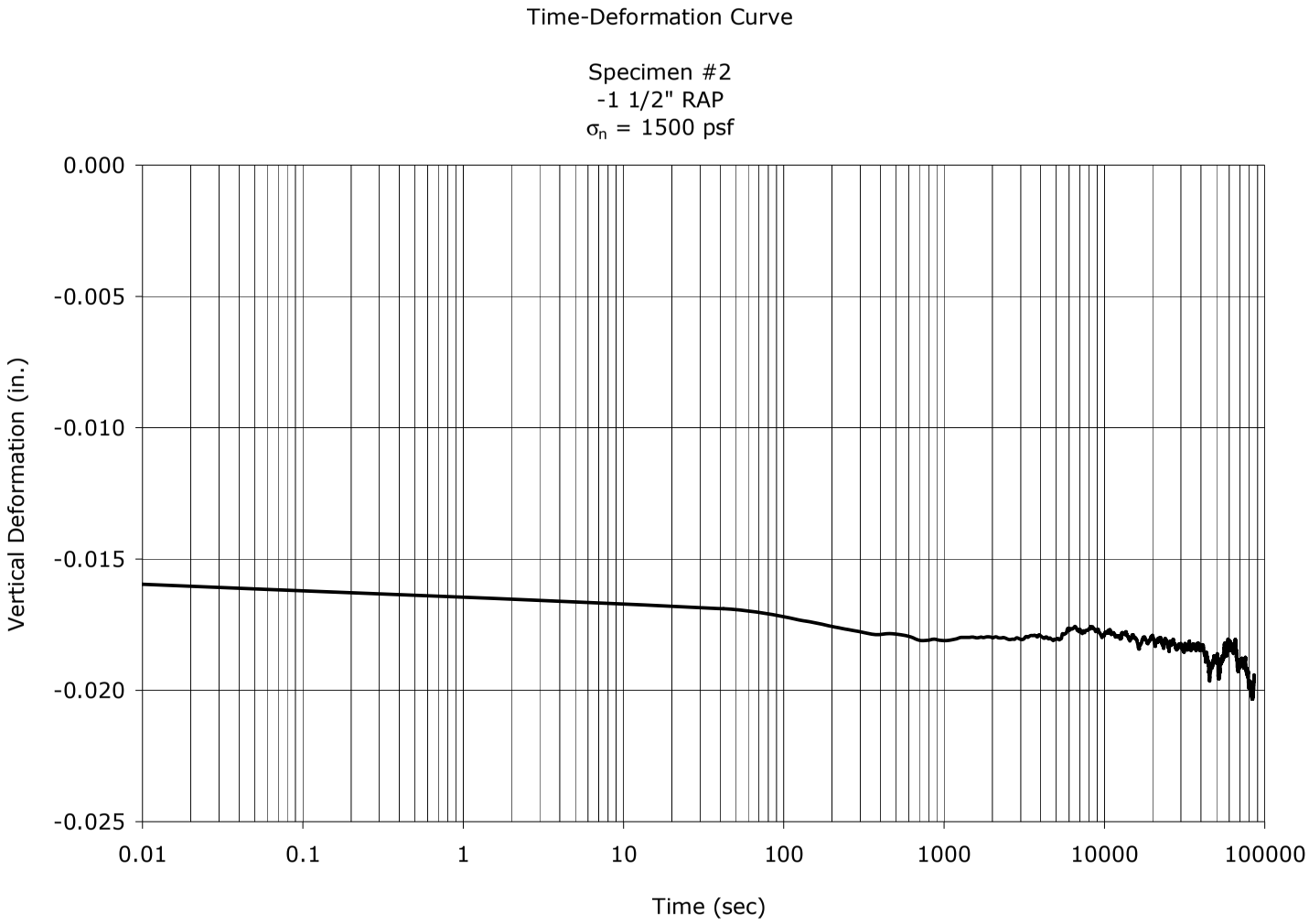
Time-Deformation Curve
Specimen #2
-1 1/2" RAP
σn = 1500 psf
0.000
-0.005
-0.010
-0.015
-0.020
-0.025
Vertical Deformation (in.)
0.01
0.1
1
10
100
1000
10000
100000
Time (sec)

Time-Deformation Curve

Specimen #2
-1 1/2" RAP
σ_n = 1500 psf

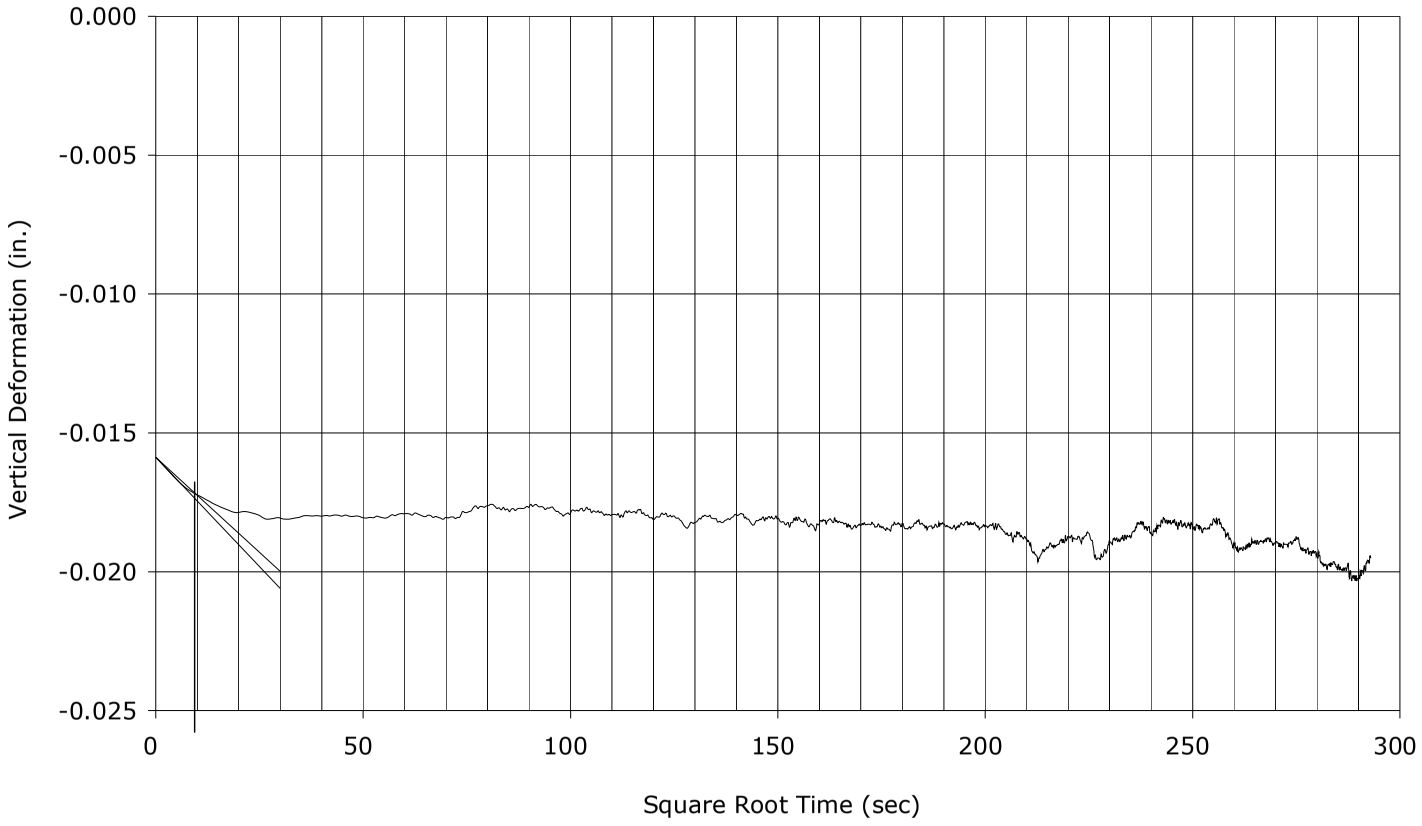

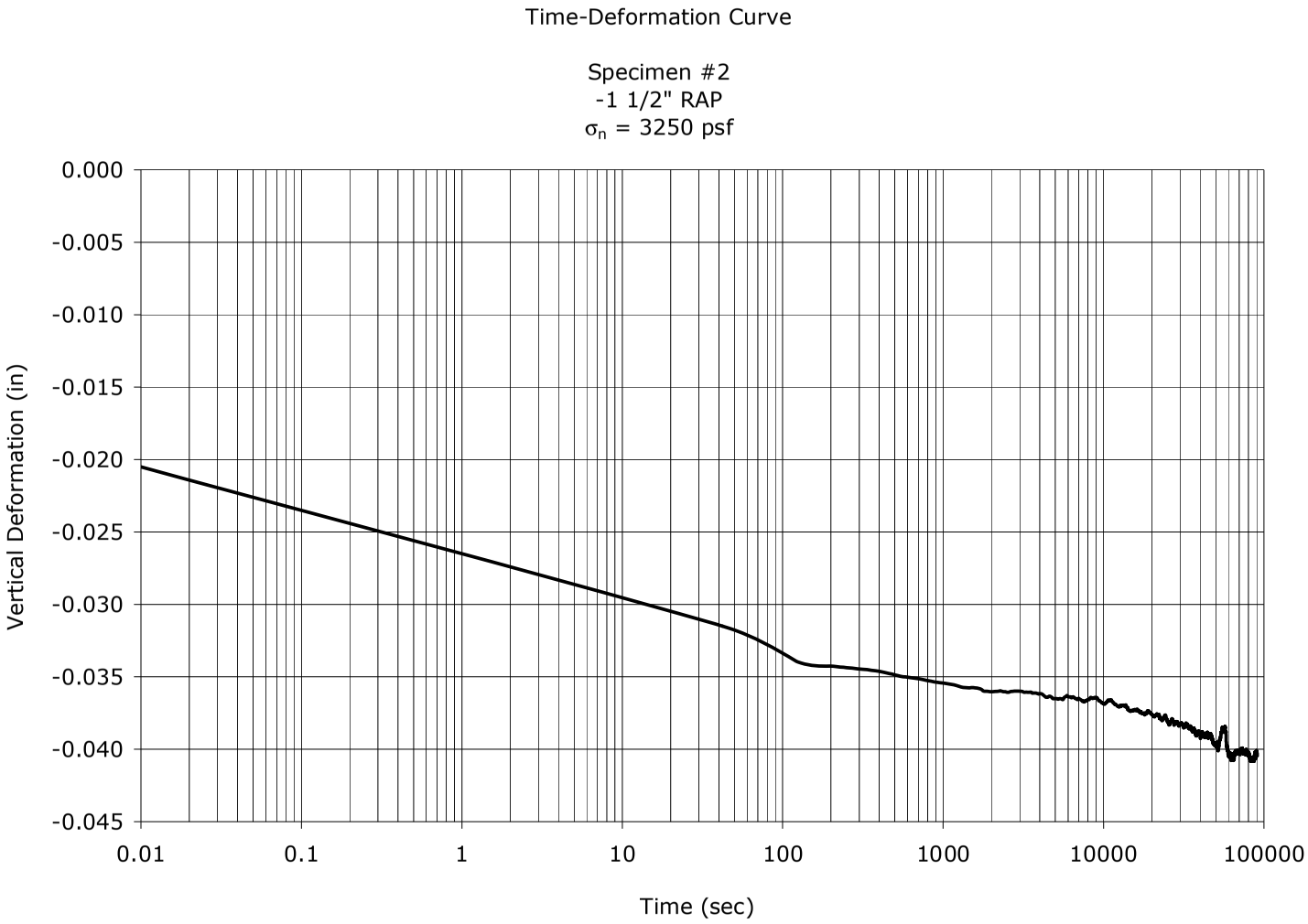
Time-Deformation Curve
Specimen #2
-1 1/2" RAP
σn = 3250 psf
0.000
-0.005
-0.010
-0.015
-0.020
-0.025
-0.030
-0.035
-0.040
-0.045
Vertical Deformation (in)
0.01
0.1
1
10
100
1000
10000
100000
Time (sec)

Time-Deformation Curve

Specimen #2
-1 1/2" RAP
σ_n = 3250 psf

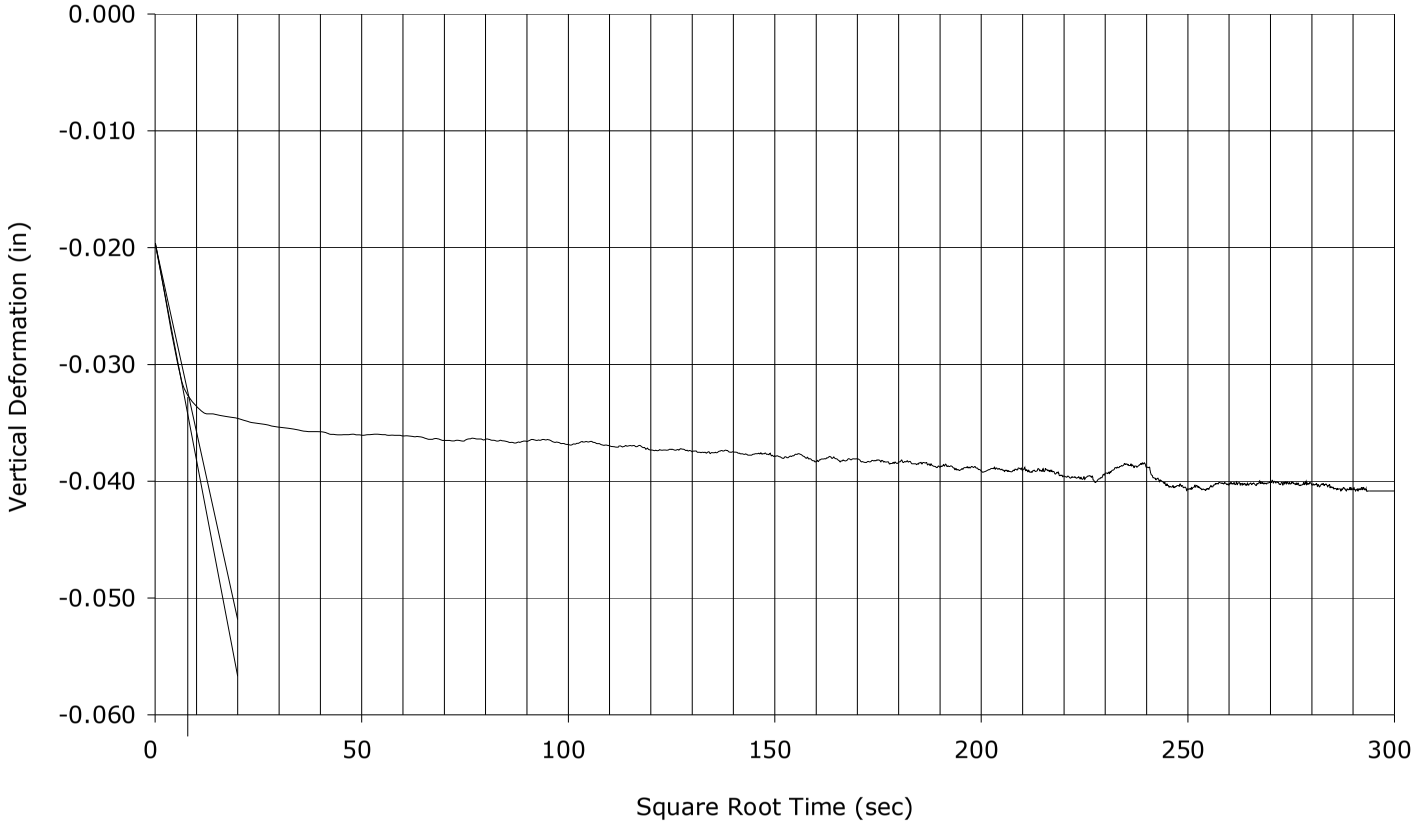

Stress-Strain Curve

Specimen #2
-1 1/2" RAP

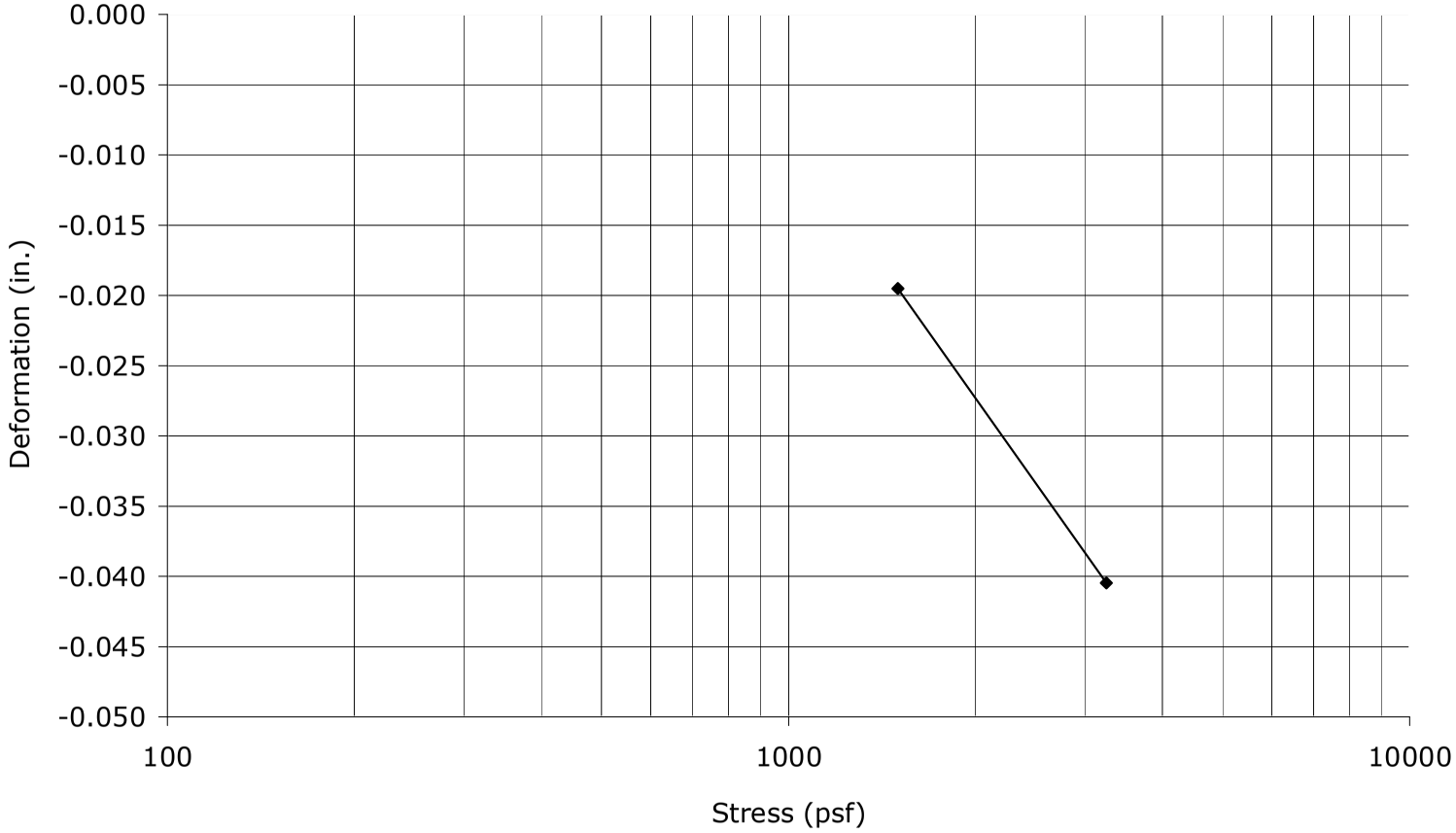

Time-Deformation Curve

Specimen #3
-1 1/2" RAP
σ_n = 1108 psf

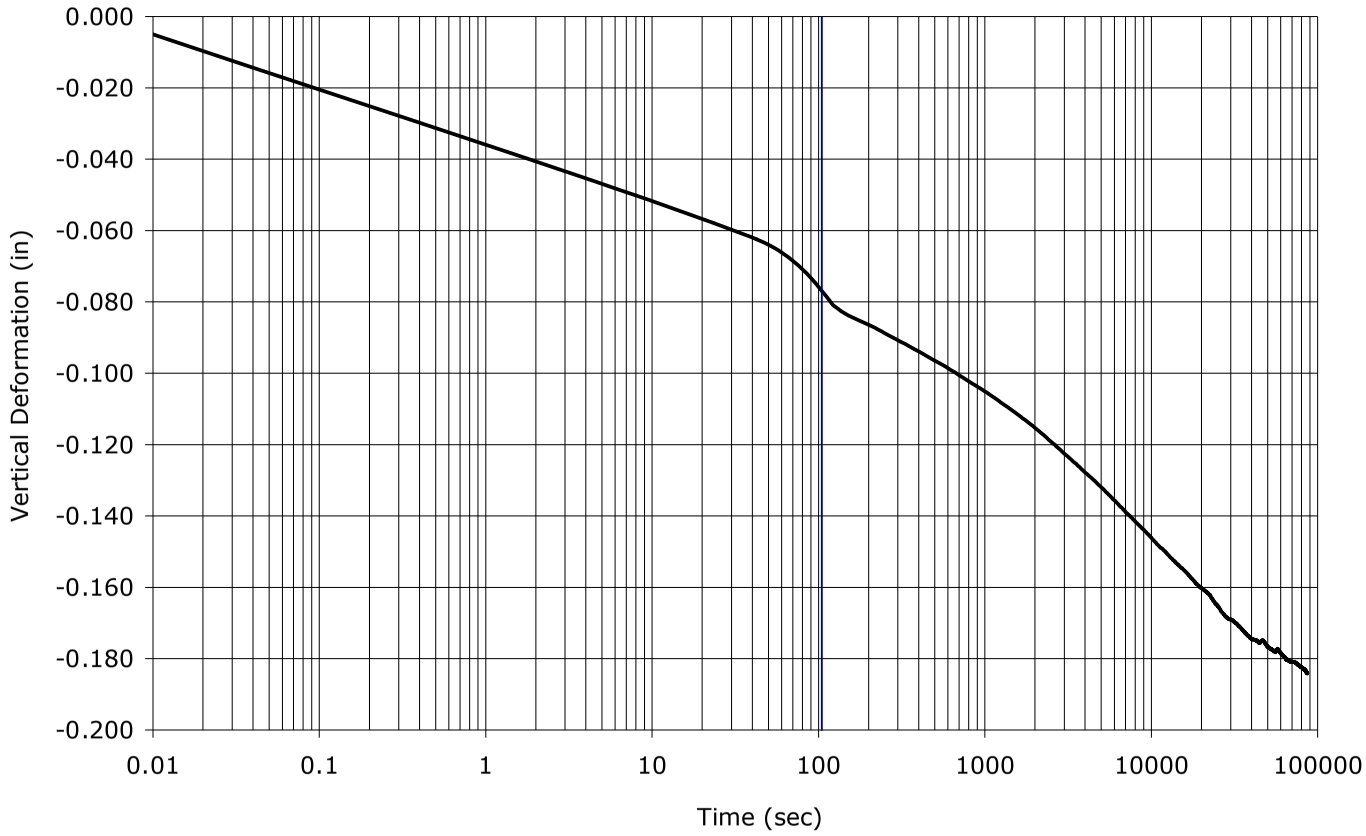

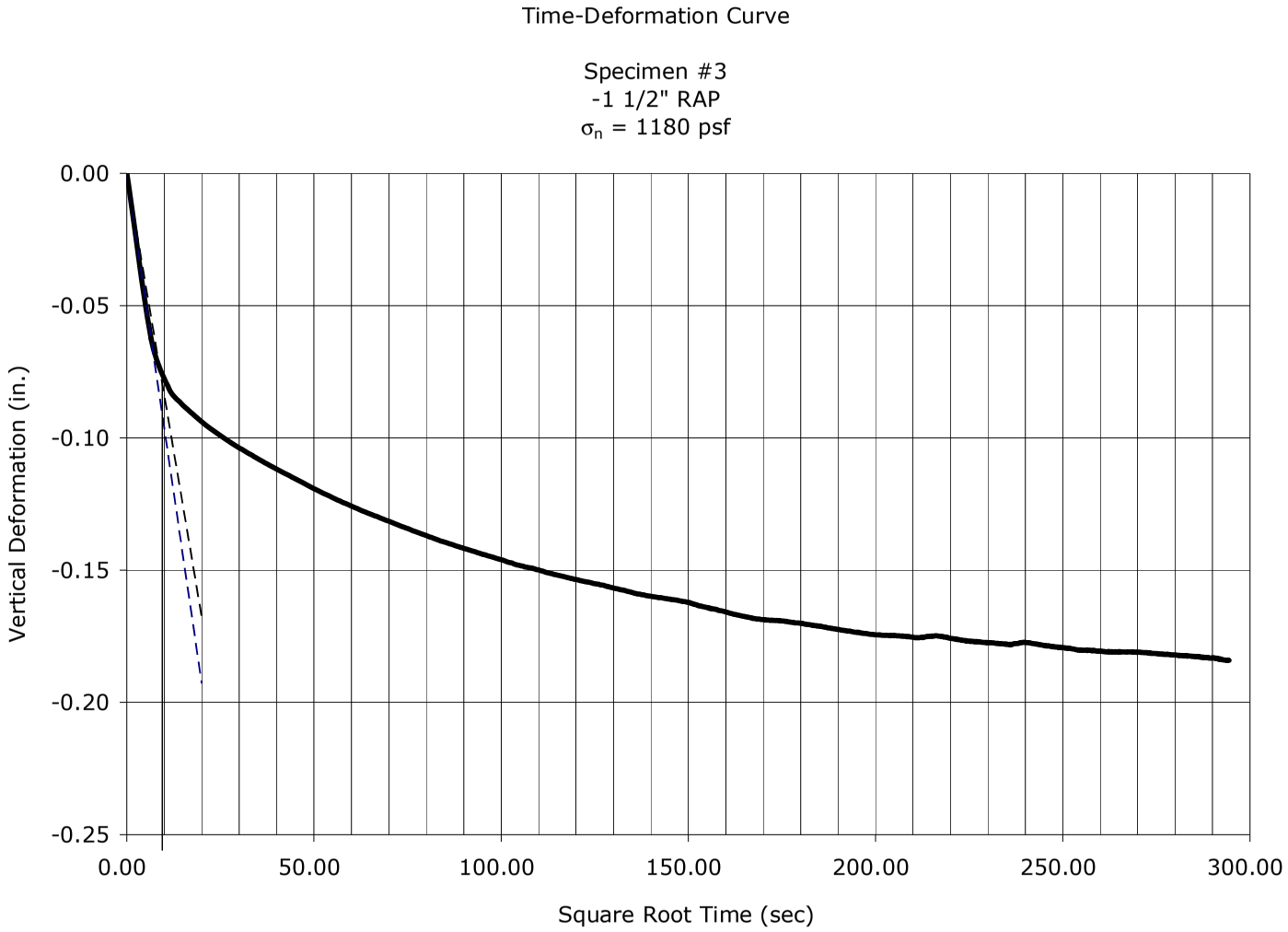
Time-Deformation Curve
Specimen #3
-1 1/2" RAP
σn = 1180 psf
Vertical Deformation (in.)
0.00
-0.05
-0.10
-0.15
-0.20
-0.25
0.00
50.00
100.00
150.00
200.00
250.00
300.00
Square Root Time (sec)

Time-Deformation Curve

Specimen #3
-1 1/2" RAP
σ_n = 2000 psf

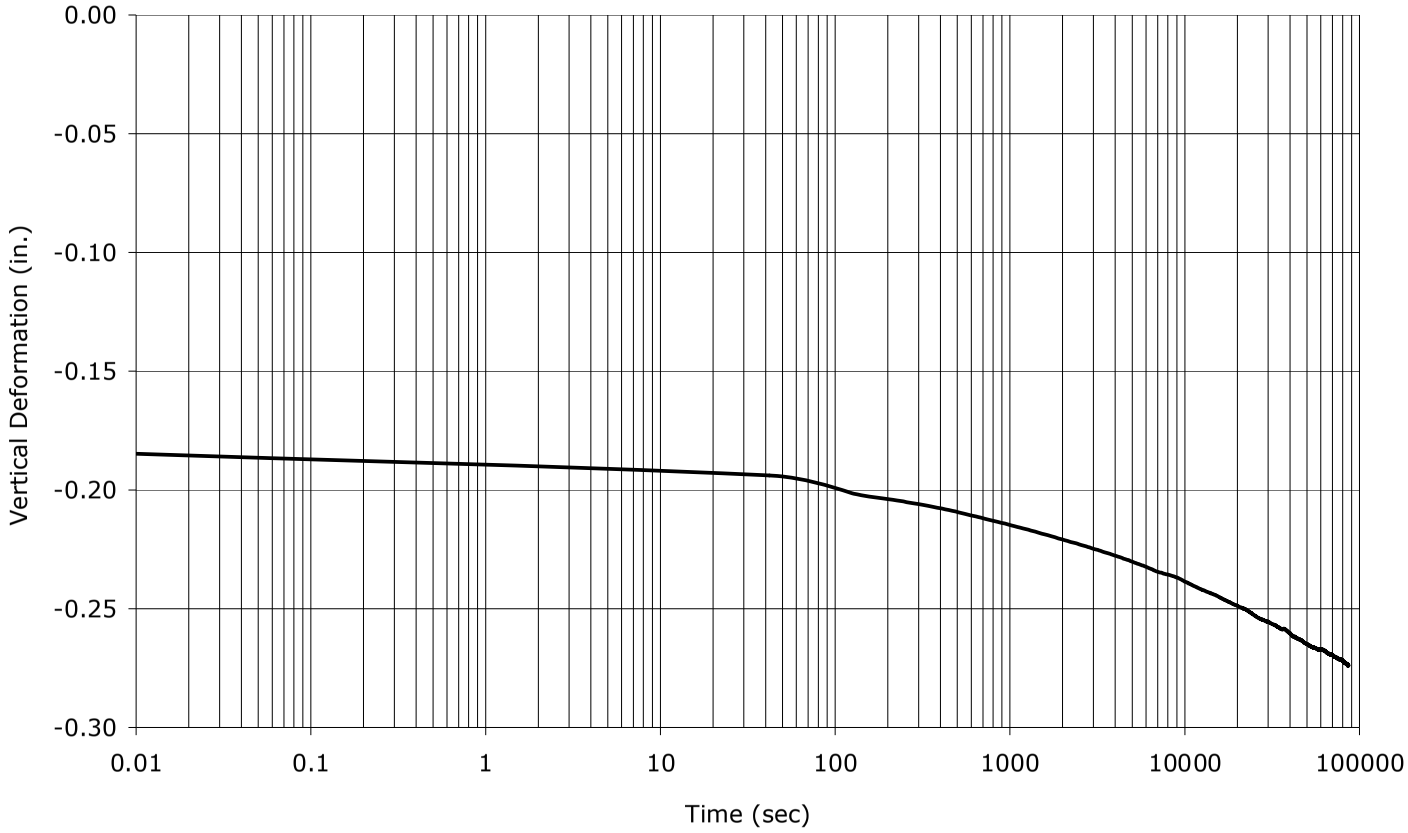

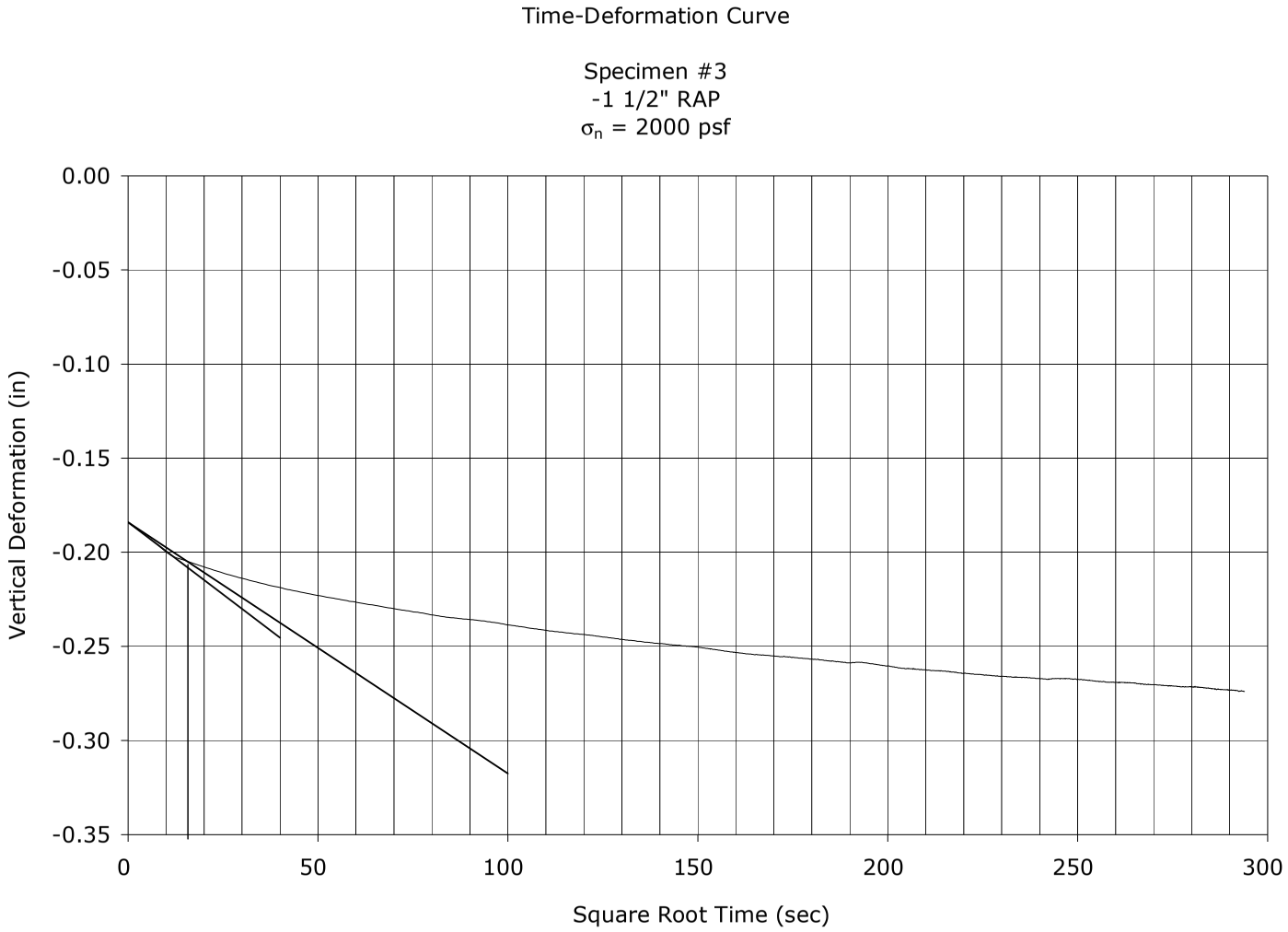
Time-Deformation Curve
Specimen #3
-1 1/2" RAP
σn = 2000 psf
Vertical Deformation (in)
0.00
-0.05
-0.10
-0.15
-0.20
-0.25
-0.30
-0.35
0
50
100
150
200
250
300
Square Root Time (sec)

06

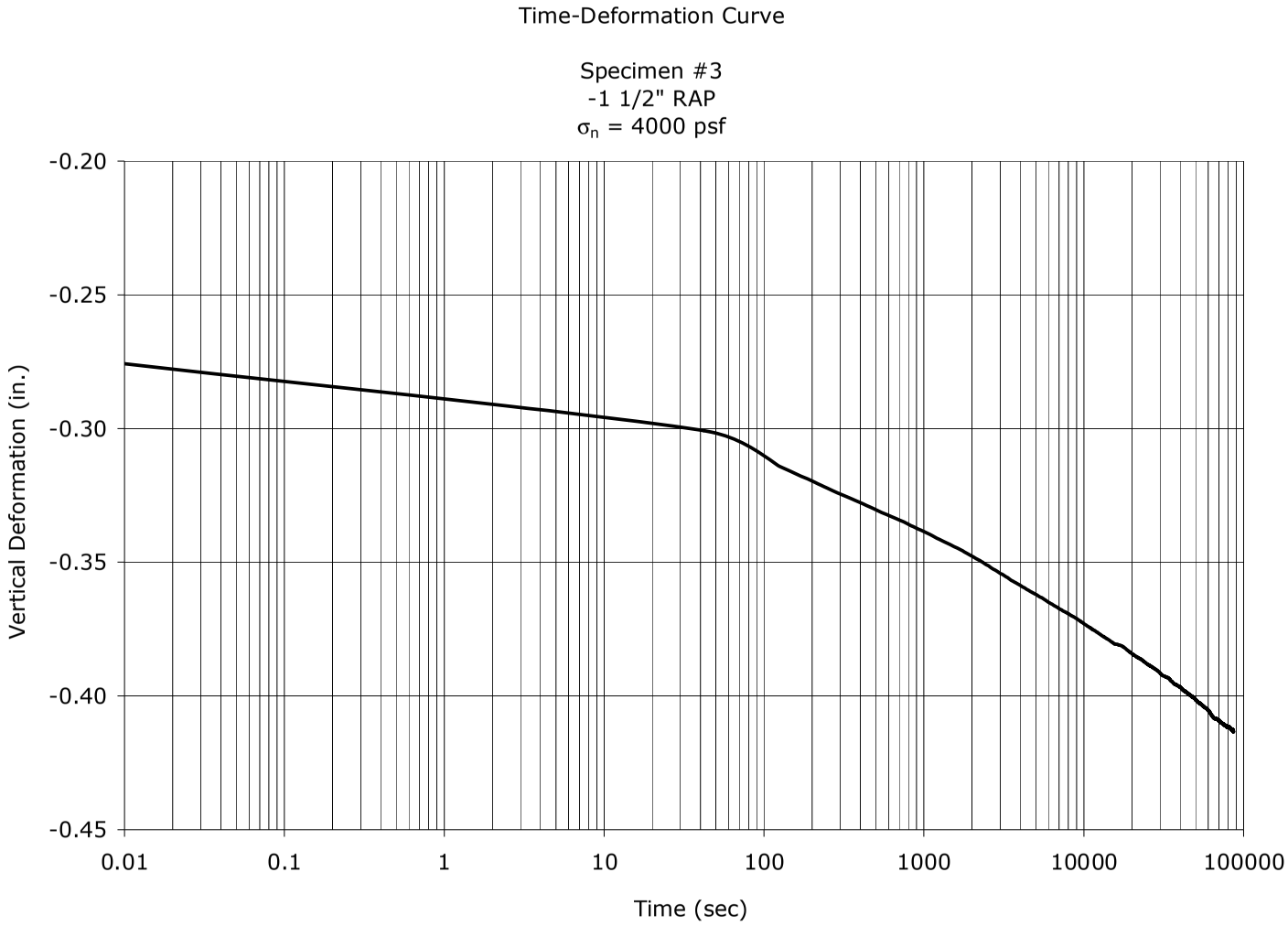
Time-Deformation Curve
Specimen #3
-1 1/2" RAP
σn = 4000 psf
Vertical Deformation (in.)
-0.20
-0.25
-0.30
-0.35
-0.40
-0.45
0.01
0.1
1
10
100
1000
10000
100000
Time (sec)

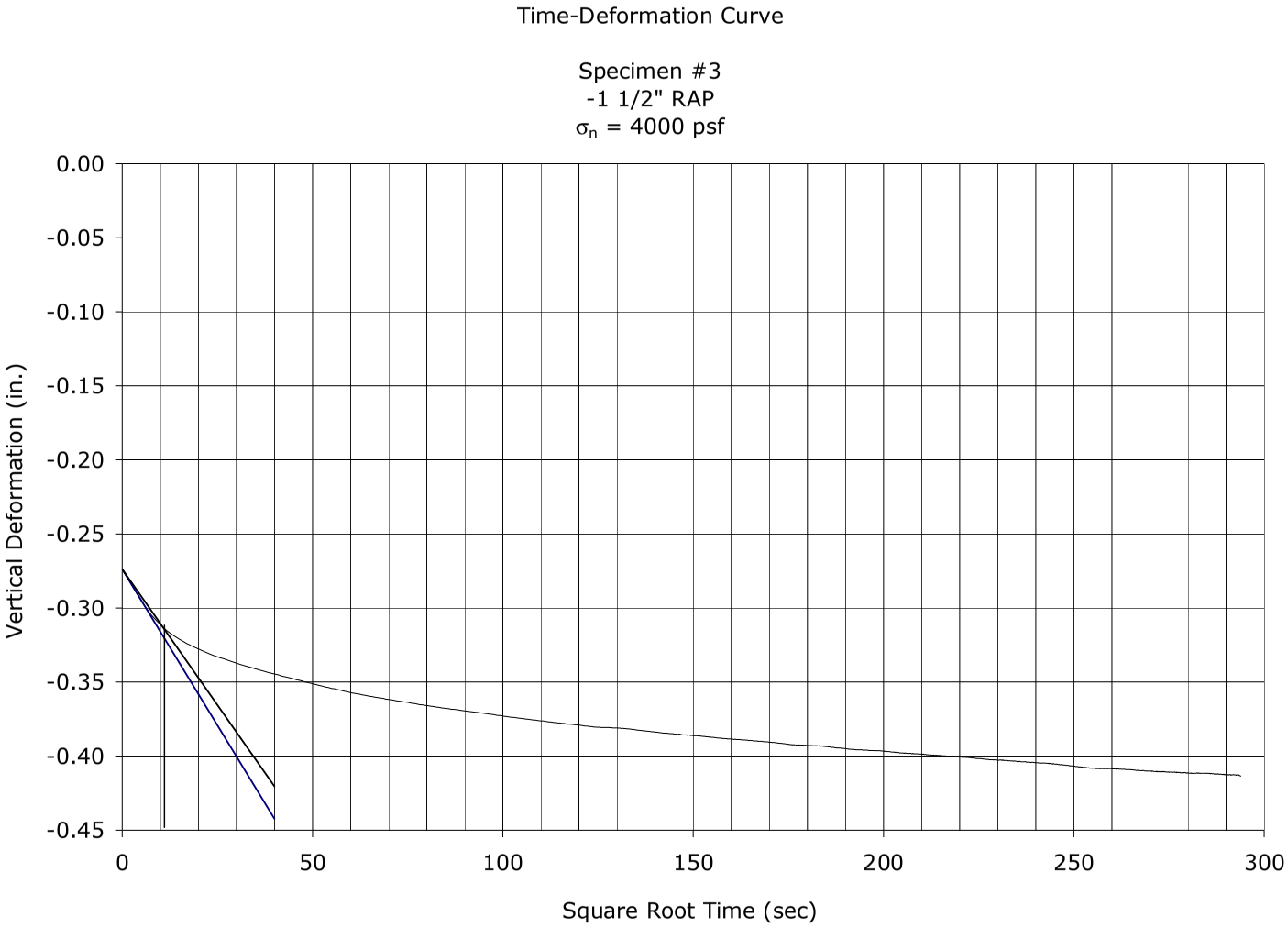
Time-Deformation Curve
Specimen #3
-1 1/2" RAP
σn = 4000 psf
Vertical Deformation (in.)
0.00
-0.05
-0.10
-0.15
-0.20
-0.25
-0.30
-0.35
-0.40
-0.45
0
50
100
150
200
250
300
Square Root Time (sec)

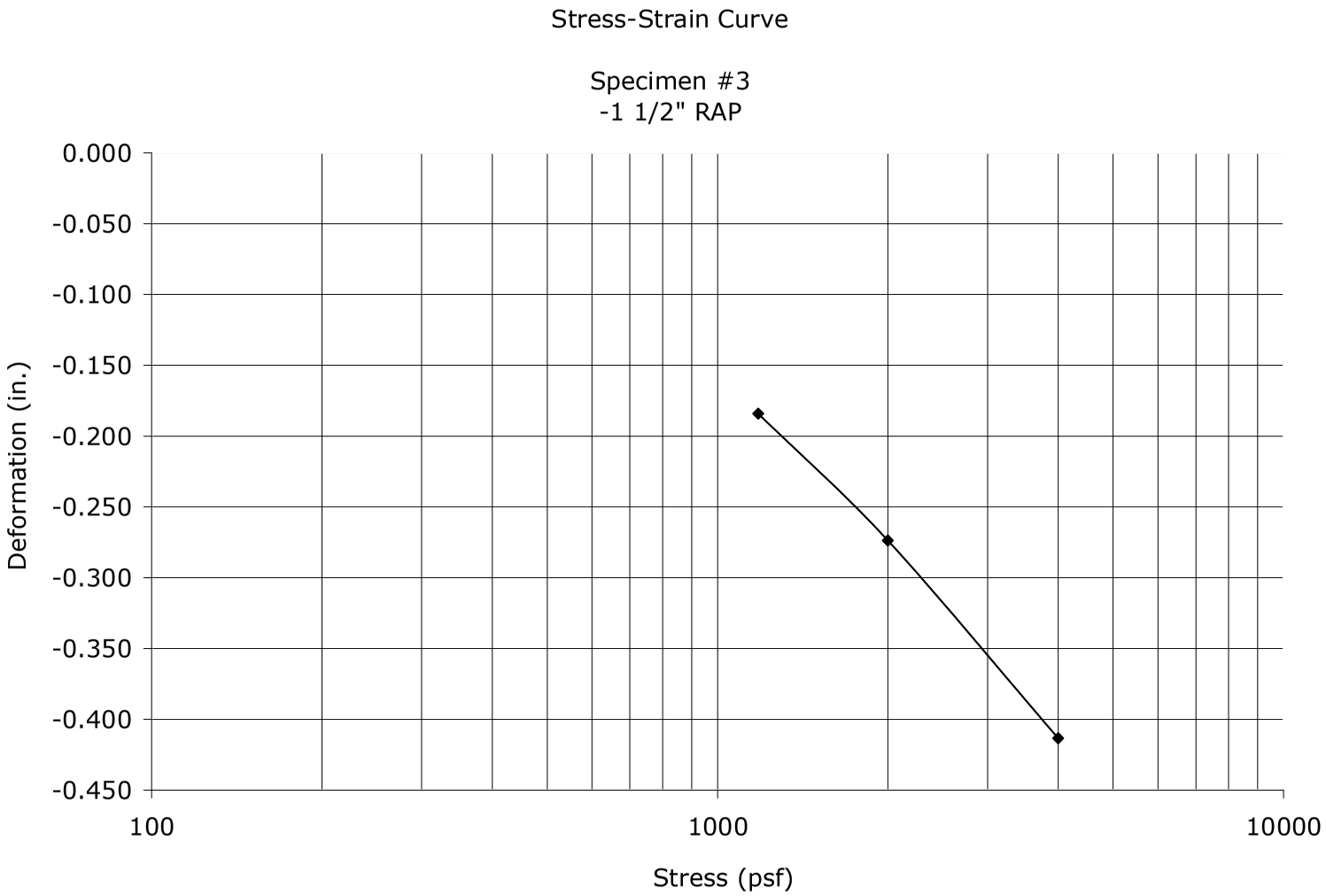
Stress-Strain Curve
Specimen #3
-1 1/2" RAP
0.000
-0.050
-0.100
-0.150
-0.200
-0.250
-0.300
-0.350
-0.400
-0.450
Deformation (in.)
100
1000
10000
Stress (psf)

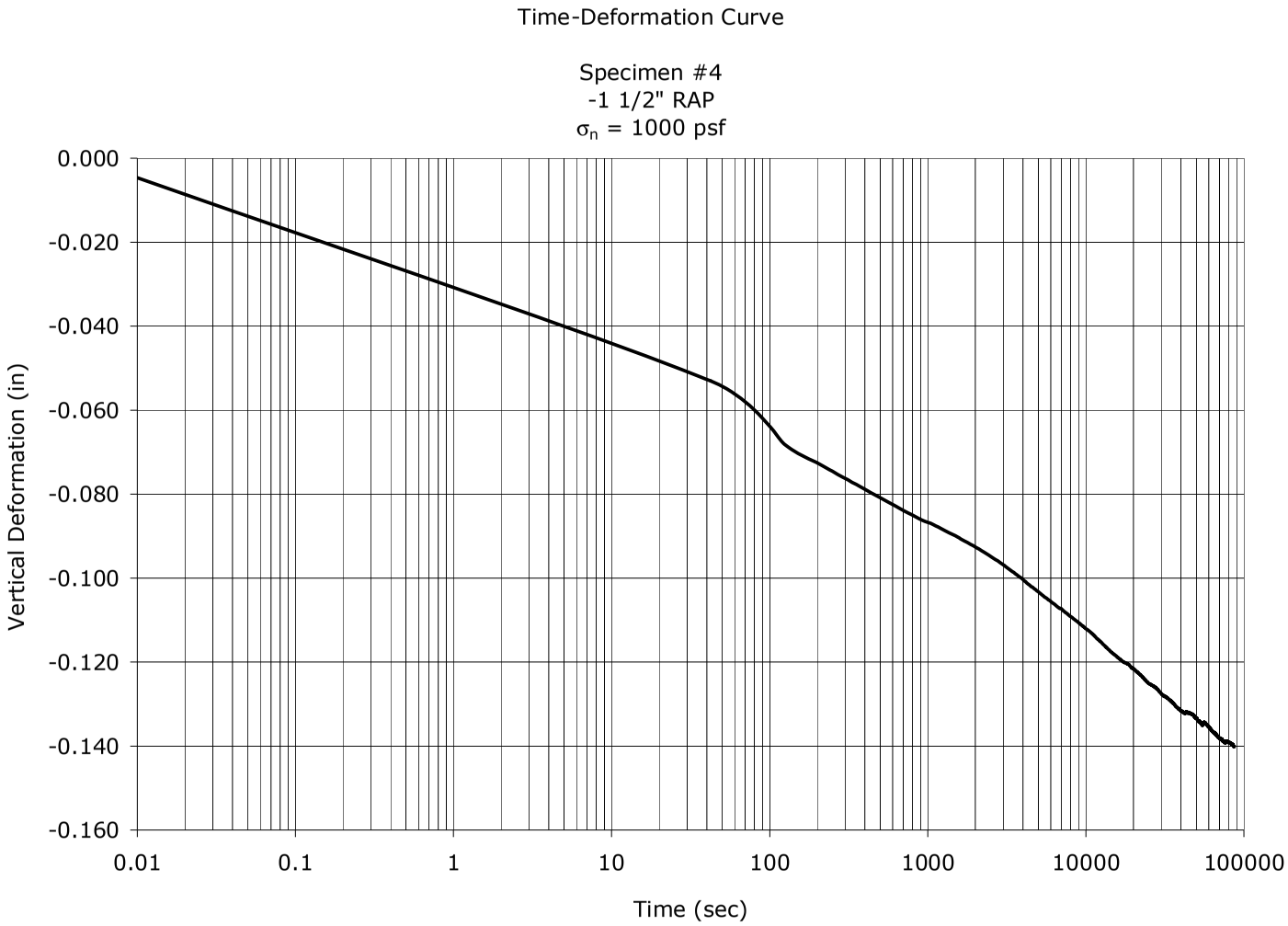
Time-Deformation Curve
Specimen #4
-1 1/2" RAP
σn = 1000 psf
0.000
-0.020
-0.040
-0.060
-0.080
-0.100
-0.120
-0.140
-0.160
Vertical Deformation (in)
0.01
0.1
1
10
100
1000
10000
100000
Time (sec)

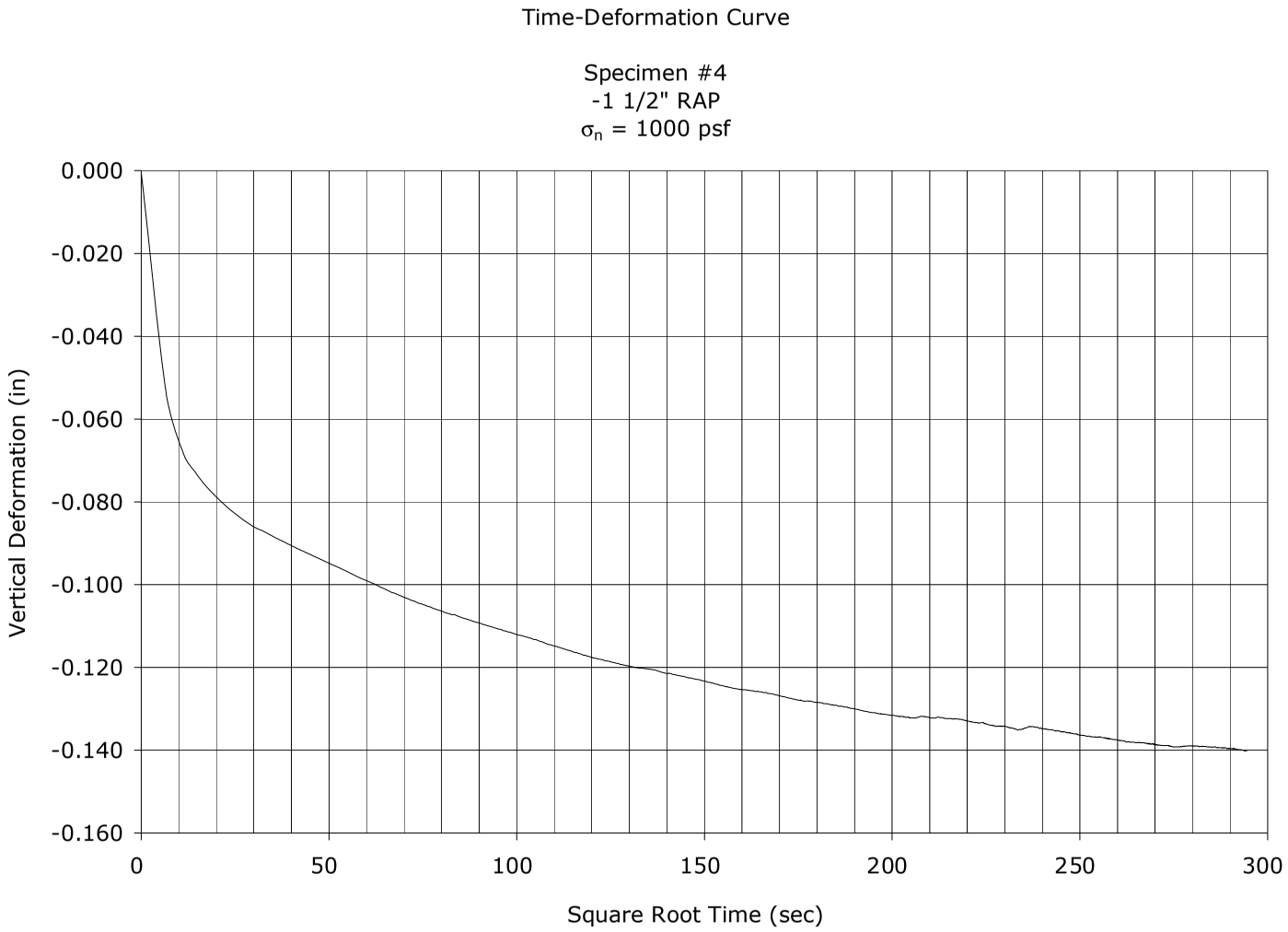
Time-Deformation Curve
Specimen #4
-1 1/2" RAP
σ_n = 1000 psf
Vertical Deformation (in)
0.000
-0.020
-0.040
-0.060
-0.080
-0.100
-0.120
-0.140
-0.160
0
50
100
150
200
250
300
Square Root Time (sec)

Time-Deformation Curve

Specimen #4
-1 1/2" RAP
σ_n = 2000 psf

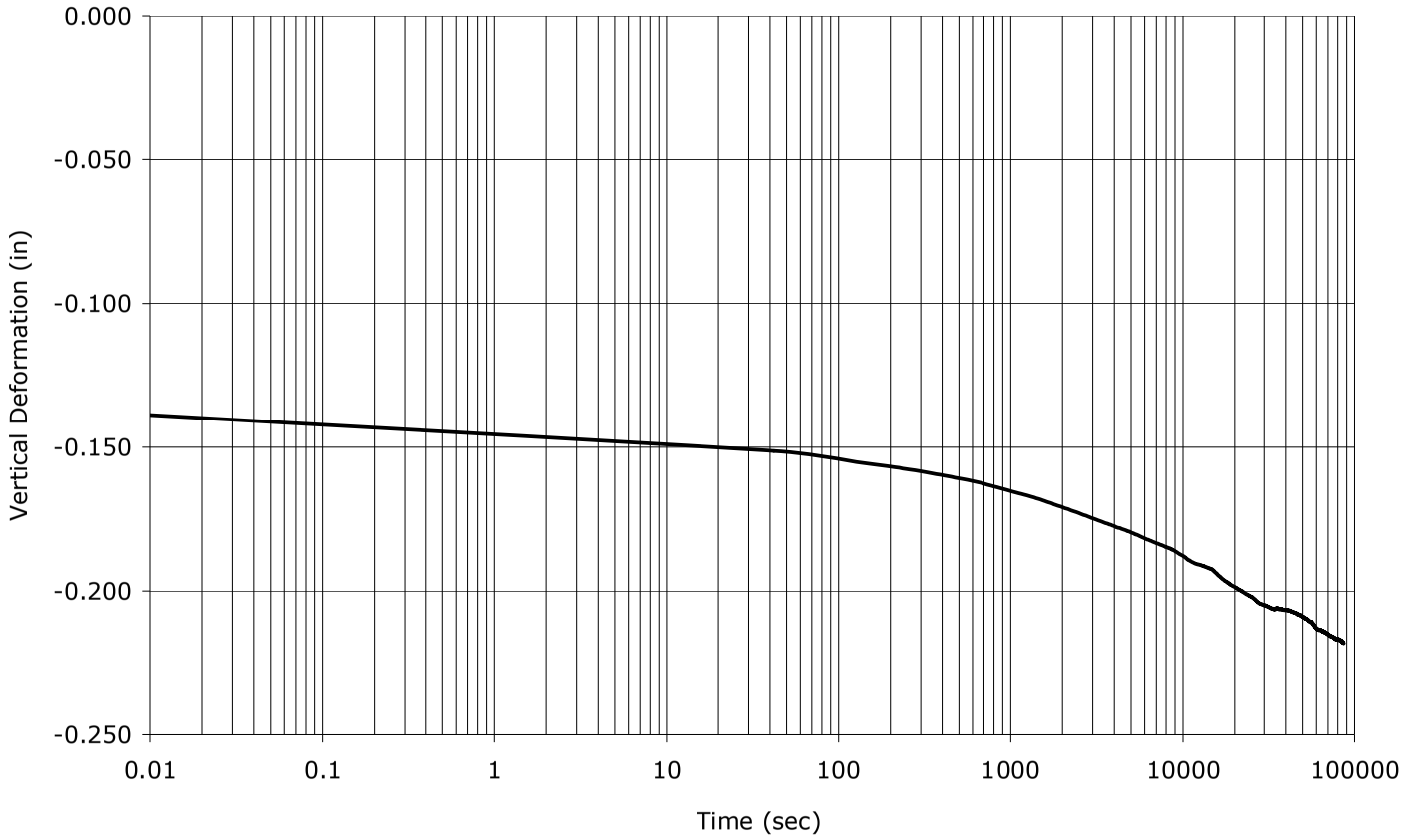

Time-Deformation Curve

Specimen #4
-1 1/2" RAP
σ_n = 2000 psf

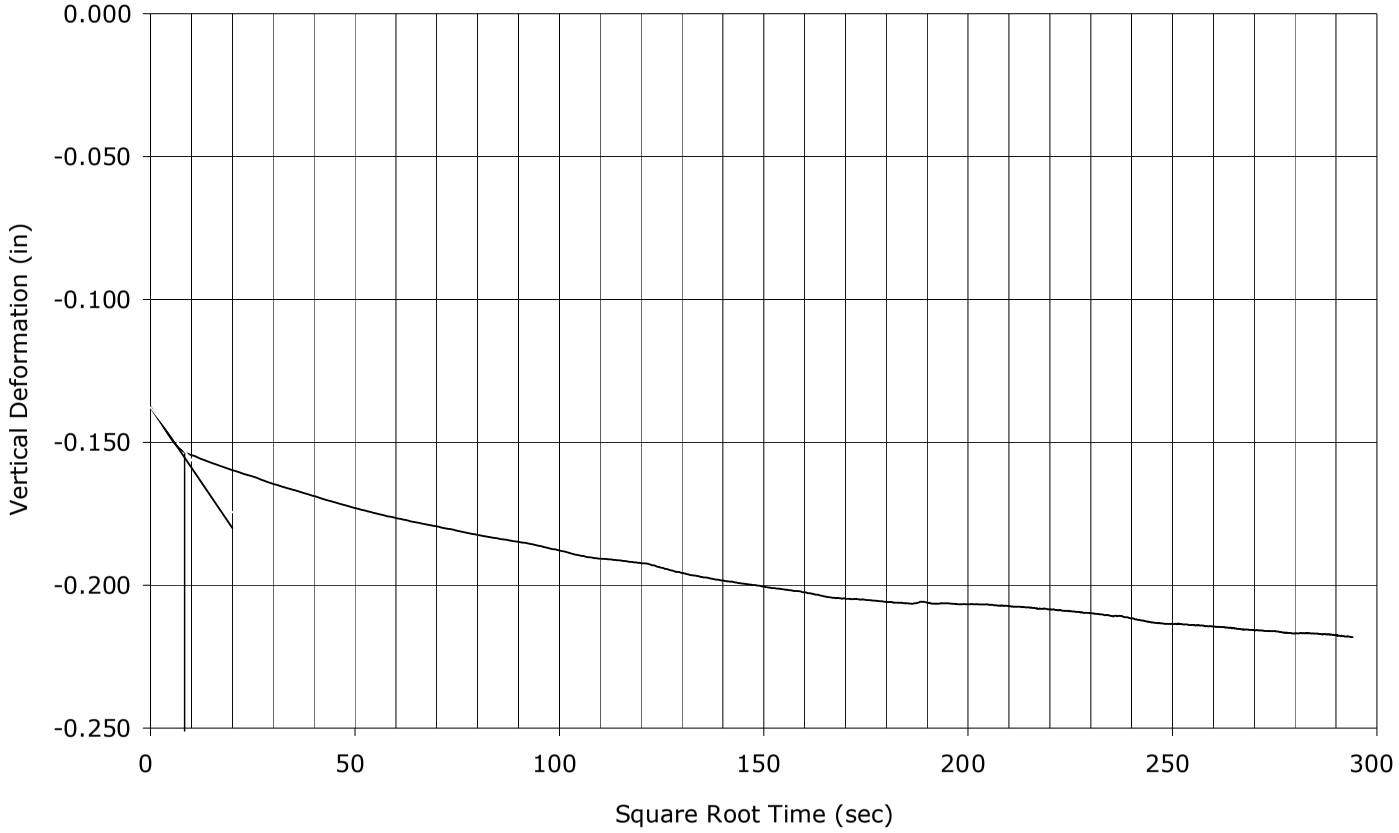

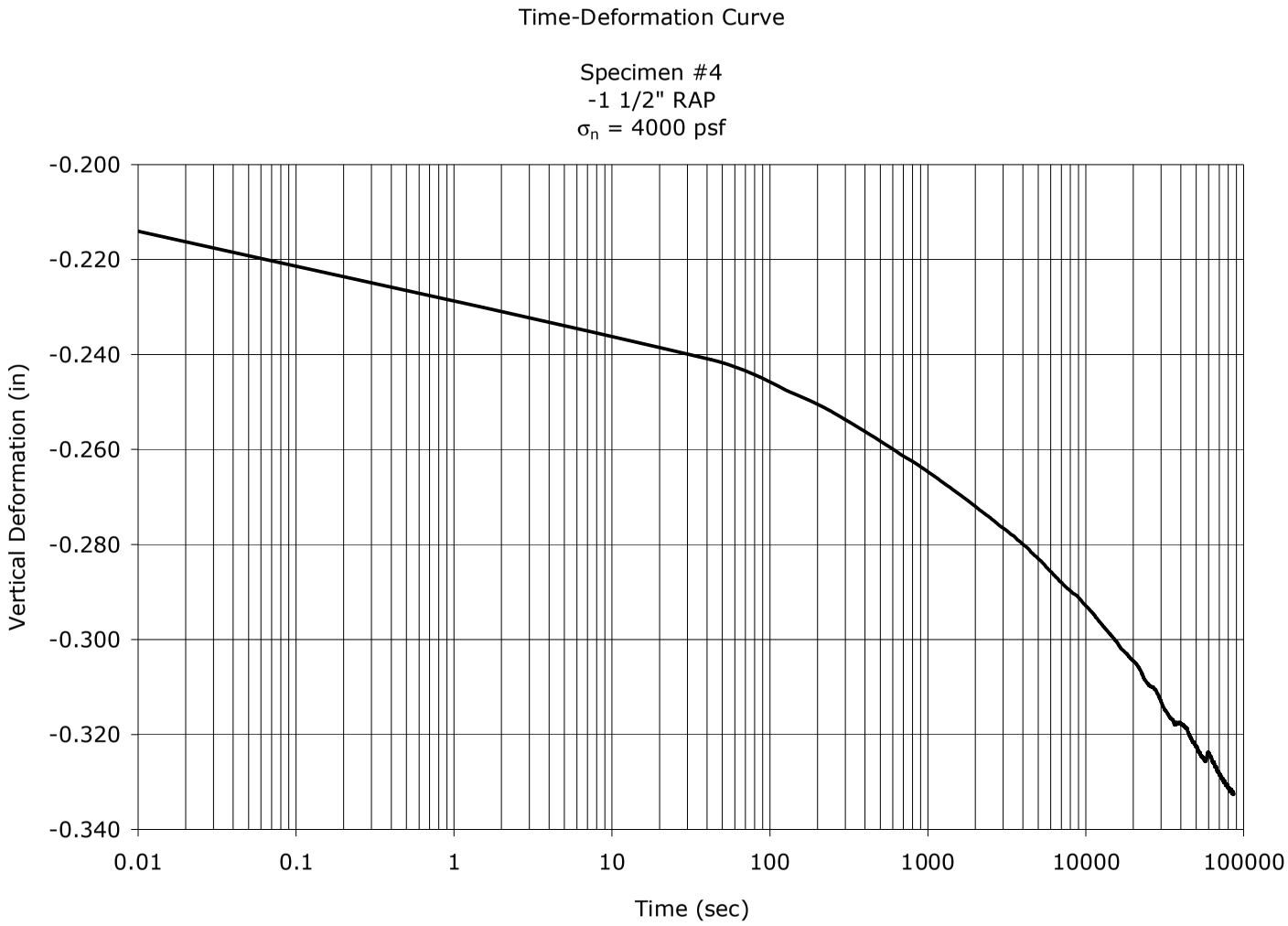
Time-Deformation Curve
Specimen #4
-1 1/2" RAP
σn = 4000 psf
Vertical Deformation (in)
-0.200
-0.220
-0.240
-0.260
-0.280
-0.300
-0.320
-0.340
0.01
0.1
1
10
100
1000
10000
100000
Time (sec)

Time-Deformation Curve

Specimen #4
-1 1/2" RAP
σ_n = 4000 psf

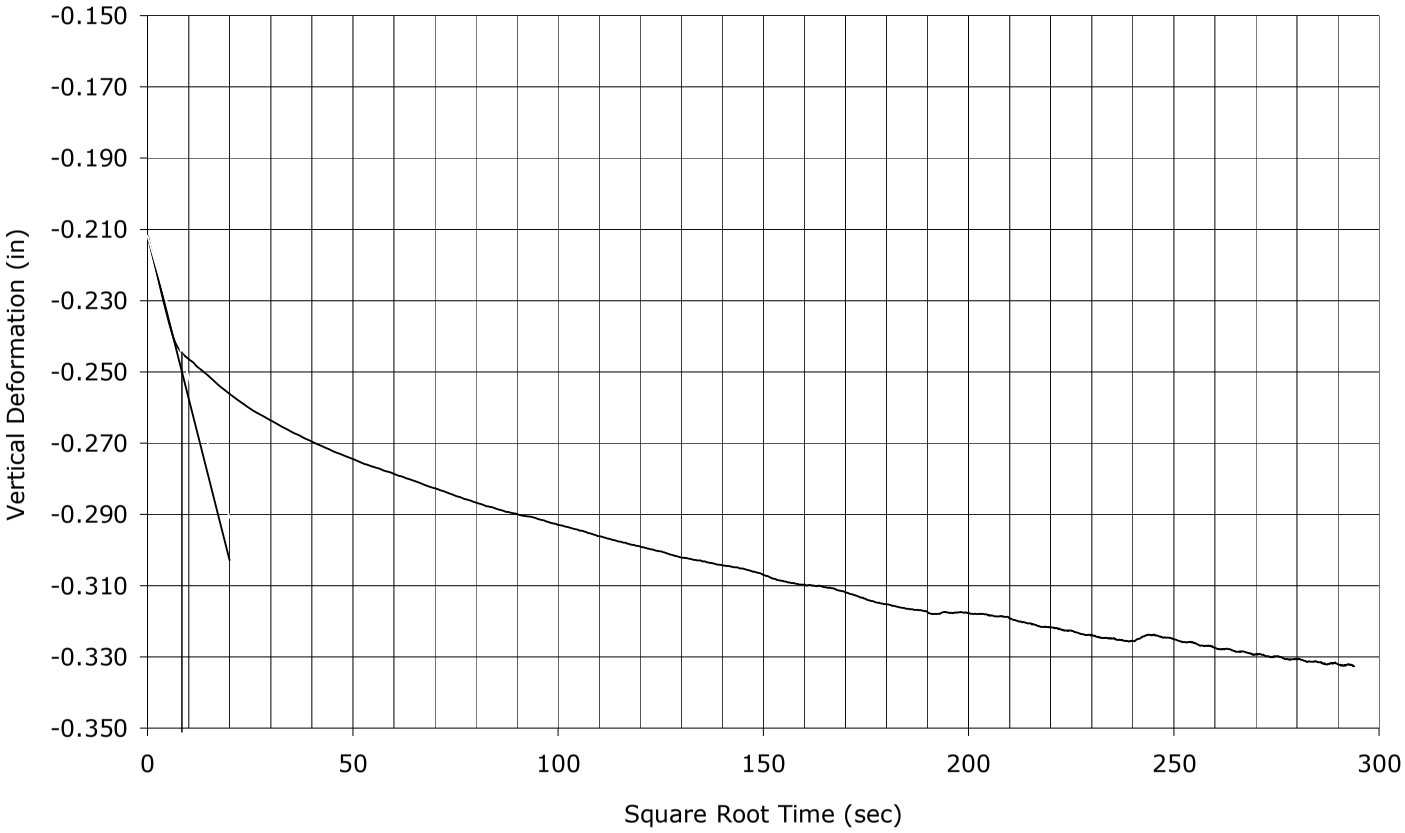

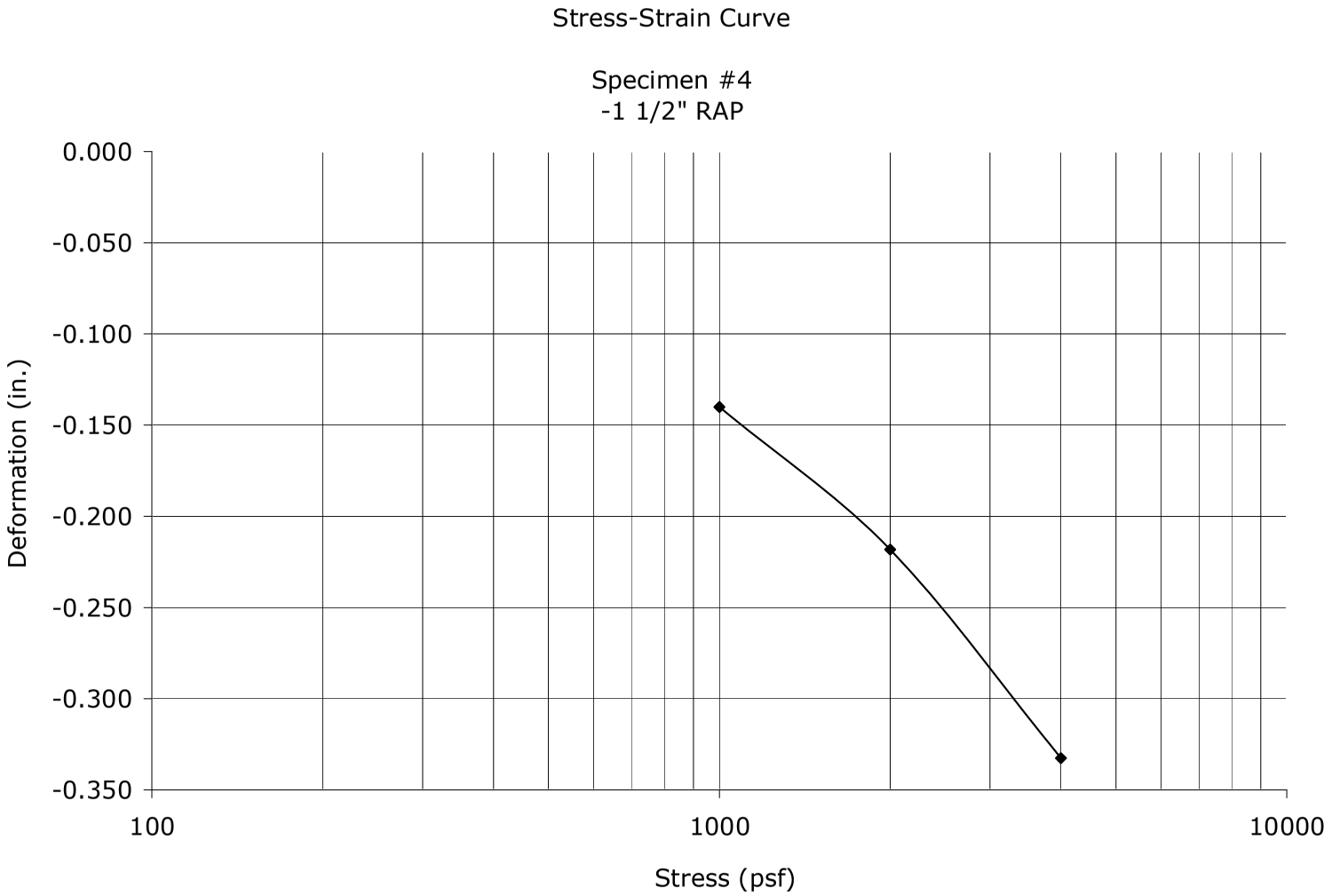
Stress-Strain Curve
Specimen #4
-1 1/2" RAP
0.000
-0.050
-0.100
-0.150
-0.200
-0.250
-0.300
-0.350
Deformation (in.)
100
1000
10000
Stress (psf)

Time-Deformation Curve

Specimen #5
-3/4" RAP
σ_n = 1000 psf

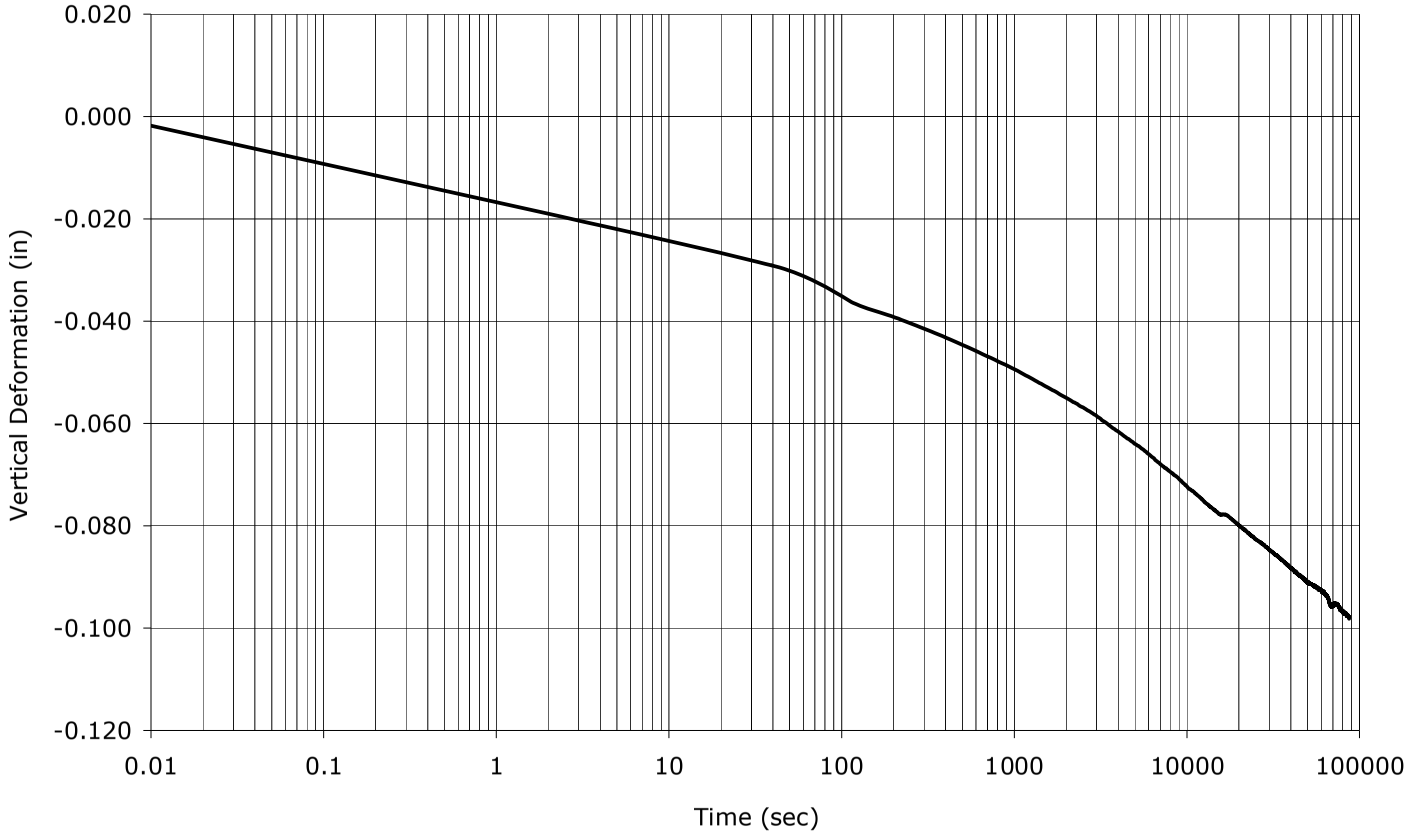

Time-Deformation Curve

Specimen #5
-3/4" RAP
σ_n = 1000 psf

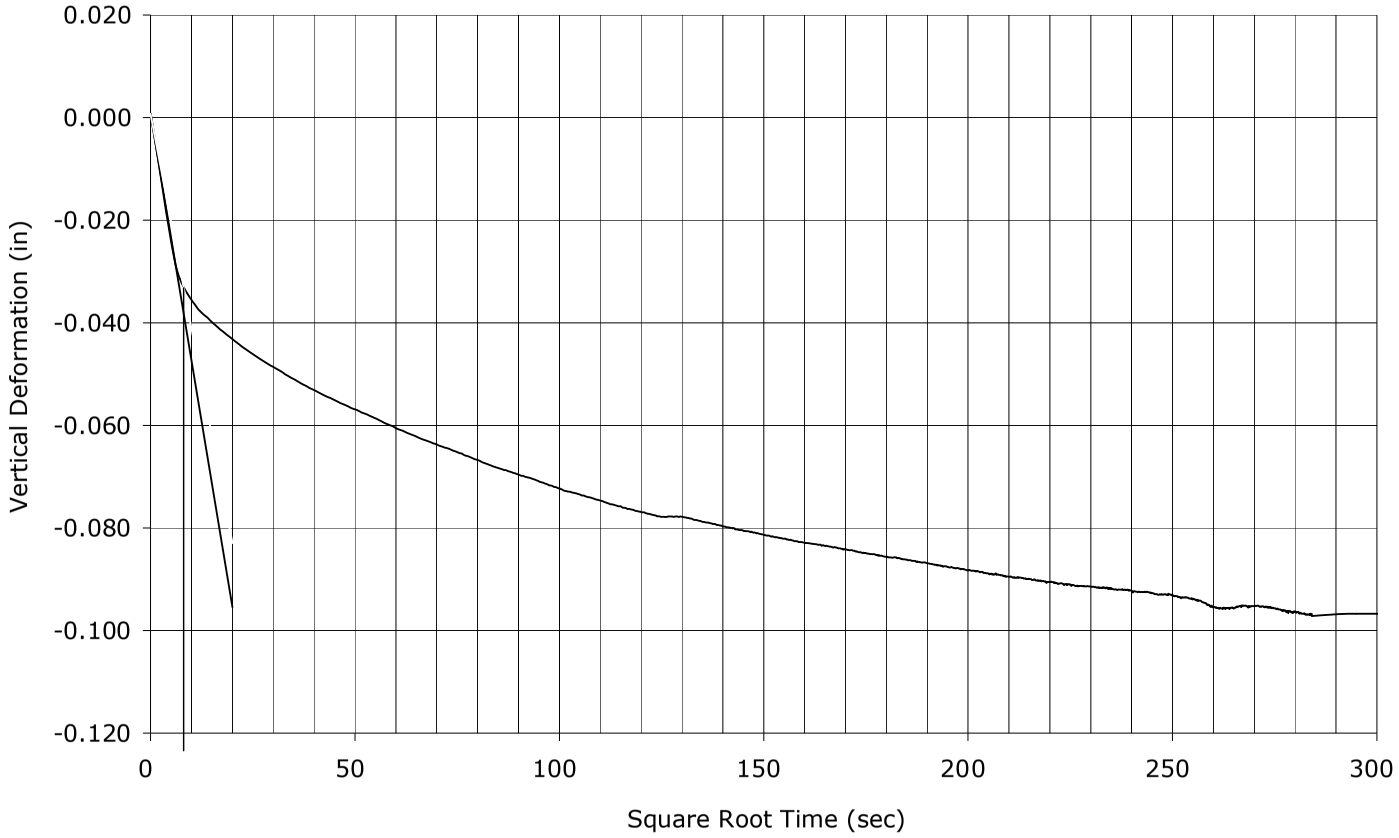

Time-Deformation Curve

Specimen #5
-3/4" RAP
σ_n = 2000 psf

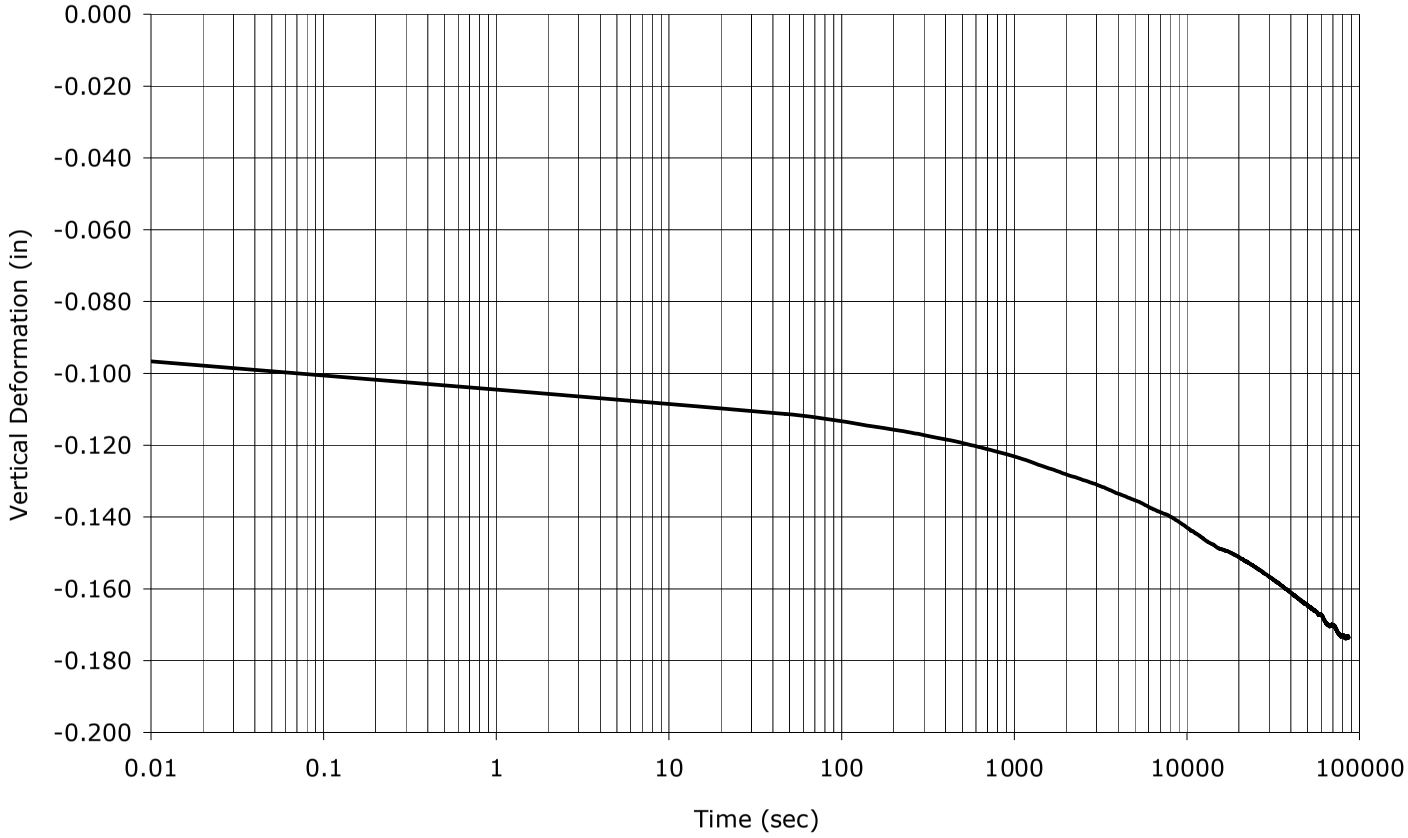

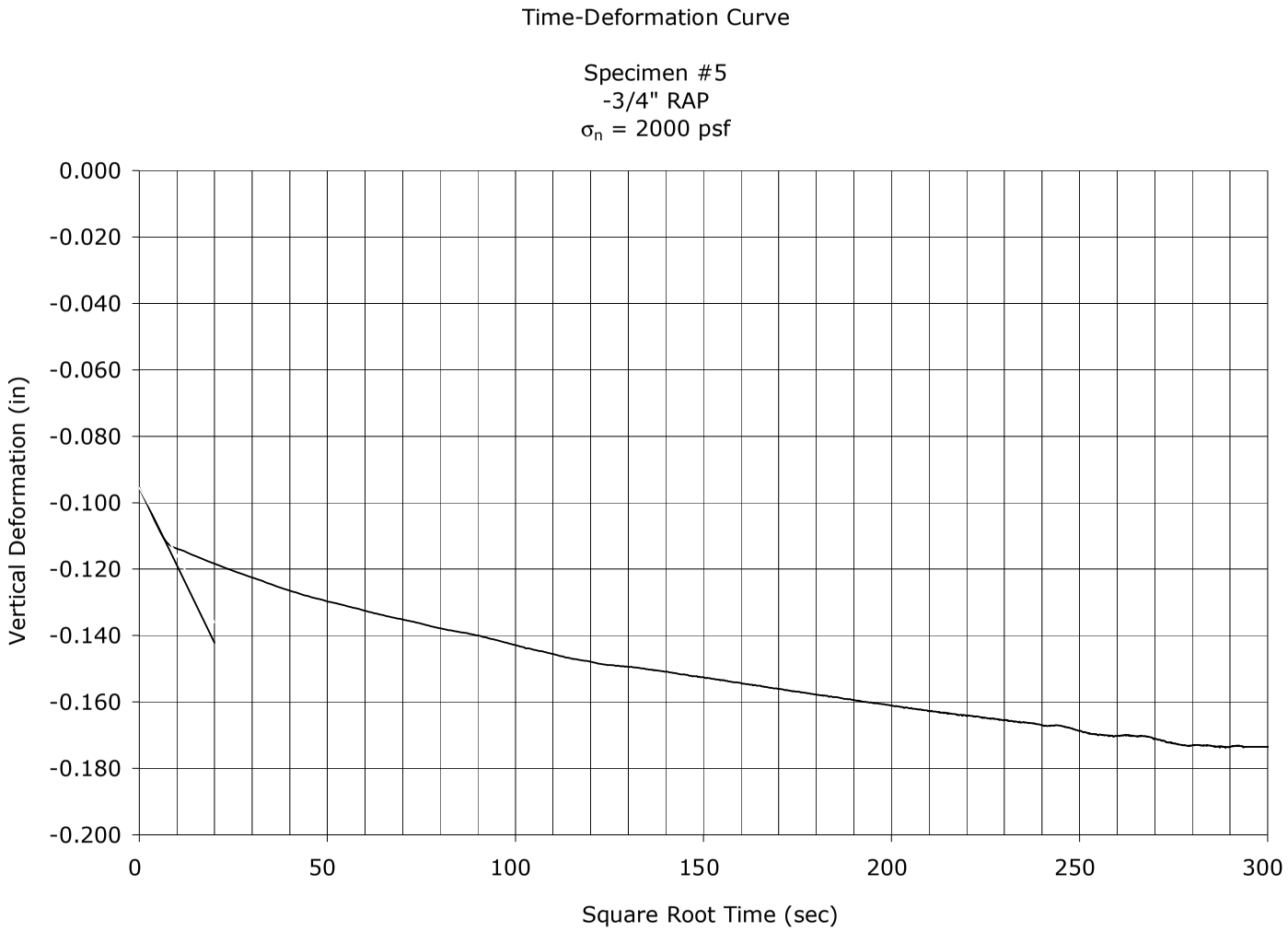
Time-Deformation Curve
Specimen #5
-3/4" RAP
σn = 2000 psf
Vertical Deformation (in)
0.000
-0.020
-0.040
-0.060
-0.080
-0.100
-0.120
-0.140
-0.160
-0.180
-0.200
0
50
100
150
200
250
300
Square Root Time (sec)

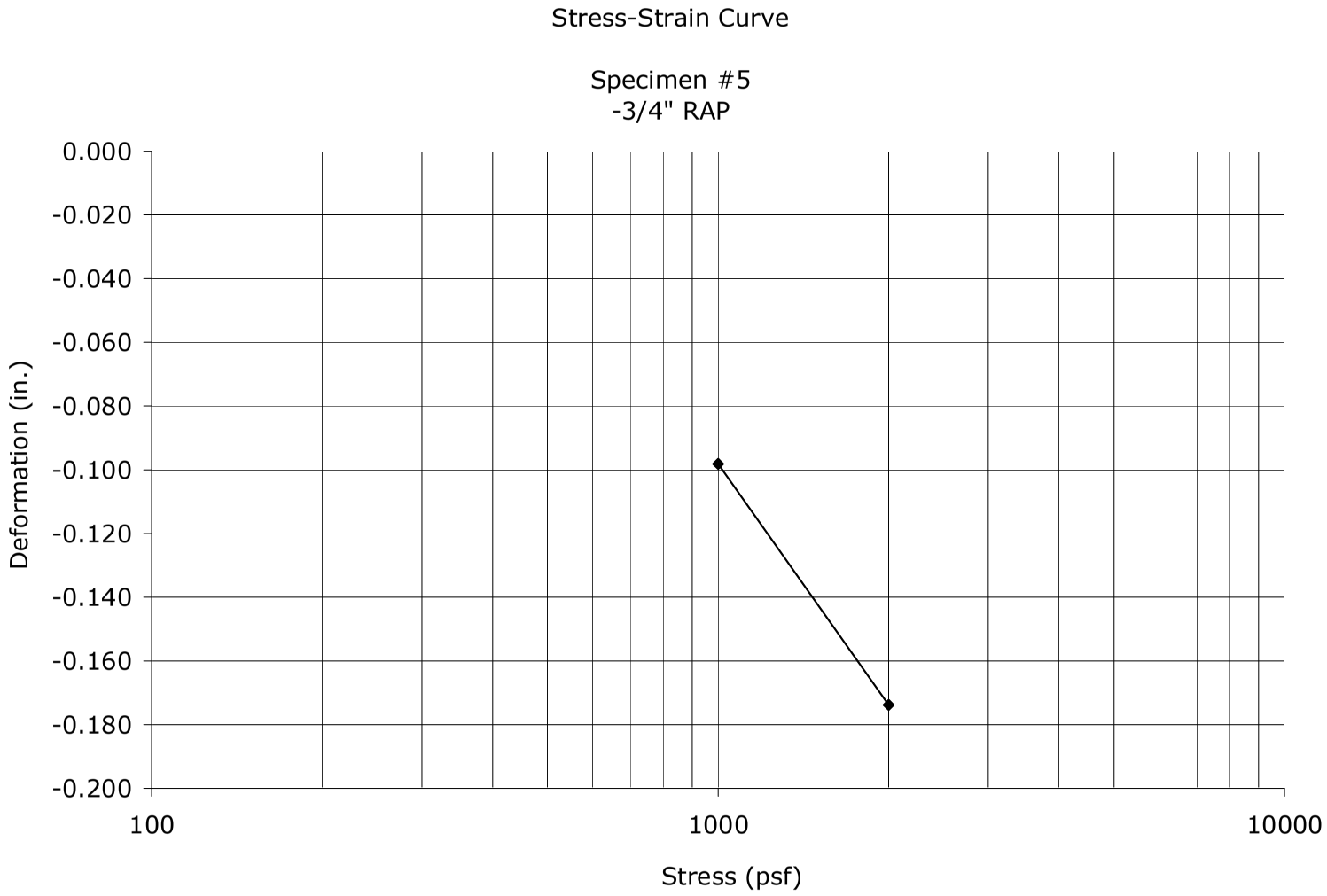
Stress-Strain Curve
Specimen #5
-3/4" RAP
0.000
-0.020
-0.040
-0.060
-0.080
-0.100
-0.120
-0.140
-0.160
-0.180
-0.200
Deformation (in.)
100
1000
10000
Stress (psf)

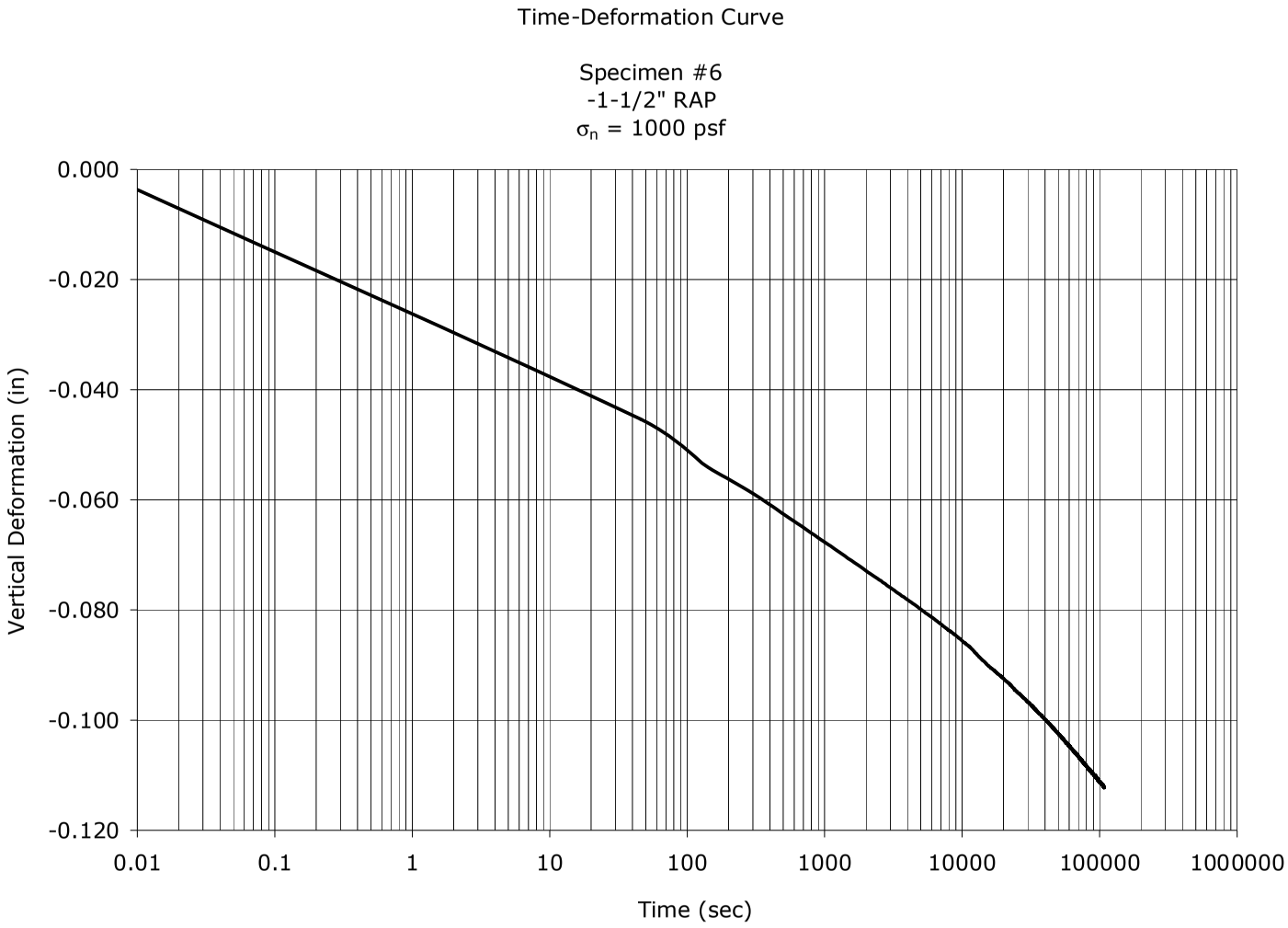
Time-Deformation Curve
Specimen #6
-1-1/2" RAP
σ_n = 1000 psf
0.000
-0.020
-0.040
-0.060
-0.080
-0.100
-0.120
Vertical Deformation (in)
0.01
0.1
1
10
100
1000
10000
100000
1000000
Time (sec)

Time-Deformation Curve

Specimen #6
-1-1/2" RAP
σ_n = 1000 psf

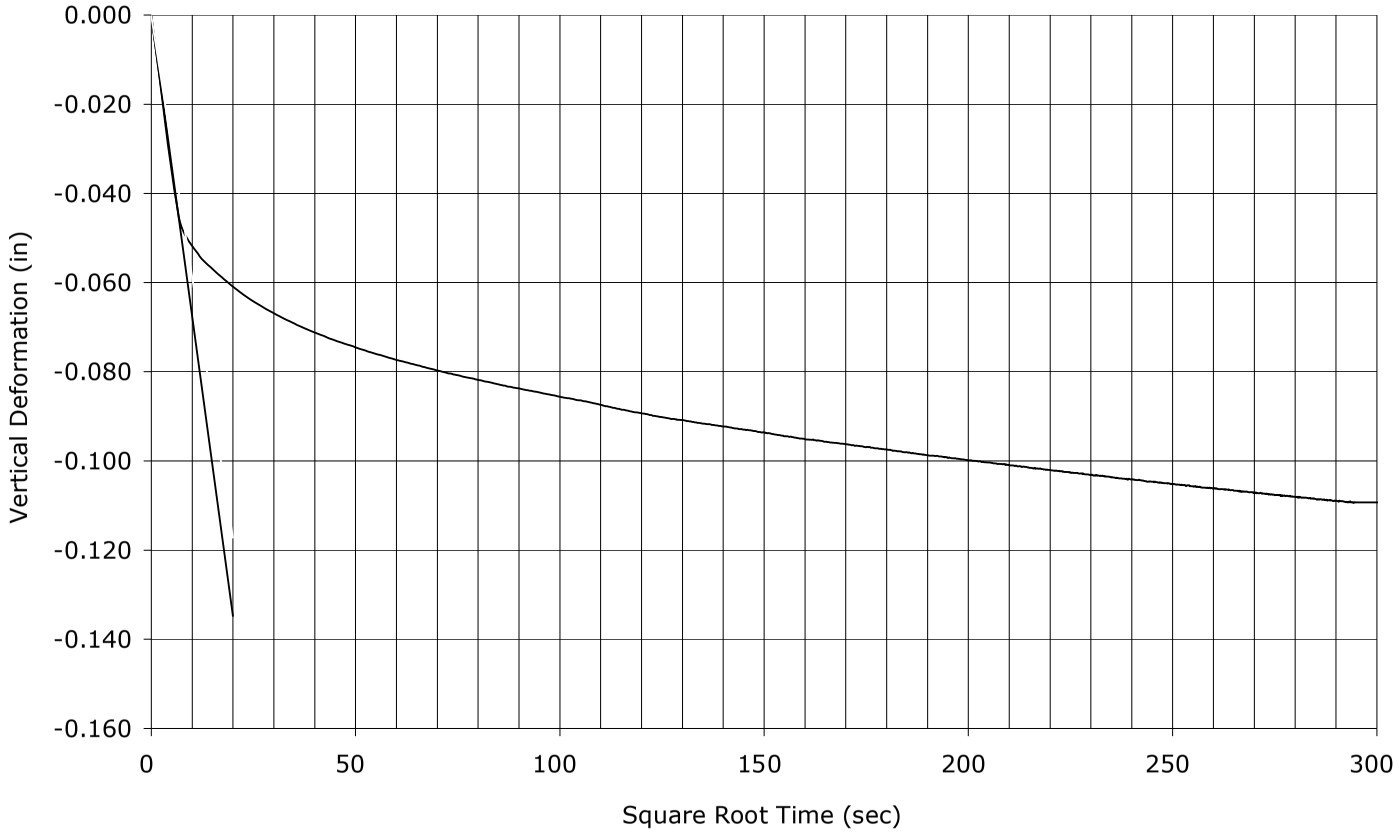

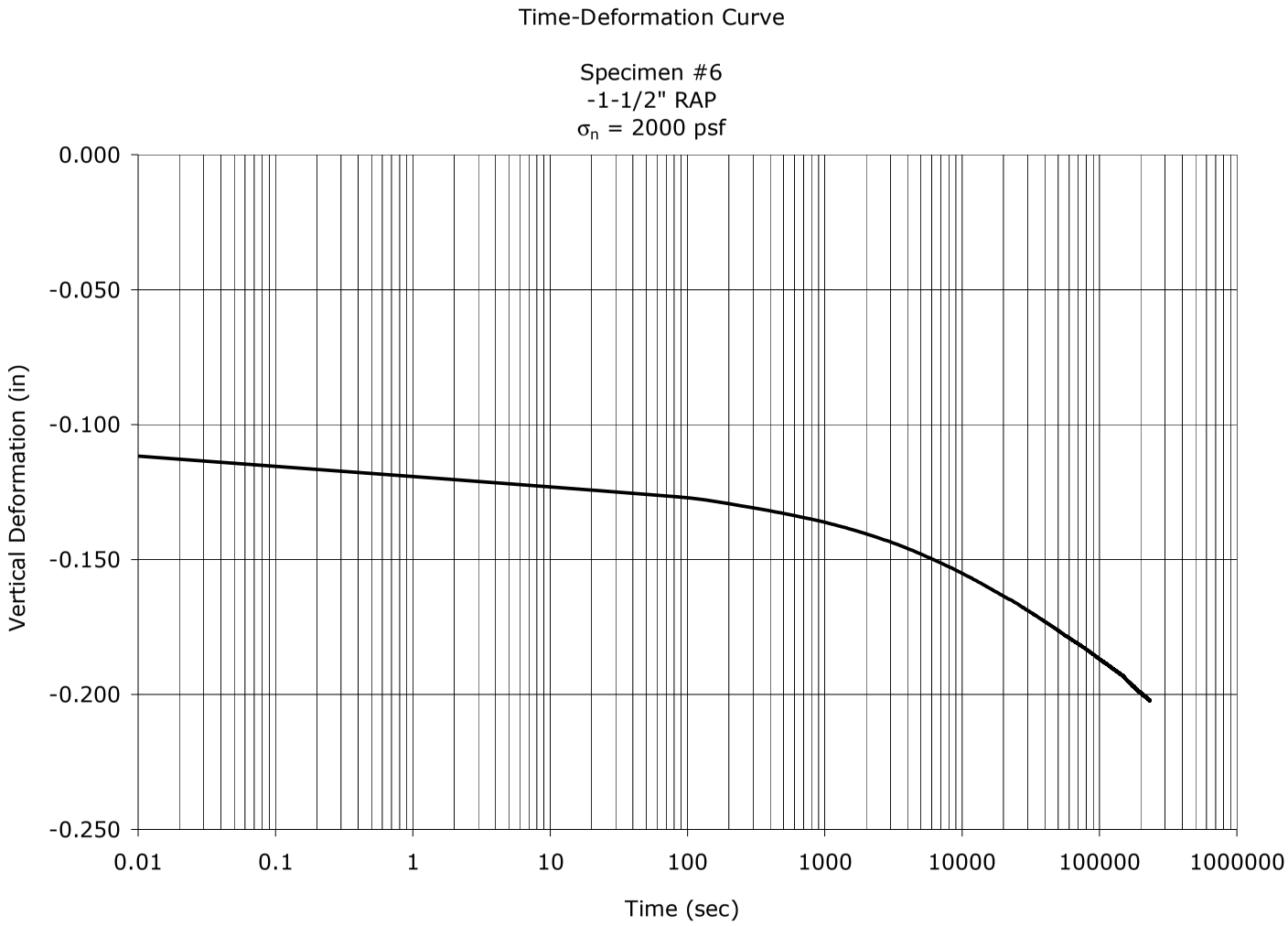
Time-Deformation Curve
Specimen #6
-1-1/2" RAP
σn = 2000 psf
0.000
-0.050
-0.100
-0.150
-0.200
-0.250
Vertical Deformation (in)
0.01
0.1
1
10
100
1000
10000
100000
1000000
Time (sec)

Time-Deformation Curve

Specimen #6
-1-1/2" RAP
σ_n = 2000 psf

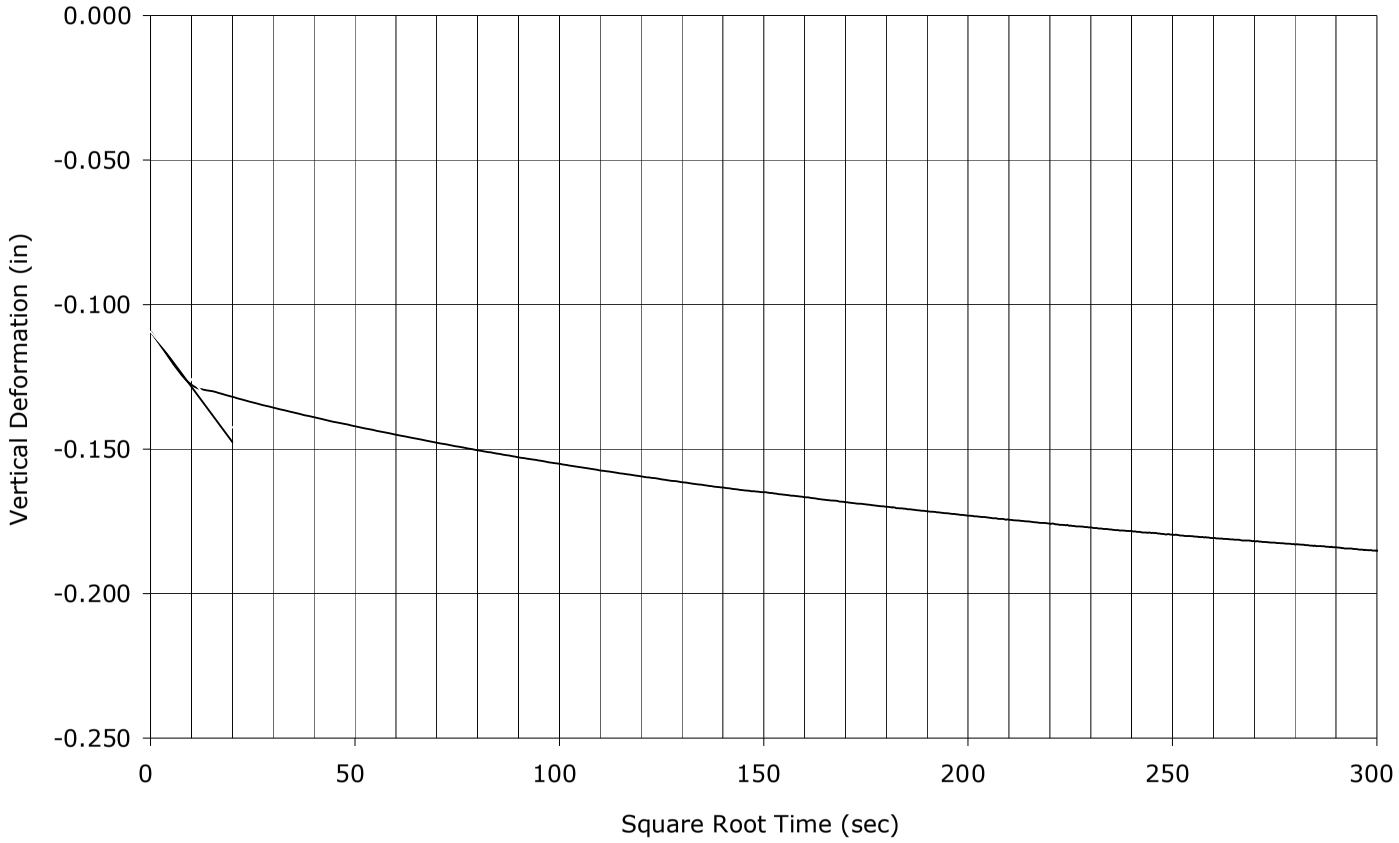

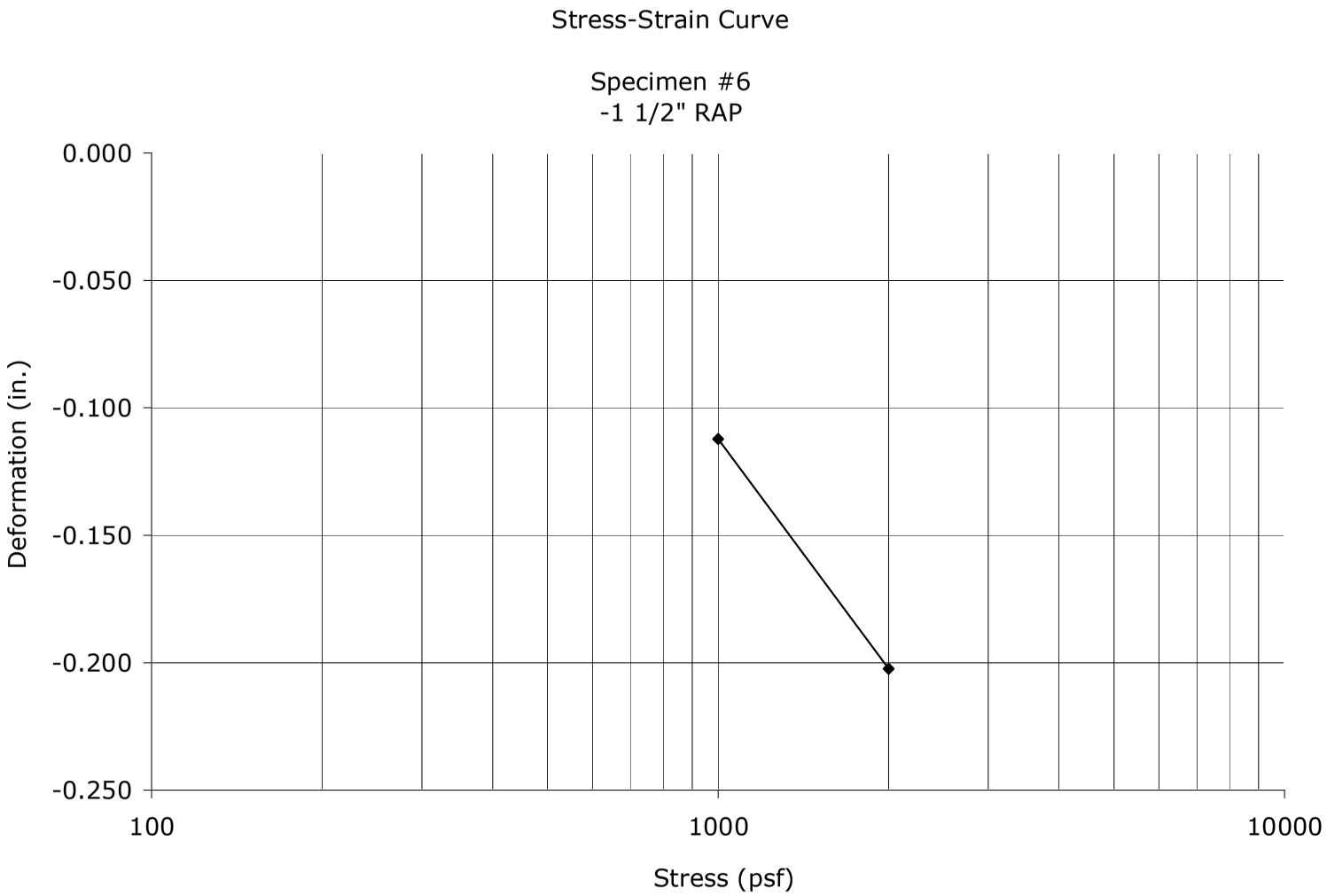
Stress-Strain Curve
Specimen #6
-1 1/2" RAP
0.000
-0.050
-0.100
-0.150
-0.200
-0.250
Deformation (in.)
100
1000
10000
Stress (psf)

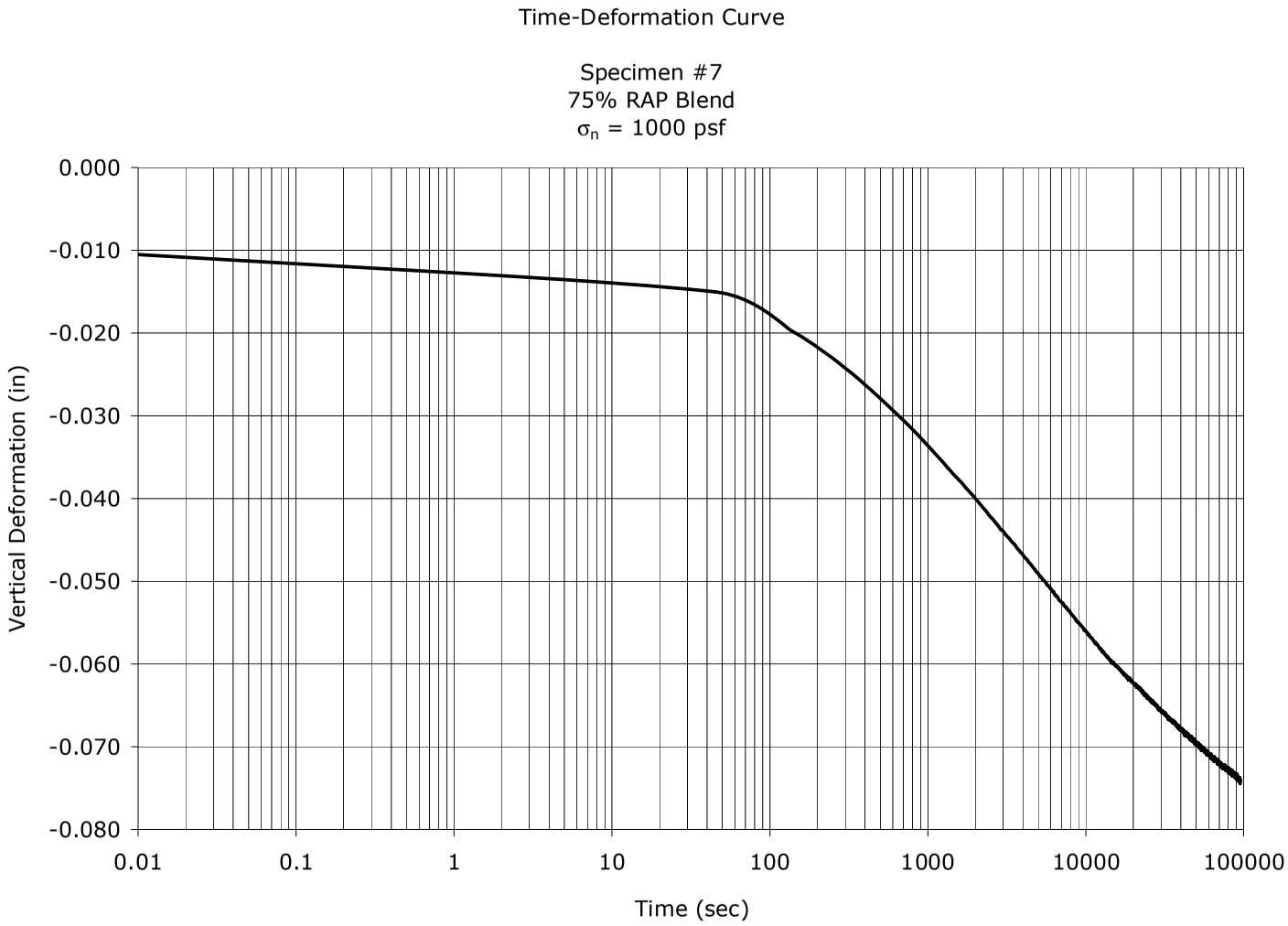
Time-Deformation Curve
Specimen #7
75% RAP Blend
σ_n = 1000 psf
Vertical Deformation (in)
0.000
-0.010
-0.020
-0.030
-0.040
-0.050
-0.060
-0.070
-0.080
0.01
0.1
1
10
100
1000
10000
100000
Time (sec)

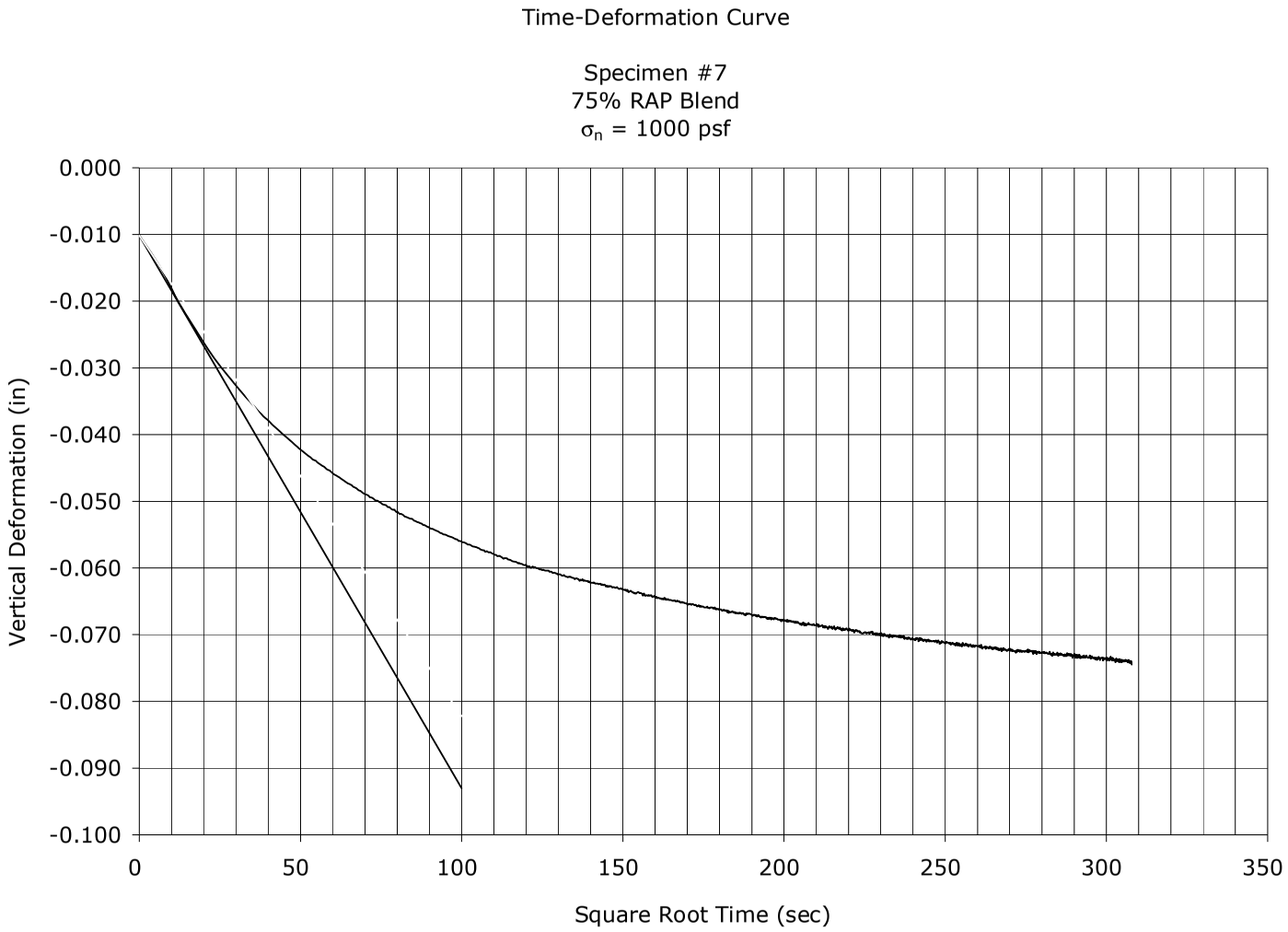
Time-Deformation Curve
Specimen #7
75% RAP Blend
σ_n = 1000 psf
Vertical Deformation (in)
0.000
-0.010
-0.020
-0.030
-0.040
-0.050
-0.060
-0.070
-0.080
-0.090
-0.100
0
50
100
150
200
250
300
350
Square Root Time (sec)

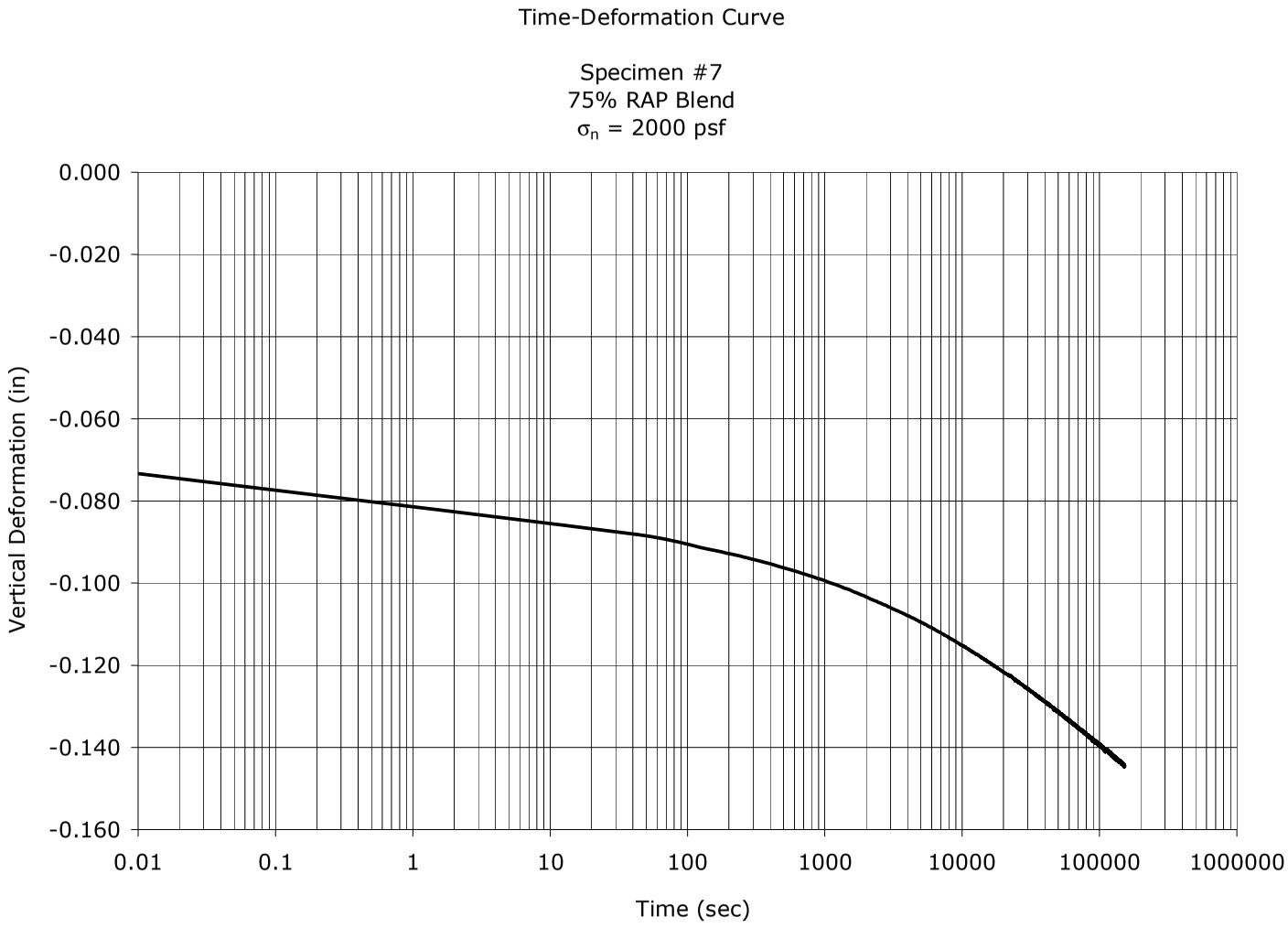
Time-Deformation Curve
Specimen #7
75% RAP Blend
σn = 2000 psf
Vertical Deformation (in)
0.000
-0.020
-0.040
-0.060
-0.080
-0.100
-0.120
-0.140
-0.160
0.01
0.1
1
10
100
1000
10000
100000
1000000
Time (sec)

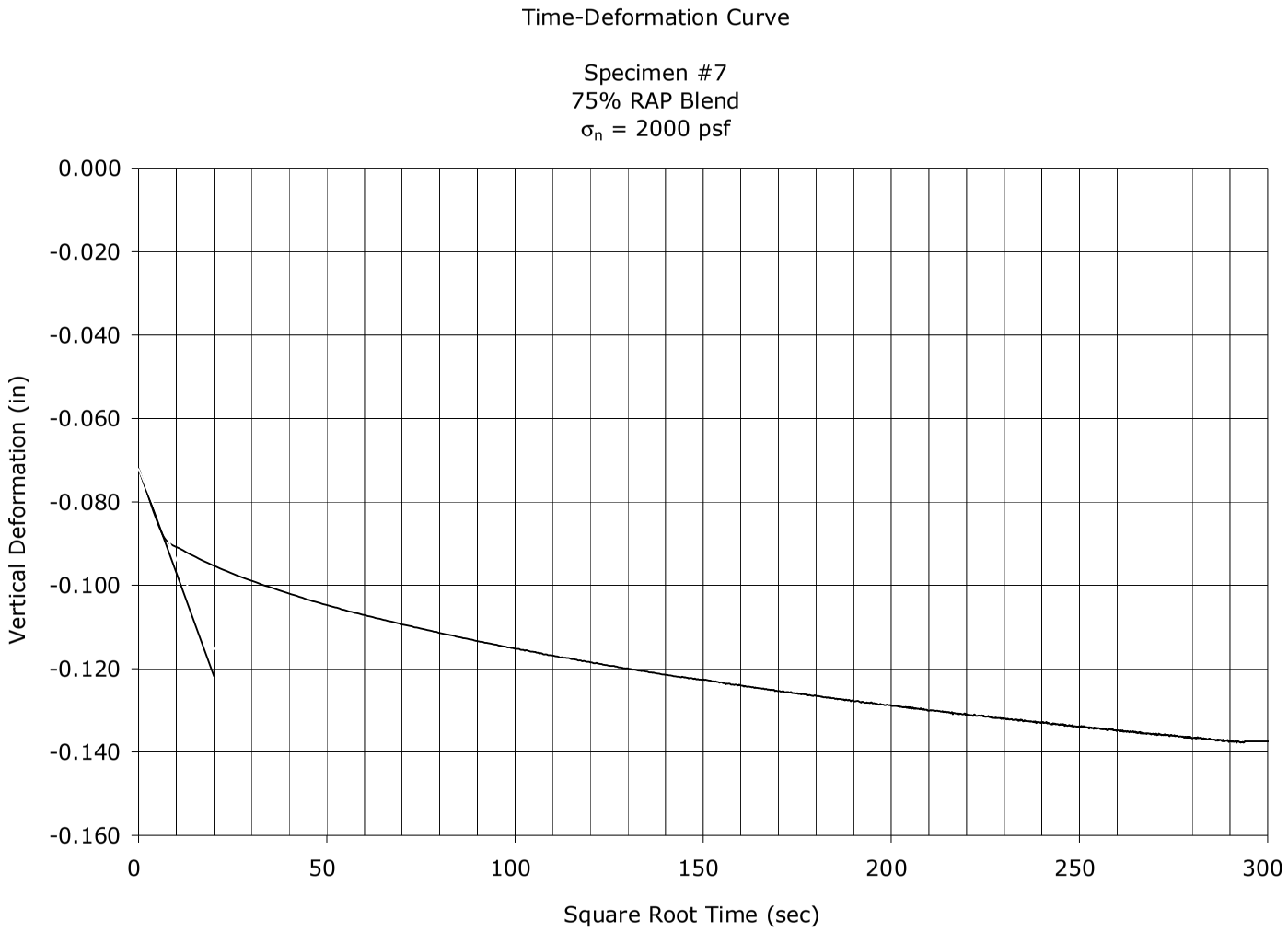
Time-Deformation Curve
Specimen #7
75% RAP Blend
σ_n = 2000 psf
Vertical Deformation (in)
0.000
-0.020
-0.040
-0.060
-0.080
-0.100
-0.120
-0.140
-0.160
0
50
100
150
200
250
300
Square Root Time (sec)

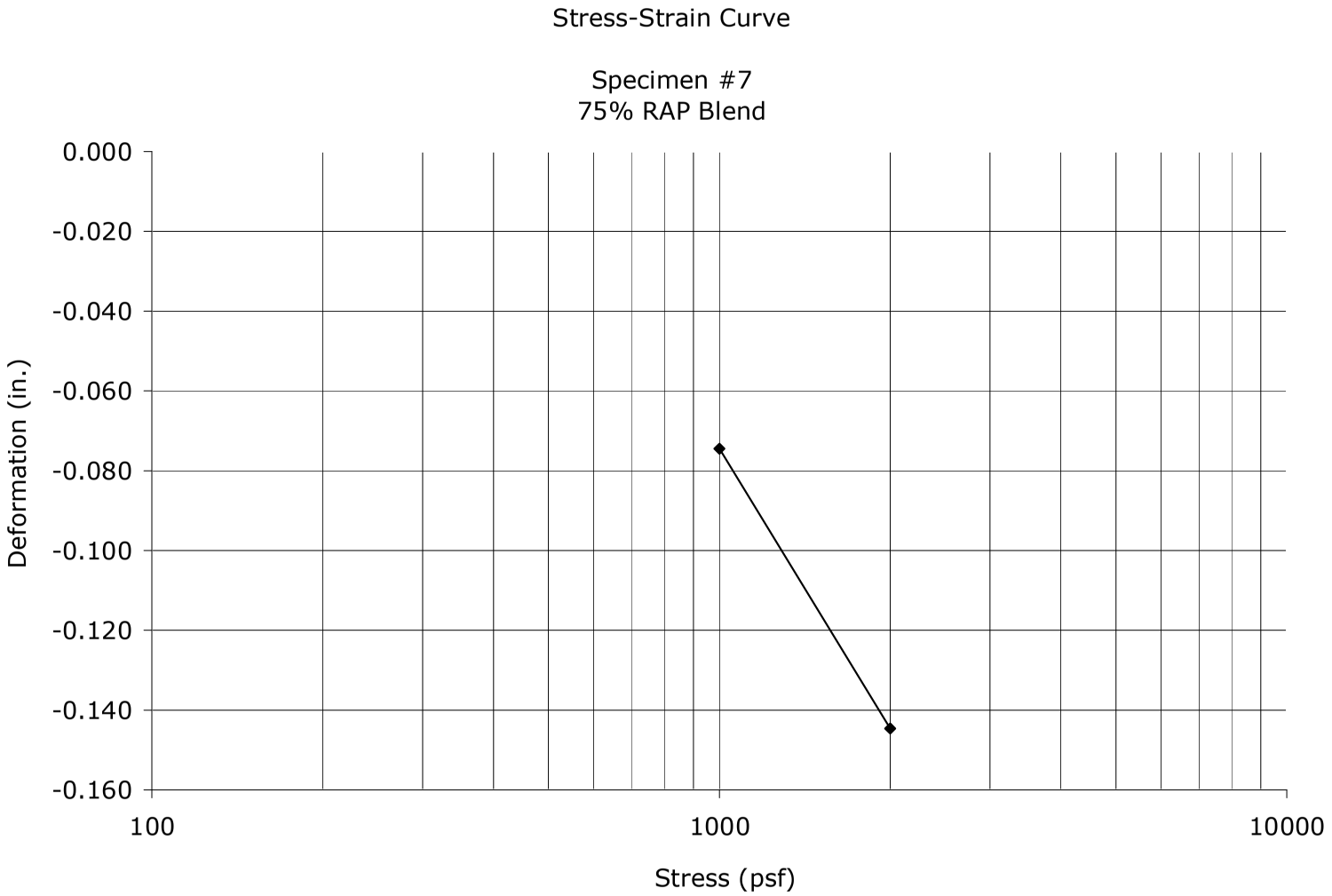
Stress-Strain Curve
Specimen #7
75% RAP Blend
0.000
-0.020
-0.040
-0.060
-0.080
-0.100
-0.120
-0.140
-0.160
Deformation (in.)
100
1000
10000
Stress (psf)

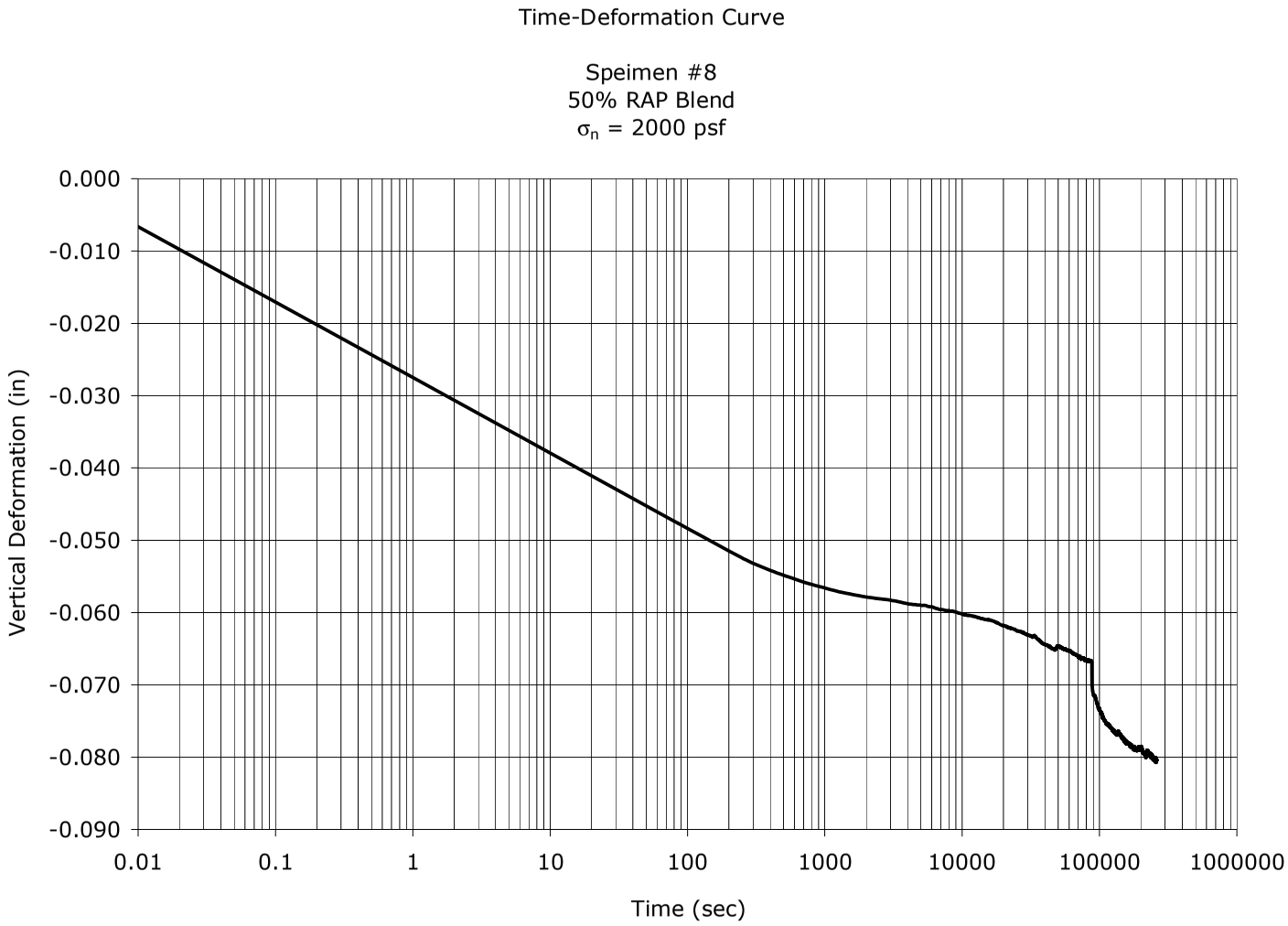
Time-Deformation Curve
Speimen #8
50% RAP Blend
σ_n = 2000 psf
Vertical Deformation (in)
0.000
-0.010
-0.020
-0.030
-0.040
-0.050
-0.060
-0.070
-0.080
-0.090
0.01
0.1
1
10
100
1000
10000
100000
1000000
Time (sec)

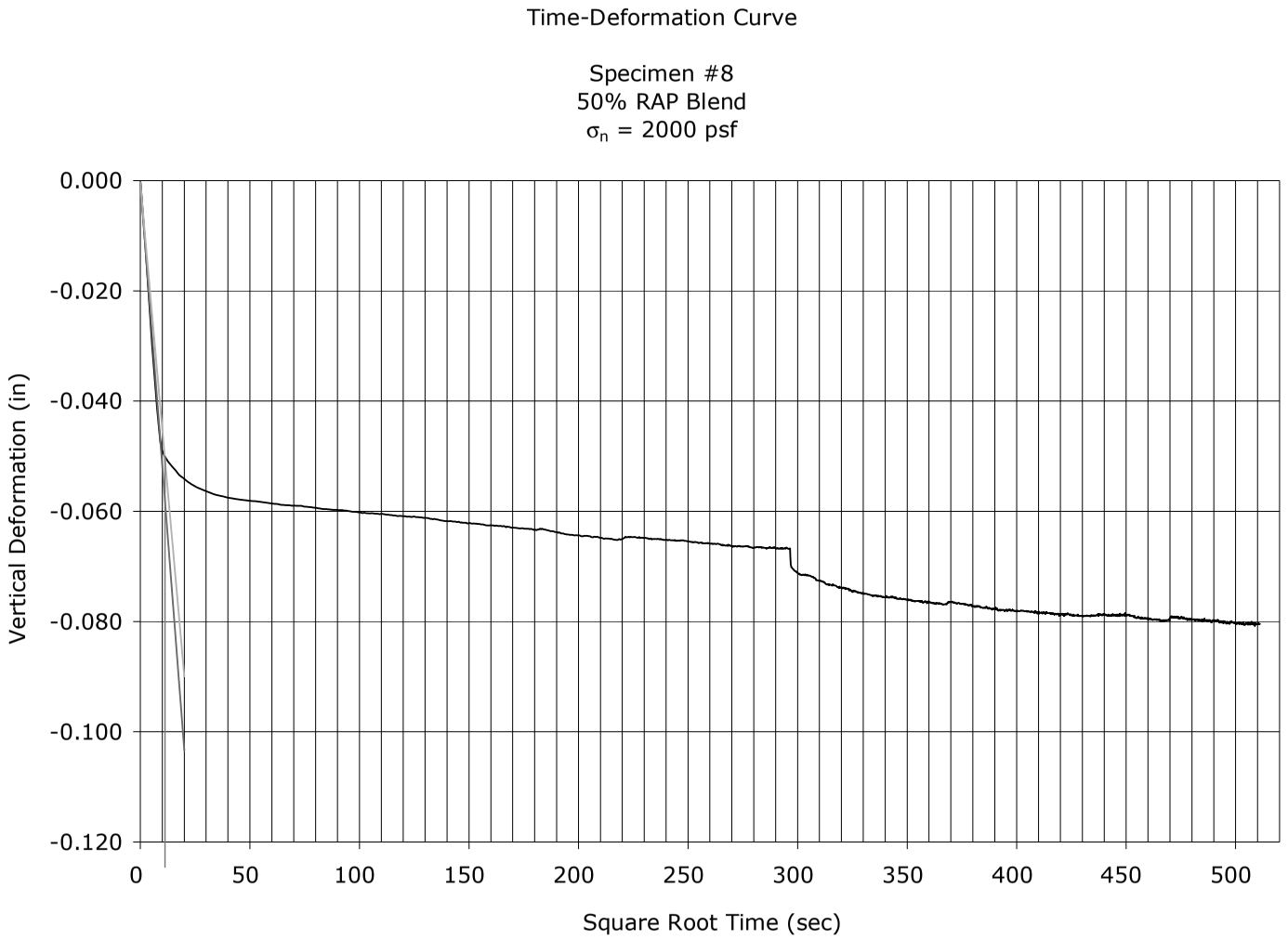
Time-Deformation Curve
Specimen #8
50% RAP Blend
σ_n = 2000 psf
Vertical Deformation (in)
0.000
-0.020
-0.040
-0.060
-0.080
-0.100
-0.120
0
50
100
150
200
250
300
350
400
450
500
Square Root Time (sec)

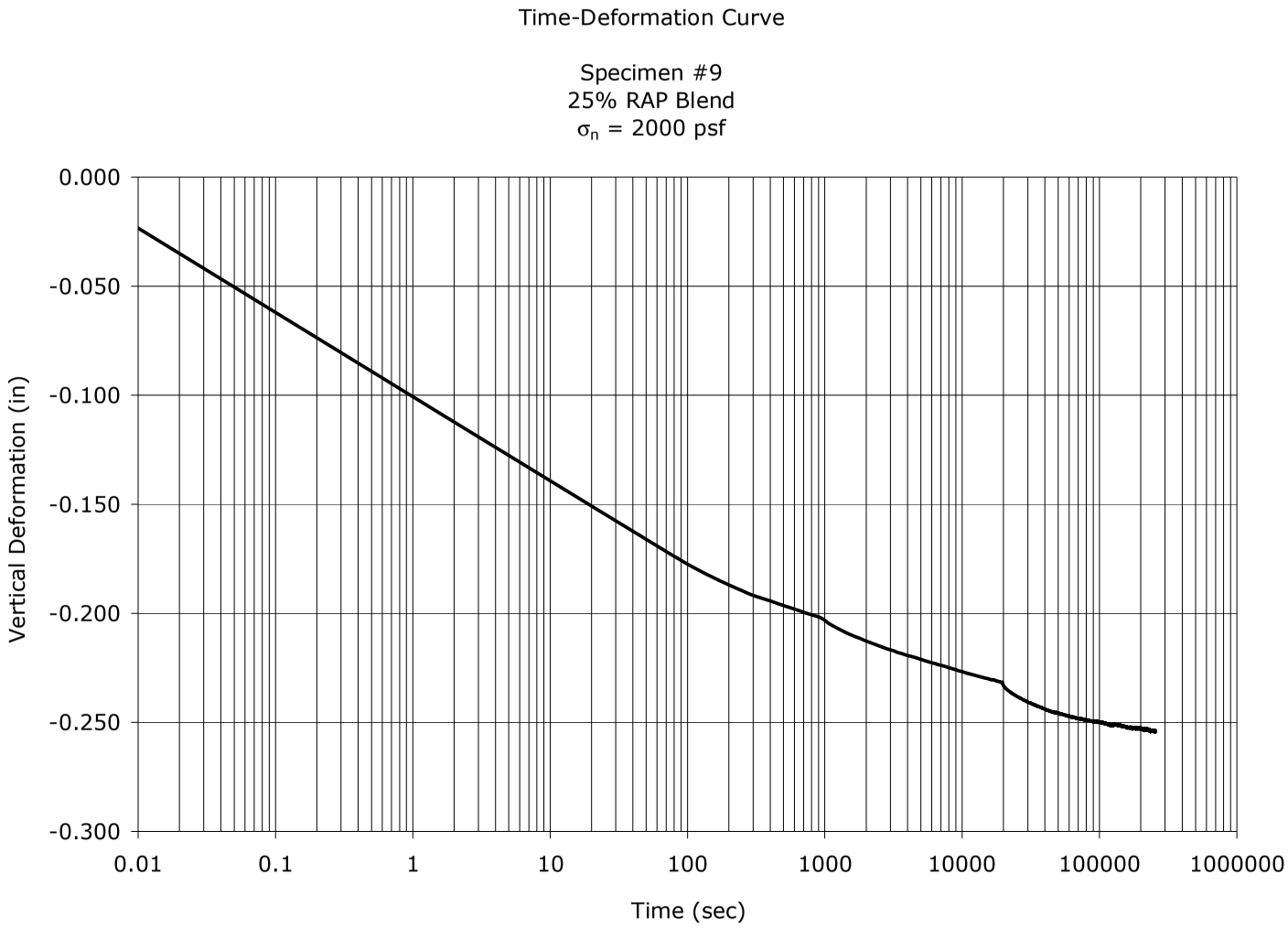
Time-Deformation Curve
Specimen #9
25% RAP Blend
σ_n = 2000 psf
0.000
-0.050
-0.100
-0.150
-0.200
-0.250
-0.300
Vertical Deformation (in)
0.01
0.1
1
10
100
1000
10000
100000
1000000
Time (sec)

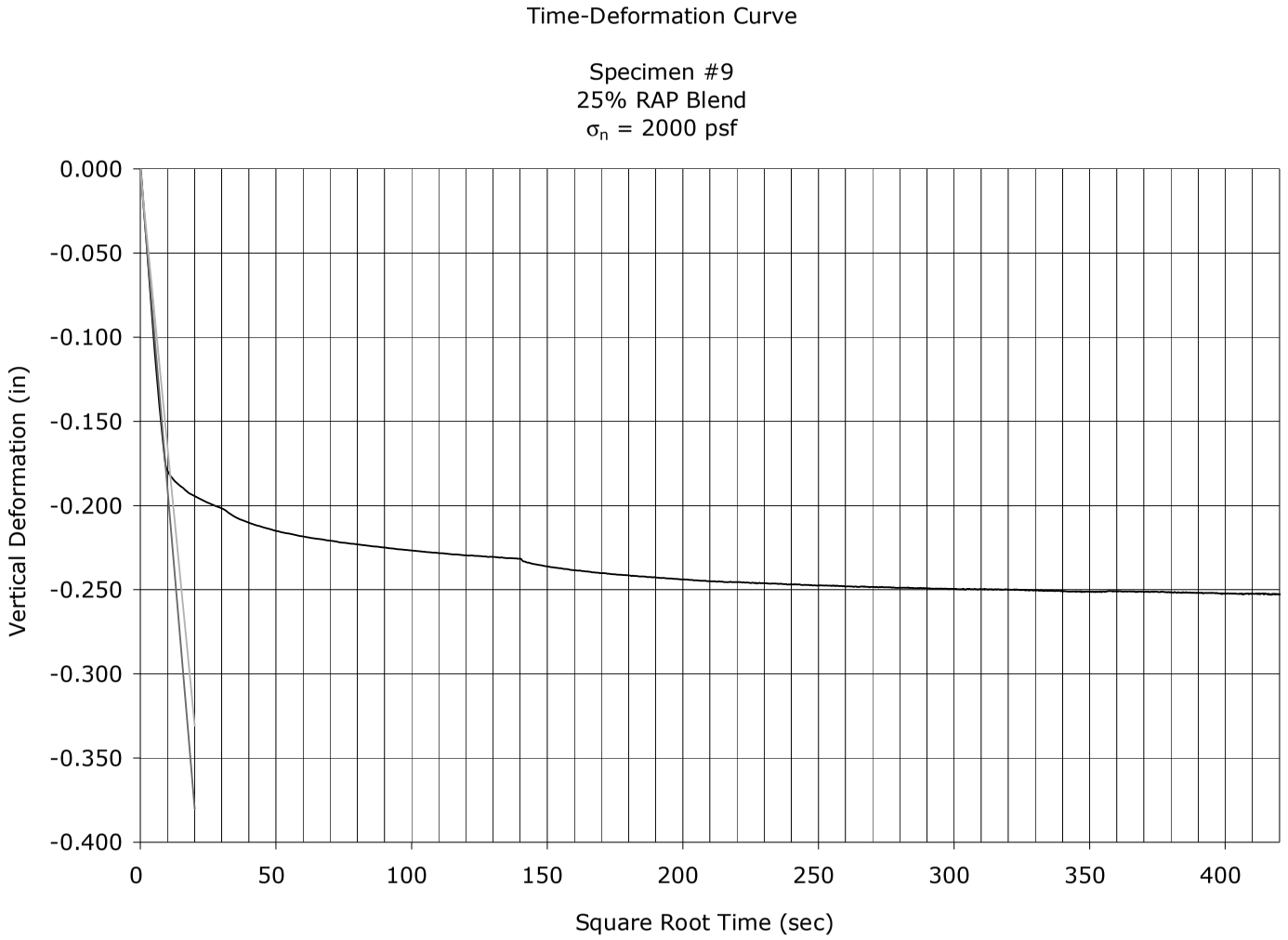
Time-Deformation Curve
Specimen #9
25% RAP Blend
σn = 2000 psf
Vertical Deformation (in)
0.000
-0.050
-0.100
-0.150
-0.200
-0.250
-0.300
-0.350
-0.400
0
50
100
150
200
250
300
350
400
Square Root Time (sec)

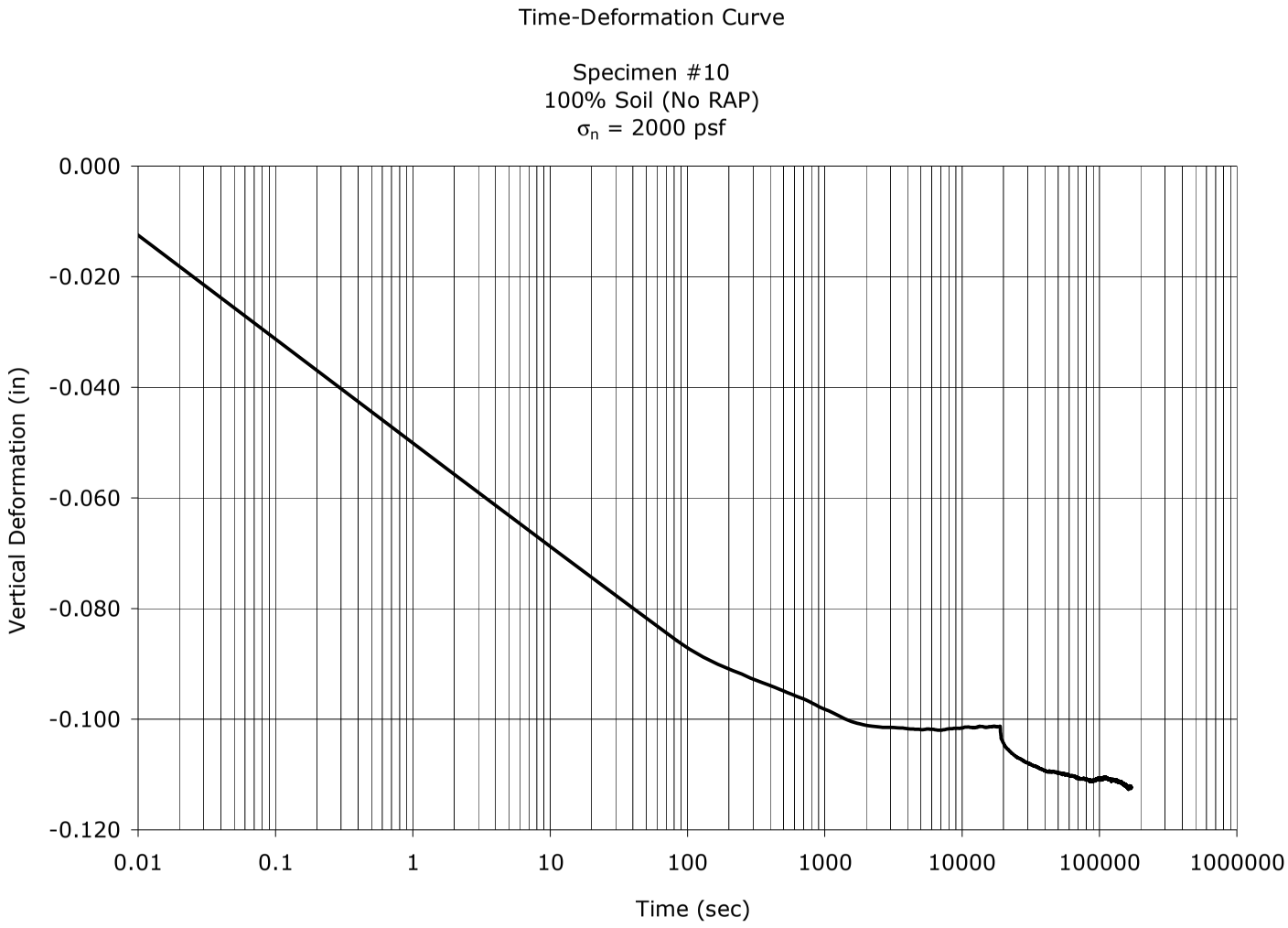
Time-Deformation Curve
Specimen #10
100% Soil (No RAP)
σn = 2000 psf
Vertical Deformation (in)
0.000
-0.020
-0.040
-0.060
-0.080
-0.100
-0.120
0.01
0.1
1
10
100
1000
10000
100000
1000000
Time (sec)

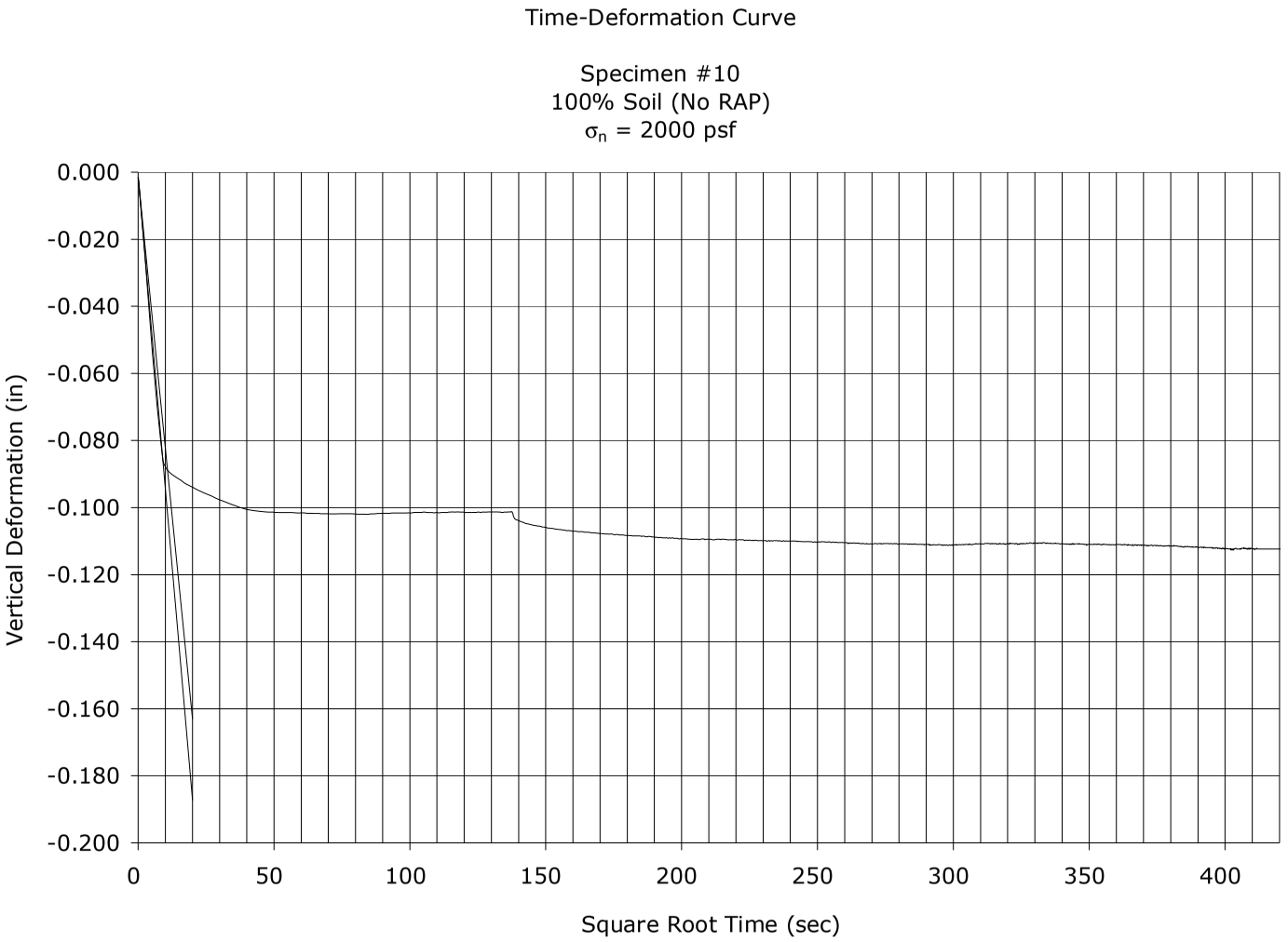
Time-Deformation Curve
Specimen #10
100% Soil (No RAP)
σ_n = 2000 psf
Vertical Deformation (in)
0.000
-0.020
-0.040
-0.060
-0.080
-0.100
-0.120
-0.140
-0.160
-0.180
-0.200
0
50
100
150
200
250
300
350
400
Square Root Time (sec)

APPENDIX C

SHEAR STRENGTH TEST DATA

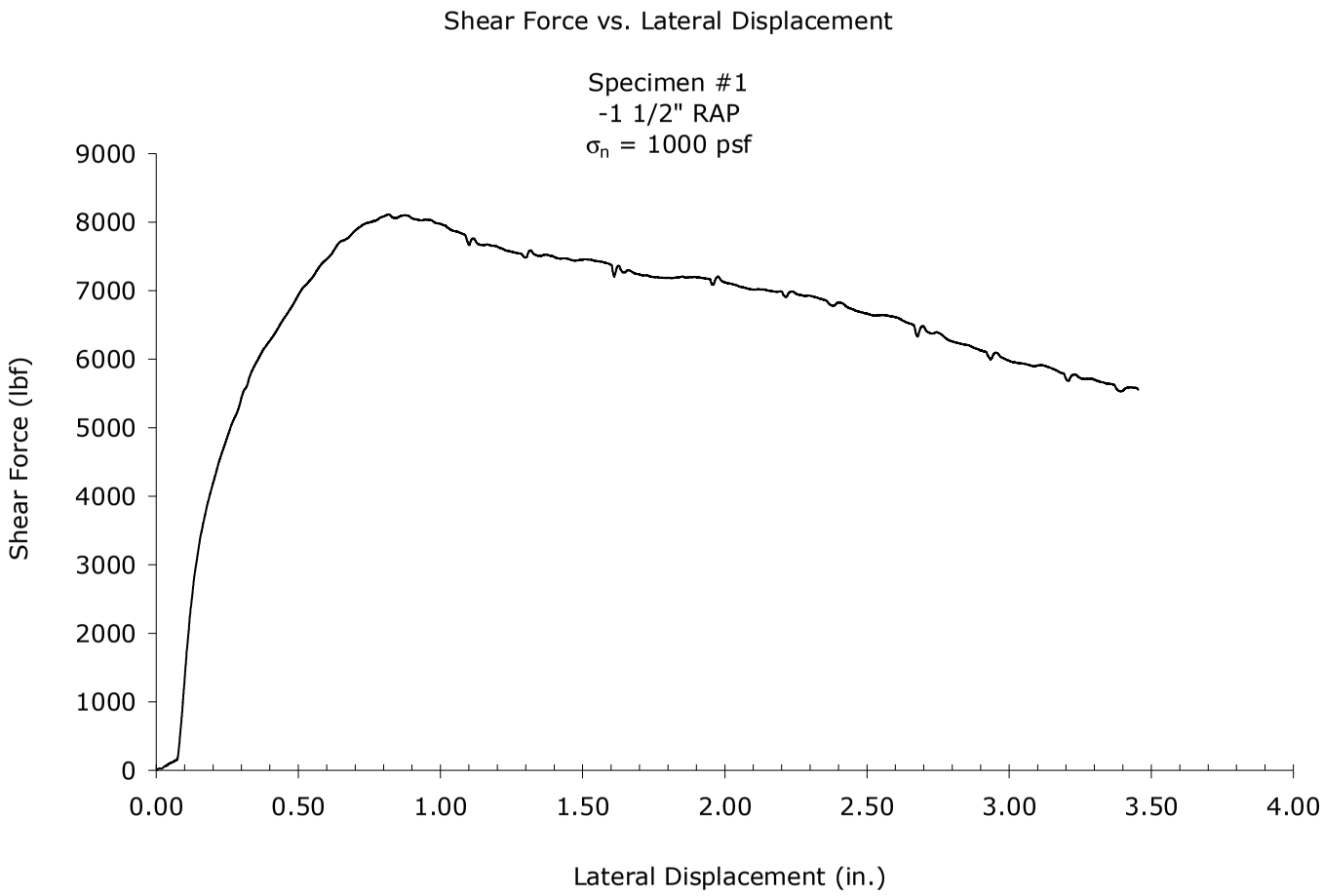
Shear Force vs. Lateral Displacement
Specimen #1
-1 1/2" RAP
σn = 1000 psf
Shear Force (lbf)
9000
8000
7000
6000
5000
4000
3000
2000
1000
0
0.00
0.50
1.00
1.50
2.00
2.50
3.00
3.50
4.00
Lateral Displacement (in.)

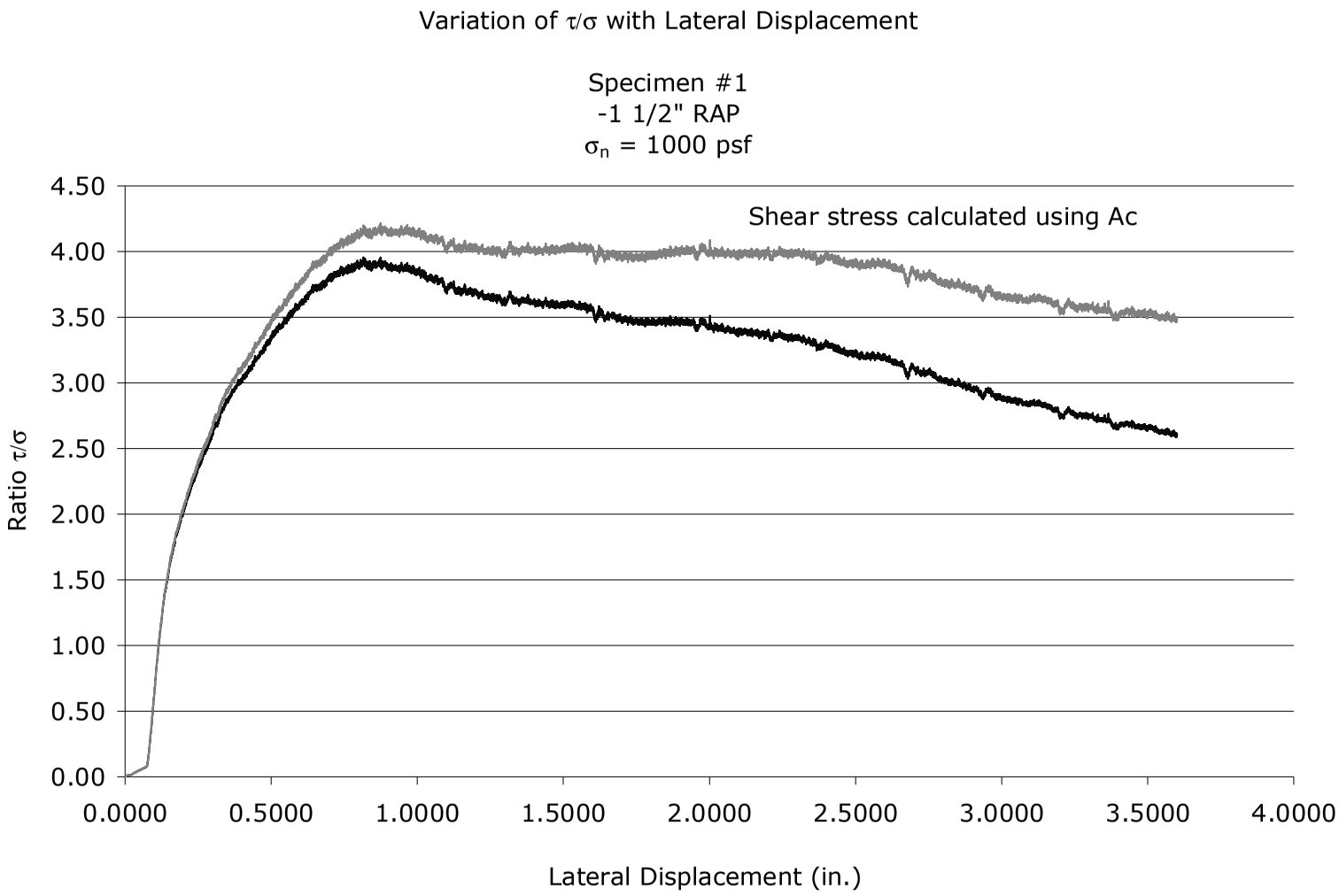
Variation of τ/σ with Lateral Displacement
Specimen #1
-1 1/2" RAP
σn = 1000 psf
Shear stress calculated using Ac
Ratio τ/σ
4.50
4.00
3.50
3.00
2.50
2.00
1.50
1.00
0.50
0.00
0.0000
0.5000
1.0000
1.5000
2.0000
2.5000
3.0000
3.5000
4.0000
Lateral Displacement (in.)

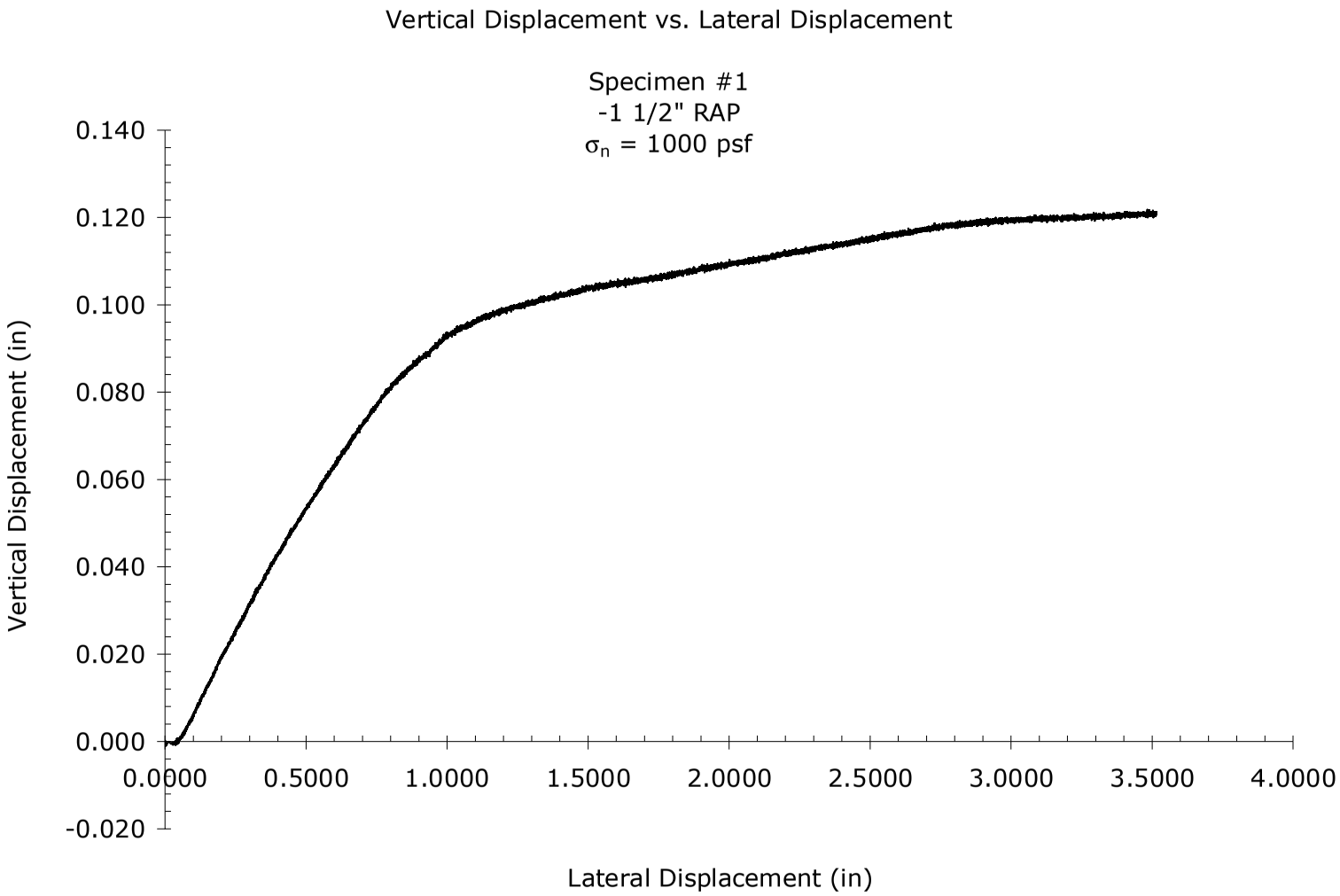
Vertical Displacement vs. Lateral Displacement
Specimen #1
-1 1/2" RAP
σn = 1000 psf
Vertical Displacement (in)
0.140
0.120
0.100
0.080
0.060
0.040
0.020
0.000
-0.020
0.0000
0.5000
1.0000
1.5000
2.0000
2.5000
3.0000
3.5000
4.0000
Lateral Displacement (in)

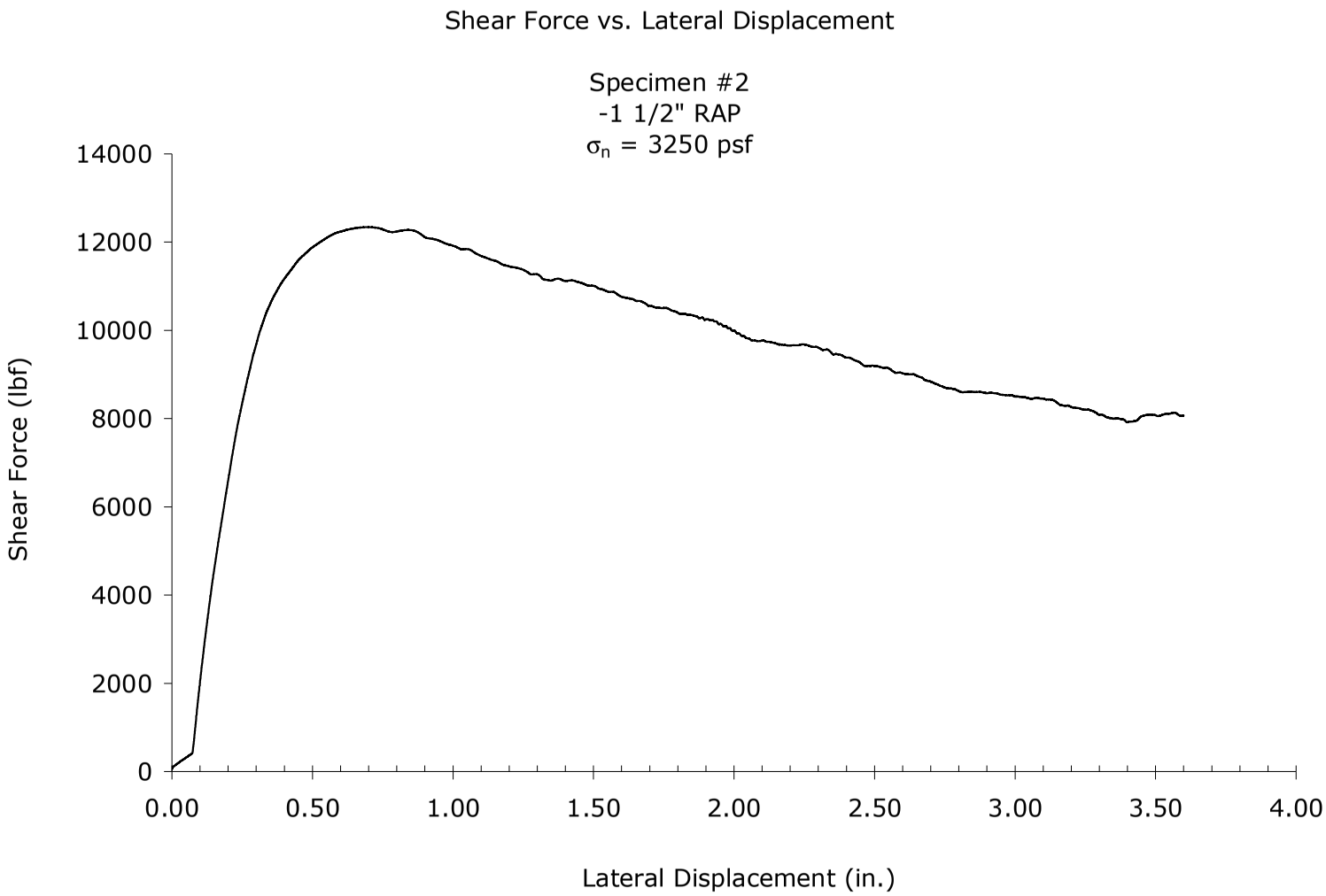
Shear Force vs. Lateral Displacement
Specimen #2
-1 1/2" RAP
σn = 3250 psf
Shear Force (lbf)
14000
12000
10000
8000
6000
4000
2000
0
0.00
0.50
1.00
1.50
2.00
2.50
3.00
3.50
4.00
Lateral Displacement (in.)

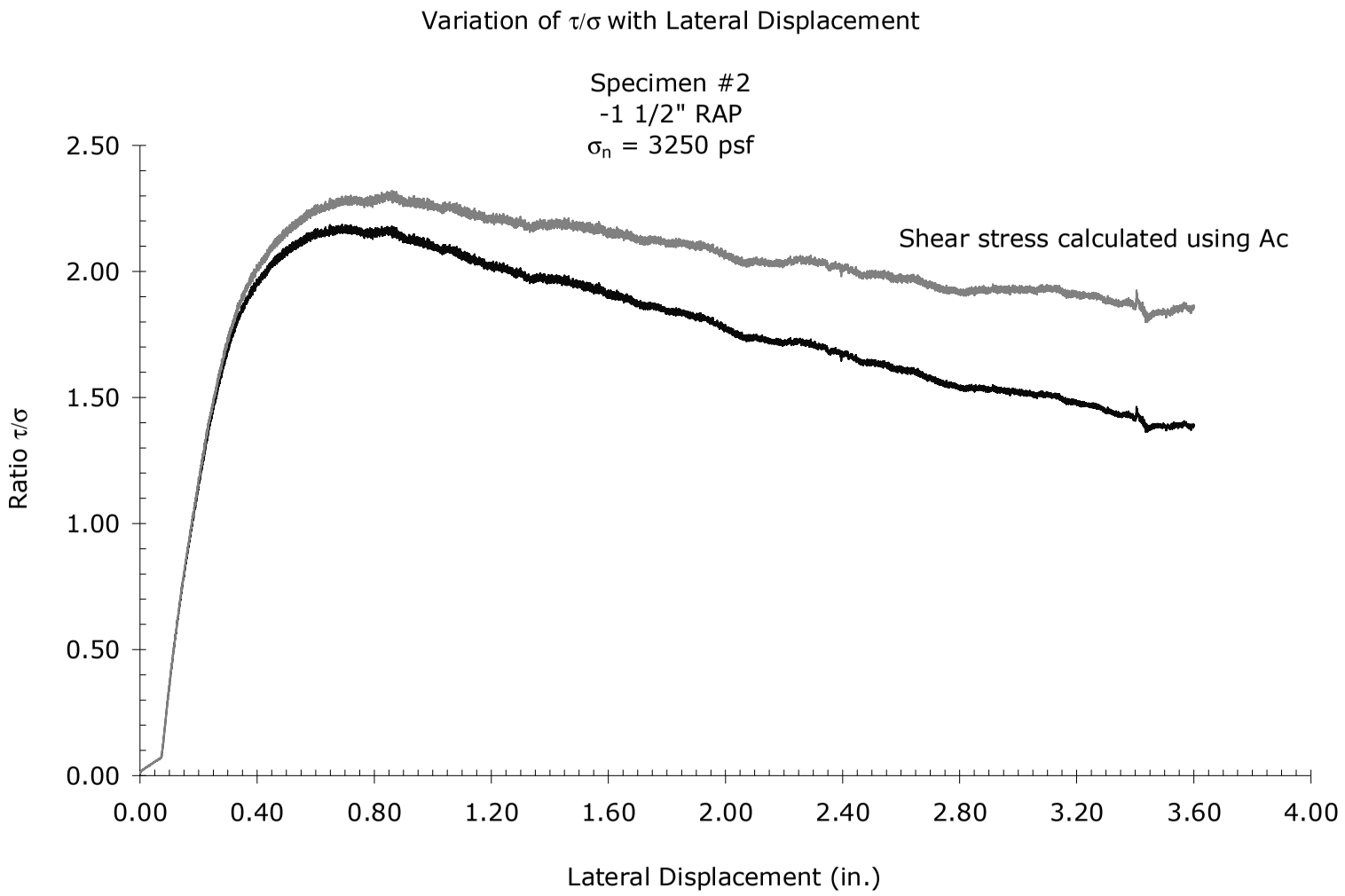
Variation of τ/σ with Lateral Displacement
Specimen #2
-1 1/2" RAP
σn = 3250 psf
Shear stress calculated using Ac
Ratio τ/σ
2.50
2.00
1.50
1.00
0.50
0.00
0.00
0.40
0.80
1.20
1.60
2.00
2.40
2.80
3.20
3.60
4.00
Lateral Displacement (in.)

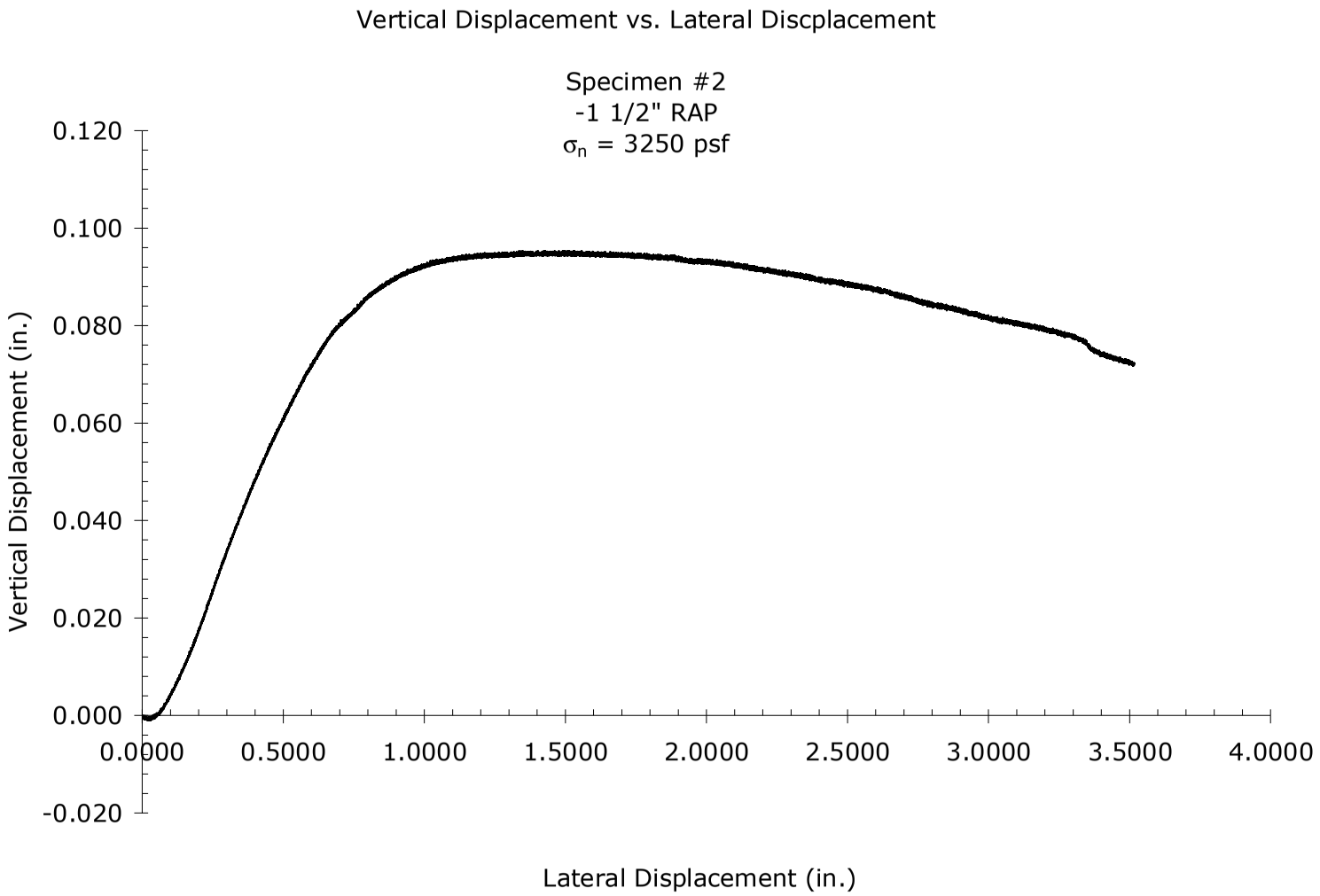
Vertical Displacement vs. Lateral Discplacement
Specimen #2
-1 1/2" RAP
σn = 3250 psf
0.120
0.100
0.080
0.060
0.040
0.020
0.000
-0.020
Vertical Displacement (in.)
0.0000
0.5000
1.0000
1.5000
2.0000
2.5000
3.0000
3.5000
4.0000
Lateral Displacement (in.)

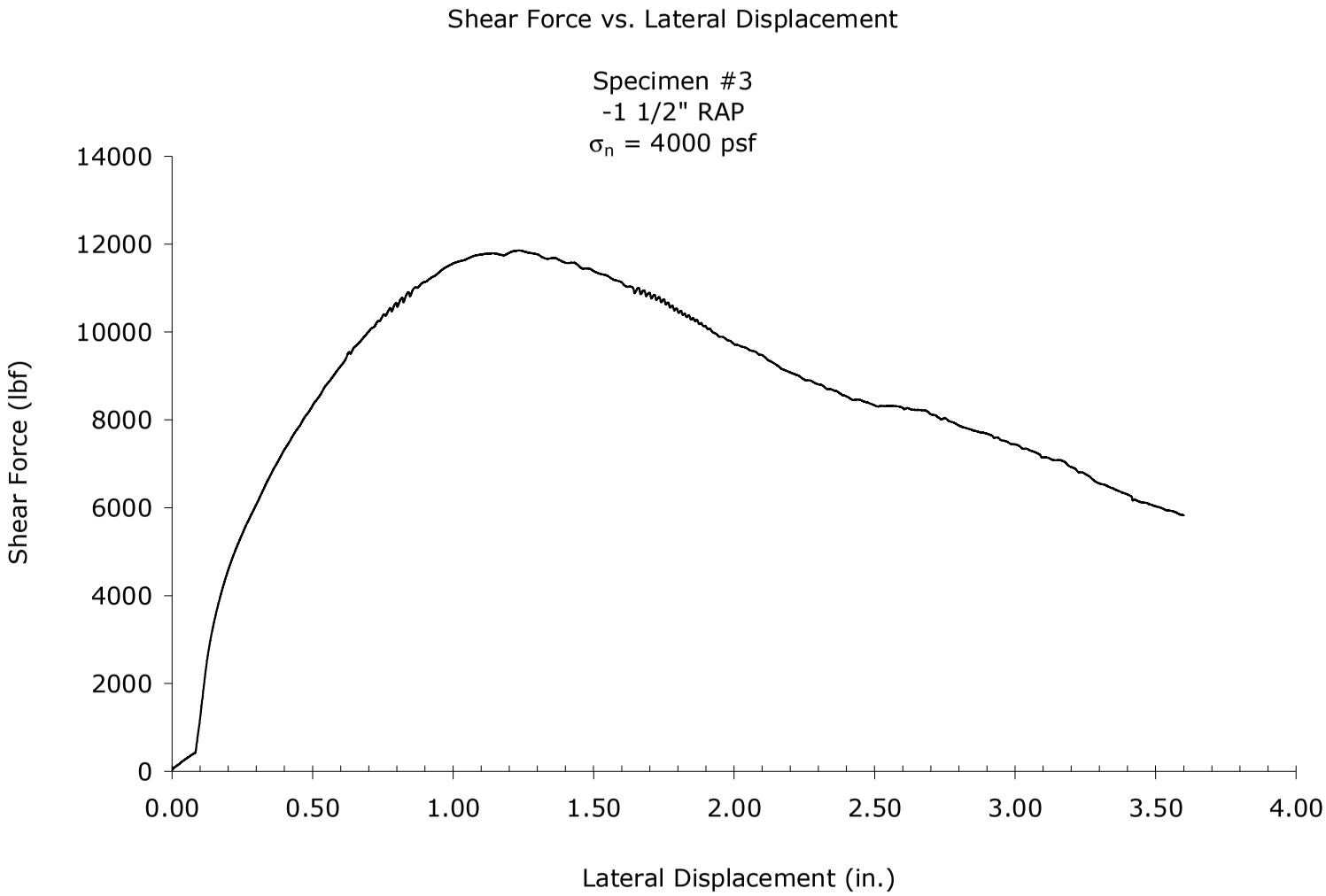
Shear Force vs. Lateral Displacement
Specimen #3
-1 1/2" RAP
σn = 4000 psf
Shear Force (lbf)
14000
12000
10000
8000
6000
4000
2000
0
0.00
0.50
1.00
1.50
2.00
2.50
3.00
3.50
4.00
Lateral Displacement (in.)

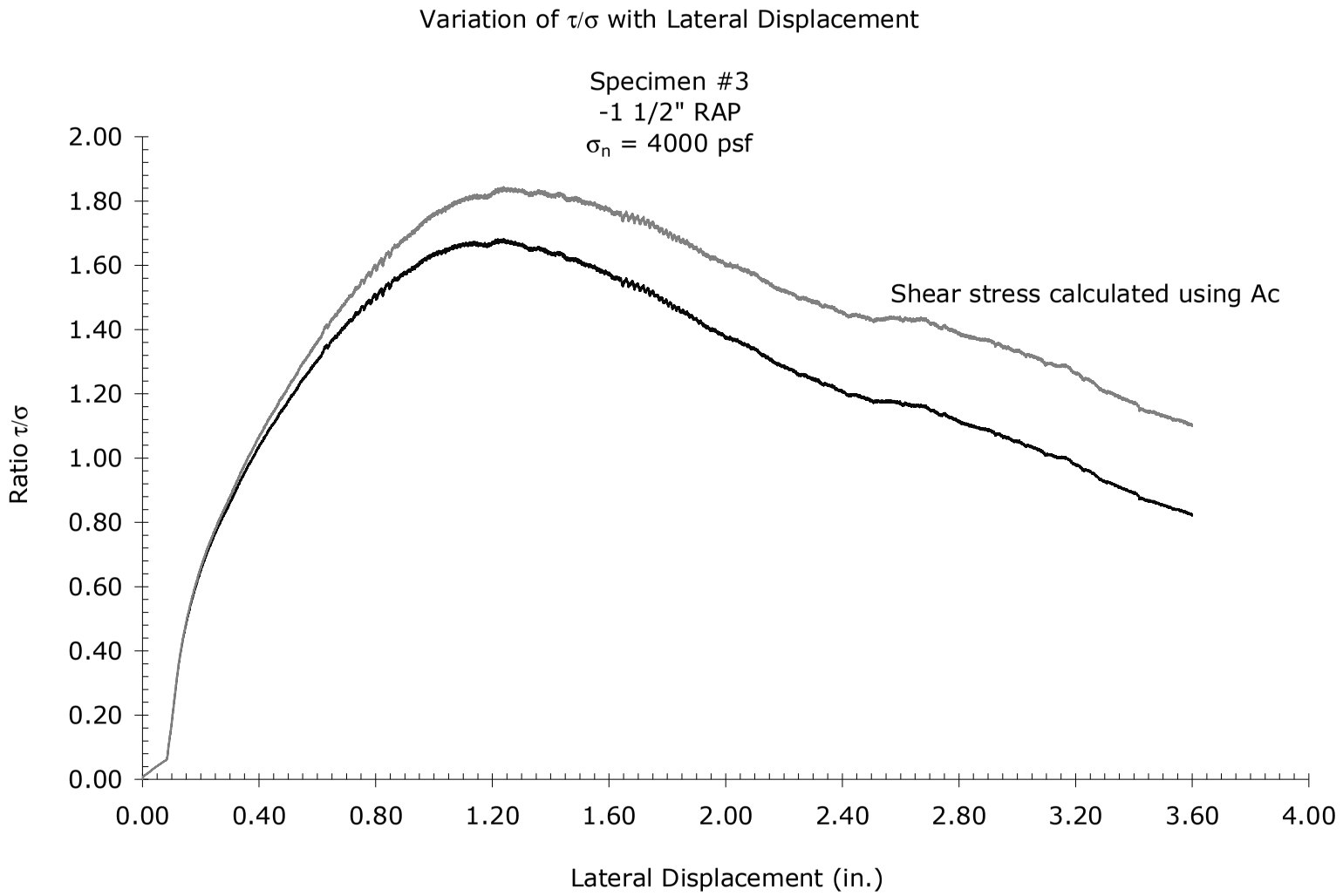
Variation of τ/σ with Lateral Displacement
Specimen #3
-1 1/2" RAP
σn = 4000 psf
Shear stress calculated using Ac
Ratio τ/σ
2.00
1.80
1.60
1.40
1.20
1.00
0.80
0.60
0.40
0.20
0.00
0.00
0.40
0.80
1.20
1.60
2.00
2.40
2.80
3.20
3.60
4.00
Lateral Displacement (in.)

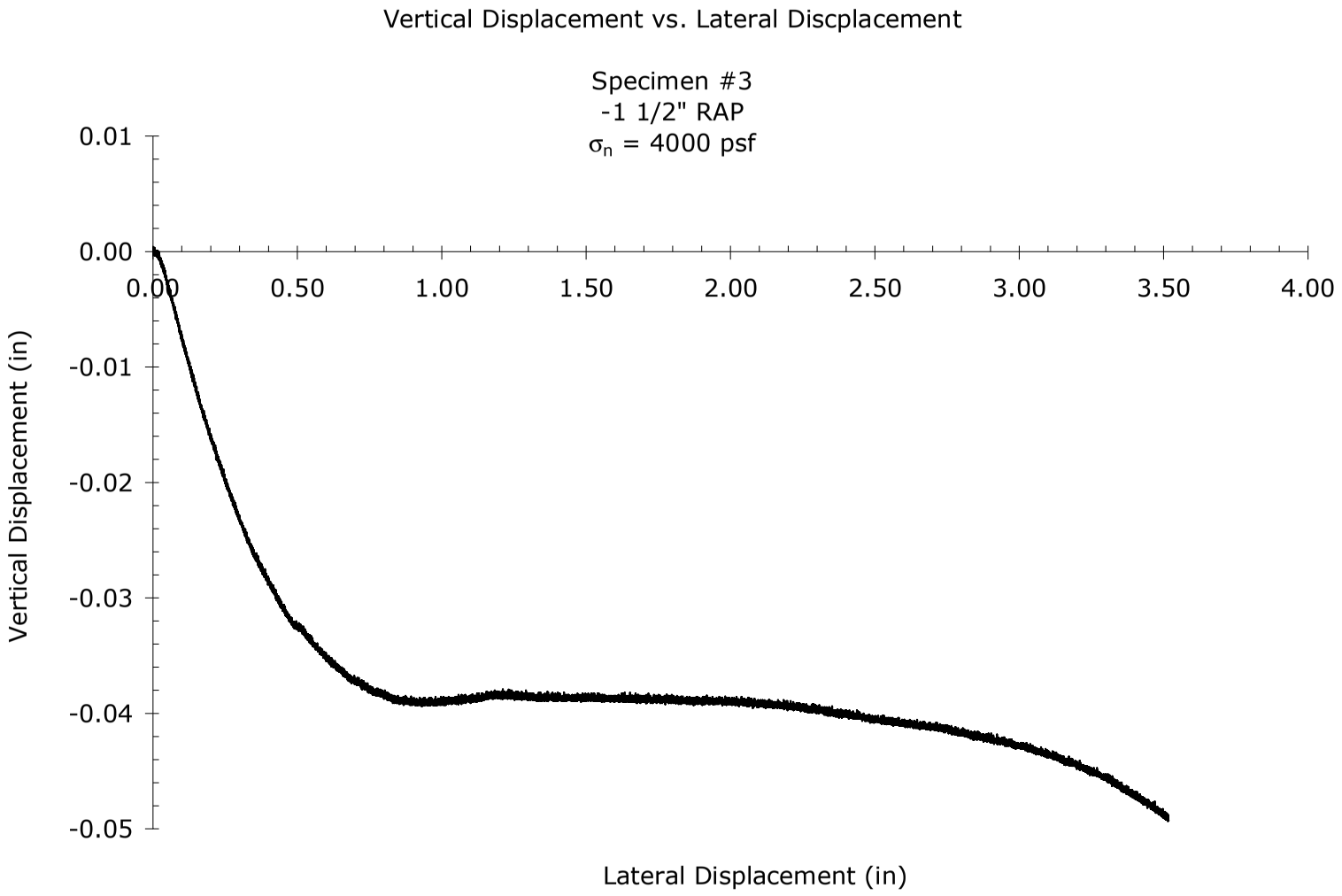
Vertical Displacement vs. Lateral Discplacement
Specimen #3
-1 1/2" RAP
σn = 4000 psf
0.01
0.00
-0.01
-0.02
-0.03
-0.04
-0.05
0.00
0.50
1.00
1.50
2.00
2.50
3.00
3.50
4.00
Vertical Displacement (in)
Lateral Displacement (in)

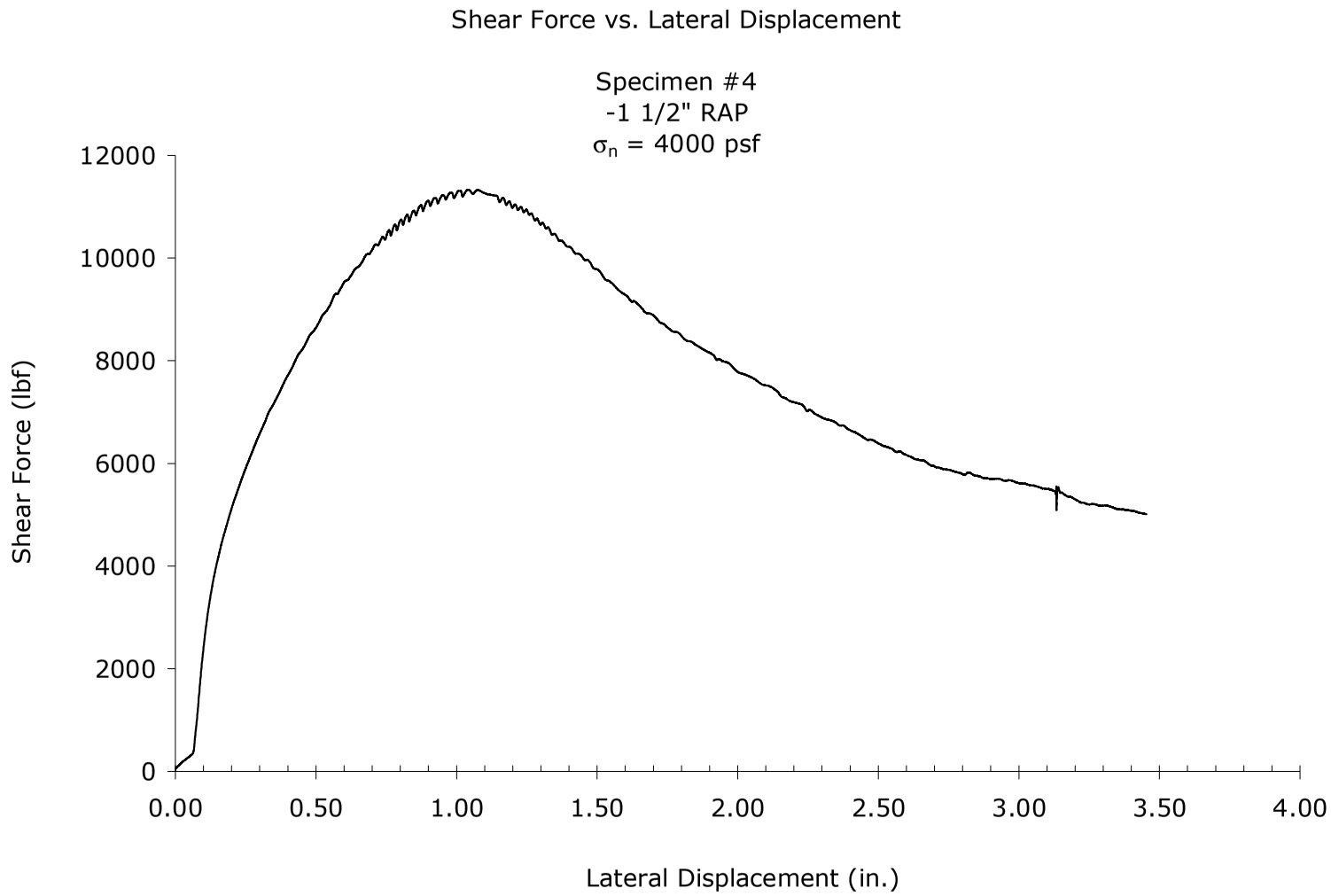
Shear Force vs. Lateral Displacement
Specimen #4
-1 1/2" RAP
σn = 4000 psf
Shear Force (lbf)
12000
10000
8000
6000
4000
2000
0
0.00
0.50
1.00
1.50
2.00
2.50
3.00
3.50
4.00
Lateral Displacement (in.)

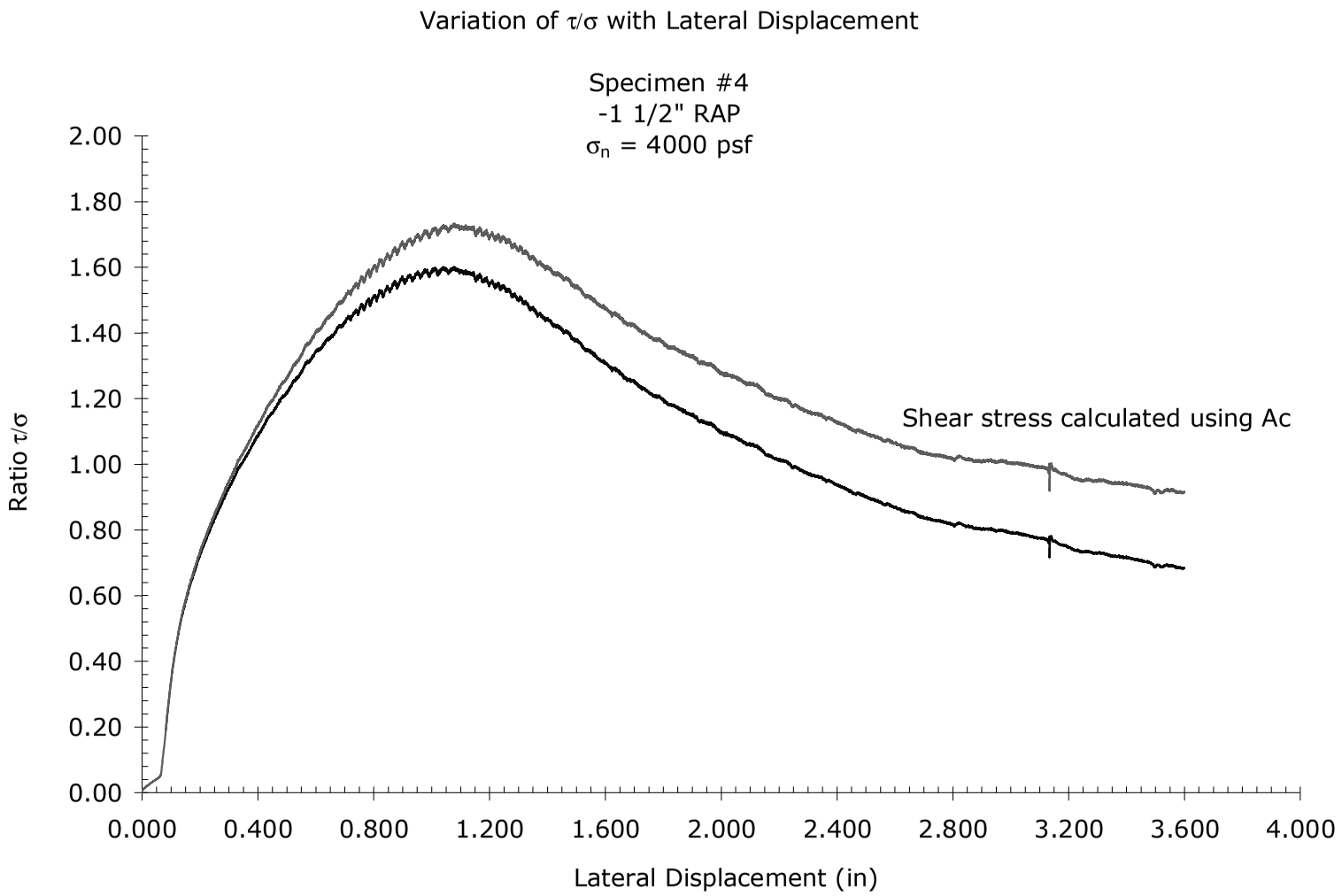
Variation of τ/σ with Lateral Displacement
Specimen #4
-1 1/2" RAP
σn = 4000 psf
Ratio τ/σ
2.00
1.80
1.60
1.40
1.20
1.00
0.80
0.60
0.40
0.20
0.00
0.000
0.400
0.800
1.200
1.600
2.000
2.400
2.800
3.200
3.600
4.000
Lateral Displacement (in)
Shear stress calculated using Ac

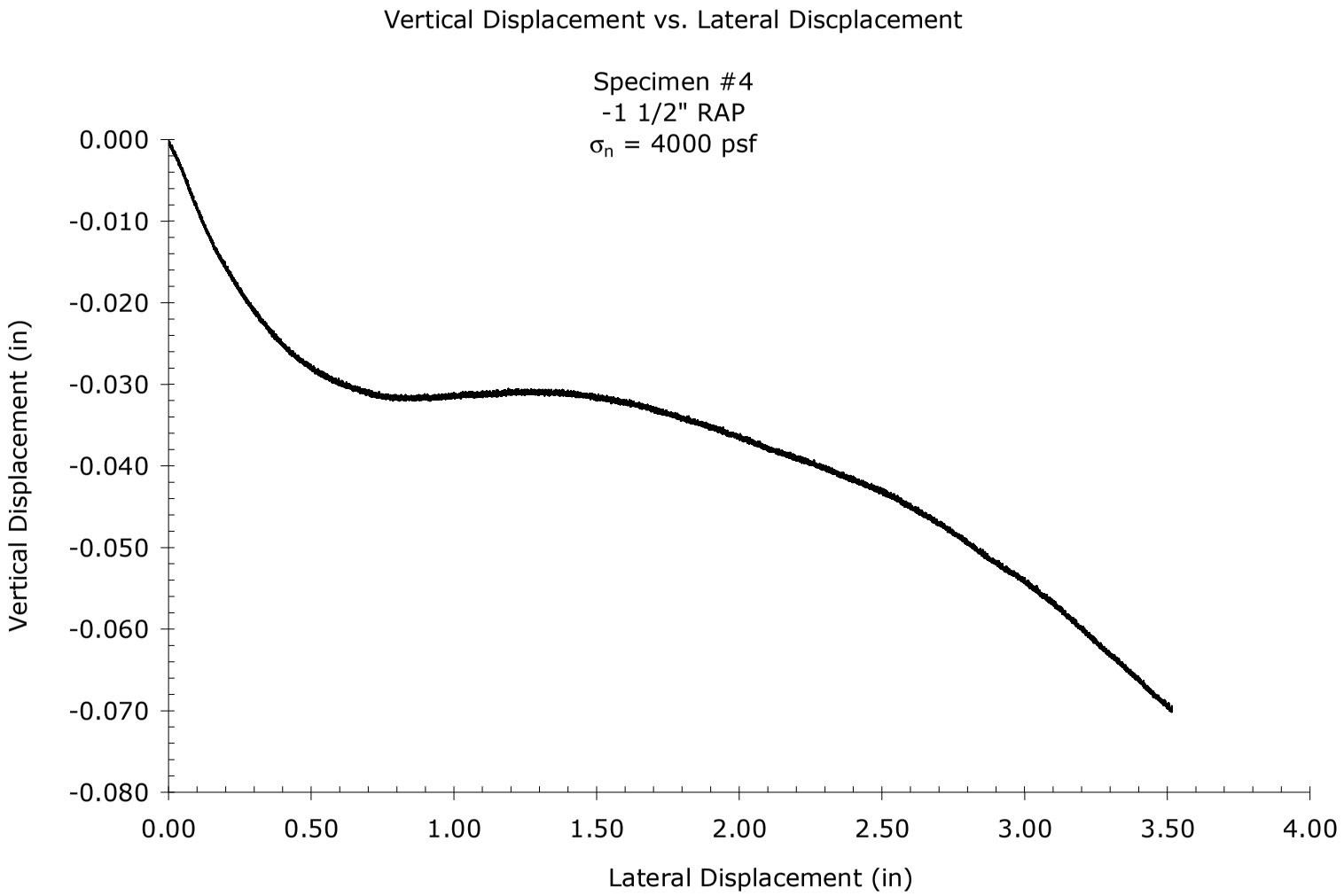
Vertical Displacement vs. Lateral Discplacement
Specimen #4
-1 1/2" RAP
σn = 4000 psf
Vertical Displacement (in)
0.000
-0.010
-0.020
-0.030
-0.040
-0.050
-0.060
-0.070
-0.080
0.00
0.50
1.00
1.50
2.00
2.50
3.00
3.50
4.00
Lateral Displacement (in)

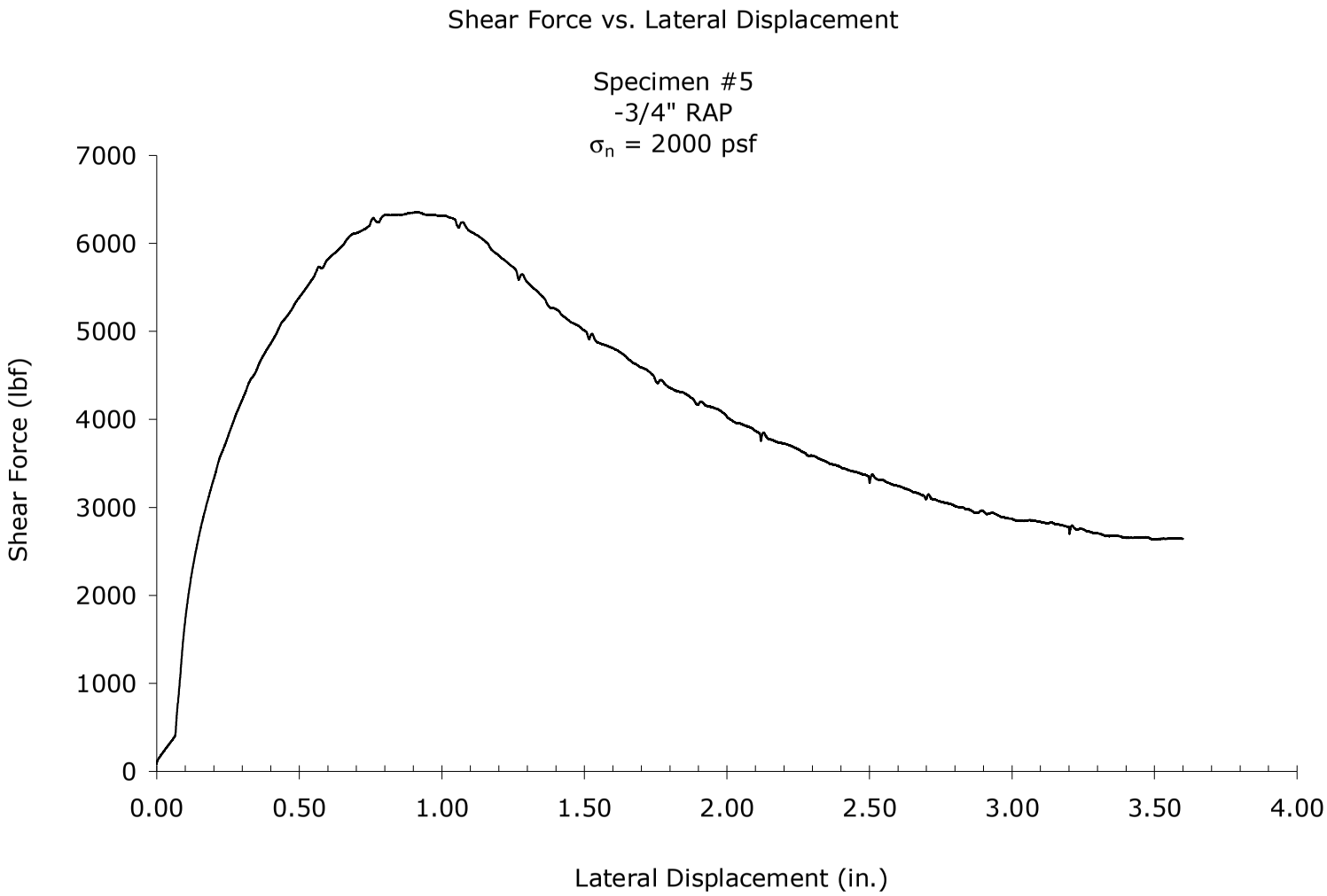
Shear Force vs. Lateral Displacement
Specimen #5
-3/4" RAP
σn = 2000 psf
Shear Force (lbf)
7000
6000
5000
4000
3000
2000
1000
0
0.00
0.50
1.00
1.50
2.00
2.50
3.00
3.50
4.00
Lateral Displacement (in.)

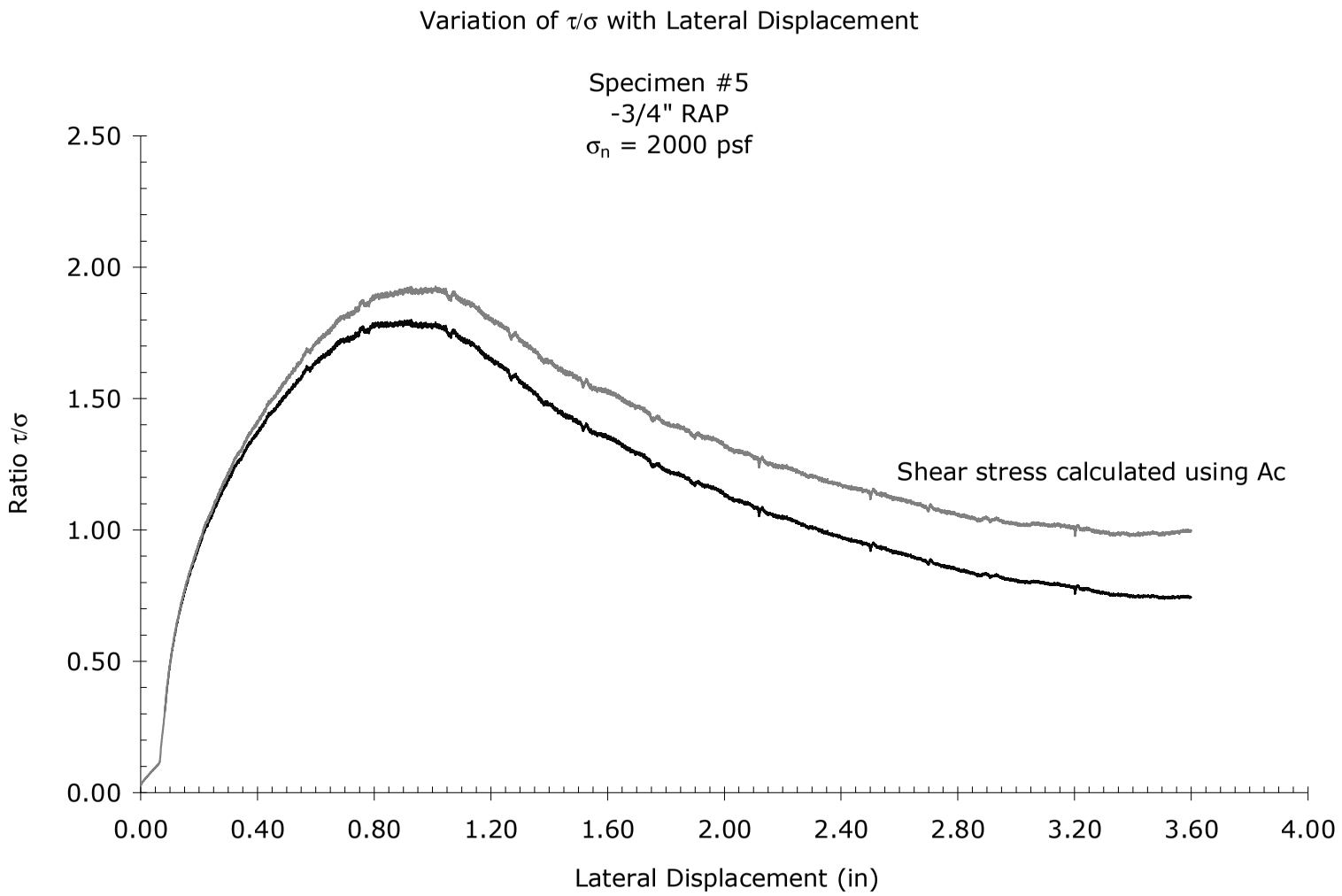
Variation of τ/σ with Lateral Displacement
Specimen #5
-3/4" RAP
σn = 2000 psf
Ratio τ/σ
2.50
2.00
1.50
1.00
0.50
0.00
0.00
0.40
0.80
1.20
1.60
2.00
2.40
2.80
3.20
3.60
4.00
Lateral Displacement (in)
Shear stress calculated using Ac

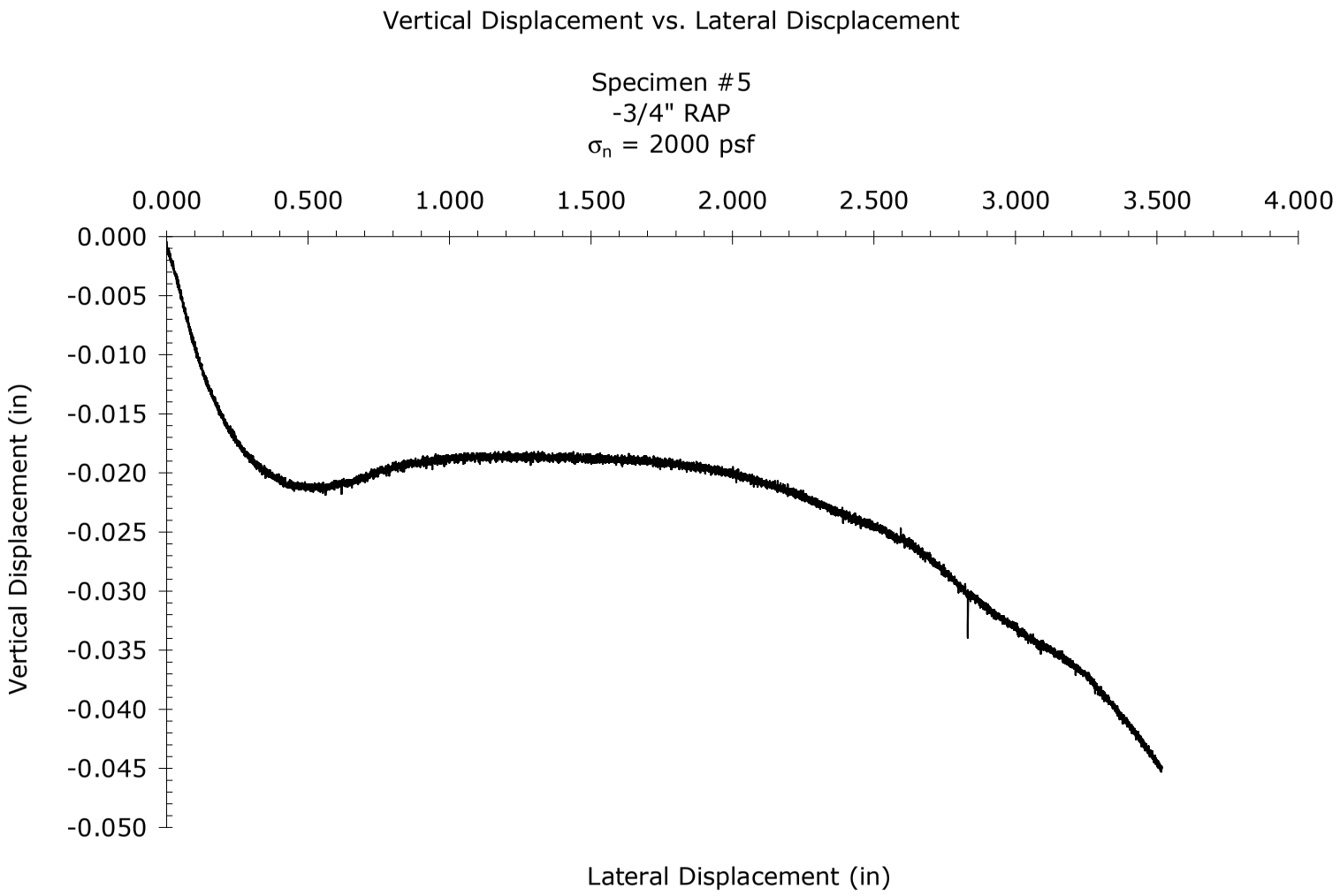
Vertical Displacement vs. Lateral Discplacement
Specimen #5
-3/4" RAP
σn = 2000 psf
0.000
0.500
1.000
1.500
2.000
2.500
3.000
3.500
4.000
0.000
-0.005
-0.010
-0.015
-0.020
-0.025
-0.030
-0.035
-0.040
-0.045
-0.050
Vertical Displacement (in)
Lateral Displacement (in)

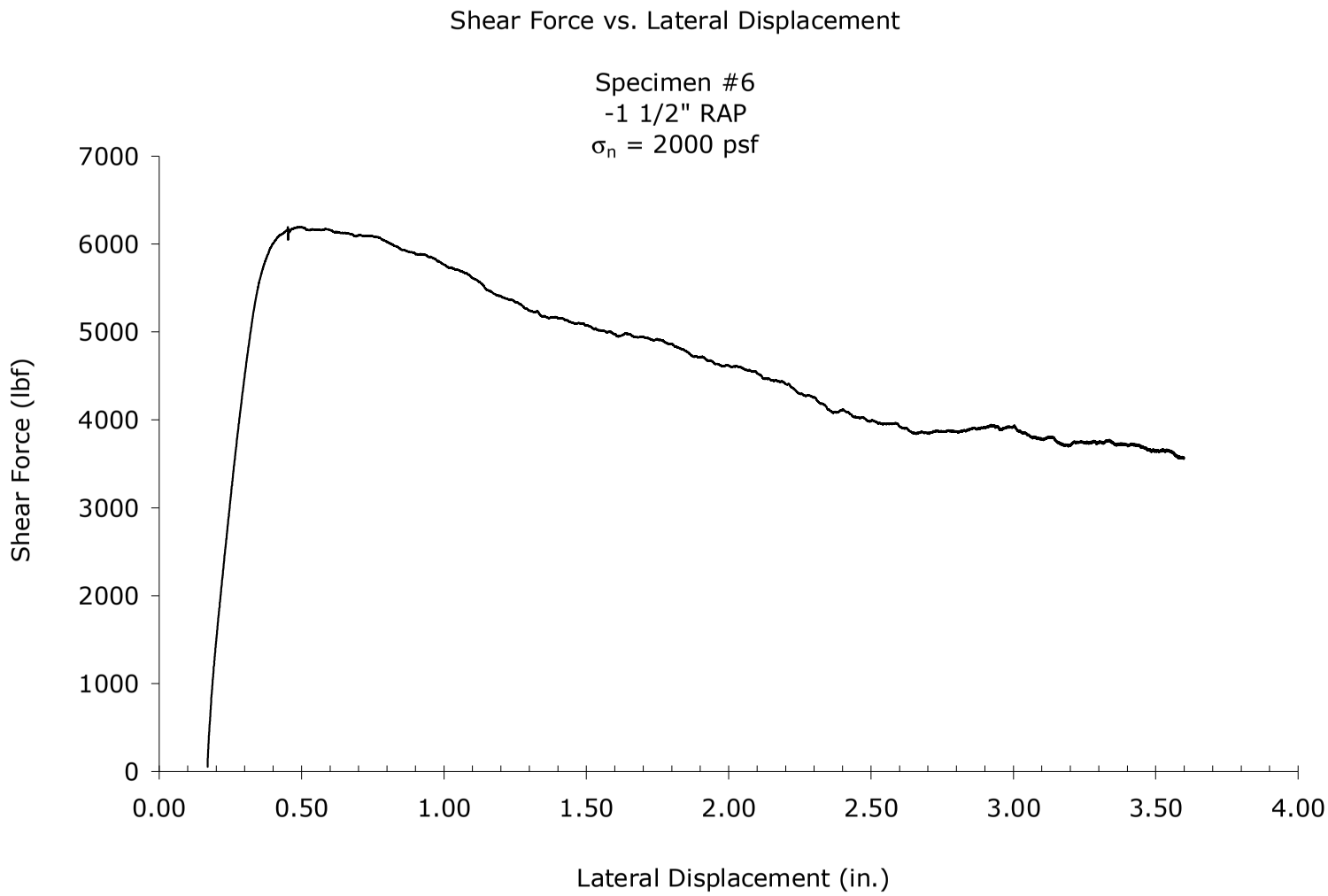
Shear Force vs. Lateral Displacement
Specimen #6
-1 1/2" RAP
σn = 2000 psf
Shear Force (lbf)
7000
6000
5000
4000
3000
2000
1000
0
0.00
0.50
1.00
1.50
2.00
2.50
3.00
3.50
4.00
Lateral Displacement (in.)

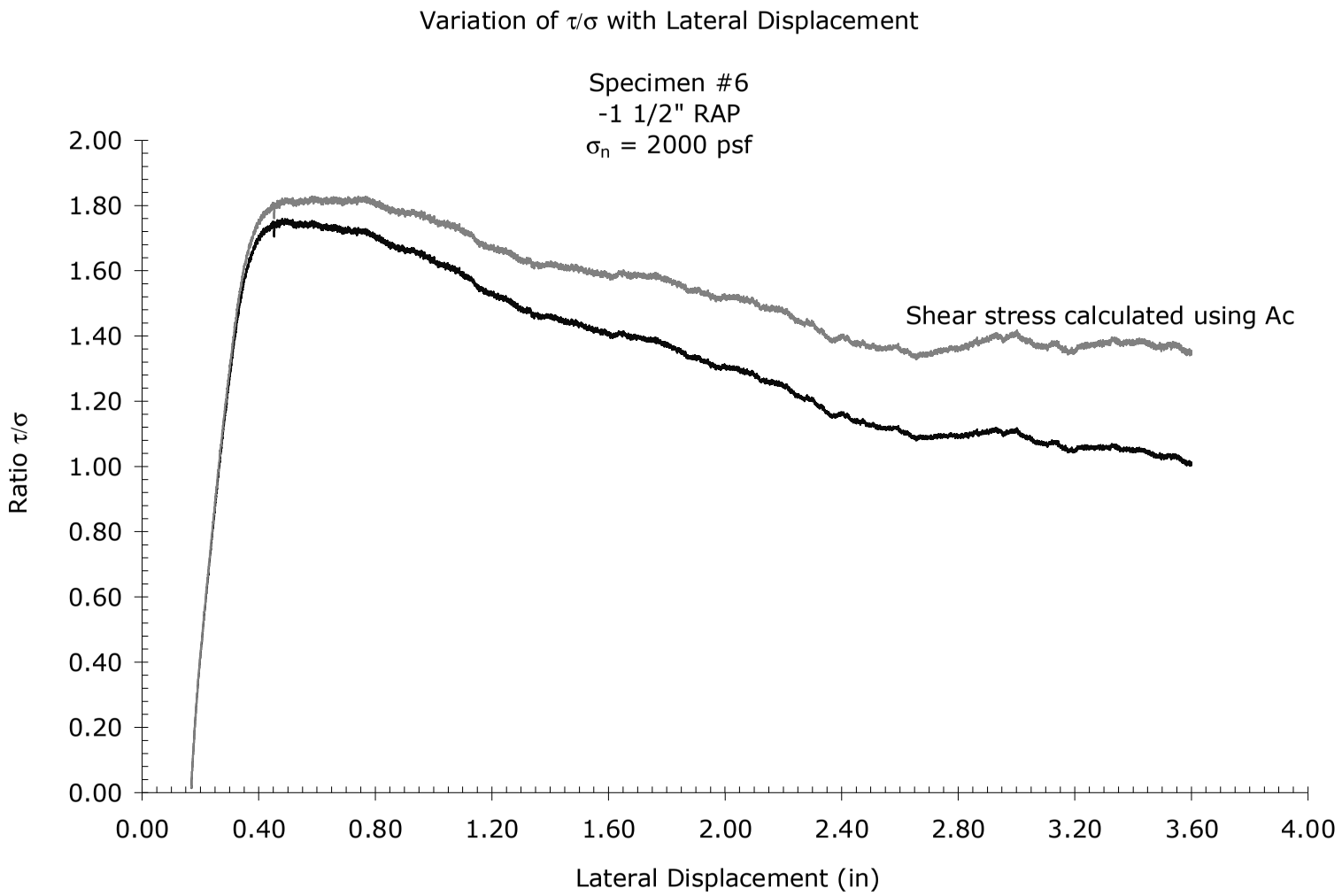
Variation of τ/σ with Lateral Displacement
Specimen #6
-1 1/2" RAP
σn = 2000 psf
Shear stress calculated using Ac
Ratio τ/σ
Lateral Displacement (in)
2.00
1.80
1.60
1.40
1.20
1.00
0.80
0.60
0.40
0.20
0.00
0.00
0.40
0.80
1.20
1.60
2.00
2.40
2.80
3.20
3.60
4.00

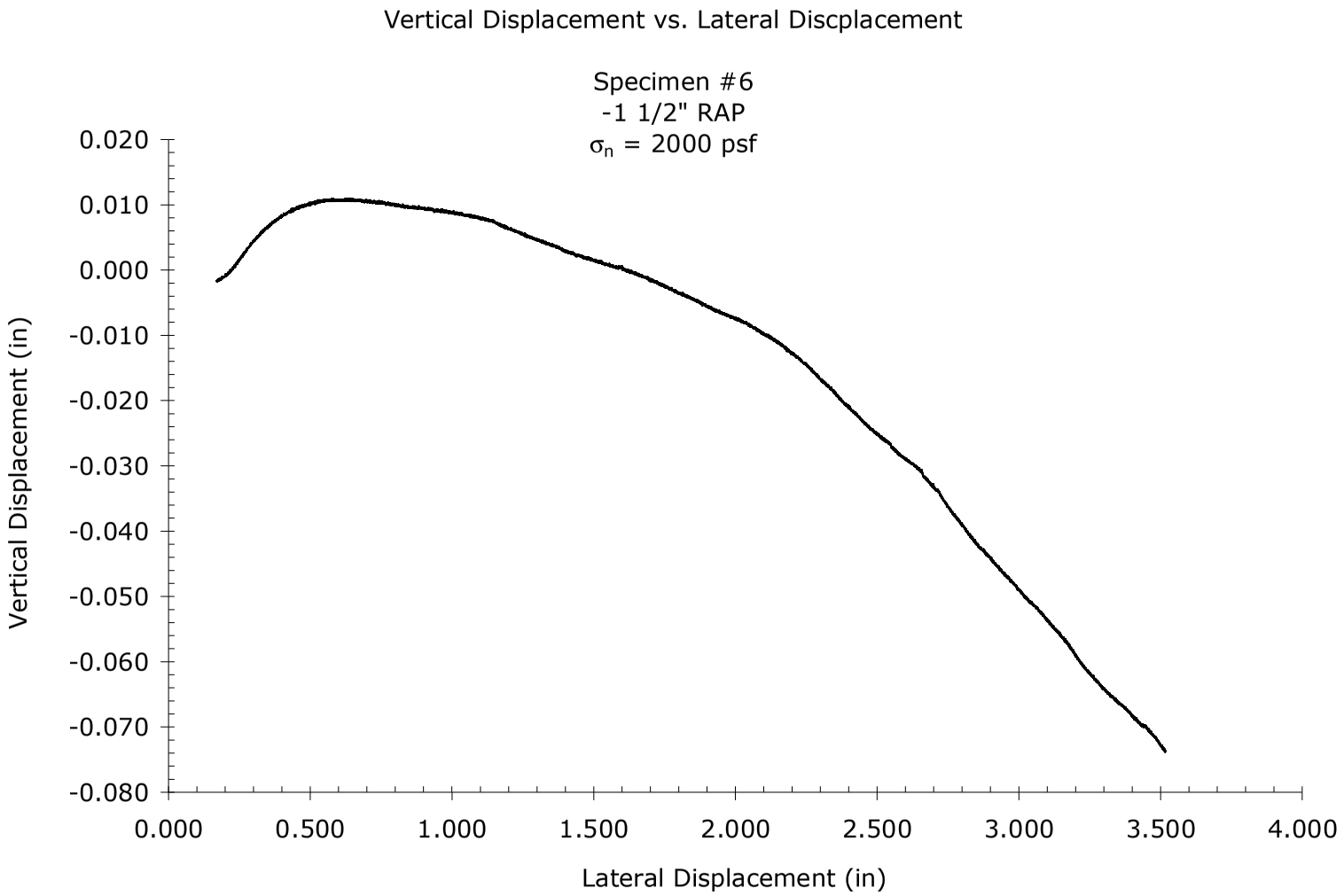
Vertical Displacement vs. Lateral Discplacement
Specimen #6
-1 1/2" RAP
σn = 2000 psf
Vertical Displacement (in)
0.020
0.010
0.000
-0.010
-0.020
-0.030
-0.040
-0.050
-0.060
-0.070
-0.080
0.000
0.500
1.000
1.500
2.000
2.500
3.000
3.500
4.000
Lateral Displacement (in)

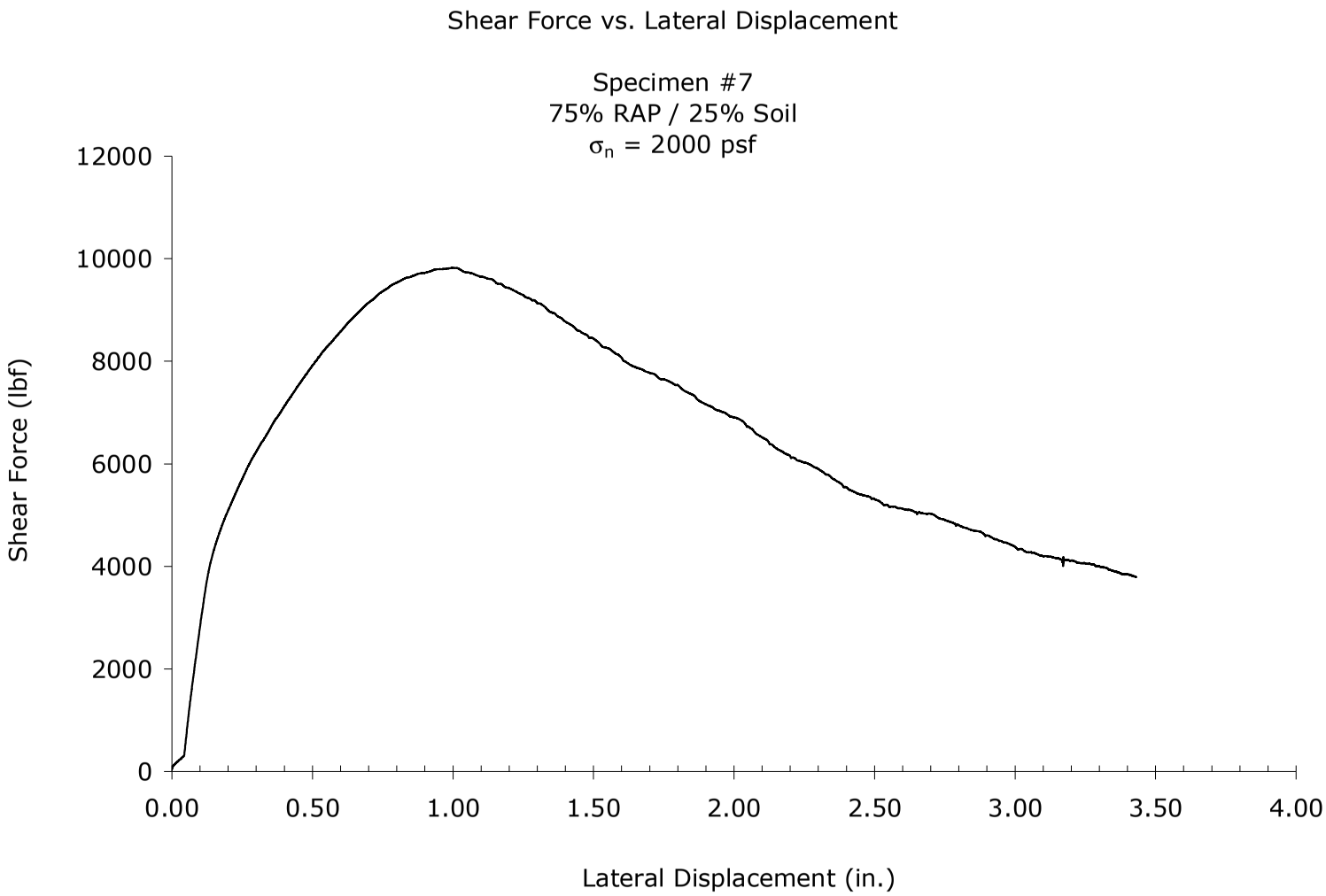
Shear Force vs. Lateral Displacement
Specimen #7
75% RAP / 25% Soil
σn = 2000 psf
Shear Force (lbf)
12000
10000
8000
6000
4000
2000
0
0.00
0.50
1.00
1.50
2.00
2.50
3.00
3.50
4.00
Lateral Displacement (in.)

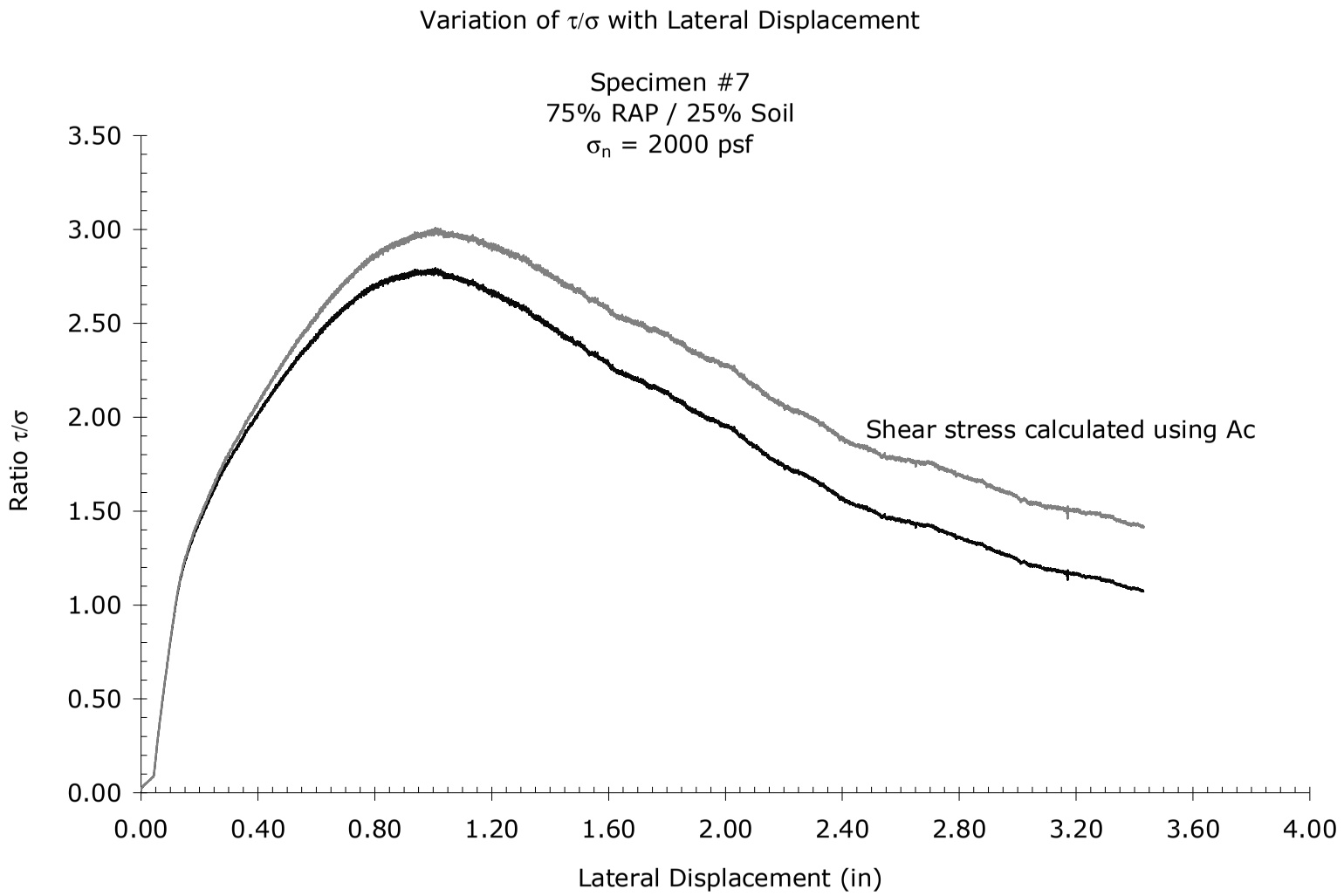
Variation of τ/σ with Lateral Displacement
Specimen #7
75% RAP / 25% Soil
σn = 2000 psf
Ratio τ/σ
3.50
3.00
2.50
2.00
1.50
1.00
0.50
0.00
0.00
0.40
0.80
1.20
1.60
2.00
2.40
2.80
3.20
3.60
4.00
Lateral Displacement (in)
Shear stress calculated using Ac

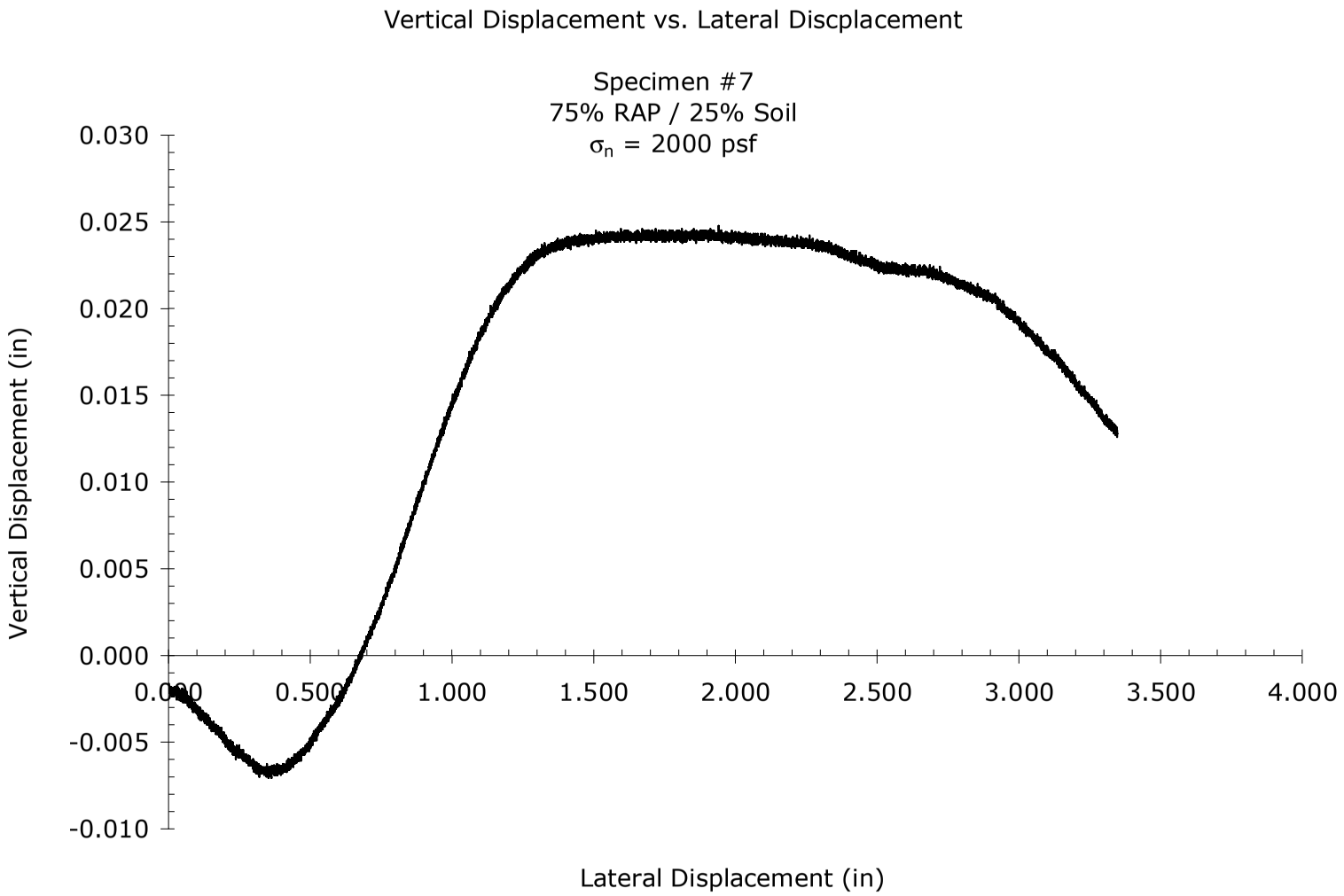
Vertical Displacement vs. Lateral Discplacement
Specimen #7
75% RAP / 25% Soil
σn = 2000 psf
Vertical Displacement (in)
0.030
0.025
0.020
0.015
0.010
0.005
0.000
-0.005
-0.010
0.000
0.500
1.000
1.500
2.000
2.500
3.000
3.500
4.000
Lateral Displacement (in)

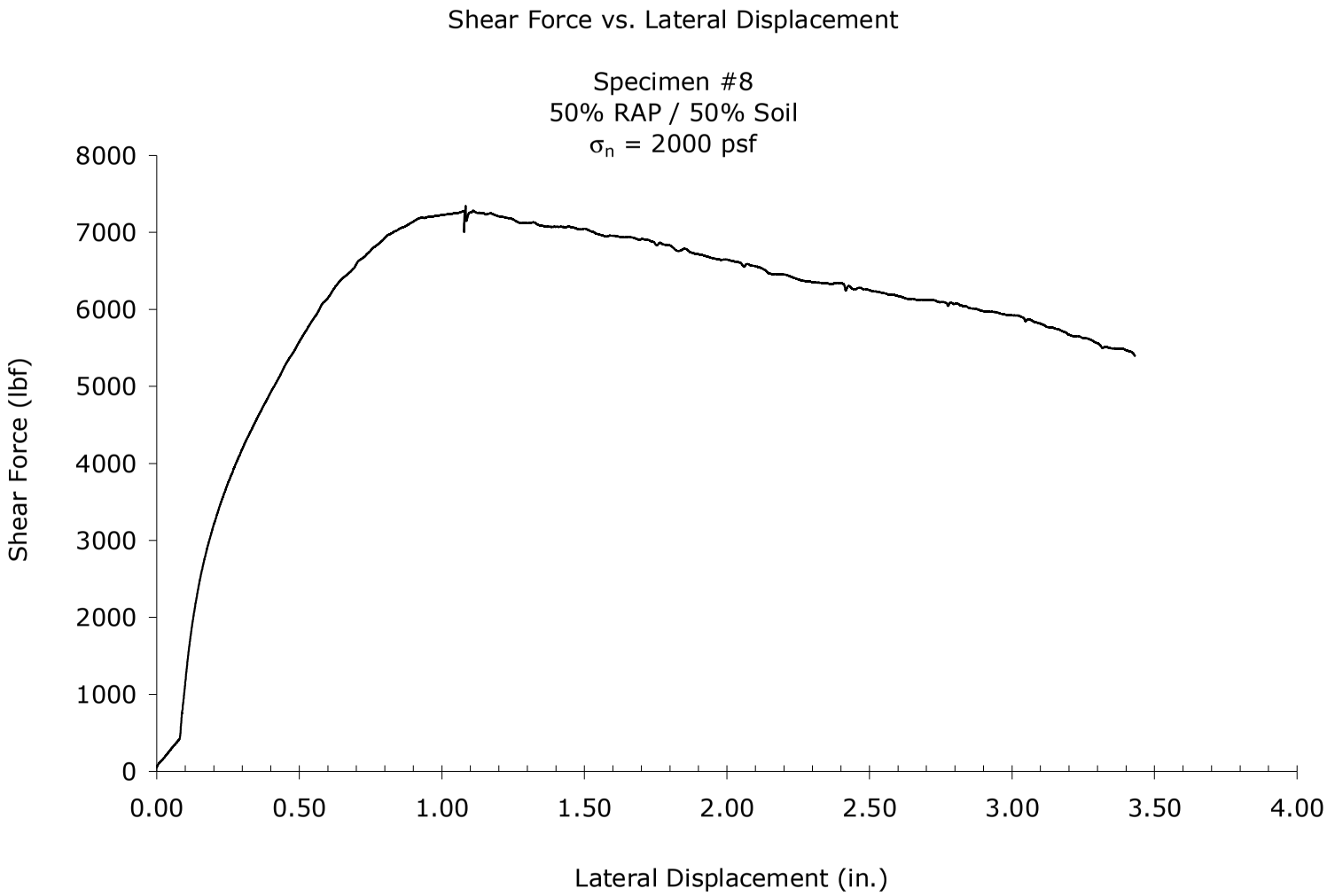
Shear Force vs. Lateral Displacement
Specimen #8
50% RAP / 50% Soil
σn = 2000 psf
Shear Force (lbf)
8000
7000
6000
5000
4000
3000
2000
1000
0
0.00
0.50
1.00
1.50
2.00
2.50
3.00
3.50
4.00
Lateral Displacement (in.)

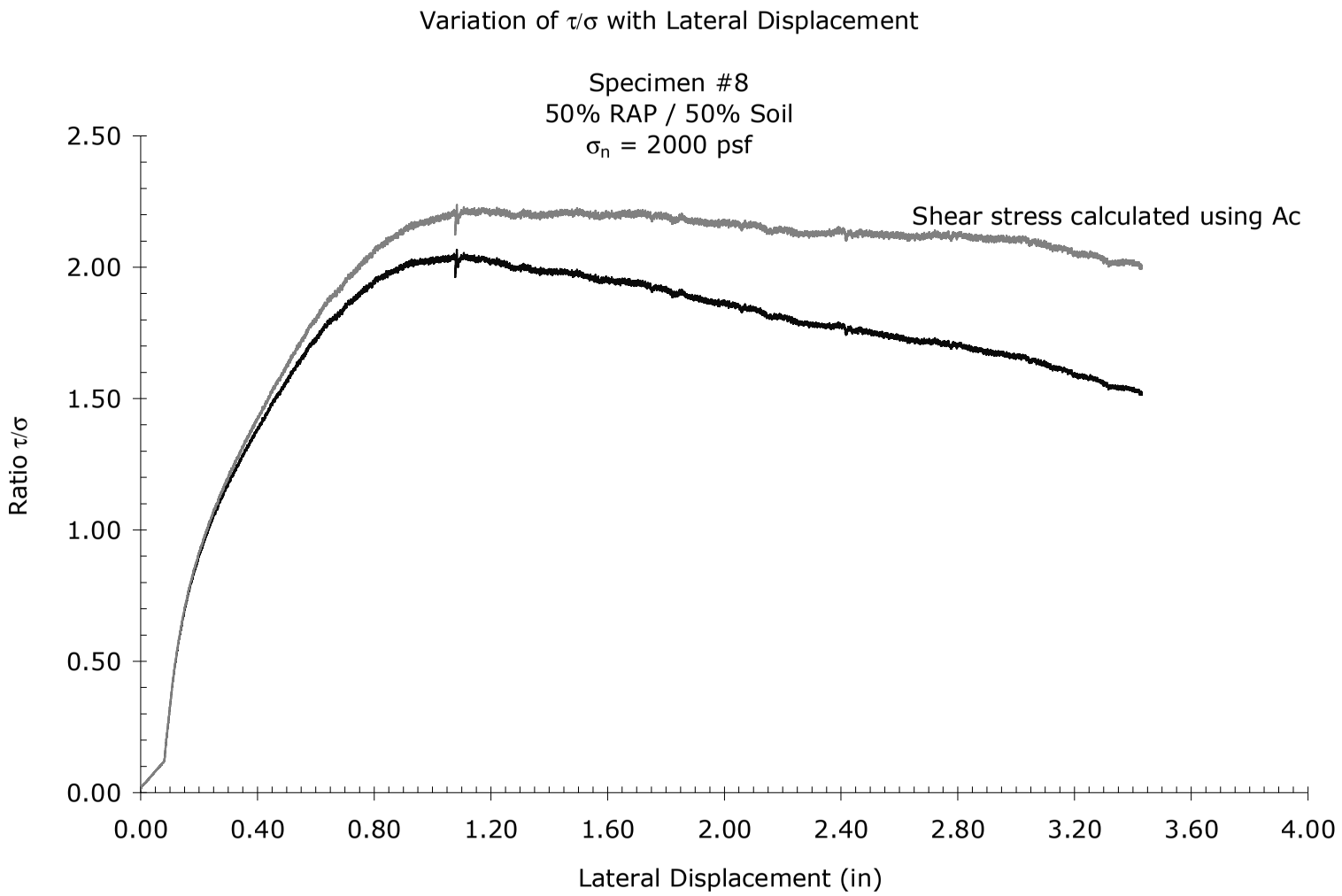
Variation of τ/σ with Lateral Displacement
Specimen #8
50% RAP / 50% Soil
σn = 2000 psf
Shear stress calculated using Ac
Ratio τ/σ
2.50
2.00
1.50
1.00
0.50
0.00
0.00
0.40
0.80
1.20
1.60
2.00
2.40
2.80
3.20
3.60
4.00
Lateral Displacement (in)

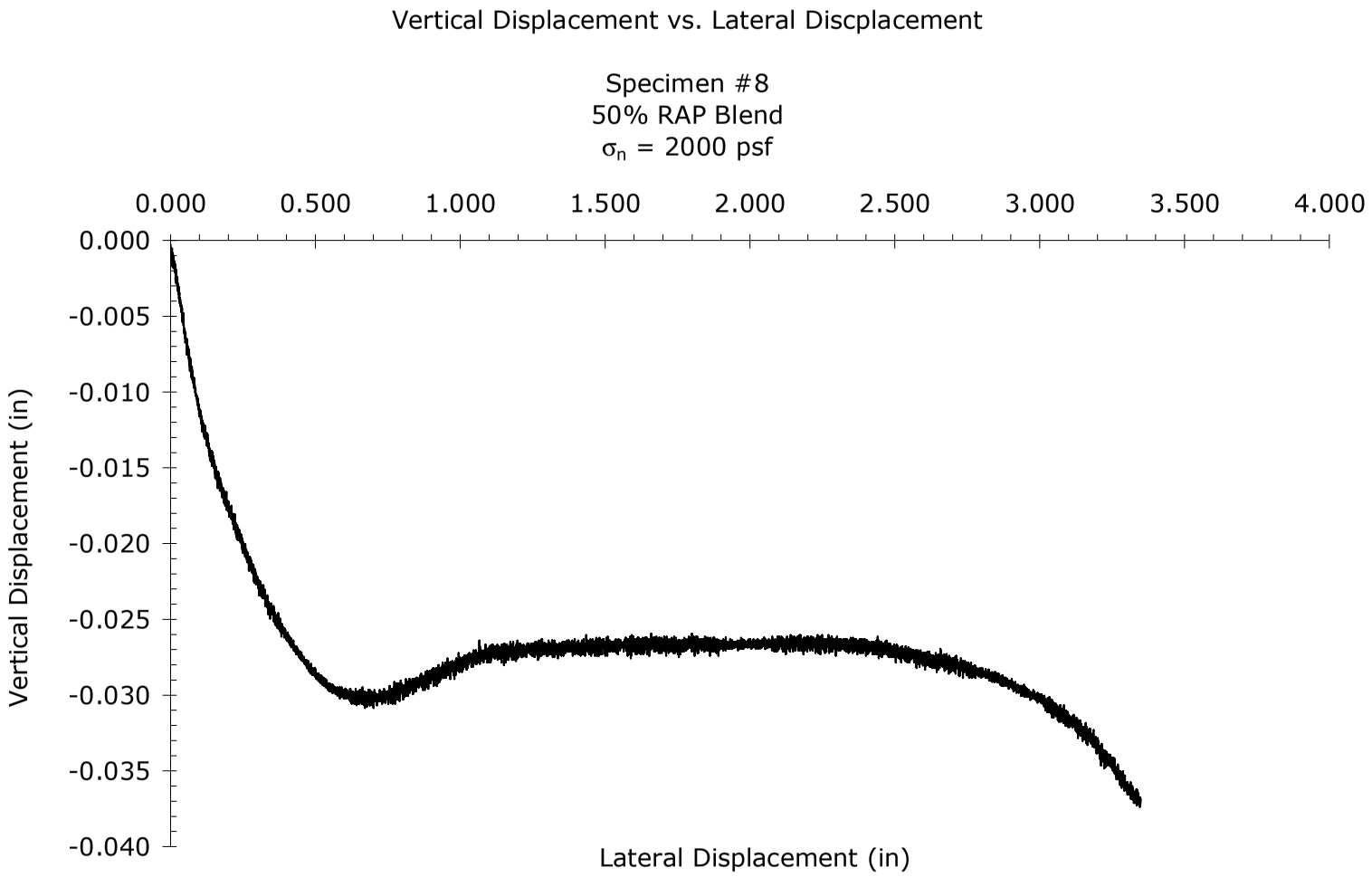
Vertical Displacement vs. Lateral Discplacement
Specimen #8
50% RAP Blend
σn = 2000 psf
0.000
0.500
1.000
1.500
2.000
2.500
3.000
3.500
4.000
0.000
-0.005
-0.010
-0.015
-0.020
-0.025
-0.030
-0.035
-0.040
Vertical Displacement (in)
Lateral Displacement (in)

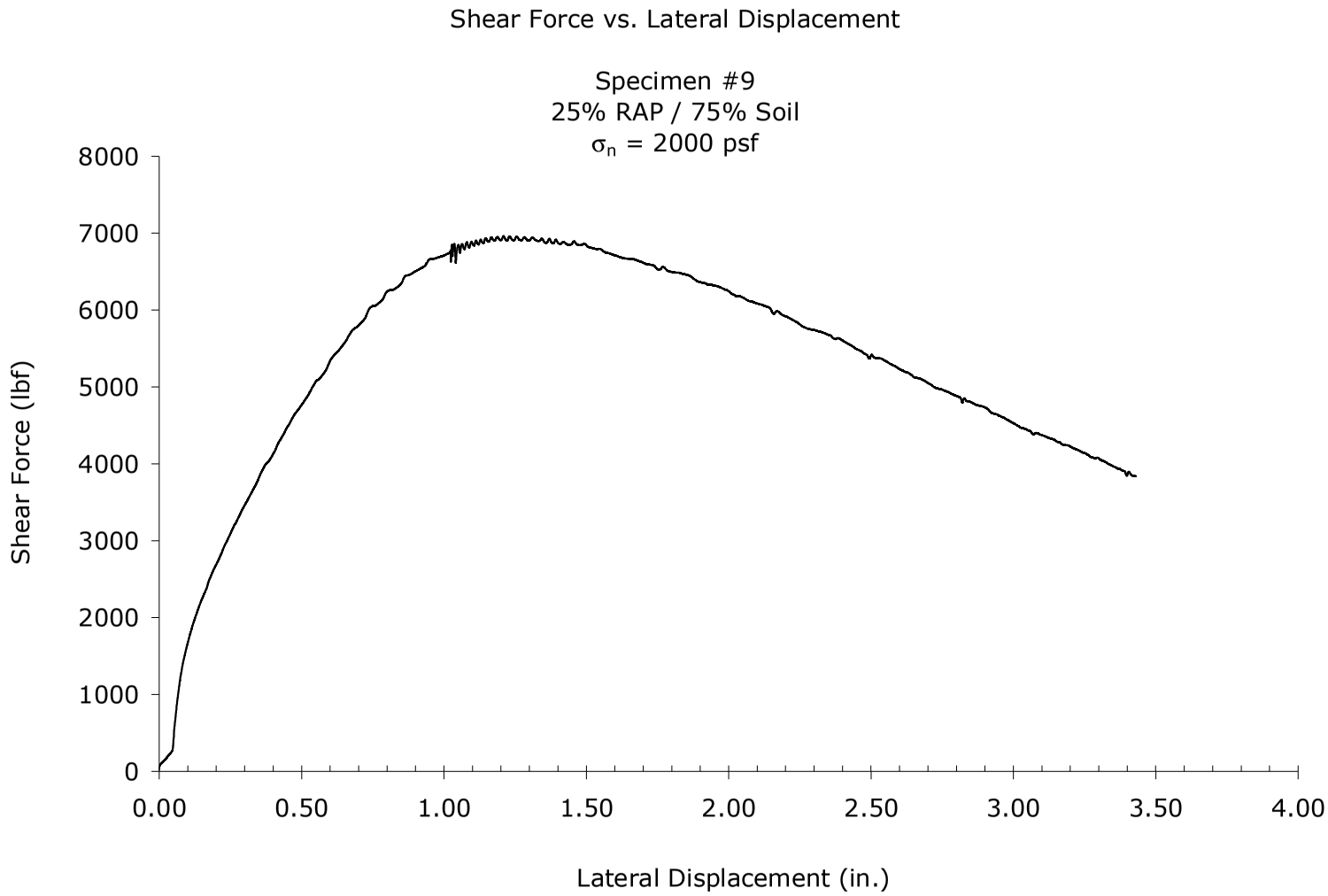
Shear Force vs. Lateral Displacement
Specimen #9
25% RAP / 75% Soil
σn = 2000 psf
Shear Force (lbf)
8000
7000
6000
5000
4000
3000
2000
1000
0
0.00
0.50
1.00
1.50
2.00
2.50
3.00
3.50
4.00
Lateral Displacement (in.)

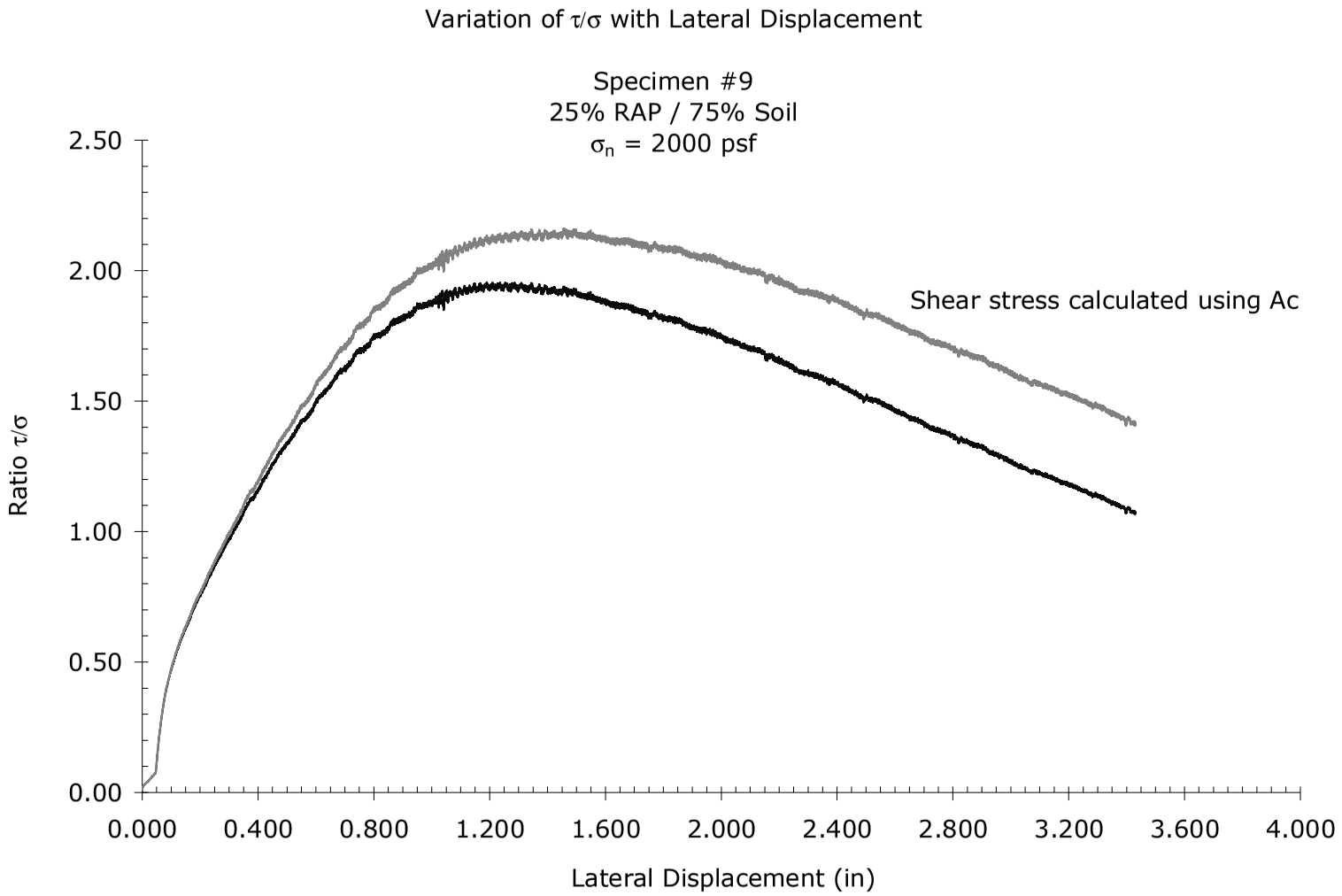
Variation of τ/σ with Lateral Displacement
Specimen #9
25% RAP / 75% Soil
σn = 2000 psf
Shear stress calculated using Ac
Ratio τ/σ
2.50
2.00
1.50
1.00
0.50
0.00
0.000
0.400
0.800
1.200
1.600
2.000
2.400
2.800
3.200
3.600
4.000
Lateral Displacement (in)

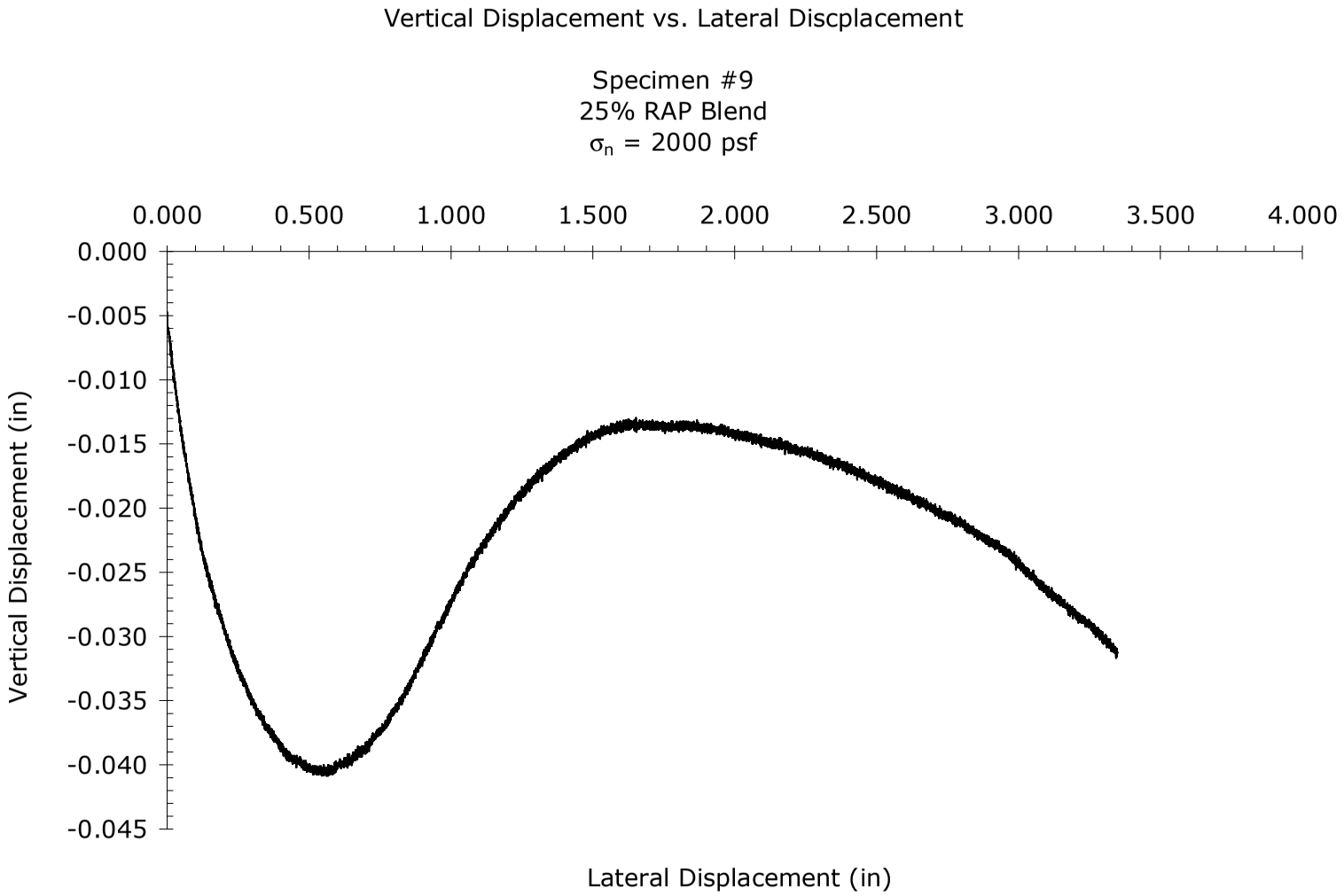
Vertical Displacement vs. Lateral Discplacement
Specimen #9
25% RAP Blend
σn = 2000 psf
0.000
0.500
1.000
1.500
2.000
2.500
3.000
3.500
4.000
0.000
-0.005
-0.010
-0.015
-0.020
-0.025
-0.030
-0.035
-0.040
-0.045
Vertical Displacement (in)
Lateral Displacement (in)

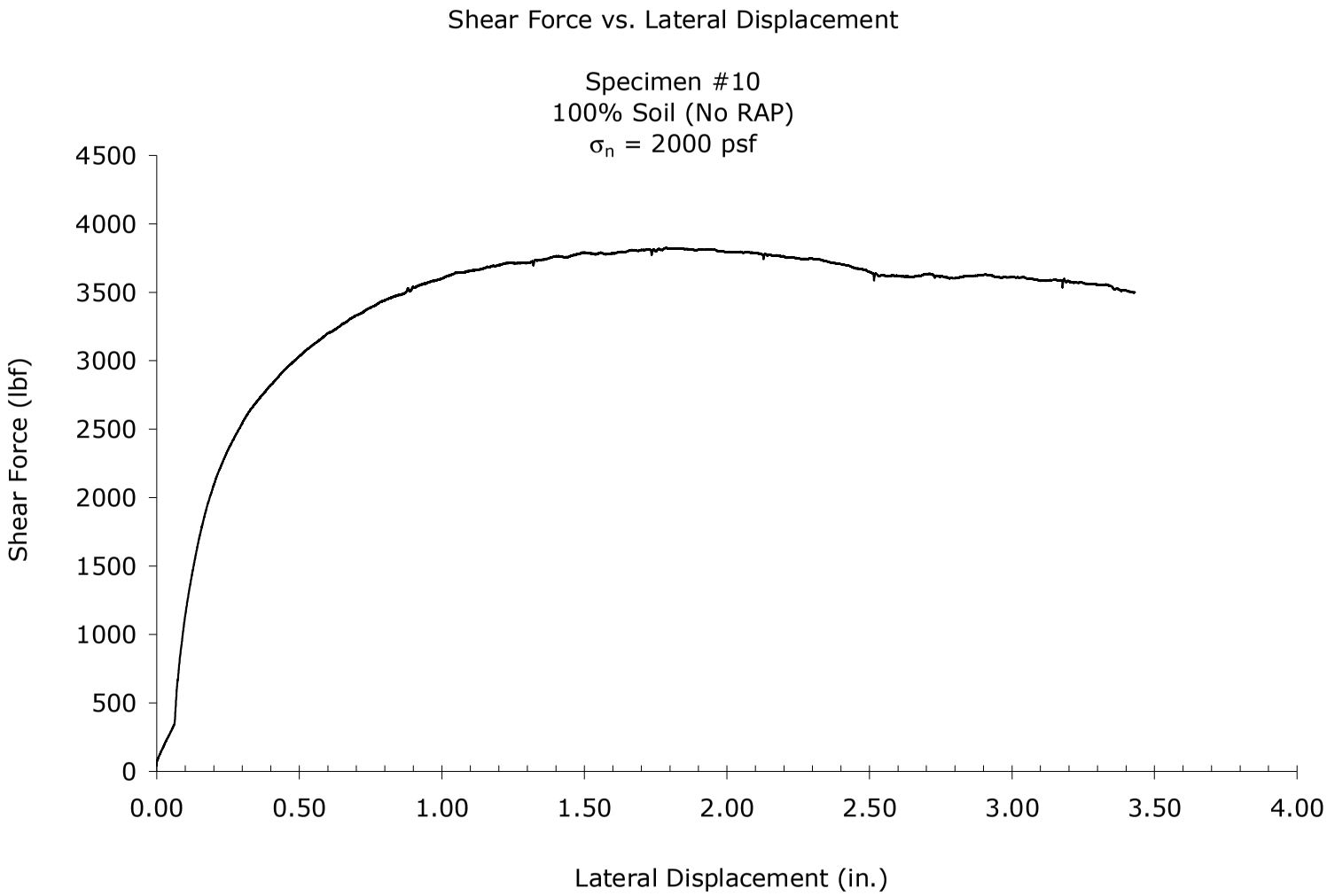
Shear Force vs. Lateral Displacement
Specimen #10
100% Soil (No RAP)
σn = 2000 psf
Shear Force (lbf)
4500
4000
3500
3000
2500
2000
1500
1000
500
0
0.00
0.50
1.00
1.50
2.00
2.50
3.00
3.50
4.00
Lateral Displacement (in.)

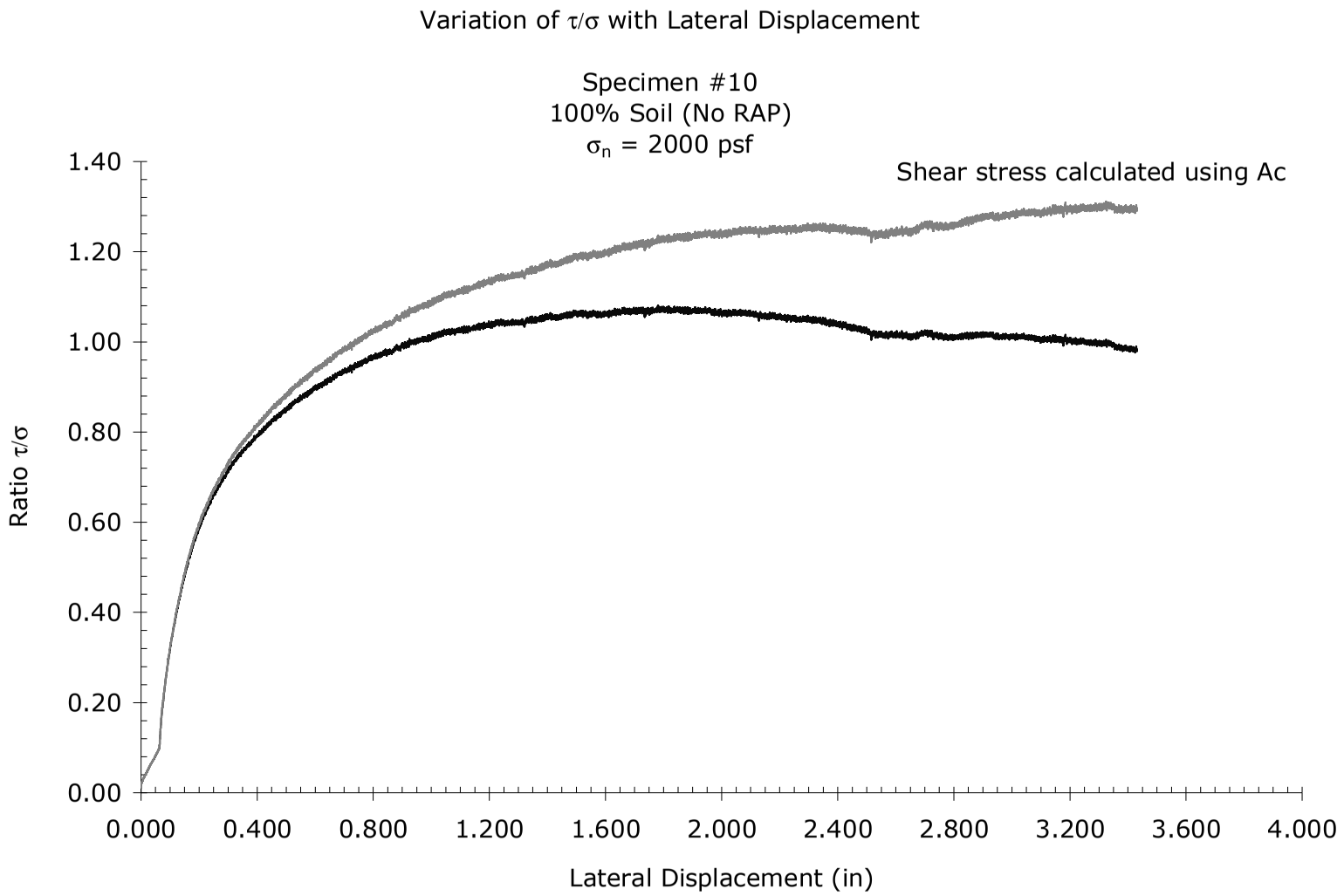
Variation of τ/σ with Lateral Displacement
Specimen #10
100% Soil (No RAP)
σn = 2000 psf
Shear stress calculated using Ac
Ratio τ/σ
1.40
1.20
1.00
0.80
0.60
0.40
0.20
0.00
0.000
0.400
0.800
1.200
1.600
2.000
2.400
2.800
3.200
3.600
4.000
Lateral Displacement (in)

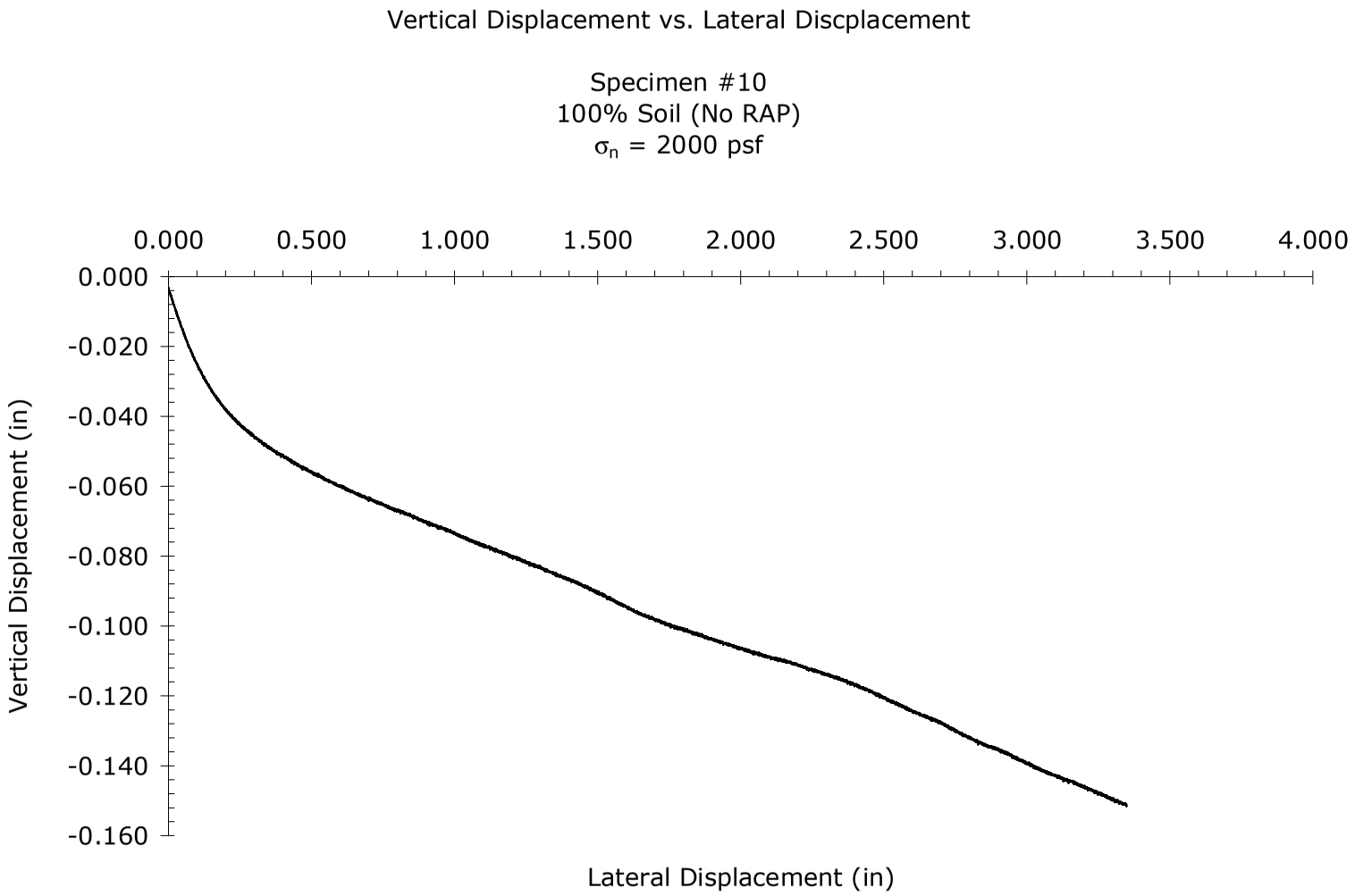
Vertical Displacement vs. Lateral Discplacement
Specimen #10
100% Soil (No RAP)
σ_n = 2000 psf
0.000
0.500
1.000
1.500
2.000
2.500
3.000
3.500
4.000
0.000
-0.020
-0.040
-0.060
-0.080
-0.100
-0.120
-0.140
-0.160
Vertical Displacement (in)
Lateral Displacement (in)

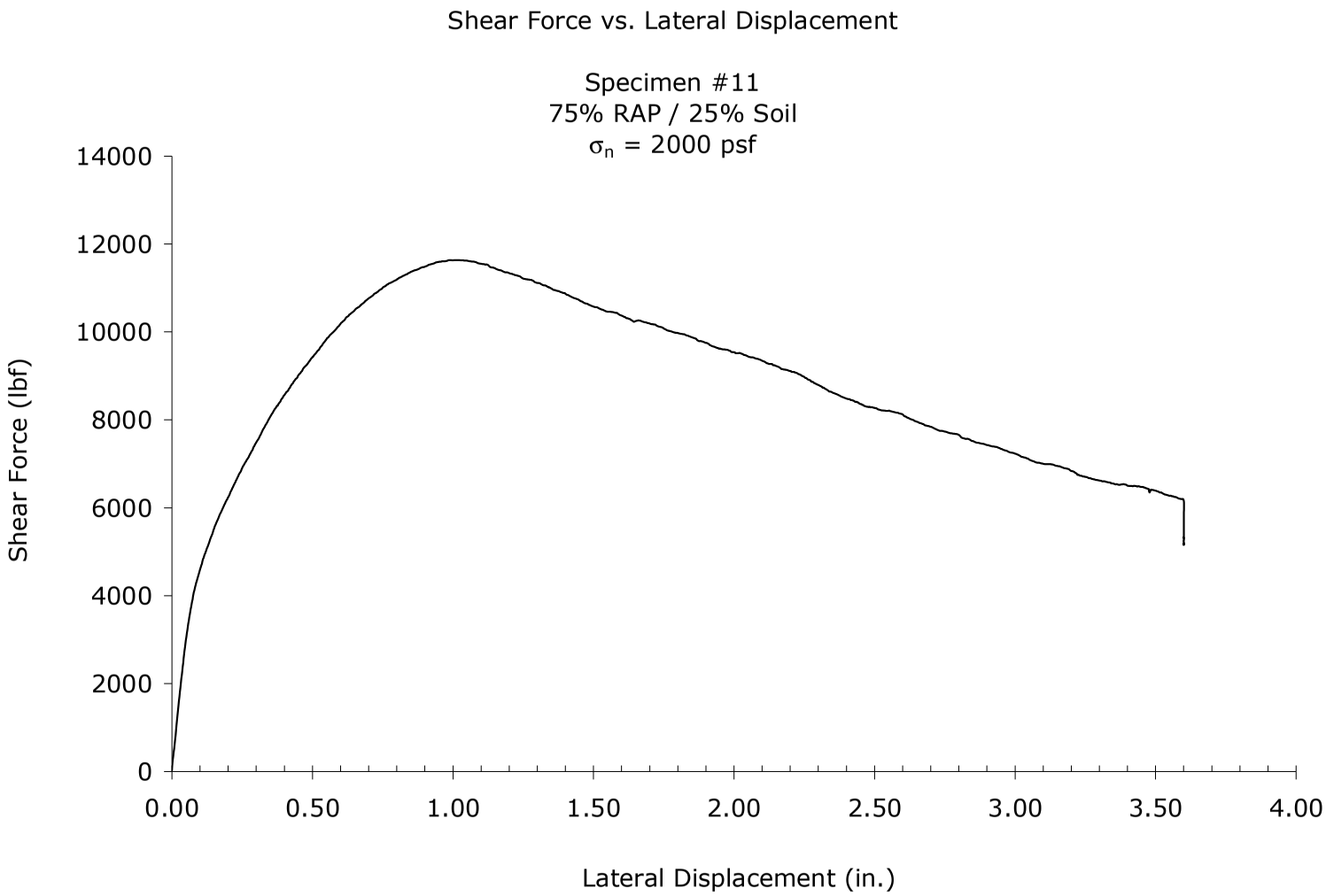
Shear Force vs. Lateral Displacement
Specimen #11
75% RAP / 25% Soil
σn = 2000 psf
Shear Force (lbf)
14000
12000
10000
8000
6000
4000
2000
0
0.00
0.50
1.00
1.50
2.00
2.50
3.00
3.50
4.00
Lateral Displacement (in.)

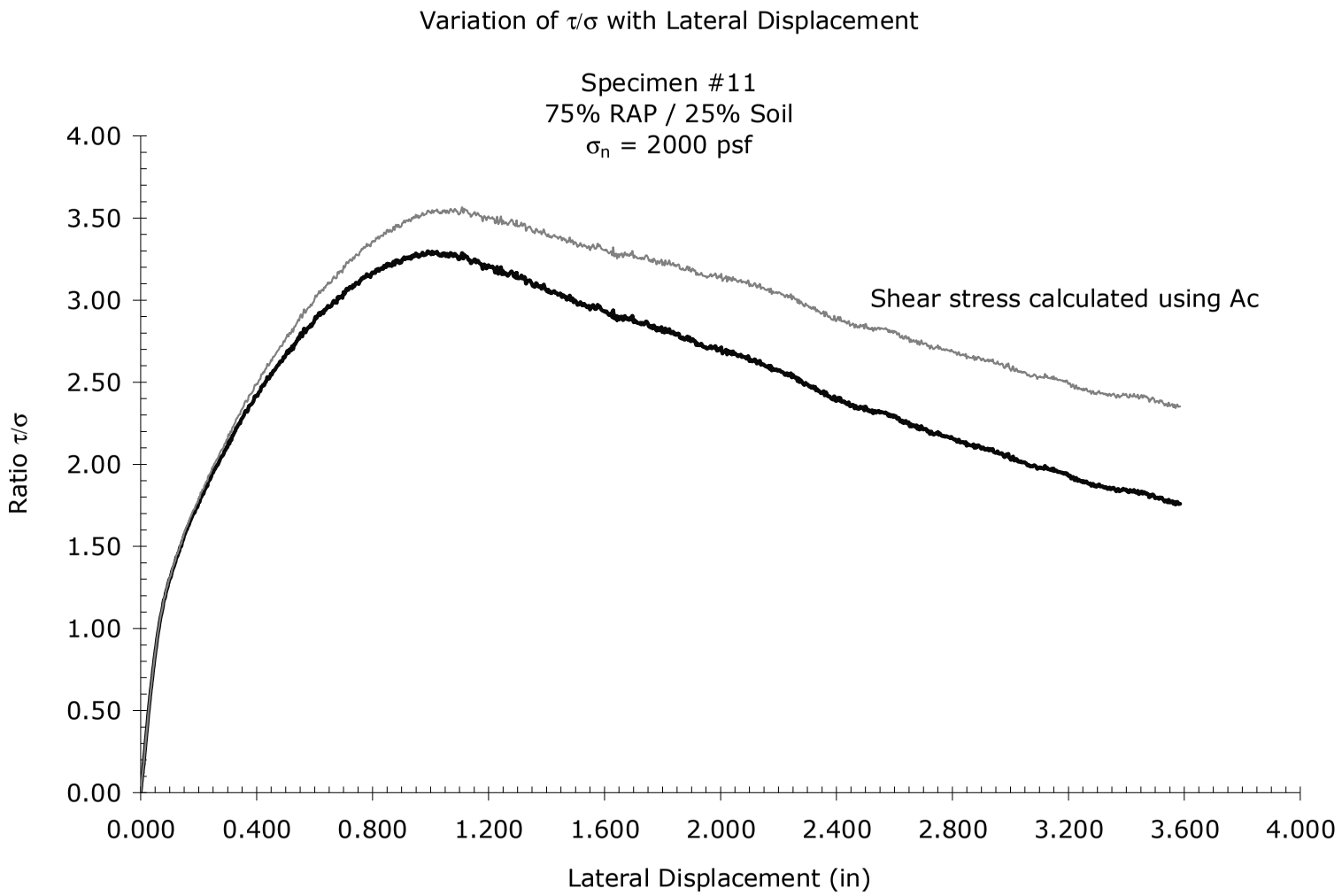
Variation of τ/σ with Lateral Displacement
Specimen #11
75% RAP / 25% Soil
σn = 2000 psf
Shear stress calculated using Ac
Ratio τ/σ
4.00
3.50
3.00
2.50
2.00
1.50
1.00
0.50
0.00
0.000
0.400
0.800
1.200
1.600
2.000
2.400
2.800
3.200
3.600
4.000
Lateral Displacement (in)

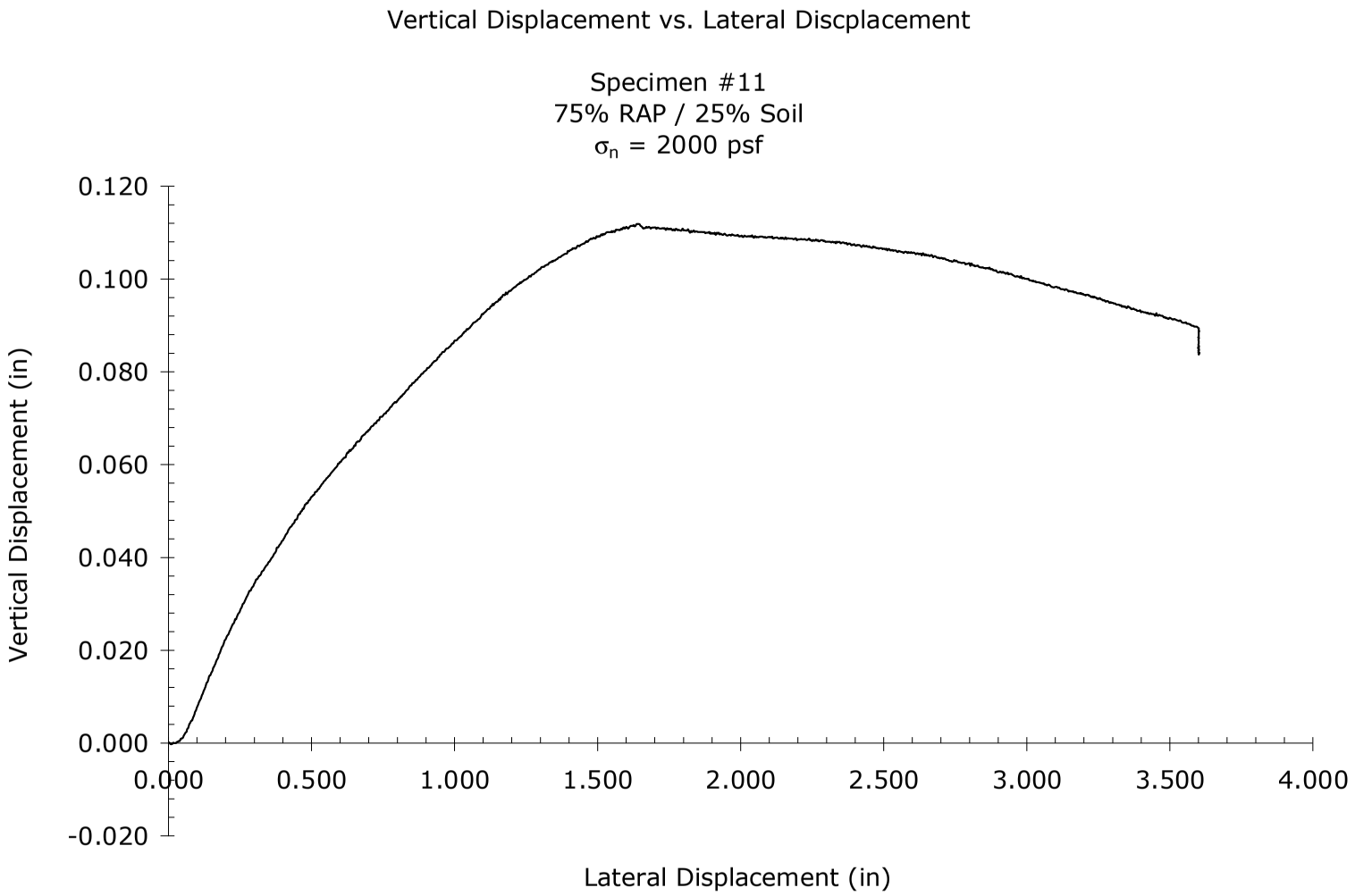
Vertical Displacement vs. Lateral Discplacement
Specimen #11
75% RAP / 25% Soil
σn = 2000 psf
Vertical Displacement (in)
0.120
0.100
0.080
0.060
0.040
0.020
0.000
-0.020
0.000
0.500
1.000
1.500
2.000
2.500
3.000
3.500
4.000
Lateral Displacement (in)

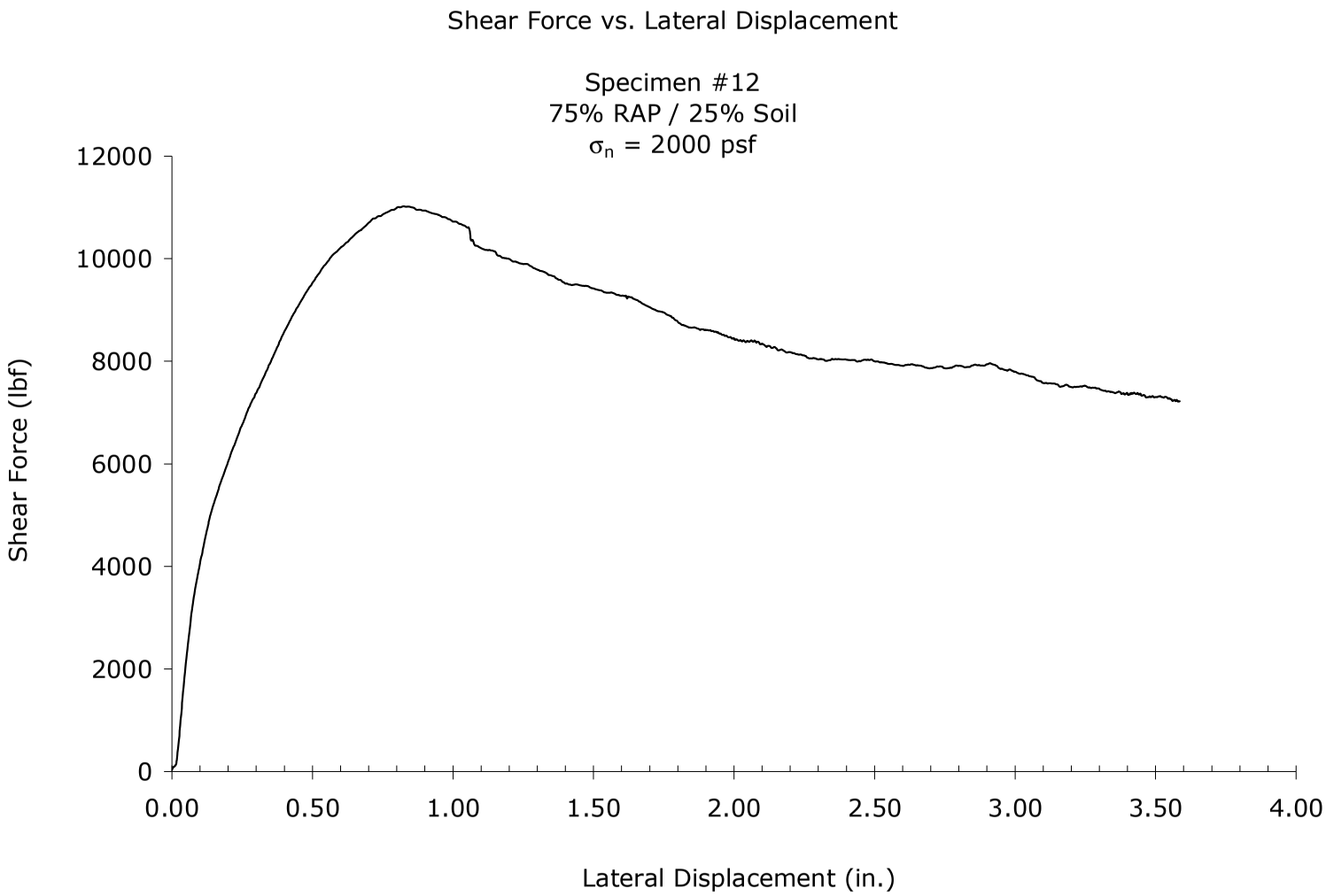
Shear Force vs. Lateral Displacement
Specimen #12
75% RAP / 25% Soil
σn = 2000 psf
Shear Force (lbf)
12000
10000
8000
6000
4000
2000
0
0.00
0.50
1.00
1.50
2.00
2.50
3.00
3.50
4.00
Lateral Displacement (in.)

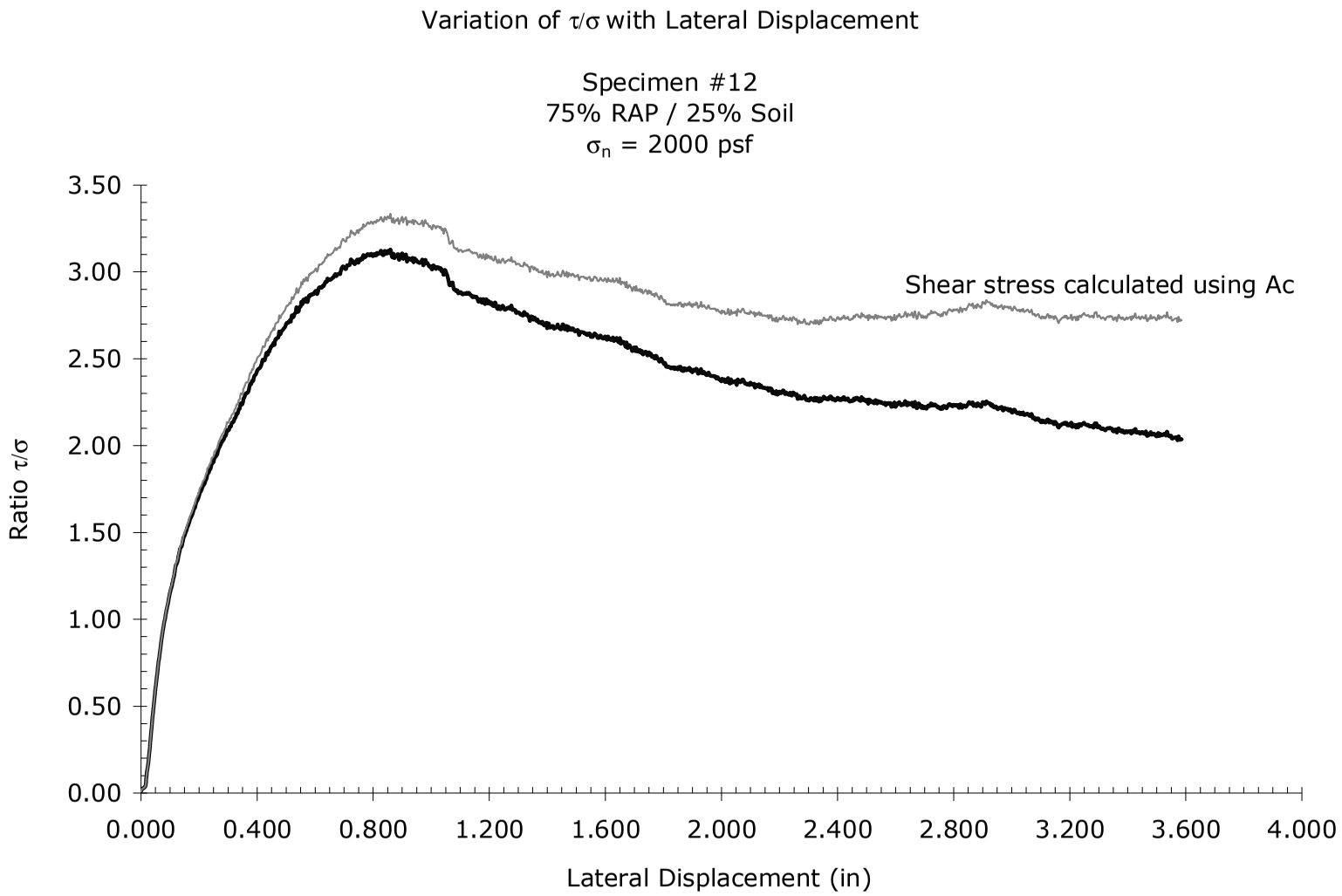
Variation of τ/σ with Lateral Displacement
Specimen #12
75% RAP / 25% Soil
σn = 2000 psf
Shear stress calculated using Ac
Ratio τ/σ
3.50
3.00
2.50
2.00
1.50
1.00
0.50
0.00
0.000
0.400
0.800
1.200
1.600
2.000
2.400
2.800
3.200
3.600
4.000
Lateral Displacement (in)

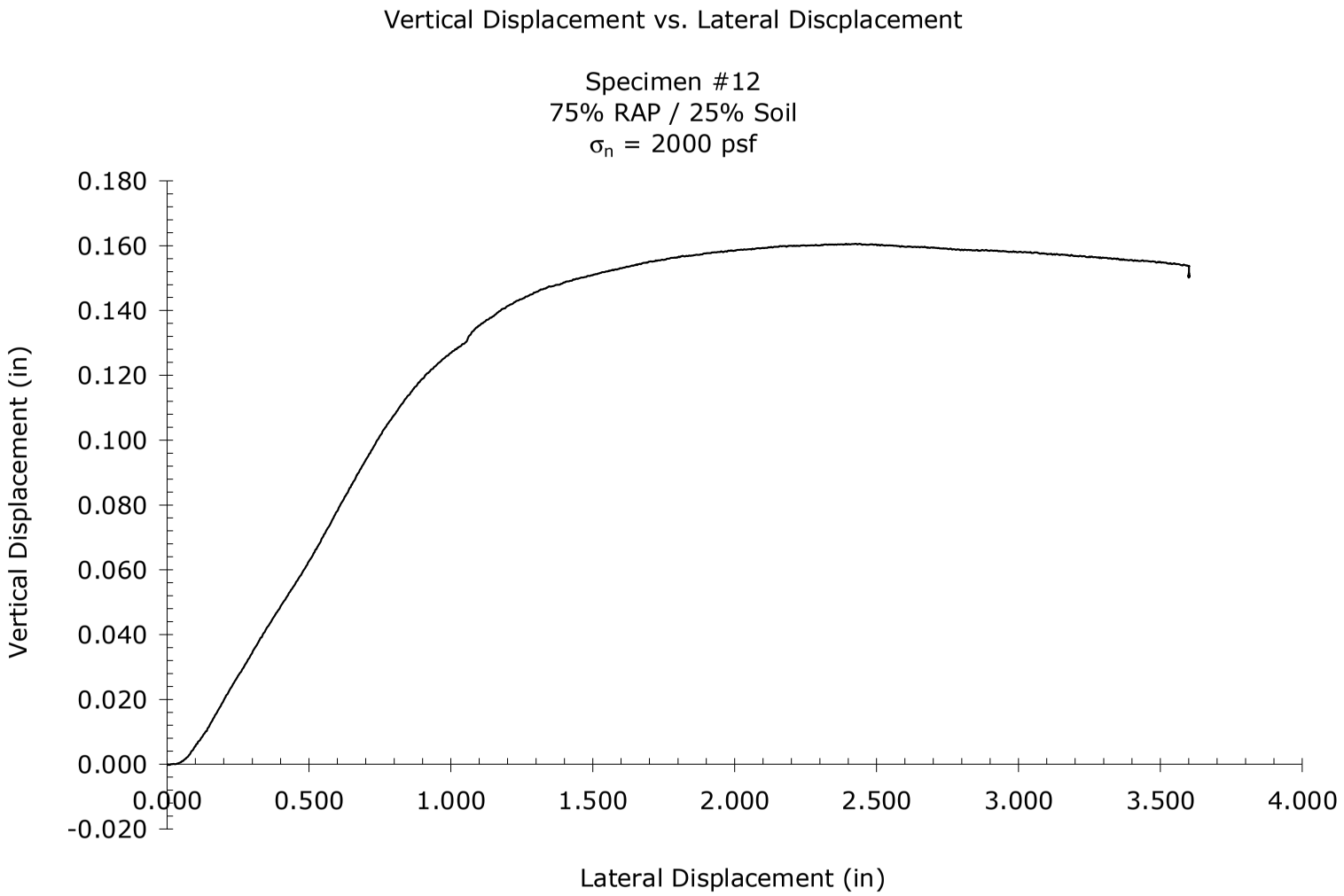
Vertical Displacement vs. Lateral Discplacement
Specimen #12
75% RAP / 25% Soil
σn = 2000 psf
Vertical Displacement (in)
0.180
0.160
0.140
0.120
0.100
0.080
0.060
0.040
0.020
0.000
-0.020
0.000
0.500
1.000
1.500
2.000
2.500
3.000
3.500
4.000
Lateral Displacement (in)

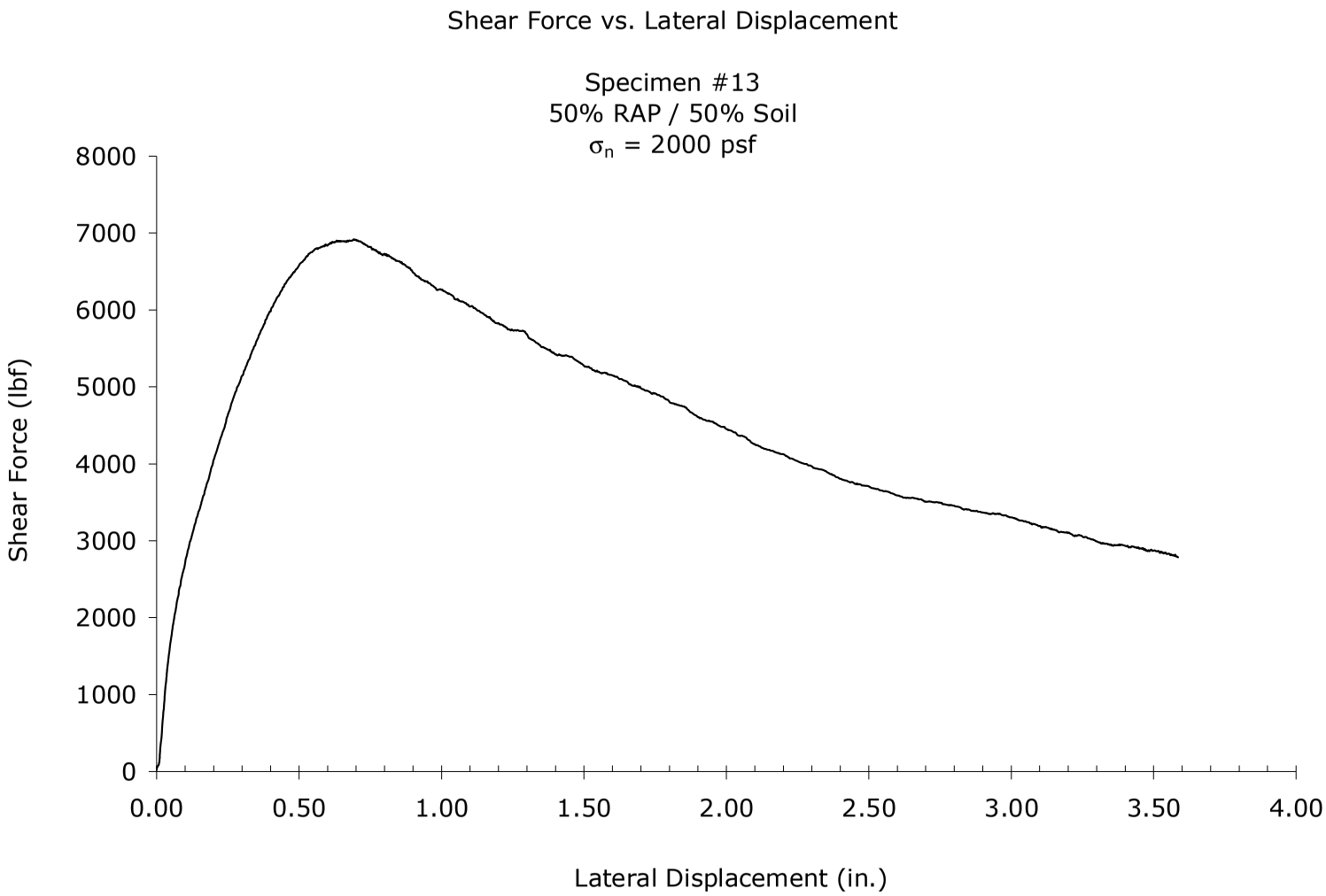
Shear Force vs. Lateral Displacement
Specimen #13
50% RAP / 50% Soil
σn = 2000 psf
Shear Force (lbf)
8000
7000
6000
5000
4000
3000
2000
1000
0
0.00
0.50
1.00
1.50
2.00
2.50
3.00
3.50
4.00
Lateral Displacement (in.)

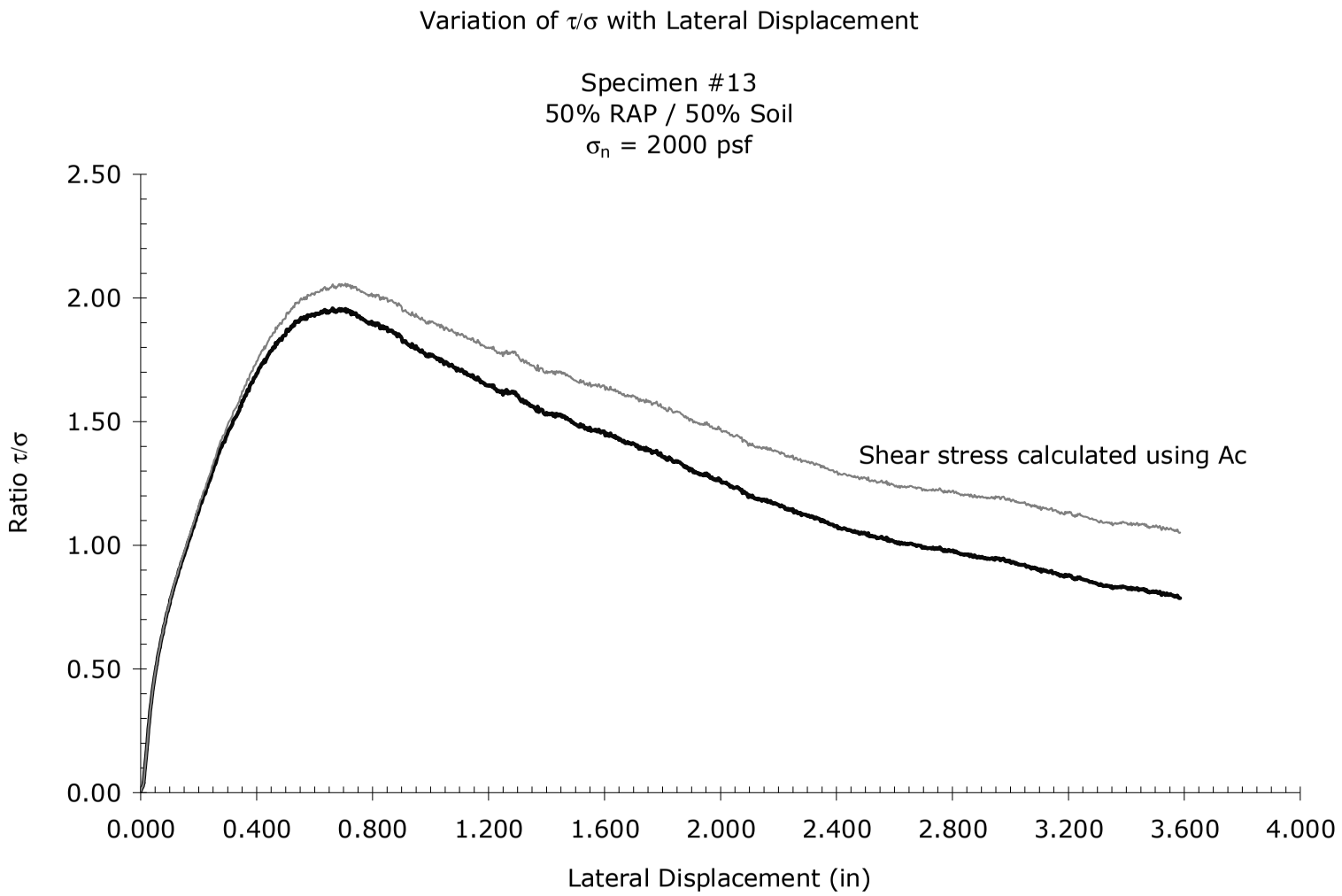
Variation of τ/σ with Lateral Displacement
Specimen #13
50% RAP / 50% Soil
σn = 2000 psf
Ratio τ/σ
2.50
2.00
1.50
1.00
0.50
0.00
Shear stress calculated using Ac
0.000
0.400
0.800
1.200
1.600
2.000
2.400
2.800
3.200
3.600
4.000
Lateral Displacement (in)

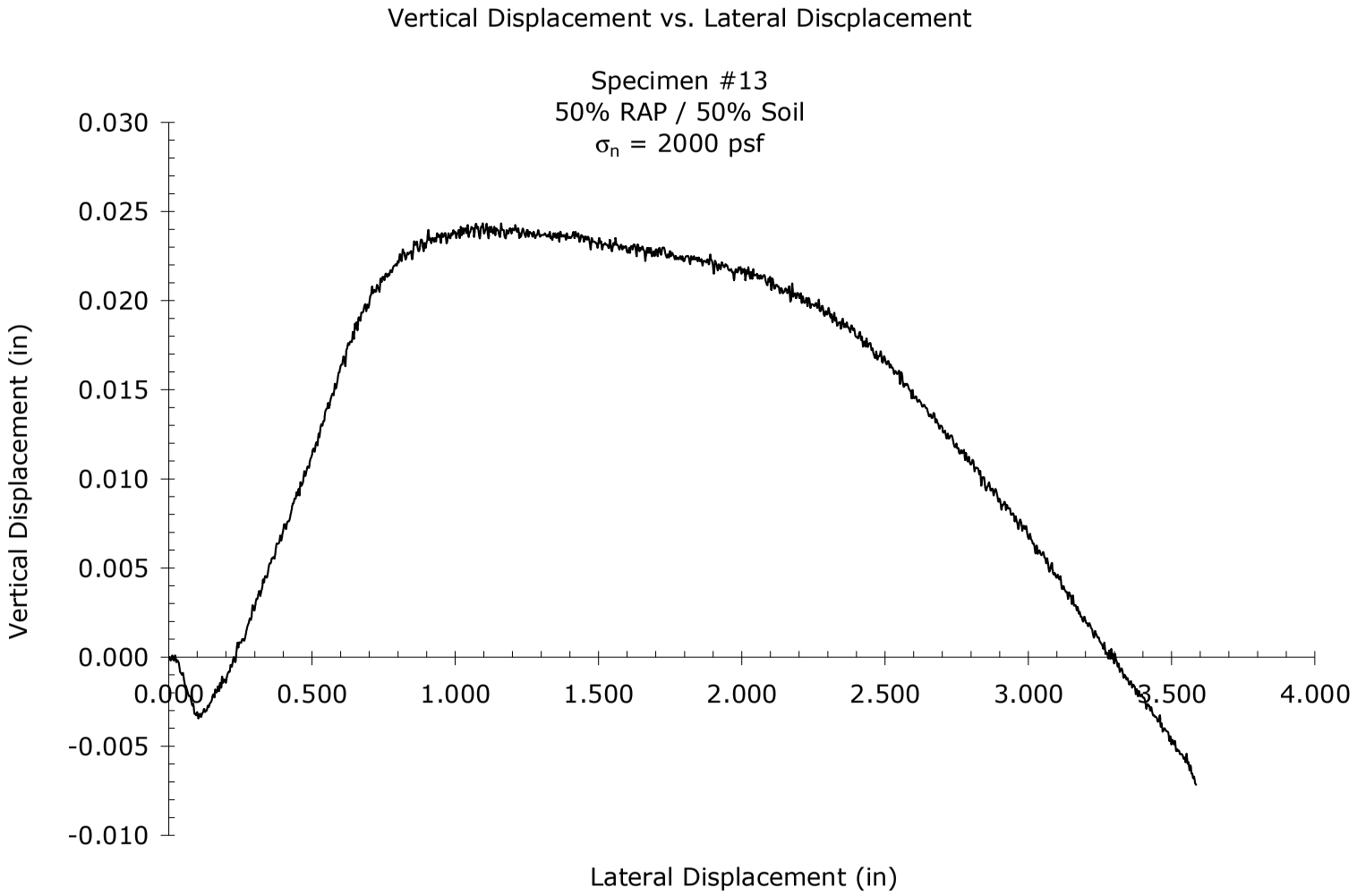
Vertical Displacement vs. Lateral Discplacement
Specimen #13
50% RAP / 50% Soil
σn = 2000 psf
Vertical Displacement (in)
0.030
0.025
0.020
0.015
0.010
0.005
0.000
-0.005
-0.010
0.000
0.500
1.000
1.500
2.000
2.500
3.000
3.500
4.000
Lateral Displacement (in)